

Supplementary information

Tracking the origins of Yakutian horses and the genetic basis for their fast adaptation to arctic environments

Pablo Librado^{1*}, Clio Der Sarkissian^{1*}, Luca Ermini¹, Mikkel Schubert¹, Hákon Jónsson¹, Anders Albrechtsen², Matteo Fumagalli³, Melinda A. Yang⁴, Cristina Gamba¹, Andaine Seguin-Orlando^{1,5}, Cecilie D. Mortensen⁵, Bent Petersen⁶, Cindi A. Hoover⁷, Belen Lorente-Galdos⁸, Artem Nedoluzhko⁹, Eugenia Boulygina⁹, Svetlana Tsygankova⁹, Markus Neuditschko¹⁰, Vidhya Jagannathan¹¹, Catherine Thèves¹², Ahmed H. Alfarhan¹³, Saleh A. Alquraishi¹³, Khaled A.S. Al-Rasheid¹³, Thomas Sicheritz-Ponten⁶, Ruslan Popov¹⁴, Semyon Grigoriev¹⁵, Anatoly N. Alekseev¹⁵, Edward M. Rubin⁷, Molly McCue¹⁶, Stefan Rieder¹⁰, Tosso Leeb¹¹, Alexei Tikhonov¹⁷, Eric Crubézy¹², Montgomery Slatkin⁴, Tomas Marques-Bonet⁸, Rasmus Nielsen¹⁸, Eske Willerslev¹, Juha Kantanen^{19,20}, Egor Prokhortchouk⁹, Ludovic Orlando^{1,12}.

¹Centre for GeoGenetics, Natural History Museum of Denmark, University of Copenhagen, Øster Voldgade 5-7, 1350K Copenhagen, Denmark;

²The Bioinformatics Centre, Department of Biology, University of Copenhagen, Copenhagen, Denmark;

³UCL Genetics Institute, Department of Genetics, Evolution and Environment; University College London; London, WC1E 6BT; UK

⁴Department of Integrative Biology, VLSB 3060, University of California, Berkeley, CA 94720-3140, USA;

⁵National High-Throughput DNA Sequencing Centre, University of Copenhagen, Øster Farimagsgade 2D, 1353K Copenhagen, Denmark;

⁶Center for Biological Sequence Analysis, Department of Systems Biology, Technical University of Denmark, 2800 Lyngby, Denmark;

⁷DOE Joint Genome Institute, Walnut Creek, California 94598, USA;

⁸ICREA (Universitat Pompeu Fabra/Consejo Superior de Investigaciones Científicas), 08003 Barcelona, Spain; Centro Nacional de Análisis Genómico, 08028 Barcelona, Spain;

⁹National Research Centre Kurchatov Institute, 1, Akademika Kurchatova, Moscow, 123182, Russian Federation;

¹⁰Agroscope, Swiss National Stud Farm, 1580 Avenches, Switzerland;

¹¹Institute of Genetics, University of Bern, 3001 Bern, Switzerland;

¹²Université de Toulouse, University Paul Sabatier (UPS), Laboratoire AMIS, CNRS UMR 5288, 37 allées Jules Guesde, 31000 Toulouse, France;

¹³Zoology Department, College of Science, King Saud University, P.O. Box 2455, Riyadh 11451, Saudi Arabia;

¹⁴Yakutian Research Institute of Agriculture, 677002 Yakutsk, Sakha, Russia

¹⁵North-Eastern Federal University, Yakutsk, Russian Federation;

¹⁶College of Veterinary Medicine, University of Minnesota, 1365 Gortner Avenue, St Paul, MN 55108, USA;

¹⁷Zoological Institute of Russian Academy of Sciences, Universitetskaya nab. 1, 199034 Saint-Petersburg, Russia;

¹⁸Center for Theoretical Evolutionary Genomics, University of California, Berkeley, Berkeley, California, USA;

¹⁹Biotechnology and Food Research, MTT Agrifood Research Finland, Jokioinen, Finland;

²⁰Department of Biology, University of Eastern Finland, Kuopio, Finland;

*Contributed equally.

AUTHOR CONTRIBUTIONS

- LO initially conceived and headed the project.
- CT, ANA, AT, EC, and EP provided ancient horse samples.
- JK and EP provided access to modern Yakutian horse samples.
- SR and TL provided access to the Franches-Montagnes horse genomes.
- MM provided access to the Morgan, American Quarter Horse and Standardbred horse genomes.
- ASO, KM, BP, CH, CT, AHA, SAA, KASAR, TSP, SG, AA, AN, EB, EMR, MM, SR, TL, AT, EC, MS, TMB, EW, JH, EP, LO provided reagents and materials.
- LO performed ancient DNA extractions and constructed ancient DNA libraries, with input from CAH, CD and LE.
- JK and RP coordinated sampling and DNA extraction from modern Yakutian horses (Yak1-Yak9).
- AN, EB and EP extracted DNA from modern Yakutian horses (Horse1-Horse3), and performed sequencing at the Kurchatov Institute, Russia.
- ST constructed DNA libraries from modern Yakutian horses (Horse1-Horse3) at the Kurchatov Institute, Russia.
- CD and LE constructed DNA libraries from modern Yakutian horses (Yak1-Yak9).
- ASO and KM sequenced DNA libraries at the Danish National High-Throughput DNA Sequencing Center, Copenhagen, Denmark.
- MN and VJ performed modern DNA extractions and constructed modern DNA libraries for Franches-Montagnes horses sequenced at the Institute of Genetics of the University of Bern.
- MSc performed read mapping, variant calling, and functional characterization, and generated genome alignments; performed DNA damage pattern analyses, BAM rescaling and trimming; did phylogenomics reconstructions based on exome data, with input from BP.
- CD and LE examined DNA damage patterns.
- CD and LE performed metagenomic analyses.
- LO performed phylogenetic reconstruction of mitochondrial genomes with input from LE.
- CD and LE performed phylogenetic reconstructions based on Y-chromosome data.
- HJ performed genotype-based Principal Component Analyses.
- LO performed genotype likelihood-based Principal Component Analyses, NGSAdmix analyses.
- LO computed F_{ST} values, and HJ detected outlier regions.
- MSc performed the analyses of segmental duplications, with input from BL and TMB.
- MSc and HJ estimated genome-wide heterozygosity and inbreeding coverage.
- AA estimated sequencing error rates and performed admixture tests based on the D-statistics.
- CD analysed the results of the admixture tests based on the D-statistics.
- LE did Pairwise-Sequential Markovian Coalescent Inference analyses.
- HJ performed TreeMix and f3-statistics analyses.

- MAY and MSI designed and performed projection analyses, with input from CD and LO.
- PL investigated the relative contribution of *cis*-regulatory elements and protein-coding regions to adaptation, with input from LO.
- LO performed enrichment analyses.
- CD, PL and LO examined outputs enrichment analyses.
- PL, CD, LE, MSc, MAY and LO wrote the supplementary information, with input from CG.
- LO wrote the manuscript, with input from all coauthors.

TABLE OF CONTENT

Section 1: Sample Information	8
1.1 Environmental conditions and inhabitants of Yakutia	8
1.2 Yakutian horses.....	8
1.3 Sampling	8
1.4 Supplementary Tables for Section 1	10
2 Section 2: Genome sequencing.....	11
2.1 DNA extraction and library preparation for modern Yakutian horses	11
2.2 DNA extraction and library preparation for ancient horses from Yakutia	12
2.3 DNA Shotgun sequencing.....	13
2.4 Comparative horse dataset.....	14
2.5 Sequence read processing and alignment against reference genomes	14
2.6 Characterizing and correcting the sequencing patterns of post-mortem damage of ancient samples.....	18
2.7 Sample-wise error rates.....	25
2.8 Supplementary Tables for Section 2	29
3 Section 3: Microbial profiling of ancient horses DNA.....	36
3.1 Supplementary Tables for Section 3	40
4 Section 4: Genomic variation	41
4.1 SNP variation	41
4.1.1 Variant calling against the horse reference EquCab2.0.....	41
4.1.2 Functional categorization of SNPs variation	41
4.1.3 Non-synonymous mutations specific to Yakutian horses.	41
4.1.4 Analysis of loci associated with important Mendelian traits in horses	42
4.2 Screening for segmental duplications	43
4.3 Inbreeding and heterozygosity	44
4.3.1 Genome-wide heterozygosity estimates	44
4.3.2 Inbreeding estimates	46
4.4 Supplementary Tables for Section 4	49
5 Section 5: Phylogenomic inference	67
5.1 Phylogenetic inference from mitochondrial sequences	67
5.1.1 Dataset and substitution models	67
5.1.2 Maximum likelihood phylogeny	67
5.1.3 Bayesian phylogeny.....	69
5.2 Y-chromosome phylogenetic inference	71
5.3 Phylogenetic inference using a super-matrix of nuclear coding sequences.....	72
5.4 Supplementary Tables for Section 5	74
6 Section 6: Demographic history of the Yakutian horses	79
6.1 Reconstructing their long and short-term effective population sizes.....	79
6.1.1 Pairwise Sequentially Markov Coalescent	79
6.1.2 Diffusion approximation for demographic inference	80
6.2 Genome projections of Yakutian and other domesticated horses	81
6.2.1 Test horse genomes and reference panels	82
6.2.2 Projection results	82
6.3 Principal component analysis	85
6.3.1 PCA based on genotype calls	85
6.3.2 PCA in a genotype likelihood framework	86
6.4 Admixture tests	87
6.4.1 D-statistics	87
6.4.2 f_3 -statistics and TreeMix analyses	91

6.4.3	Genetic Clustering based on genotype likelihoods	92
6.5	Supplementary Tables for Section 6	95
7	Section 7: Genetic determinants of the Yakutian horse adaptations	102
7.1	Selection scans	102
7.1.1	Genetically differentiated regions: F_{ST} -outlier approach.....	102
7.2	Coding vs. non-coding contribution to adaptation	104
7.2.1	Genetic distances across functional site categories	104
7.3	Functional enrichment analyses	107
7.4	Supplementary Tables for Section 7	108

FIGURE LIST

Figure S2.1. Size distribution of horse library inserts for the present-day and ancient Yakutian specimens	16
Figure S2.2. Size distribution of horse library inserts for the comparative dataset of modern horses	17
Figure S2.3. Nucleotide mis-incorporation patterns at 5'- and 3'- read termini for the ancient samples Batagai and CGG101397.....	19
Figure S2.4. DNA fragmentation patterns at 5'- and 3'- read termini for ancient the samples Batagai and CGG101397.	21
Figure S2.5. Nucleotide mis-incorporation patterns at 5'- and 3'- read termini for the ancient samples ODJ6 and Yukagir.....	22
Figure S2.6. DNA fragmentation patterns at 5'- and 3'- read termini for the ancient samples ODJ6 and Yukagir.	24
Figure S2.7. Posterior distributions estimated for three DNA damage parameters (δ_d , δ_s and $1/\lambda - 1$) for ancient samples Batagai and CGG101397.....	25
Figure S2.8. Estimated error rates for ancient and present-day horse genomes without quality filtering.....	27
Figure S2.9. Estimated error rates for ancient and present-day horse genomes with quality filtering (mapQ \geq 30, baseQ \geq 20).....	28
Figure S3.1. Relative abundance of microbial classes in the DNA extracts of ancient horse remains preserved in the permafrost.	37
Figure S3.2. Principal Coordinate Analysis of Bray-Curtis distances between microbial DNA profiles at the genus level in the DNA extracts of ancient horse remains preserved in the permafrost.	38
Figure S3.3. Hierarchical clustering of Manhattan distances between microbial DNA at the genus level in the DNA extracts of ancient horse remains preserved in the permafrost.	38
Figure S3.4. Principal Coordinate Analysis of Bray-Curtis distances between microbial DNA profiles at the genus level in various human associated microbiomes, soils and ancient permafrost horse remains.	39
Figure S4.1. Distribution of copy-numbers called for control regions in modern Yakutian horses and the Thoroughbred Twilight individual underpinning the horse reference genome.	44
Figure S4.2. Average autosomal heterozygosity in ancient and modern horses.	45
Figure S4.3. Average autosomal heterozygosity in ancient and modern horses, disregarding transitions.	46
Figure S4.4. Inbreeding coverage estimates for Yakutian and Late Pleistocene horses.	47
Figure S4.5. Inbreeding coverage estimates for other domesticated horses.	48
Figure S5.1. Mitochondrial ML phylogeny of ancient and modern horses.	68
Figure S5.2. Mitochondrial Bayesian phylogeny of ancient and modern horses.	70
Figure S5.3: Bayesian Skyline plot reconstructed from mitochondrial genome data..	71
Figure S5.4. Y-chromosome Maximum Likelihood phylogeny.	72
Figure S5.5. Exome-based phylogenetic inference.	73
Figure S6.1. Unscaled PSMC profiles.	80
Figure S6.2. Projections of modern Yakutian horses onto the refYAK panel.....	83
Figure S6.3. Projections of Przewalski's horses onto the refFM panel.	84
Figure S6.4. Projections of modern Yakutian horses onto the refFM panel.....	84

Figure S6.5. Projections of non-Yakutian and non-Franches-Montagnes modern horses onto the refYAK panel.....	84
Figure S6.6. Projections of ancient horse genomes onto the refYAK panel.	85
Figure S6.7. PCA plot depicting the genetic affinities of ancient and modern horses, based on genotype calls.	86
Figure S6.8. PCA plot depicting the genetic affinities of ancient and modern horses, based on genotype likelihoods.	87
Figure S6.9. Admixture tests based on D-statistics and transversions.	90
Figure S6.10. Schematic illustration depicting the notation used to estimate f_3 -statistics values.....	91
Figure S6.11. TreeMix population splits between modern and ancient horses.	93
Figure S6.12. Admixture plot representing from $K=2$ to 20 ancestry components.	94
Figure S7.1. Illustrative examples of F_{ST} outlier regions identified by the “Region peaks” smoothing method (YAK-DOM).	103
Figure S7.2. Illustrative examples of F_{ST} outlier regions identified by the “Region-peaks” smoothing method (YAK-FM).	103
Figure S7.3. Relationship between protein-coding gene density and F_{ST} in 50Kb sliding windows.	104
Figure S7.4. Boxplot of the d_A estimates across different site categories, for the YAK-DOM population pair.....	106
Figure S7.5. Proportion of adaptive sites for each site category in the YAK-DOM population pair.	106

Section 1: Sample Information

1.1 Environmental conditions and inhabitants of Yakutia

Yakutia, or the Sakha Republic (Russia), is located at the most North-Eastern part of the Russian territory and shows very low population densities. Climatic conditions are extreme and represent the coldest region in the northern hemisphere, with winter temperature records sometimes below -70°C and almost half of the territory consisting of permafrozen soils. The population of Yakutia mainly consists of two human groups, the Russians and the Yakuts. The latter migrated in the region probably between the 13th-15th century (1, 2), leaving their native range in the south, supposedly in the Altai-Sayan and/or Baykal regions (3, 4). Present-day Yakuts constitute a semi-nomadic group specialized in animal husbandry, especially of horse and cattle (5).

Historically, Yakutian horses have represented the main branch of the economy of the Yakuts (6), providing meat, milk, transportation, as well as primary products for clothes (mainly hairs, tendons, and skins). Today, Yakutian horses are mostly exploited as sources of meat and milk, with most males being slaughtered at the end of their first autumn, but still represent an essential part of the Yakutian culture, as shown by the horse symbol featured on the national Yakutian flag.

1.2 Yakutian horses

In this study, we investigate the evolutionary history of Yakutian horses, the most northerly distributed domesticated horse breed in the planet (above the 70 North latitude line), which survive extremely cold conditions with minimal human attention. These horses live in the open air all year round, grazing on vegetation lying under deep snow cover for 7-8 months (6).

They show characteristic morphological traits likely reflecting their adaptation to the extreme climatic conditions of Yakutia, such as a long back, a coarse head, a straight neck, a deep and wide chest (7). They are massively built, with average height at withers not higher than 1.40 m and carry a rump generally higher than withers. Yakutian horses have short limbs and are extremely hairy with small hoof, ears and collar. The mane and tail are very thick and long, and the body hair is thick and long and can reach 10 cm in winter (7).

Yakutian horses also exhibit characteristic metabolic features. For example, during the extremely short period of vegetation growth (late May – late September), they can accumulate important fat reserves and regulate their own metabolic needs according to the seasonal conditions. They have lower winter metabolic levels than outbred horses (8), and show seasonality patterns in aspartate aminotransferase and alanine transaminase activities, which likely reflects the increased participation of carbohydrate metabolism in spring for supporting metabolism recovery, higher energy expenditure and fetal growth (9).

1.3 Sampling

Hair samples from nine Yakutian horses (Yak1 to Yak9) living in rural localities of Yakutia, were collected in 2001 by Pr. Juha Kantanen in the Eveno-Bytantaj District. Three additional hair samples (Horse1 to Horse3) from Yakutian horses were collected by Dr. Alexei Tikhonov in February 2012. These samples originate from three different regions (Kazachie village, in the lower course of the

Yana river; the Srednekolymsk district, in the middle course of the Kolyma river; and, the Betenkes village by the Adycha river, close to Verkhoyansk) and are considered to represent the descendants of the most ancient Yakutian breeds (**Table S1.1**).

We also sampled a series of nine ancient horse bones and teeth excavated in Yakutia, corresponding to specimens that lived prior to (~5,000-5,500 years Before Present, yBP) and after (~300 yBP) the arrival of the Yakuts in the area (**Table S1.2**). Samples pre-dating the Yakut settlement include two samples: sample “Yukagir” excavated at the “Yuka” site, on the southern coast of the Dmitry Laptev Strait (between Bolshoi Lyakhowski Island and mainland, Novosoborskie islands, Yakutia, Russia) in the Oyagossky Yar area, and radiocarbon-dated to $4,630 \pm 35$ uncalibrated yBP (GrA-540209), and sample “Batagai” excavated from the Batagai site, Verkhoyansk District, and radiocarbon-dated to $4,450 \pm 35$ uncalibrated yBP (Gr 50842). These dates correspond to 3,517-3,351 Before Christ (BC) and 2,939-3,337 BC, respectively, using the IntCal13 calibration in OxCal 4.2 online (<http://www.c14.arch.ox.ac.uk/oxcal.html>). Six of the samples post-dating the arrival of Yakuts (CGG101392, CGG101393, CGG101394, CGG101395, CGG101396, CGG101397) were presented in (10) and were dated ~200-300 years yBP. Sample ODJ6 was excavated from the Odjuluun site during the MAFSO 2006 expedition (French Archaeological Mission in Oriental Siberia) and was dated to ~250 yBP.

1.4 Supplementary Tables for Section 1

Table S1.1. Sample Information for the modern Yakutian horses analysed in this study.

Horse ID	Gender	Tissue type	Geographical coordinates	Region of Origin
Yak1	Male	Hair	68°11N, 131°41E	Kustur, Sakha Republic, Russia
Yak2	Female	Hair	68°11N, 131°41E	Kustur, Sakha Republic, Russia
Yak3	Female	Hair	68°11N, 131°41E	Kustur, Sakha Republic, Russia
Yak4	Male	Hair	68°11N, 131°41E	Kustur, Sakha Republic, Russia
Yak5	Female	Hair	68°11N, 131°41E	Kustur, Sakha Republic, Russia
Yak6	Female	Hair	67°47N, 130°24E	Batagay-Alyta, Sakha Republic, Russia
Yak7	Female	Hair	67°47N, 130°24E	Batagay-Alyta, Sakha Republic, Russia
Yak8	Male	Hair	67°47N, 130°24E	Batagay-Alyta, Sakha Republic, Russia
Yak9	Male	Hair	67°47N, 130°24E	Batagay-Alyta, Sakha Republic, Russia
Horse1	n/a	Hair	n/a	Kazachie village, Sakha Republic, Russia
Horse2	n/a	Hair	n/a	Srednekolymsk, Sakha Republic, Russia
Horse3	n/a	Hair	n/a	Betenkes, Sakha Republic, Russia

Table S1.2. Sample Information for the ancient Yakutian horses analysed in this study.

Horse ID	Tissue type	Age	Collection date	Site name and coordinates	Region of origin	Reference
Yukagir	Bone	4,630 ± 35 uncalibrated yBP	August 2012	Yuka: 72°42N, 142°50E	Verkhoyansk	This study
Batagai	Bone	4,450 ± 35 uncalibrated yBP	February 2012	Batagai: 67°34N, 134°46E	Verkhoyansk	This study
CGG101392	Tooth	19 th century AD	MAFSO 2012	OursSire2: 66°51N, 131°45.21E	Verkhoyansk	Der Sarkissian et al. 2014 (10)
CGG101393	Bone	18 th /19 th century AD	MAFSO 2011	Bakhtakh: 67°09N, 134°31.01E	Verkhoyansk	Der Sarkissian et al. 2014 (10)
CGG101394	Tooth	19 th century AD	MAFSO 2012	Yakutia: near 66°53N, 131°51E	Verkhoyansk	Der Sarkissian et al. 2014 (10)
CGG101395	Bone	18 th century AD	MAFSO 2012	Tysarastaak2: 66°54N, 131°50E	Verkhoyansk	Der Sarkissian et al. 2014 (10)
CGG101396	Tooth	19 th century AD	MAFSO 2010	Targana1: 66°59 N, 132°59E	Verkhoyansk	Der Sarkissian et al. 2014 (10)
CGG101397	Bone	19 th century AD	MAFSO 2012	Tumeski: 66°56N, 131°55E	Verkhoyansk	Der Sarkissian et al. 2014 (10)
ODJ6	Bone	First half of 18 th century AD	MAFSO 2006	Odjuluun: 61°52N, 132°24E	Central Yakutia	This study

“yBP”: years Before Present; “MAFSO”: Mission Archéologique Française en Sibérie Orientale led by Prof. Eric Crubézy.

2 Section 2: Genome sequencing

2.1 DNA extraction and library preparation for modern Yakutian horses

Genomic DNA from the nine modern Yakutian horse samples, Yak1 to Yak9, was extracted at the Institute of Veterinary Medicine and Animal Sciences (Estonian University of Life Sciences, Estonia). DNA extraction was performed on hair roots using Puregene® Genomic DNA Purification Kit (Gentra Systems. USA), following the manufacturer's protocol. Genomic DNA from three modern Yakutian horse samples, Horse1 to Horse3, was extracted at the Kurchatov Institute (Moscow, Russia) from hair root and shaft, using the methods described by Gilbert and colleagues (11), with the modifications from (12). More specifically, hair shafts were sliced into small pieces and digested at 55°C for 24 hours in 5ml of digestion buffer (10mM Tris, 10mM NaCl, 5mM CaCl, 2.5mM EDTA, 1% SDS, 10mb/ml DTT and 0.5mb/ml proteinase K). The digestion supernatant was recovered by spinning at 2,500g for 2 minutes and concentrated to 50-100 µL using 30KDa centricons. The final DNA extract was obtained following a terminal purification of MinElute columns (Qiagen).

Indexed Illumina DNA libraries were constructed from the Yak1-Yak9 DNA extracts at the Centre for GeoGenetics (University of Copenhagen, Denmark) in laboratory facilities dedicated to the molecular analysis of fresh DNA. Overall, we followed the procedure for constructing libraries by blunt-end ligation described in the Supplementary Information section 3.1.b.3 of (13) with slight modifications. Briefly, 1 µg of DNA extract was sheared with the Bioruptor (Diagenode) using 4 cycles of 15 seconds on high energy, and 90 seconds off. Sheared DNA extracts were then purified on MinElute columns (Qiagen) and eluted in 22 µL of EB. The whole eluted sheared DNA was used for library construction using the NEBNext Quick DNA Library Prep Master Mix Set for 454 (New England BioLabs, ref: #E60700), with the following modifications. We worked with 25 µL reaction volumes at each step and used a final concentration of 500 nM of Illumina multiplex blunt-end adapters. We used two different adapters that we prepared according to Meyer and Kircher (14). After the end-repair reaction, we used a MinElute PCR purification kit (Qiagen) with an elution in 16 µL EB buffer following a 10 min-incubation at 37°C. Ligation was then performed for 20 minutes at 20°C following a purification step in MinElute columns (Qiagen) with elution in 22 µL of buffer EB (10 min at 37°C). A final fill-in reaction step was performed at 37°C for 20 minutes adding 4 µL of Bst DNA polymerase enzyme mix to each library, consisting of 2.5 µL of adapter-fill in reaction buffer and 1.5 µL of Bst DNA polymerase. The Bst polymerase was then inactivated by incubation at 80°C for 20 min. DNA library were obtained in a final volume of 25 µL.

DNA libraries were then PCR-amplified in a final volume of 25 µL containing: 12.5 µL of DNA library, 1 µL Illumina inPE1.0 primer (25 µM, 5'-AAT GAT ACG GCG ACC ACC GAG ATC TAC ACT CTT TCC CTA CAC GAC GCT CTT CCG ATC T), 1 µL Multiplex Index Primer (25 µM, 5'-CAA GCA GAA GAC GGC ATA CGA GAT NNN NNN GTG ACT GGA GTT CAG ACG TGT GCT CTT CCG, where the N stretch corresponds to a 6 nucleotides index tag), 5 units of AmpliTaq Gold DNA polymerase (Life Technologies), 1x Gold Buffer, 25 mM MgCl₂, 1 mg/mL BSA, and 0.25 µM of each dNTP. PCR cycling conditions consisted of an initial denaturation and enzyme activation for 10 minutes at 92°C, followed by 9 cycles of 30 second denaturation at 92°C, 30 seconds annealing at 60°C and 30 second elongation at 72°C, and terminated by a final 7 minute elongation step at 72°C. The resultant amplified DNA fragments were then purified on MinElute columns (Qiagen), and eluted in 25 µL

of EB buffer. A blank library was built by replacing DNA samples with EB buffer to monitor contamination and a PCR blank was also included. All blanks were negative after library amplification.

For samples Horse1-Horse3, DNA libraries were prepared at the Kurchatov Institute (Moscow, Russia) using a NEBNext Quick DNA Library Prep Master Mix set for 454 (New England Biolabs), with adapter primers on an Illumina Sequencing Platform and following the manufacturer's instructions. DNA libraries were then PCR-amplified in a final volume of 50 µL containing: 15 µL of DNA library, 5 µL NEBNext®universal primer (10 µM 5'-AAT GAT ACG GCG ACC ACC GAG ATC TAC ACT CTT TCC CTA CAC GAC GCT CTT CCG ATC T-3'), 5 µL NEBNext® Multiplex Index Primer (10 µM, 5'-CAA GCA GAA GAC GGC ATA CGA GAT NNN NNN GTG ACT GGA GTT CAG ACG TGT GCT CTT CCG ATC T-3', where the N stretch corresponds to a 6 nucleotides index tag), 2x NEBNext® Q5® Hot Start HiFi PCR Master Mix (NEB) cycling conditions consisted of 3 minutes at 98°C, followed by 7 cycles of 30 seconds denaturation at 98°C and 75 seconds annealing/extension at 65°C, and terminated by a final 5 minute elongation step at 65°C. The resultant amplified DNA fragments were then purified with 45mkl AMPure XP Beads (Beckman Coulter), and eluted in 25 µL H2O. A blank library was built by replacing DNA samples with EB buffer to monitor contamination and a PCR blank was also included. All blanks were negative after library amplification. The purity and amount of DNA libraries were evaluated using a 2100 Bioanalyser (Agilent, USA) and HS Qubit (Invitrogen, USA).

2.2 *DNA extraction and library preparation for ancient horses from Yakutia*

We performed DNA extraction and library preparation from ancient bones and teeth at the ancient DNA facilities of the Centre for GeoGenetics, University of Copenhagen, Denmark, following strict procedures for limiting contamination by modern DNA. Importantly, those facilities are located in separate buildings (i.e., at about a five minute walking distance) from the post-PCR facilities, where DNA of the modern samples was handled.

For bones, the outer surface was first abraded to a depth of 1-2 mm and bone powder was generated drilling within the sample with a Dremel grinding tool, at low speed. For teeth, powder was obtained by drilling. Digestion of the samples was carried out in 5 mL of 0.5 M EDTA (pH 8.5), 0.1% N-lauryl-sarcosyl, and 1 mg/mL proteinase K (Invitrogen) at 37 °C for 24 hours under rotation. The supernatant was stored and a second digestion was performed on the pellets' leftover from the first digestion. The supernatant from this second digestion was then used for DNA extraction using the silica-based method described in (13) and (10), and the resulting DNA extract was further build into DNA libraries. For samples CGG101392 to CGG101397, the remaining fraction of the first digestion (hereafter referred to as 'simple digestion') was also fully extracted, and prepared into DNA libraries (see below).

For Batagai, a total of 4 indexed TruSeq Illumina DNA libraries were built using the procedure already described in (15) and (16). Briefly, End Repair reaction was performed on 16.5 µL of DNA extract using End-It™ DNA End-Repair Kit (Epicentre) with a first incubation at 4°C for 2 minutes followed by a second incubation at 37°C for 45 minutes. End-repaired DNA templates were then purified with MinElute columns (Qiagen), using 10 volumes of PN buffer (from QIAQuick, Qiagen) and 17.5 µL of Elution Buffer (EB, Qiagen). The whole purified volume was then used for Klenow exo-polyA-tailing (37°C for 30 minutes) and adapter ligation with standard

indexed TruSeq adapters. Each DNA library underwent a final purification with Ampure XP beads using 1.8:1 volume ratio between beads and DNA. Purified DNA was eluted in 20 µL of EB solution. Two libraries were then PCR amplified with AmpliTaq Gold DNA polymerase (Life Technologies), and the other two with Accuprime Pfx (Life Technologies). We amplified 7 µL of DNA library in a final PCR volume of 25 µL using 300 nM Illumina PCR primers (PCR primer 1.0: 5'-AAT GAT ACG GCG ACC ACC GAG ATC TAC ACT CTT TCC CTA CAC GA; PCR primer 2.0: 5'-CAA GCA GAA GAC GGC ATA CGA GAT), a concentration of 1mg/mL BSA, 1µM dXTP (Invitrogen) and 5U of Taq Gold or Accuprime Pfx. For Taq Gold, PCR cycling conditions consisted of a first DNA denaturation at 95 °C for 10 minutes, followed by 15 cycles of denaturation (95°C, 30 seconds), annealing (60°C, 30 seconds) and elongation (72°C, 60 seconds). A final elongation was performed at 72°C for 7 minutes before amplified DNA was purified into 25 µL EB with using Qiagen Minelute purification kit. For Accuprime Pfx, PCR cycling conditions consisted of a first DNA denaturation at 95 °C for 2 minutes, followed by 15 cycles of denaturation (95°C, 15 seconds), annealing (68°C, 30 seconds) and elongation (68°C, 40 seconds). A final elongation was performed at 68°C for 3 minutes before amplified DNA was purified into 25 µL EB with using Qiagen Minelute purification kit.

For sample Batagai, we also prepared one indexed Illumina DNA library based on blunt-end ligation, following the procedure described in (10) and in **section S2.1**, without prior DNA shearing and using PN buffer (from QIAQuick, Qiagen) instead of PB for MinElute (Qiagen) purification steps. The same type of DNA libraries was prepared for samples CGG101392 to CGG101397, ODJ6, and Yukagir, for which no other library types (e.g. TruSeq) were prepared. For samples CGG101392 to CGG101397, one library was built per extract fraction (i.e., following simple or double digestion) as described in (10). DNA libraries were amplified using the same conditions as in **section S2.1**, except that two rounds of amplification were performed as described in (17), with the number of PCR cycles varying from 10 to 12 and 500nM of adapters. We used the whole 25 µL of DNA libraries in the first amplification round, except for sample Batagai (7 µL).

DNA contamination from the laboratory and reagents was monitored through mock DNA extractions and mock library constructions carried out at the same time as for ancient samples. All blanks were negative after final amplification of the libraries.

Our implementation of DNA libraries from fossil remains is detailed in **Table S2.1**, including the amount of fossil material processed, the type/number of DNA libraries constructed, the type of DNA polymerase used, and the number of library amplification PCR cycles performed.

2.3 DNA Shotgun sequencing

Sequencing of the genomes from the modern Yakutian horses Yak1 to Yak9 and from all ancient Yakutian horses was performed at the Danish National High-Throughput DNA Sequencing Centre, Copenhagen, Denmark, where a total number of 9,684,698,721 sequencing reads were produced. DNA libraries were first inspected and quantified on an Agilent 2100 Bioanalyzer High Sensitivity DNA chip. Modern DNA libraries were mixed in different pools and paired-end sequenced (98 bp reads, PE) on Illumina HiSeq 2000/2500 platforms (**Table S2.2**).

The DNA libraries constructed on the three modern Yakutian horses Horse1, Horse2 and Horse3 were sequenced at the Kurtchatov Institute, Moscow, Russia, on the Illumina GAIIx platform, where a total number of 155,582,799 sequencing reads were generated (**Table S2.2**).

Ancient DNA libraries were sequenced in pools that did not include any of the DNA libraries built on modern samples. Additionally, DNA libraries from Batagai and CGG101397 were sequenced separately on Illumina MiSeq and HiSeq2000/2500 platforms, using both paired-end (PE) and single-end sequencing technologies (SE; **Table S2.3**). Library pools included DNA libraries that differed in their barcode sequence by a minimum edit distance of 2 bp. Casava (version 1.8.s, Illumina) was used for basecalling, applying 100% match to the expected index of each library. Reads failing the matching filter were removed before downstream analyses.

2.4 Comparative horse dataset

We compared the complete genomes of Yakutian horses, that we characterized here for the first time, to a panel comprising 32 present-day and ancient horse genomes, representing eleven horse breeds/populations (**Table S2.4**).

Twenty of these were characterized in (18) (European Nucleotide Archive Project number PRJEB10098) and belong to the following domesticated horse breeds: Franches-Montagnes (N=12), Morgan (N=1), American Quarter Horse (later also referred to as “Quarter”, N=4) and Standardbred (N=3). Domesticated horse genomes were generated from Illumina TruSeq v2 libraries sequenced using one lane (0.5 lane for the Std_M1009 individual) of 100-bp pair-ended (PE) Illumina HiSeq (v3 chemistry) at the Institute of Genetics of the University of Bern, Switzerland and at the University of Minnesota, USA.

Our comparative panel also included previously published data from seven present-day domesticated horses belonging to the six domesticated breeds (Thoroughbred, Arabian, Standardbred, Norwegian Fjord, Icelandic horses (13, 16), and Mongolian horses (19), as well as from three Przewalski's horses (13, 19). Sequence reads for the Mongolian and Przewalski's horses published in (19) were retrieved from the Sequence Read Archive (SRA). For Mng_D2628 we used runs with SRA accession numbers SRR1167052-3, SRR1167891, SRR1167892 (mate 1 reads only), and SRR1167093. For Mng_D2629, we used runs with accession numbers SRR1167108-10, and SRR1167893. For Prz_D2630 we used runs with accession numbers SRR1167030, SRR1167031 (mate 1 reads only), SRR1167045, SRR1167257, and SRR1167890. For Prz_D2631 we used runs with accession numbers SRR1167258, and SRR1167048-50.

The published data of two Late Pleistocene horses, pre-dating domestication, were also included in the comparative datasets. These horses, labelled CGG10022 and CGG10023, were excavated in the Taymyr peninsula, Russia, and dated to $42,692 \pm 891$ (UBA-16478) and $16,099 \pm 192$ calibrated years before present (yBP; UBA-16479), respectively (13, 16). This is equivalent to 39,851-41,633 BC and 13,957-14,341 BC.

2.5 Sequence read processing and alignment against reference genomes

The sequencing reads obtained from present-day and ancient Yakutian horses, as well as from all the horses in our comparative panel, were processed using the PALEOMIX pipeline (20) and following the procedure described in (16). Mapping results are reported in **Tables S2.5-2.6**. The sequencing data are available from the European Nucleotide Archive Project number PRJEB10854.

The three modern Yakutian horses Horse1, Horse2 and Horse3 were not sequenced at sufficient depth (i.e. their average depth-of-coverage was 0.34X, 0.21X and 0.13X, respectively) to enable their complete nuclear genome characterization. For

those samples, we thus restricted our analyses to their mitochondrial genome (sequenced at 69.63, 47.66 and 43.94X; see **section S5.1**).

Preliminary screening of libraries constructed from ancient Yakutian horse specimens showed that the Batagai and CGG101397 samples were characterized by endogenous contents compatible with the cost-effective sequencing of their complete genome (their final endogenous content estimates are provided in **Table S2.6** and respectively correspond to 38.22% and 45.39% of the reads sequenced and passing quality filters). These specimens were therefore whole-genome sequenced at relatively high coverage (18.29-20.25X). Two other ancient horses, Yukagir and ODJ6, showed lower endogenous content (0.93% and 9.46%; **Table S2.6**) and were not further sequenced. For these samples, we therefore restricted our analyses to their complete mitochondrial genomes (sequenced at 911.47 and 30.60X; see **section S5.1**). Likewise, specimens CGG101392 to CGG101396 were excluded from further horse genomic analyses, as they showed low endogenous content (**Table S2.6**). As their DNA libraries consisted of a majority of reads of exogenous origin (probably from micro-organisms), these were included in metagenomic analyses (see **section S3**).

Read length distributions were computed for all samples based on collapsed and non-collapsed PE reads. For non-collapsed PE reads, we only considered pairs of reads in which both mates were mapped to the same chromosome, to different strands, and where the mate mapped to the positive strand was located 5' to the mate mapped to the negative strand. Each collapsed read or pair of mates was counted once. To exclude extreme outliers (potentially) resulting from mis-alignments, we truncated the distribution at the 99.9th quantile. The distributions are shown in **Figures S2.1-2.2**.

A ca. 10-bp periodicity was observed for modern specimens Yak1 to Yak9, but was more pronounced for ancient specimens CGG101397 and Batagai. This pattern has been proposed by (15) as a nucleosome protection footprint, possibly resulting from apoptotic degradation of DNA in hair shafts (21) and *post-mortem* fragmentation in bones (15). This pattern is in line with previous observations for a series of other ancient samples, including the Palaeo-Saqqaq Eskimo (22), Mesolithic hunter-gatherers (23), Siberian and North mammoths (24) and Late Pleistocene horses (16).

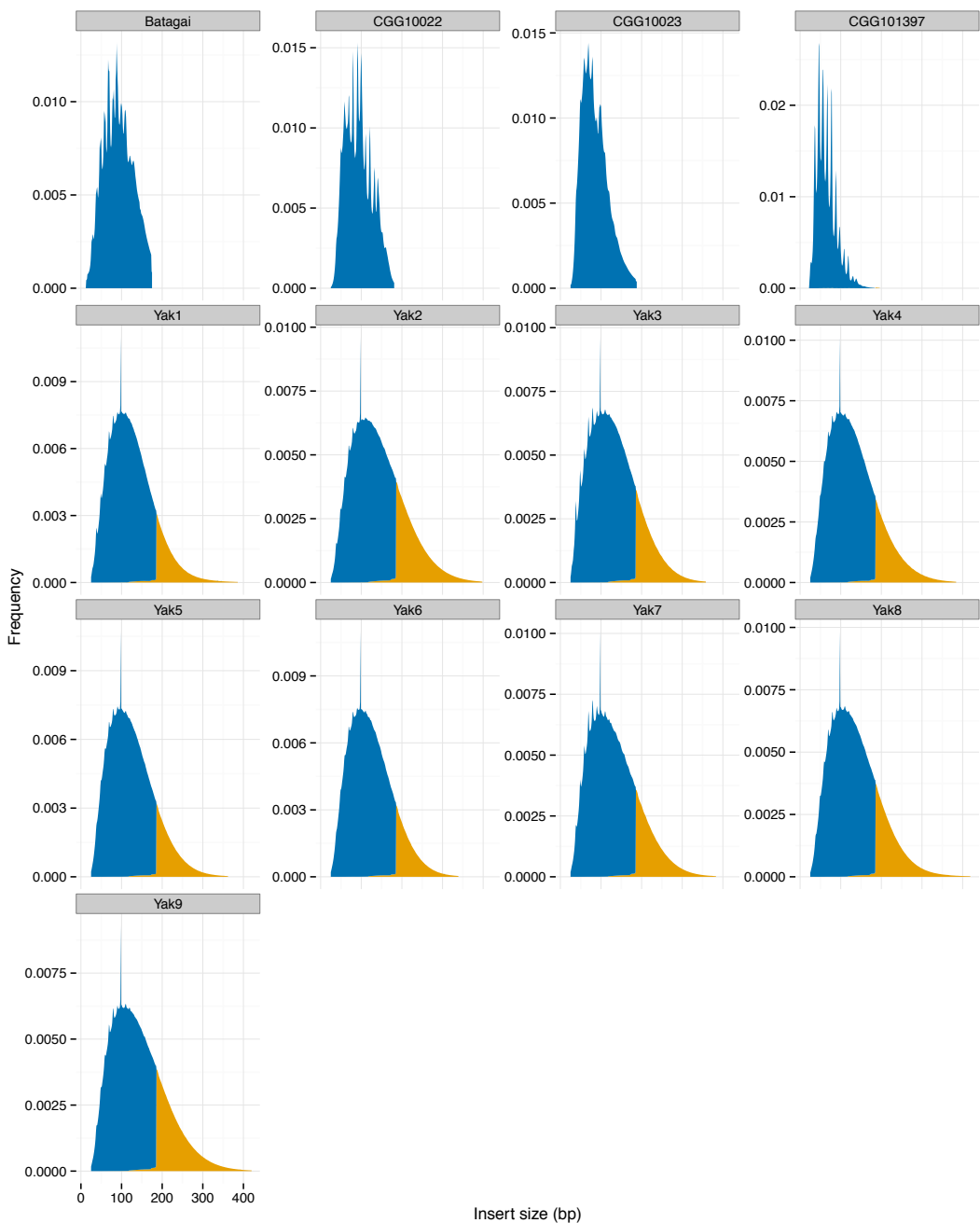


Figure S2.1. Size distribution of horse library inserts for the present-day and ancient Yakutian specimens.

Collapsed reads are indicated in blue. The physical distance covered between retained mate pairs is shown in yellow). The distribution of insert sizes observed for two Late Pleistocene horse genomes previously characterized, CGG10022 and CGG10023 (16), are shown for comparison.

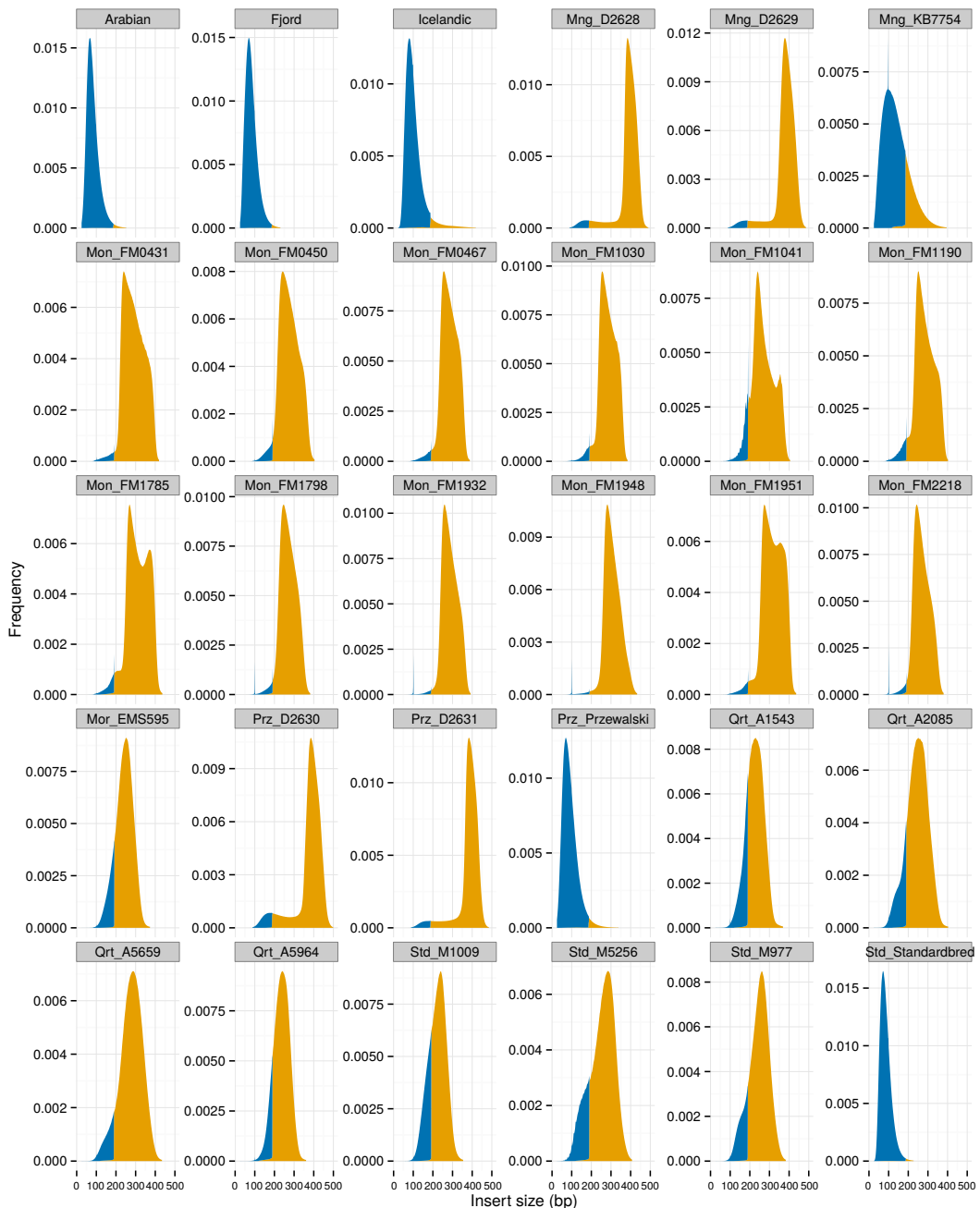


Figure S2.2. Size distribution of horse library inserts for the comparative dataset of modern horses.
The Arabian, Fjord, Icelandic, St_Standardbred, Thoroughbred (Twilight) and Prz_Przewalski genomes were characterized in (13); Mng_D2628, Mng_D2629, Prz_D2630 and Prz_D2631 were characterized in (19); the others were characterized in (18). See **Figure S2.1** for additional captions.

2.6 Characterizing and correcting the sequencing patterns of post-mortem damage of ancient samples

We assessed the presence of sequence patterns typical of *post-mortem* damage in each library generated from the ancient samples Batagai, CGG101397, Yukagir and ODJ6 in order to validate the authenticity of the data (25). This was achieved using the program mapDamage v2.02 (26) with default parameters.

Batagai showed expected nucleotide mis-incorporation signatures of *post-mortem* DNA damage, with increasing C→T substitution rates towards 5' read termini, and increasing complementary G→A substitution levels towards 3' read ends (**Figure S2.3A**). In addition, we observed an excess of purines at the genomic position preceding sequencing starts, in line with depurination driving *post-mortem* DNA fragmentation (**Figure S2.4A**). Similar patterns were observed in the sequence data underlying the genome of samples CGG101397, Yukagir and ODJ6. For CGG101397 and ODJ6 C→T and G→A mis-incorporation rates were more limited, most likely due to the younger age of the specimens (**Figures S2.3-2.6**). For sample ODJ6, we observed abnormally elevated error rates for all classes of mis-incorporations at the 7th and the 17th positions from the 3' end (**Figure S2.5A**). As these libraries were sequenced as part of the same sequencing run, this indicates a bias in the base call or in the sequencing at cycles 7 and 17. This, however, does not impact the accuracy of the complete mitochondrial genome sequence for ODJ6, as we estimated that these errors involve only 0.03% of the bases mapped, these errors being randomly distributed along the mitochondrial genome sequence obtained at 30.6X coverage. We also noticed elevated mis-incorporation rates in the last ~7 nucleotides sequenced for four of the DNA libraries of sample Batagai (**Figure S2.3A**). These are likely due to palindromic artifacts, previously observed in TruSeq DNA library data (27), which introduce, during library formation, copies of the sequence starts towards sequence ends, as long as native templates show some level of sequence complementarity.

In order to limit the impact of such palindromic artifacts and other types of nucleotide mis-incorporations in the downstream analyses of the Batagai and CGG101397 complete genomes, we trimmed low-quality regions from both read termini as described in **Table S2.7**. We also used a statistical model of DNA damage to rescale the quality scores of likely damaged positions. More specifically, approximate Bayesian estimation of damage parameters was first computed in mapDamage v2.02 (26) with default parameters for each library of both ancient samples. Resulting posterior distribution estimates of cytosine deamination rates at both double stranded regions (δ_d) and single stranded overhangs (δ_s), and the probabilities of reads not terminating in overhangs (λ) are shown in **Figure S2.7**. We then rerun mapDamage v2.02 for rescaling quality scores of likely damaged positions of each library using the per-library options, as shown in (**Table S2.7**), in addition to the parameter --seq-length=15, which was used to fit the model based on the first 15 bases at both 5' and 3' ends for all libraries. All subsequent analyses involving the nuclear genome sequences of the ancient horses Batagai and CGG101397 rely on the sequences post-trimming and rescaling.

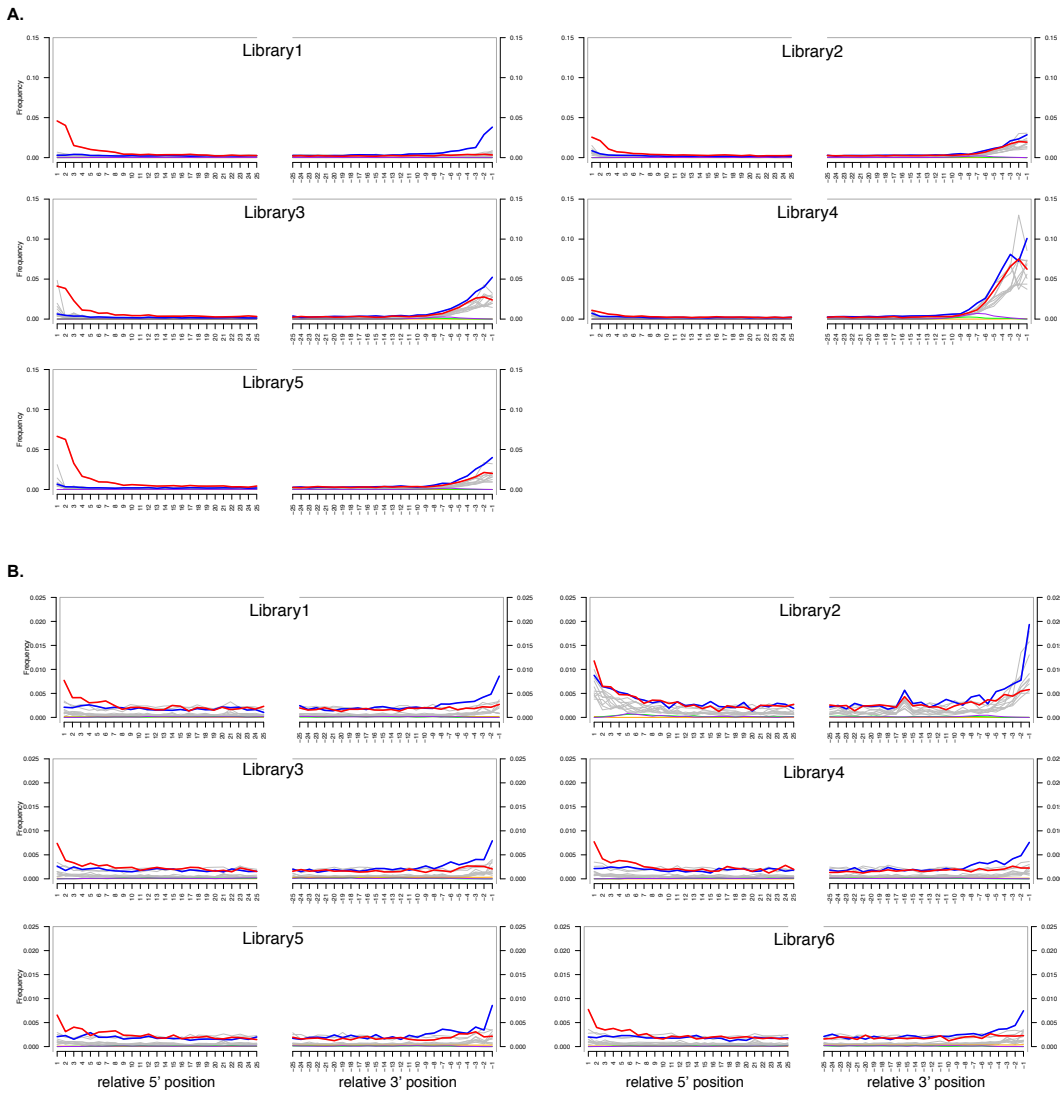
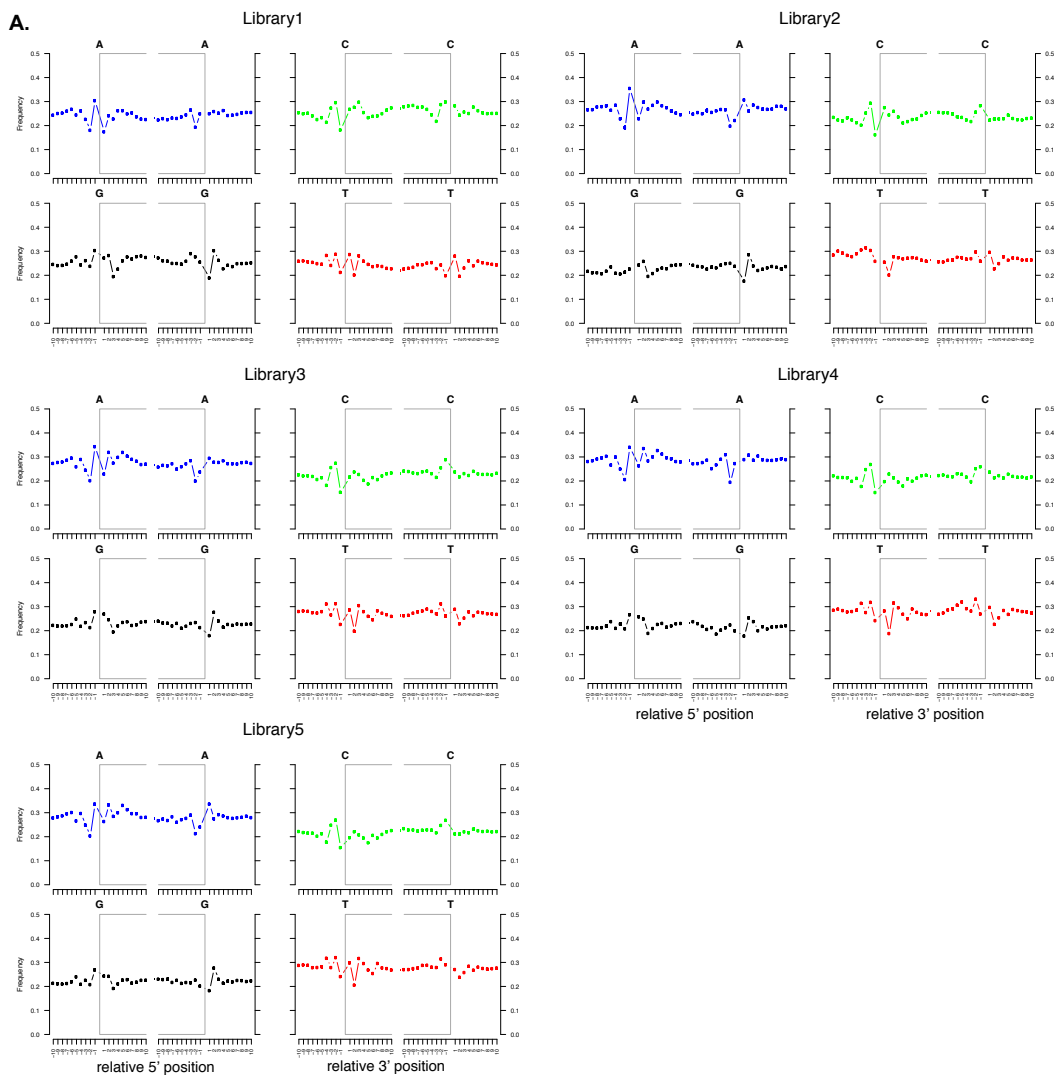


Figure S2.3. Nucleotide mis-incorporation patterns at 5'- and 3'- read termini for the ancient samples Batagai and CGG101397.

Nucleotide mis-incorporation patterns along the first and last 25 read positions obtained for the Batagai (A) and the CGG101397 (B) before trimming and rescaling. A. For Batagai, Library 1 is a blunt-ended library (New England Biolabs) amplified with AmpliTaq Gold DNA polymerase (Life Technologies), Library2, Library3 and Library5 are TruSeq libraries (Illumina) amplified with AmpliTaq Gold DNA polymerase, Library4 is a TruSeq library amplified with Accuprime Pfx (Life Technologies). B. For CGG101397, all libraries are blunt-ended libraries amplified with AmpliTaq Gold DNA polymerase. Mis-incorporation frequencies are shown for the first and the 25 nucleotides of the reads aligned to the horse reference nuclear genome EquCab2.0. The x-axis provides read positions relative to read starts (positive numbers) and/or read ends (negative numbers).



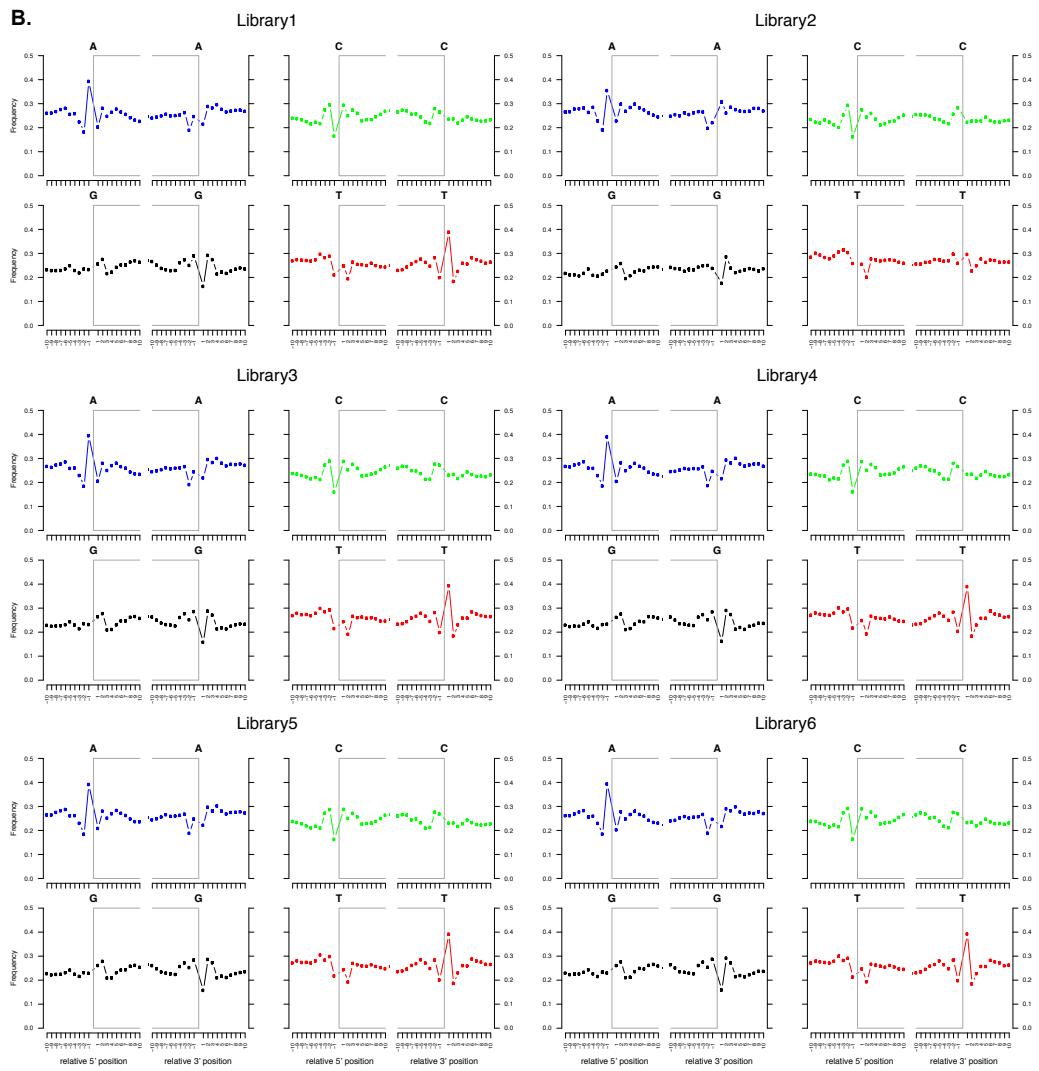


Figure S2.4. DNA fragmentation patterns at 5'- and 3'- read termini for ancient samples Batagai and CGG101397.

DNA fragmentation patterns obtained for the Batagai (A) and the CGG101397 (B) specimens before trimming and rescaling. DNA fragmentation is shown for reads aligned to the horse reference nuclear genome EquCab2.0: within 10 bp preceding read starts (positions -1 to -10 on the left panels of each base composition profile) and within the 10 bp following read ends (post-adapter and/or quality trimming; positions 1 to 10 on the right panels of each base composition profile). See **Figure S2.3** for additional captions.

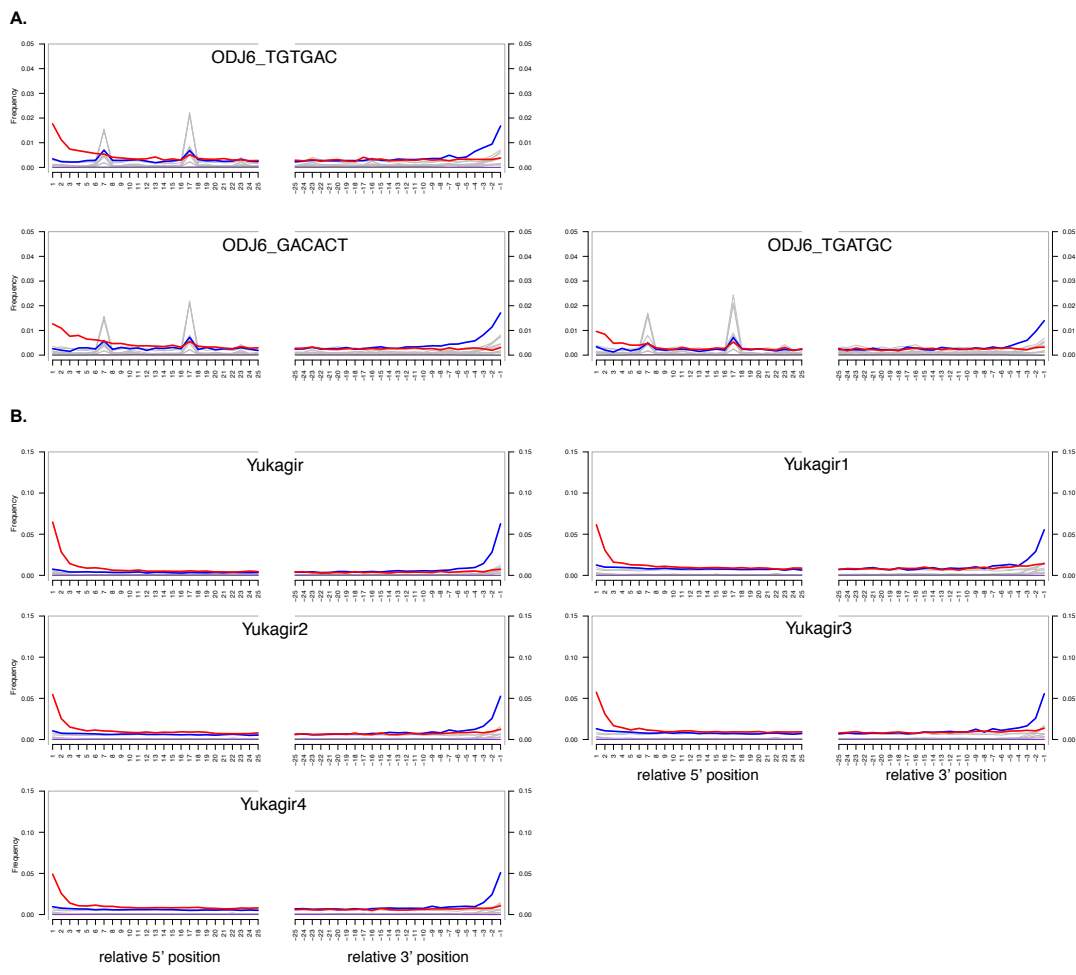
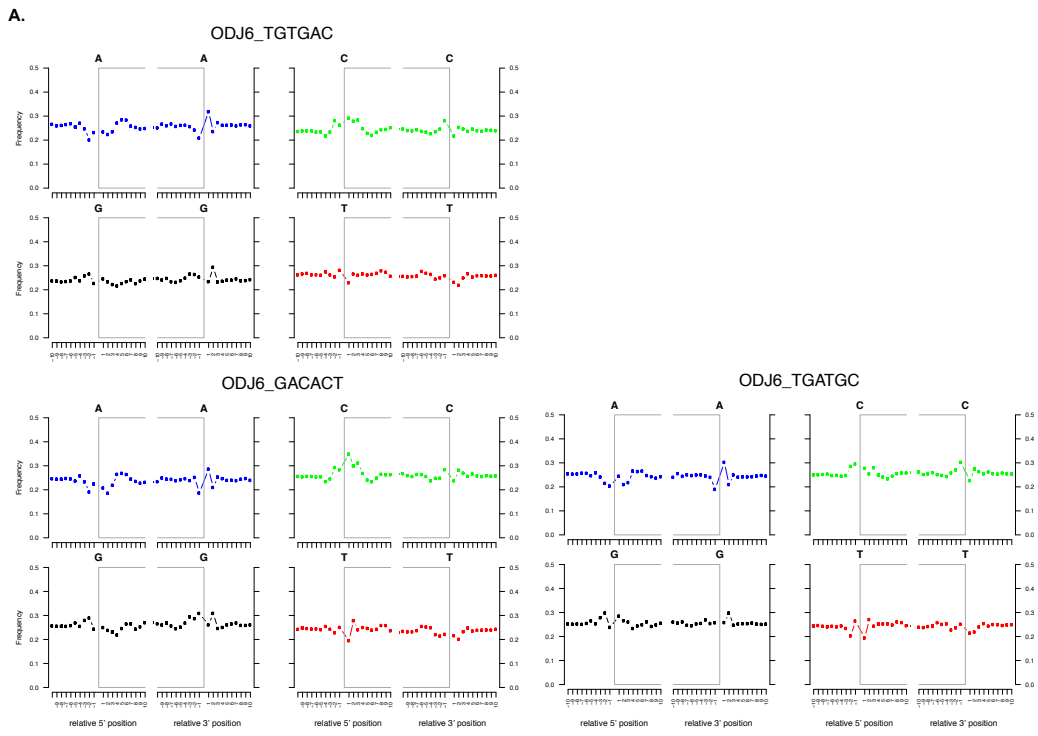


Figure S2.5. Nucleotide mis-incorporation patterns at 5'- and 3'- read termini for the ancient samples ODJ6 and Yukagir.

Nucleotide mis-incorporation patterns along the first and last 25 read positions obtained for the ODJ6 (A) and the Yukagir (B) specimens. All libraries are blunt-ended libraries (New England Biolabs) amplified with AmpliTaq Gold DNA polymerase (Life Technologies). See **Figure S2.3** for additional captions.



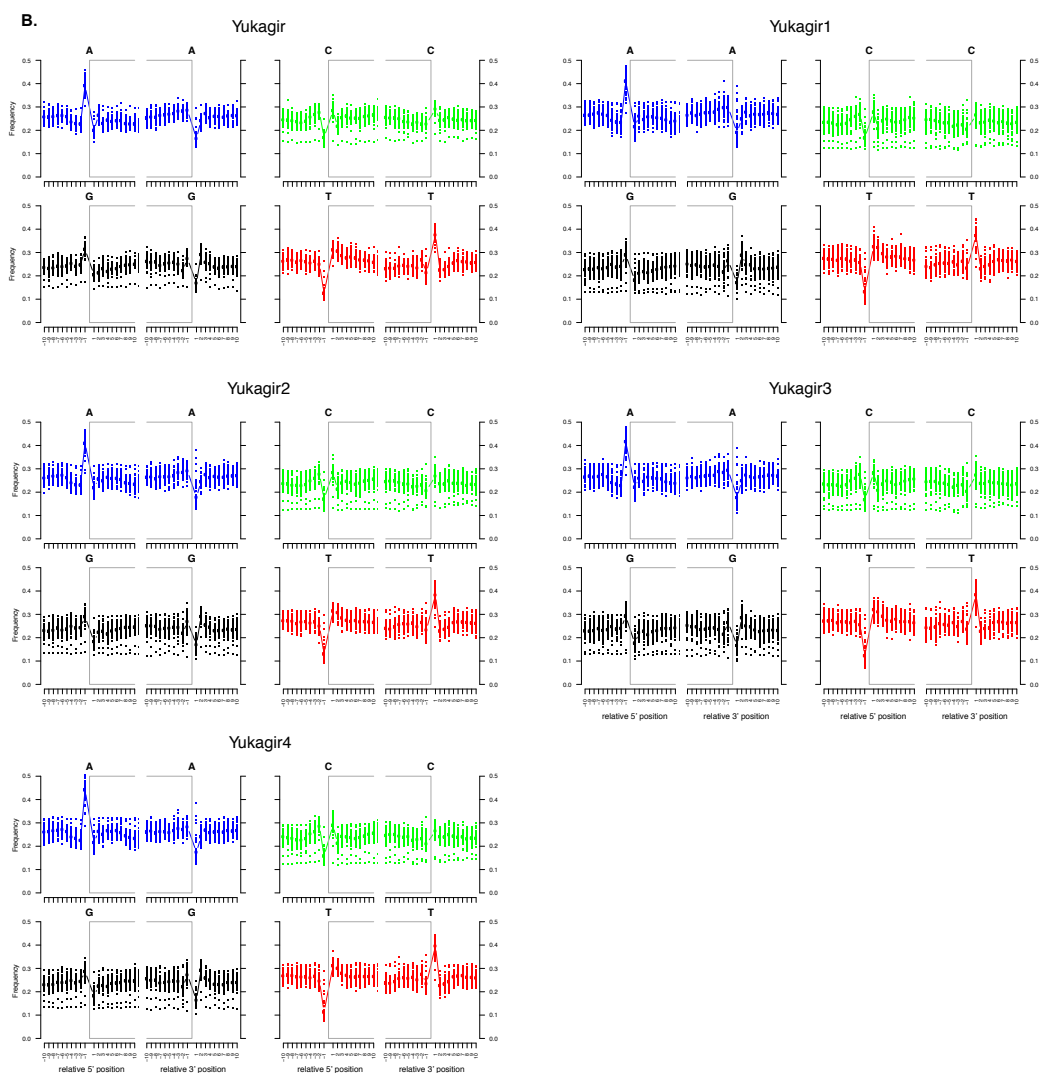


Figure S2.6. DNA fragmentation patterns at 5'- and 3'- read termini for the ancient samples ODJ6 and Yukagir.

DNA fragmentation patterns obtained for the ODJ6 (A) and the Yukagir (B) specimens. See **Figures S2.3 and S2.4** for additional captions.

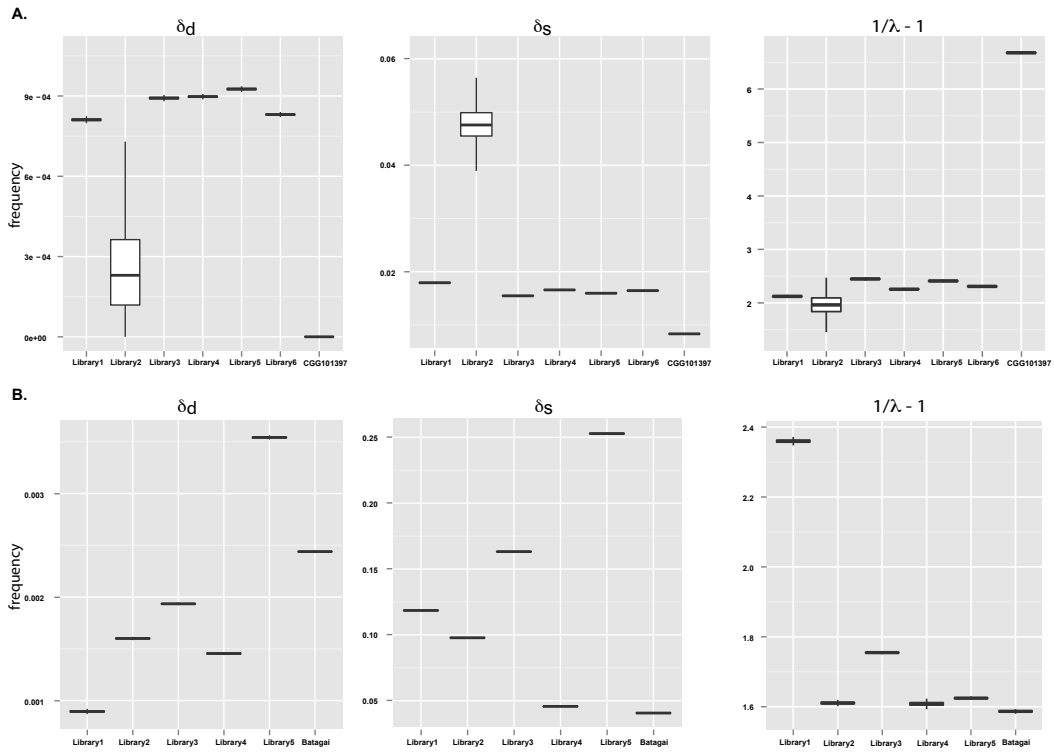


Figure S2.7. Posterior distributions estimated for three DNA damage parameters (δ_d , δ_s and $1/\lambda - 1$) for ancient samples Batagai and CGG101397.

“ δ_d ”, cytosine deamination rates at double stranded regions; “ δ_s ”, at single stranded overhangs (δ_s); “ λ ”, probability of reads not terminating in overhangs. Parameter distributions are shown on a per-library and a per-sample basis. A. CGG101397. B. Batagai. For clarity, λ is converted in a size estimate of average overhang length (in bp) using the following formula: $(1/\lambda - 1)$, following (13) and (16).

2.7 Sample-wise error rates

The sequencing error rate was estimated using a methodology similar to the one described in (28), and implemented in the Supplementary section S4.4 of (13). The method is based on the idea that genomes from the same species should have the same expected number of derived alleles when compared to an outgroup sequence. We used the high-quality genome of EquCab2.0 (Thoroughbred horse Twilight; (29)) as the prototype horse genome for comparison, and the genome of *Equus africanus somaliensis* (30) as the outgroup defining ancestral alleles. More specifically, let A_i and a_i be the true and observed number of ancestral alleles for a given sample i . We define D_i and d_i as the true and observed number of derived alleles present in the same genome. Under the assumption that the genomes are phylogenetically equidistant from the outgroup, and given an error rate ε_i the expected number of derived allele is:

$$E [d_i] = d_i (1 - \varepsilon_i) + A_i \varepsilon_i \approx d_i(1 - \varepsilon_i) + a_i \varepsilon_i$$

Under the assumption that the reference high-quality genome j contains no error such as that the estimates of A_j and D_j are equal to a_j and d_j , respectively, an estimate of the overall error rate can then be obtained as

$$\varepsilon_i = (d_i - d_j) / (a_j - d_j)$$

Here, the high-quality genome j is represented by the Illumina sequencing data generated by Orlando and colleagues (13) for the individual Twilight, which underpins the EquCab2.0 reference genome. Error rates for each substitution category are estimated on a maximum likelihood framework summing over the true state of the allele in the sequenced genome, as described in (13). We estimated the sequencing error rates for each sequenced genome with and without stringent quality filtering (minimal mapping quality, mapQ, of 30 and minimal base quality, baseQ, of 20). For both the high-quality horse and outgroup genomes, we considered Phred-mapping score mapQ>35 and Phred-base quality score baseQ>25 in order to match the expectations of high-quality data.

For unfiltered data, we observed very low average sequencing error rate for the genomes of modern Yakutian horses, spanning 0.14%-0.18% errors per base, for samples Yak5 and Yak2, respectively (**Figure S2.8**). The per-base error rate of the genomes newly characterized in our comparative panel (18) was on average equal to 0.25% and ranged from 0.17% (sample Mon_FM0450) to 0.44% (sample Mon_FM1948). In absence of quality filtering, the genome of the sample CGG101397 showed an overall error rate similar to that of modern individuals (0.09%, **Figure S2.8**). The per-base error rate of sample Batagai was found to be larger, and equal to 0.23%, reminiscent of the quality estimated within our comparative genome panel (**Figure S2.8**). Importantly, error rates were particularly increased for G→A and C→T base substitutions within the most ancient sample Batagai (0.14% each). Those substitution types are known to correspond to nucleotide mis-incorporations at cytosine residues that have been deaminated into uracil residues post-mortem (25) (see also **section S2.6**).

We also calculated sequencing error rates after quality filtering (baseQ≥20 and mapQ≥30) and we estimated overall average error rate per base to range from 0.04% (Yak6) to 0.07% (Batagai). We found remarkably low sequencing error rates (<0.01% to 0.09%) across all substitution types (**Figure S2.9**). The highest error rates were again observed for G→A and C→T base substitutions for the ancient genome of sample Batagai (0.05% each) and the modern genomes of the Yak2 and Yak3 horses (0.09% each for both), most likely due to significant cytosine deamination levels in the hair tissues analysed for these samples (**Figure S2.9**).

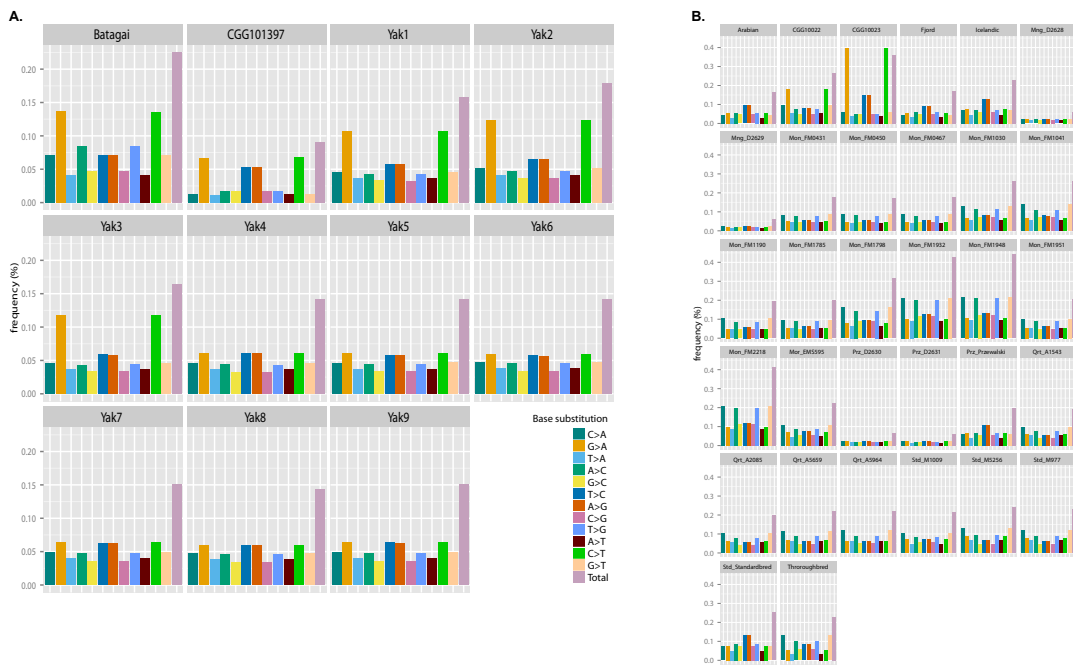


Figure S2.8. Estimated error rates for ancient and present-day horse genomes without quality filtering.

A. Ancient and present-day horse genomes characterized in this study. B. Ancient and present-day horse genomes of the comparative panel. Error rates are provided for each substitution type and across all substitution types (“Total”). “High-quality genome” = EquCab2.0; outgroup genome = *Equus asinus somaliensis*, both filtered to keep bases with mapping scores >35 and base-quality scores >25.

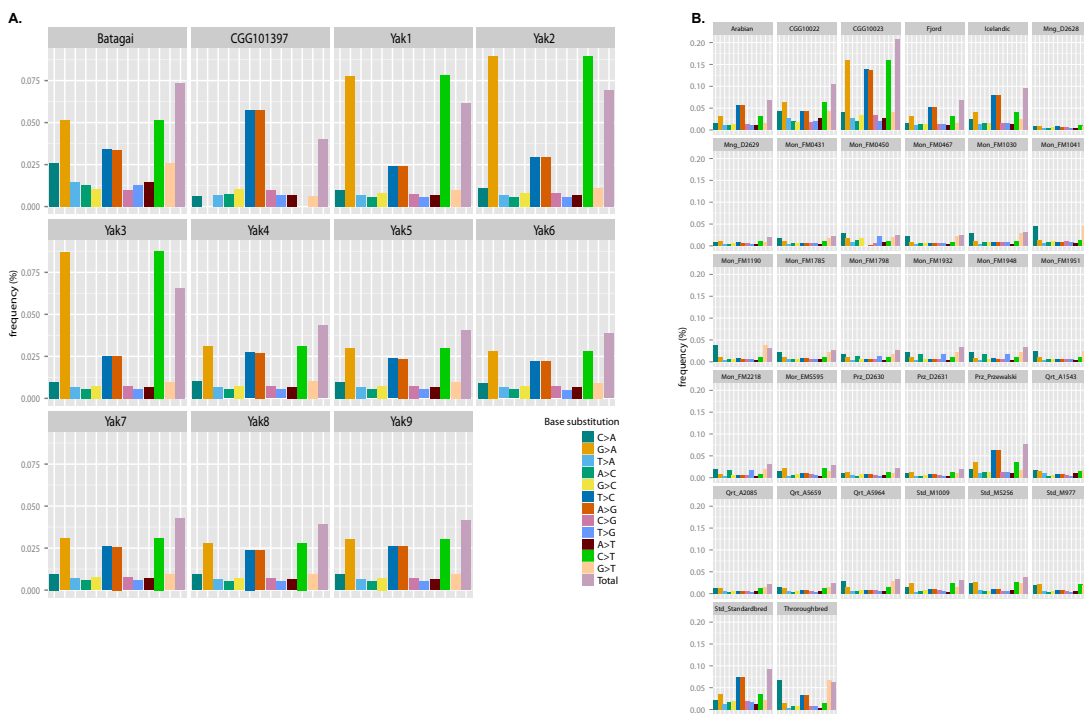


Figure S2.9. Estimated error rates for ancient and present-day horse genomes with quality filtering (mapQ \geq 30, baseQ \geq 20).

A. Ancient and present-day horse genomes characterized in this study. B. Ancient and present-day horse genomes of the comparative panel. See **Figure S2.8** for additional captions.

2.8 Supplementary Tables for Section 2

Table S2.1. Ancient DNA extraction and library information.

Horse ID	Tissue type	Powder used (mg)	Library	Library type	Polymerase	PCR cycles
Yukagir	Bone	348	Yukagir	BE	TG	12+10
			Yukagir1	BE	TG	12+10
			Yukagir2	BE	TG	12+10
			Yukagir3	BE	TG	12+10
			Yukagir4	BE	TG	12+10
Batagai	Bone	225	Library1	BE	TG	12+10
			Library2	TS	TG	15
			Library3	TS	TG	15
			Library4	TS	AP	15
			Library5	TS	TG	15
CGG101392	Tooth	605	CGG101392	BE	TG	12+10
			CGG101392R	BE	TG	12+10
CGG101393	Bone	673	CGG101393AR	BE	TG	12+10
			CGG101393B	BE	TG	12+10
		263	CGG101393BR	BE	TG	12+10
CGG101394	Tooth	482	CGG101394	BE	TG	12+10
			CGG101394R	BE	TG	12+10
CGG101395	Bone	326	CGG101395	BE	TG	12+10
			B CGG101395R	BE	TG	12+10
CGG101396	Tooth	361	CGG101396	BE	TG	12+10
			CGG101396R	BE	TG	12+10
CGG101397	Bone	727	Library1 (TuRE\$)	BE	TG	12+10
			Library2 (Tu\$)	BE	TG	12+10
			Library3	BE	TG	12+10
			Library4	BE	TG	12+10
			Library5	BE	TG	12+10
			Library6	BE	TG	12+10
ODJ6	Bone	241	TGTGAC	BE	TG	10+10
			TGATGC	BE	TG	10+10
			GACACT	BE	TG	10+10

“BE”: Blunt-Ended library (New England Biolabs); “TS”: TruSeq library (Illumina); “TG”: AmpliTaq Gold DNA polymerase (Life Technologies); “AG”: Accuprime Pfx (Life Technologies). When two amplification rounds were performed, the number of PCR cycles used in the first and second rounds are indicated prior and following the + sign, respectively. \$: labels from (10).

Table S2.2. Sequencing information for the present-day Yakutian horses.

Horse ID	Library	Sequencing Run	Number of raw reads	Number of retained reads	Number of collapsed pairs
Yak1	Yak1_1	98PE	515,474,672	286,081,689	225,881,271
	Yak1_2	98PE	63,444,452	41,497,687	21,671,067
	Total	98PE	578,919,124	327,579,376	247,552,338
Yak2	Yak2_1	98PE	891,452,624	541,301,679	343,163,472
	Yak2_2	98PE	49,195,198	31,384,438	17,622,213
	Total	98PE	940,647,822	572,686,117	360,785,685
Yak3	Yak3_1	98PE	516,321,776	299,198,159	213,417,404
	Yak3_2	98PE	56,254,278	35,359,754	20,654,528
	Total	98PE	572,576,054	334,557,913	234,071,932
Yak4	Yak4_1	98PE	430,886,056	249,367,905	178,365,934
	Yak4_2	98PE	58,496,056	37,195,922	21,057,224
	Total	98PE	489,382,112	286,563,827	199,423,158
Yak5	Yak5_1	98PE	530,254,434	299,574,265	226,771,443
	Yak5_2	98PE	49,402,642	31,394,424	17,788,042
	Total	98PE	579,657,076	330,968,689	244,559,485
Yak6	Yak6_1	98PE	587,021,086	331,444,133	251,436,596
	Yak6_2	98PE	43,036,440	26,425,349	16,437,552
	Total	98PE	630,057,526	357,869,482	267,874,148
Yak7	Yak7_1	98PE	1,153,069,686	676,648,042	467,572,888
	Yak7_2	98PE	22,598,580	15,139,546	7,352,490
	Total	98PE	1,175,668,266	691,787,588	474,925,378
Yak8	Yak8_1	98PE	440,059,126	258,885,881	178,074,119
	Yak8_2	98PE	38,375,780	26,238,927	11,975,400
	Total	98PE	478,434,906	285,124,808	190,049,519
Yak9	Yak9_1	98PE	458,586,934	279,105,845	175,926,495
	Yak9_2	98PE	30,194,094	20,356,673	9,705,442
	Total	98PE	488,781,028	299,462,518	185,631,937
Horse1	Library1	50SE/98SE	33,495,082	14,752,467	n/a
	Library2	50SE/98SE	19,533,897	7,518,876	n/a
	Library3	50SE/98SE	70,896,686	66,503,514	n/a
	Total	50SE	123,925,665	88,774,857	n/a
Horse2	Library4	50SE	21,980,216	20,782,070	n/a
Horse3	Library4	98SE	9,676,918	9,379,056	n/a

“Number of retained reads”: number of sequencing reads retained after adapter removal; “Number of collapsed pairs”: number of overlapping read pairs collapsed into a single sequence; “98PE”: 98 bp pair-ended sequencing reads (PE); “50SE/98SE”: 50/98 bp single-ended reads.

Table S2.3. Sequencing information for the ancient horses from Yakutia.

Horse ID	Library	Sequencing Run	Number of PE reads	Number of SE reads	Number of retained reads (PE and SE)	Number of collapsed pairs
Yukagir	Yukagir	94SE	n/a	48,101,535	47,813,678	n/a
	Yukagir1	94SE	n/a	4,866,139	4,711,842	n/a
	Yukagir2	94SE	n/a	7,560,056	7,255,501	n/a
	Yukagir3	94SE	n/a	4,394,290	4,319,878	n/a
	Yukagir4	94SE	n/a	6,237,908	6,113,260	n/a
	Total		n/a	71,159,928	70,214,159	n/a
Batagai	Library1	94SE	n/a	60,936,512	60,624,116	n/a
	Library2	94SE	n/a	262,457,296	218,190,094	n/a
	Library3	51SE, 94SE, 98PE	615,757,748	300,147,502	562,609,645	216,372,041
	Library4	51SE, 94SE, 98PE	874,262,382	31,595,163	397,541,599	254,737,837
	Library5	94SE, 98PE	44,142,598	278,586,185	232,218,000	15,226,633
	Total		1,534,162,728	933,722,658	1,471,183,454	486,336,511
CGG101392	CGG101392	94SE	n/a	12,545,745	12,393,476	n/a
	CGG101392R	94SE	n/a	16,379,222	10,871,116	n/a
	Total		n/a	28,924,967	23,264,592	n/a
CGG101393	CGG101393AR	94SE	n/a	18,302,900	11,862,758	n/a
	CGG101393B	94SE	n/a	10,401,702	9,491,647	n/a
	CGG101393BR	94SE	n/a	9,849,670	8,969,882	n/a
	Total		n/a	38,554,272	30,324,287	n/a
CGG101394	CGG101394	94SE	n/a	8,645,215	8,531,157	n/a
	CGG101394R	94SE	n/a	7,267,126	7,033,095	n/a
	Total		n/a	15,912,341	15,564,252	n/a
CGG101395	CGG101395	94SE	n/a	11,693,072	11,259,928	n/a
	B_CGG101395R	94SE	n/a	12,187,372	12,023,328	n/a
	Total		n/a	23,880,444	23,283,256	n/a
CGG101396	CGG101396	94SE	n/a	12,009,410	11,709,424	n/a
	CGG101396R	94SE	n/a	29,418,042	12,384,464	n/a
	Total		n/a	41,427,452	24,093,888	n/a
CGG101397	Library1	51SE, 98PE	322,207,922	1,998,389	162,988,335	158,261,243
	Library2	51SE	n/a	642,694	565,437	n/a
	Library3	51SE, 98PE	614,836,976	2,030,628	309,052,534	304,207,048
	Library4	51SE, 98PE	806,664,104	1,629,180	404,510,458	399,065,920
	Library5	51SE, 98PE	761,335,186	1,729,611	382,214,058	376,946,693
	Library6	51SE, 98PE	875,205,176	1,157,255	436,691,907	430,865,890
	Total		3,380,249,364	9,187,757	1,696,022,729	1,669,346,794
ODJ6	TGTGAC	94SE	n/a	17,507,548	17,669,585	n/a
	TGATGC	94SE	n/a	20,127,349	20,216,200	n/a
	GACACT	94SE	n/a	92,964,045	93,269,115	n/a
	Total		n/a	130,598,942	131,154,900	n/a

“Number of retained reads”: number of sequencing reads retained after adapter removal; “Number of collapsed pairs”: number of overlapping read pairs collapsed into a single sequence; “PE”: pair-ended; “SE”: single-ended.

Table S2.4. Genome characteristics for the ancient and present-day horses of the comparative panel.

Horse ID	Breed	Gender	Reference	# Mapped	Cov. (X)
Mon_FM1798	Franches-Montagnes	M	Der Sarkissian et al. 2015 (18)	42,505,483	22.62
Mon_FM1932	Franches-Montagnes	M	Der Sarkissian et al. 2015 (18)	20,527,420	10.82
Mon_FM1948	Franches-Montagnes	M	Der Sarkissian et al. 2015 (18)	16,600,211	8.72
Mon_FM2218	Franches-Montagnes	M	Der Sarkissian et al. 2015 (18)	22,771,087	12.05
Mon_FM1190	Franches-Montagnes	M	Der Sarkissian et al. 2015 (18)	30,749,884	16.37
Mon_FM1041	Franches-Montagnes	M	Der Sarkissian et al. 2015 (18)	14,695,522	7.96
Mon_FM1951	Franches-Montagnes	M	Der Sarkissian et al. 2015 (18)	36,627,376	19.24
Mon_FM0467	Franches-Montagnes	M	Der Sarkissian et al. 2015 (18)	28,836,871	15.29
Mon_FM_431	Franches-Montagnes	M	Der Sarkissian et al. 2015 (18)	21,988,334	11.62
Mon_FM1785	Franches-Montagnes	M	Der Sarkissian et al. 2015 (18)	28,230,241	14.89
Mon_FM1030	Franches-Montagnes	M	Der Sarkissian et al. 2015 (18)	32,187,975	17.02
Mon_FM0450	Franches-Montagnes	M	Der Sarkissian et al. 2015 (18)	29,840,675	16.15
Mor_EMS595	Morgan	F	Der Sarkissian et al. 2015 (18)	25,216,660	14.02
Qrt_A5964	American Quarter Horse	F	Der Sarkissian et al. 2015 (18)	25,565,430	13.97
Qrt_A5659	American Quarter Horse	F	Der Sarkissian et al. 2015 (18)	25,576,377	13.67
Qrt_A1543	American Quarter Horse	F	Der Sarkissian et al. 2015 (18)	22,265,239	12.55
Qrt_A2085	American Quarter Horse	M	Der Sarkissian et al. 2015 (18)	22,456,409	12.32
Std_M977	Standardbred	F	Der Sarkissian et al. 2015 (18)	22,685,006	12.35
Std_M5256	Standardbred	M	Der Sarkissian et al. 2015 (18)	20,975,678	11.44
Std_M1009	Standardbred	M	Der Sarkissian et al. 2015 (18)	13,252,954	7.68
Std_Standardbred	Standardbred	M	Orlando et al. 2013; Schubert et al. 2014 (13, 16)	27,145,773	12.31
Mng_D2629	Mongolian	F	Do et al. 2014 (19)	44,899,823	24.09
Mng_D2628	Mongolian	M	Do et al. 2014 (19)	43,833,220	23.54
Fjord	Norwegian Fjord	F	Orlando et al. 2013; Schubert et al. 2014 (13, 16)	17,734,587	7.73
Icelandic	Icelandic	M	Orlando et al. 2013; Schubert et al. 2014 (13, 16)	16,814,503	8.51
Arabian	Arabian	F	Orlando et al. 2013; Schubert et al. 2014 (13, 16)	24,648,073	10.82
Thoroughbred	Thoroughbred	F	Wade et al. 2009 (29)	74,144,230	41.14
Prz_D2630	Przewalski	M	Do et al. 2014 (19)	31,465,668	16.91
Prz_D2631	Przewalski	F	Do et al. 2014 (19)	47,061,560	25.25
Prz_Przewalski	Przewalski	M	Orlando et al. 2013; Schubert et al. 2014 (13, 16)	20,310,866	9.65
CGG10022	Late Pleistocene	F	Orlando et al. 2013; Schubert et al. 2014 (13, 16)	53,947,568	25.60
CGG10023	Late Pleistocene	M	Schubert et al. 2014 (16)	18,032,105	7.72

“F”: Female; “M”: Male; “#Mapped”: number of sequencing reads mapping uniquely and with high confidence (mapping quality mapQ \geq 25).
 “Cov.”: genome coverage.

Table S2.5. Mapping results for present-day Yakutian horses.

Horse ID	Library			Mapped reads ^a		Coverage (X)	
		%end.	%clon.	Nuclear genome	Mitochondrial genome	Nuclear genome	Mitochondrial genome
Yak1	Yak1_1	75.22	2.82	215,185,844	168,417	9.19	1,044.85
	Yak1_2	75.09	7.59	31,158,714	21,245	1.32	132.83
	Total	75.20	3.45	246,344,558	189,662	10.52	1,177.67
Yak2	Yak2_1	74.45	6.47	403,013,210	231,724	17.37	1,470.14
	Yak2_2	75.19	7.50	23,598,996	13,693	1.01	85.76
	Total	74.49	6.53	426,612,206	245,417	18.38	1,555.91
Yak3	Yak3_1	74.79	3.22	223,770,293	155,116	9.54	965.51
	Yak3_2	73.74	7.24	26,074,838	17,190	1.11	106.46
	Total	74.68	3.65	249,845,131	172,306	10.65	1,071.97
Yak4	Yak4_1	74.27	3.47	185,197,680	154,190	7.91	976.88
	Yak4_2	73.26	7.76	27,249,122	22,023	1.16	139.33
	Total	74.14	4.04	212,446,802	176,213	9.07	1,116.20
Yak5	Yak5_1	75.18	2.82	225,218,752	217,060	9.53	1,372.03
	Yak5_2	74.60	7.25	23,421,400	21,955	0.99	138.18
	Total	75.12	3.26	248,640,152	239,015	10.52	1,510.21
Yak6	Yak6_1	76.38	3.02	253,152,852	220,636	10.79	1,404.27
	Yak6_2	75.24	7.01	19,881,239	17,349	0.85	110.31
	Total	76.29	3.32	273,034,091	237,985	11.64	1,514.58
Yak7	Yak7_1	73.59	5.11	497,929,694	496,523	21.16	3,158.80
	Yak7_2	74.53	8.46	11,282,826	10,973	0.47	68.58
	Total	73.61	5.19	509,212,520	507,496	21.63	3,227.38
Yak8	Yak8_1	77.41	2.48	200,394,370	172,475	8.64	1,106.54
	Yak8_2	75.99	8.46	19,938,048	15,680	0.84	98.74
	Total	77.28	3.05	220,332,418	188,155	9.48	1,205.28
Yak9	Yak9_1	77.06	3.17	215,068,521	196,393	9.21	1,254.99
	Yak9_2	75.45	8.20	15,359,392	13,557	0.65	85.12
	Total	76.95	3.52	230,427,913	209,950	9.85	1,340.11
Horse1	Library1	35.40	2.70	5,222,589	6,919	0.11	25.69
	Library2	46.19	1.36	3,472,669	3,815	0.09	16.05
	Library3	10.83	79.28	7,204,071	9,762	0.13	27.89
Horse2	Total	17.91	63.58	15,899,329	20,496	0.34	69.63
	Library4	50.53	3.43	10,500,497	16,170	0.21	47.66
Horse3	Library4	38.87	9.13	3,645,791	8002	0.13	43.94

^asequencing reads mapping uniquely and with high confidence (mapping quality MQ≥ 25); “%end.”: percentage of endogenous DNA calculated as 100 * Number of Mapped Reads (uniquely and with high confidence) / Number of Retained Reads (after trimming for adapters and low-quality ends); “%clon.”: percentage of reads that were PCR duplicates; %end. and %clon. were calculated considering reads mapping to the nuclear or the mitochondrial horse genomes separately.

Table S2.6. Mapping results for the ancient horses from Yakutia.

Horse ID	Library	Mapped reads ^a		Coverage (X)			
		%end.	%clon.	Nuclear genome	Mitochondrial genome	Nuclear genome ^a	X-chromosome
Yukagir	Yukagir	0.72	89.21	344,200	-	9.08x10 ⁻³	-
	Yukagir1	1.34	81.33	63,295	32,871	1.87x10 ⁻³	-
	Yukagir2	1.26	84.03	91,508	32,427	2.61x10 ⁻³	-
	Yukagir3	1.48	80.33	63,745	32,626	1.86x10 ⁻³	-
	Yukagir4	1.51	82.95	92,345	32,424	2.68x10 ⁻³	-
	Total	0.93	86.81	655,093	162,838	1.81x10⁻²	-
Batagai ^b	Library1	31.34	7.77	19,001,067	-	2,591	0.54
	Library2	50.16	3.93	109,449,139	-	13,985	3.38
	Library3	35.47	3.20	199,575,502	-	33,838	6.69
	Library4	30.48	4.27	121,150,831	-	21,837	4.28
	Library5	48.70	6.32	113,095,345	-	15,991	3.4
	Total	38.22	4.37	562,271,884	88,242	18.29	8.87
CGG101392	CGG101392	0.19	1.24	23,783	-	45	5.89x10 ⁻⁴
	CGG101392R	0.36	22.95	39,409	-	81	1.00x10 ⁻³
	Total	0.27	16.00	63,192	126	1.59x10⁻³	0.50
CGG101393	CGG101393AR	2.42	4.46	286,689	-	279	8.77x10 ⁻³
	CGG101393B	0.56	6.87	52,735	-	58	1.32x10 ⁻³
	CGG101393BR	3.21	12.02	288,377	-	167	6.24x10 ⁻³
	Total	2.07	8.28	627,801	504	1.63x10⁻²	2.06
CGG101394	CGG101394	1.69	1.25	143,836	-	37	3.95x10 ⁻³
	CGG101394R	11.24	1.96	790,281	-	749	2.14x10 ⁻²
	Total	6.00	1.85	934,117	786	2.54x10⁻²	3.12
CGG101395	CGG101395	0.82	6.93	92,883	-	24	2.52x10 ⁻³
	B CGG101395R	2.66	4.21	319,312	-	170	7.74x10 ⁻³
	Total	1.77	4.83	412,195	194	1.03x10⁻²	0.75
CGG101396	CGG101396	0.42	1.91	48,828	-	15	1.40x10 ⁻³
	CGG101396R	1.68	48.73	207,982	-	200	5.90x10 ⁻³
	Total	1.07	43.61	256,810	215	7.30x10⁻³	0.90
CGG101397 ^b	Library1	50.35	6.53	82,062,890	-	23,82	2.15
	Library2	9.95	0.49	56,265	-	15	9.5x10 ⁻³
	Library3	46.33	14.89	143,194,831	-	41,660	3.72
	Library4	44.17	18.29	178,676,610	-	50,828	4.65
	Library5	45.60	17.21	174,275,030	-	49,215	4.7
	Library6	43.86	18.25	191,542,625	-	52,707	5.03
ODJ6	Total	45.39	16.29	769,808,251	218,247	20.25	8.93
	TGTGAC	7.79	12.11	1,363,036	-	536	4.26 x10 ⁻²
	TGATGC	3.51	4.68	705,771	-	603	2.18 x10 ⁻²
	GACACT	10.34	9.40	9,610,375	-	5,157	0.30
	Total	8.94	9.46	11,679,182	6,296	0.37	-

^asequencing reads mapping uniquely and with high confidence (mapping quality MQ≥ 25); ^bstatistics relative to the mapping to the nuclear genomes are given post-trimming/rescaling (see section S2.6); "%end.": percentage of endogenous DNA calculated as 100 * Number of Mapped Reads (uniquely and with high confidence) / Number of Retained Reads (after trimming for adapters and low-quality ends); "%clon.": percentage of reads that were PCR duplicates; %end. and %clon. were calculated considering reads mapping to the nuclear or the mitochondrial horse genomes separately.

Table S2.7. Number of bases trimmed at read ends and mapDamage v2.02 parameters used for rescaling bases in the BAM file alignments to the horse nuclear genome sequence for the Batagai, the CGG101397 and two previously published Late Pleistocene genomes.

Horse ID	Library name	mapDamage2 rescaling option	#bases trimmed	
			5'-end	3'-end
Batagai	Library1	No rescaling	0	0
	Library2	--diff-hangs	0	0
	Library3	--forward	2	2
	Library4	--forward	6	6
	Library5	--forward	2	2
CGG101397	Library1	--forward	7	7
	Library2	No rescaling	3	3
	Library3	No rescaling	9	9
	Library4	No rescaling	2	2
	Library5	No rescaling	8	8
	Library6	No rescaling	1	1
CGG10022 ^a	ACTGCC DI	--diff-hangs	0	0
	ACTTGA	--diff-hangs	0	0
	CGTAGT	--diff-hangs	0	0
	CTTGTA AP	No rescaling	0	0
	CTTGTA APem	No rescaling	0	0
	CTTGTA TG	--diff-hangs	0	0
	GCAACG TI	Defaults	0	0
	TGACCA AP	No rescaling	0	0
	TGACCA TG	No rescaling	0	0
	TGCAGG SI	Defaults	0	0
CGG10023 ^a	13-idx1	--diff-hangs	0	0
	13-idx10	--diff-hangs	0	0
	13-idx11	--diff-hangs	0	0
	13-idx12	--diff-hangs	0	0
	13-idx2	--diff-hangs	0	0
	13-idx24	Defaults	0	0
	13-idx25	Defaults	0	0
	13-idx26	Defaults	0	0
	13-idx3	--diff-hangs	0	0
	13-idx4	--diff-hangs	0	0
	13-idx9	--diff-hangs	0	0

^aSchubert et al. 2014 (16); “--diff-hangs”: damage models are allowed to be different for 5'- and 3'-overhangs. “--forward”: damage models are estimated using only the 5'-end of the sequencing reads.

3 Section 3: Microbial profiling of ancient horses DNA

We performed metagenomic analyses on single end DNA sequences of each library of the four ancient specimens for which we generated shotgun-sequencing data (samples Yukagir, Batagai, CGG101397, and ODJ6). We followed the methodology implemented in the PALEOMIX pipeline (20), and applied in (10). Briefly, single-end sequencing reads were mapped to the markers of the MetaPhlAn database using the Bowtie2 v2.1.0 (31), with default parameters (sensitive global alignment strategy). PCR duplicates were then removed from each DNA library. The resultant unique high-quality hits were then profiled for their microbial content using MetaPhlAn version 1.7.7 (32). For comparison, we also generated microbial profiles on a subset of shotgun sequences of the two previously published Late Pleistocene horses (CGG10022 and CGG10023; (16)) and we also incorporated microbial profiles obtained from other six ancient horse remains (18th-19th century AD) analysed in (10) (**Table S3.1**). All the ancient samples analysed were buried in similar conditions, namely in the Yakutian permafrost. For sample CGG101397, the profile obtained from Library2 was excluded from the analyses, as no microbial taxon could be identified by MetaPhlAn from the limited number of reads generated for this library (and mapping to the MetaPhlAn database), leaving five libraries analysed here for CGG101397.

We compared taxon abundances across samples using a suite of analyses described in (20) and (10). In order to reduce stochastic effects of low-abundance taxa, we excluded those with a relative abundance <1% across all samples. The Shannon index was used as a measure of microbial diversity at the genus level and was calculated using the function ‘diversity’ of the R package ‘vegan’ (<http://cran.r-project.org/package=vegan>). Genus-level diversity was also characterized using Principal Coordinate Analyses (PCoA) of Bray-Curtis distances among microbial profiles and the R function ‘pcoa’. The structure among microbial profiles at the genus level was established using the R package ‘pvclust’, Manhattan distances and an average linkage clustering method (33). This method allowed estimating cluster support through Approximately Unbiased p-values and Bootstrap Probabilities from 10,000 bootstrap iterations. In order to identify the ecological origin of the microbial diversity retrieved from ancient horse remains, the microbial profiles were finally compared to those previously published from human (34) and soil samples (35) means of PCoA of Bray-Curtis distances at the genus level.

The relative abundances of microbial classes in the ancient horses samples (**Figure S3.1**), PCoA (**Figure S3.2**) and hierarchical clustering analyses of genus abundances (**Figure S3.3**) showed a high similarity amongst the microbial profiles characterized from the different libraries obtained from each individual sample. Per-sample clustering of microbial profiles was also supported by hierarchical clustering even when different samples showed high relative abundance similarities in PCoA, e.g., Batagai and Yukagir. We also found that the microbial diversity across all ancient samples was closer to that observed in soil samples than in human samples (**Figure S3.4**). Altogether, these results support the deposition soil as the main source of the microbial diversity recovered, as well as the low impact, if any, of contamination derived from humans during the handling of the samples post-excavation.

Our analyses identified a clear segregation between the microbial profiles of specimens Batagai and Yukagir on the one hand, and of the rest of the samples on the other hand (**Figures S3.1-3.3**). This segregation was driven by high relative abundances in the microbial class *Gammaproteobacteria* (82.2-99.5%) in the Batagai and Yukagir specimens, whereas the microbial profiles of the other samples were dominated by

Actinobacteria (22.7-100.0%; **Figure S3.1**). In Batagai and Yukagir, high abundances of *Gammaproteobacteria* were caused by high abundances of the environmental *Pseudomonas* genus (73.7-97.5% for *P. fluorescens* and unclassified *Pseudomonas*), which is identified in the other samples at lower abundances (07.5%). The *Pseudomonas* genus was previously found to dominate the microbial sequence data generated from a ~700,000 year-old horse sample preserved from the permafrost of the Yukon Territory, Canada (13).

Among the other ancient horse samples analysed here, CGG101397 appeared differentiated from the other specimens (in accordance with (10)), due to high abundances of *Actinobacteria*, the only class identified in four out of the five libraries profiled for this sample. In CGG101397, the *Actinobacteria* class was characterized by a single genus, *Mycobacterium* (unclassified species); lower but relatively high abundances in *Mycobacterium* were also detected in other samples (4.81-54.4%), together with the *Rhodococcus erythropolis* species (0.0-33.5%).

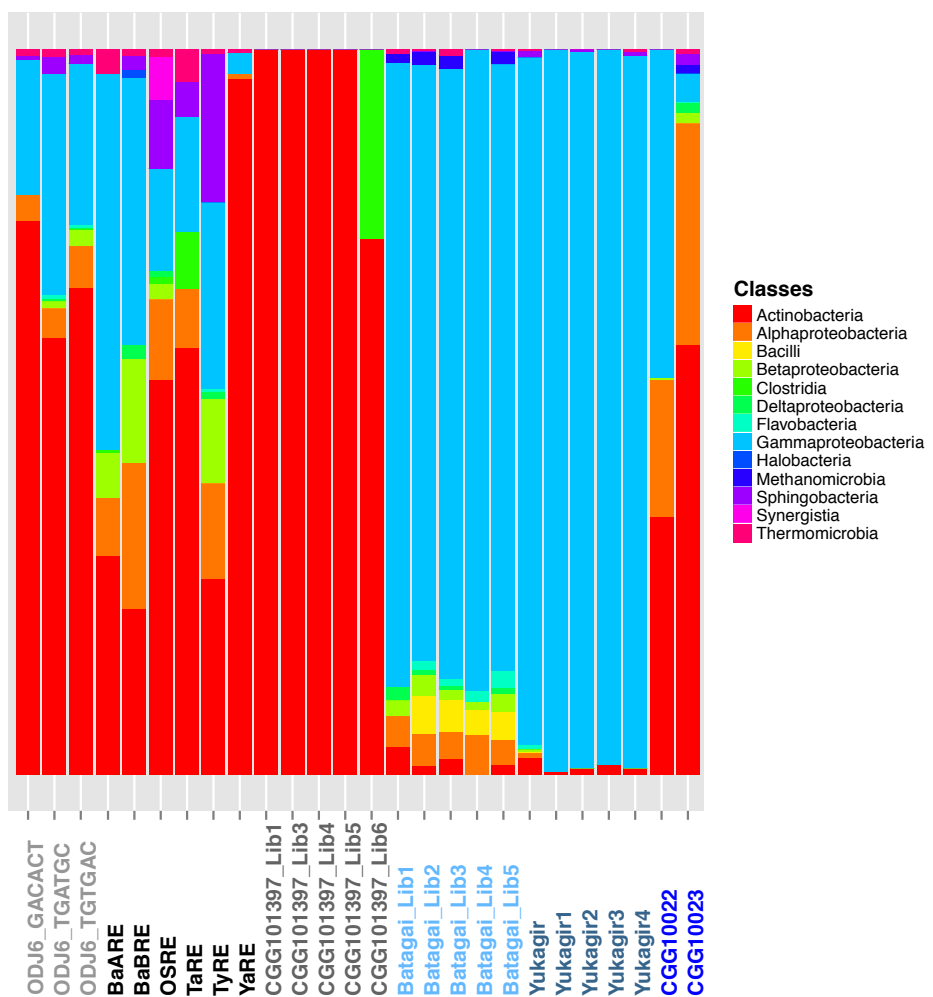


Figure S3.1. Relative abundance of microbial classes in the DNA extracts of ancient horse remains preserved in the permafrost.

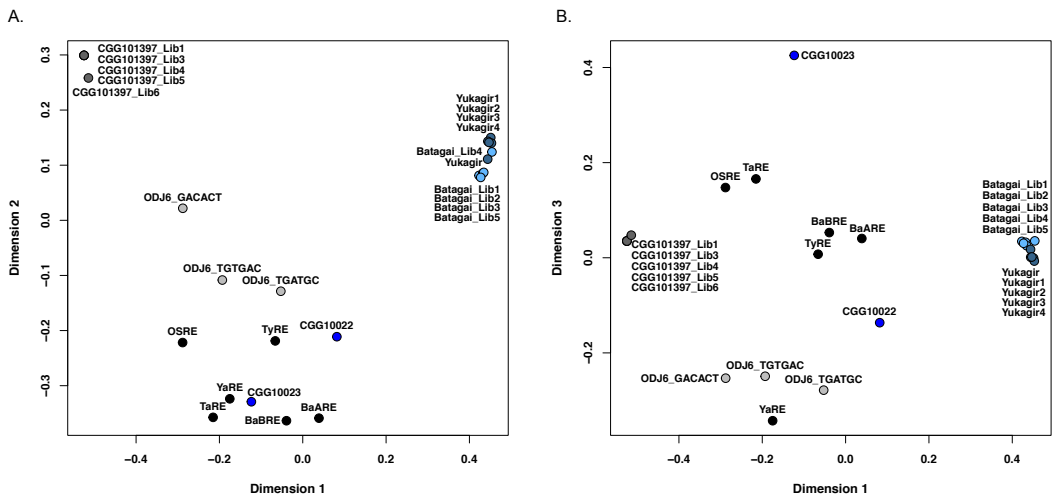


Figure S3.2. Principal Coordinate Analysis of Bray-Curtis distances between microbial DNA profiles at the genus level in the DNA extracts of ancient horse remains preserved in the permafrost.

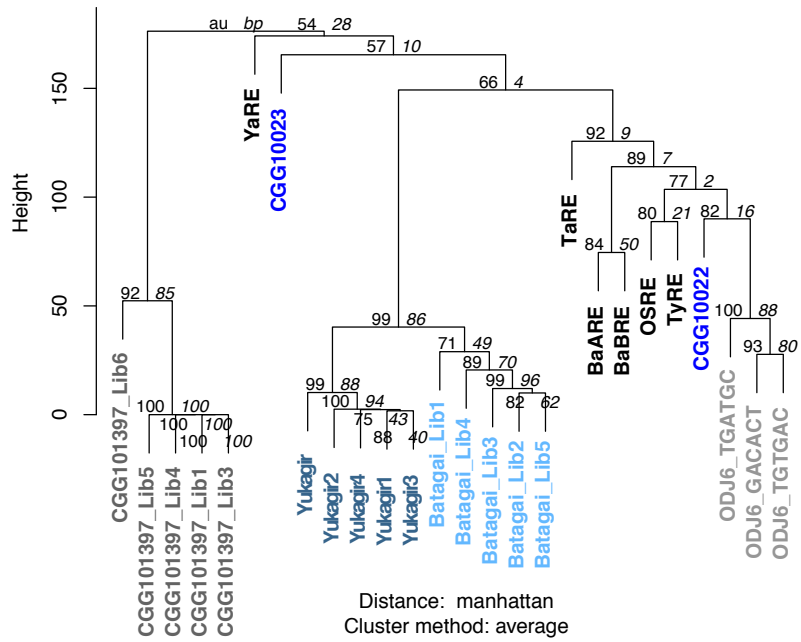


Figure S3.3. Hierarchical clustering of Manhattan distances between microbial DNA at the genus level in the DNA extracts of ancient horse remains preserved in the permafrost.

Cluster support is given approximately unbiased p-values (au) and bootstrap values (bp; 10,000 iterations).

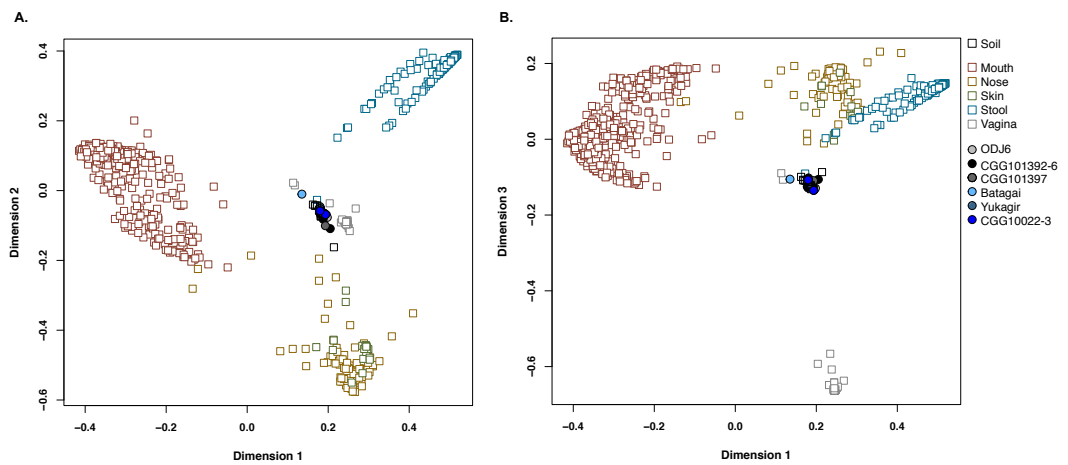


Figure S3.4. Principal Coordinate Analysis of Bray-Curtis distances between microbial DNA profiles at the genus level in various human associated microbiomes, soils and ancient permafrost horse remains.

3.1 Supplementary Tables for Section 3

Table S3.1. Information underlying the microbial DNA profiles of ancient horse specimens.

Horse ID	Reference	Library	#trimmed reads	#mapped reads ^a	# genera	Shannon index ^b
Yukagir	This study	Yukagir	47,813,678	17,208	16	0.42
		Yukagir1	4,711,842	1,790	3	0.13
		Yukagir2	7,255,501	2,977	5	0.17
		Yukagir3	4,319,878	1,598	4	0.17
		Yukagir4	6,113,260	2,327	5	0.19
Batagai	This study	Batagai_Lib1	60,624,116	5,797	11	0.74
		Batagai_Lib2	218,190,094	20,824	23	1.18
		Batagai_Lib3	241,003,960	20,576	22	1.04
		Batagai_Lib4	22,967,850	1,909	7	0.75
		Batagai_Lib5	211,992,359	17,465	22	1.17
CGG101397	This study	CGG101397_Lib1	1,981,276	408	1	0.00
		CGG101397_Lib2	565,437	59	unclassified	n/a
		CGG101397_Lib3	2,020,738	393	1	0.00
		CGG101397_Lib4	1,621,611	308	1	0.00
		CGG101397_Lib5	1,722,373	316	1	0.00
		CGG101397_Lib6	1,146,356	280	2	0.57
ODJ6	This study	ODJ6_GACACT	9,580,824	8,965	12	1.27
		ODJ6_TGATGC	20,127,349	23,725	23	1.56
		ODJ6_TGTGAC	84,990,191	75,369	32	1.73
CGG10022	Schubert et al. 2014 (16)	CGG10022	49,964,648	3,100	12	1.99
CGG10023	Schubert et al. 2014 (16)	CGG10023	31,478,854	10,952	34	1.81
BaARE	Der Sarkissian et al. 2014 (10)	CGG101393AR	11,862,758	7,858	20	2.36
BaBRE	Der Sarkissian et al. 2014 (10)	CGG101393BR	8,969,882	8,410	27	2.78
OSRE	Der Sarkissian et al. 2014 (10)	CGG101392R	10,871,116	11,421	19	2.25
TaRE	Der Sarkissian et al. 2014 (10)	CGG101396R	12,384,464	8,407	18	2.56
TyRE	Der Sarkissian et al. 2014 (10)	B_CGG101395R	12,023,328	9,276	18	2.17
YaRE	Der Sarkissian et al. 2014 (10)	CGG101394R	7,033,095	12,991	15	1.50

^ato the MetaPhlAn database. ^bat the genus level.

4 Section 4: Genomic variation

4.1 *SNP variation*

4.1.1 Variant calling against the horse reference EquCab2.0

Variants were called against the horse reference genome, as detailed in the Supplementary Information section S8.3 (13) and in (30), using the PALEOMIX pipeline (20).

4.1.2 Functional categorization of SNPs variation

Filtered SNPs were categorized according to their effect on genes, transcripts, protein sequences and regulatory regions using the Ensembl Variant Effect Predictor script and annotations from Ensembl v76 (36), as previously described in (30) and (16). Chromosomes X (chrX), which shows variable ploidy across samples, and the pseudo-chromosome Unknown (chrUn), which consists of contigs that could not be scaffolded within autosomal and sex chromosomes, were excluded from the functional characterization. When a variant was assigned to multiple classifications (e.g. variants adjacent to multiple genes/transcripts), we counted this variant only once in each category. This rule was also applied to each classification related to genes. The following categories of variants are listed:

1. Genes

- 1.1. *Intron*, intronic regions.
- 1.2. *Non-coding exon*, variant found in a non-coding region of a gene (e.g. non-coding RNA).
- 1.3. *5' UTR*, variant found in the 5' untranslated region of a gene.
- 1.4. *3' UTR*, variant found in the 3' untranslated region of a gene.
- 1.5. *Splice site*, variant found in the splice region: within 1-3 bp of the exon, or within 3-8 bp of the intron.
- 1.6. *Mature miRNA*, variant found within the sequence of mature miRNA.
- 1.7. *Coding exons*, coding regions.
 - 1.7.1. *Frameshift*, variants leading to a frameshift the amino acid sequence.
 - 1.7.2. *Synonymous*, variants not changing the encoded amino acid.
 - 1.7.3. *Non-synonymous* variants, leading to a different encoded amino acid.
 - 1.7.4. *Stop gain*, variant leading to gain a stop codon.
 - 1.7.5. *Stop loss*, variant leading to lose a stop codon.

2. Outside genes

- 2.1. *Intergenic*, variant located between genes but not in 1.1 and 1.2.
- 2.2. *Upstream*, variant found less than 5 kb upstream of the 5'-termini of a gene.
- 2.3. *Downstream*, variant found less than 5 kb downstream of the 3'-termini of a gene.

Results for all genomes sequenced in this study are shown in **Table S4.2**.

4.1.3 Non-synonymous mutations specific to Yakutian horses.

We collected mutations potentially specific to Yakutian horses, using criteria based on the work from Baye and colleagues (37). The ancient sample Batagai was found to be genetically differentiated from more recent sample CGG101397 and modern Yakutian horses (see **section S5.3**), it was then excluded from the population of Yakutian

horses in this specific analysis. Briefly, we collected all sites for which a variant was called in at least 8 out of 10 Yakutian horse genomes and 16 out of the 19 domesticated horses present in our comparative panel. We did not filter SNPs by physical proximity, (unlike (37), who suggested a minimum distance of 0.3 cM in humans) to accommodate downstream analyses for which different marker densities may be required.

We then extracted loci with differences in allele frequency superior to 0.4, corresponding to 429 SNPs, including 170 non-synonymous (in 130 genes) and 259 synonymous mutations ($dN/dS = 0.68$). The corresponding 170 non-synonymous substitutions are listed in **Table S4.3**.

We carried out functional enrichment for the 130 genes as described in **section S7.3**. Using humans as model organisms, no PheWAS or other phenotype was found to be significantly enriched; other results for functionnal enrichment can be found in **Tables S4.4-S4.8**.

4.1.4 Analysis of loci associated with important Mendelian traits in horses

Using the genotyping calls produced above (see **section S4.1.1**), we examined SNPs at 49 loci for known Mendelian traits, including traits collected in the Online Mendelian Inheritance in Animals (OMIA) database (38) in (13) and in (39) as described in (16) (**Table S4.9**). We attempted to call SNPs at all loci in both modern and ancient samples, and in cases where coverage was incompatible with our genotyping criteria, we recorded the number of high-quality nucleotides ($\text{BaseQ} \geq 35$) observed at the given site.

Results are listed in **Tables S4.10-S4.11**. In the majority of cases, Batagai and the other Late Pleistocene horses belonging to the same population cluster (specimens CGG10022 and CGG10023) carry the reference alleles with the exceptions of genes mainly associated with racing performance (*COX4/1*, *ACN9*), and body size (*ZFAT*). For example, heterozygosity is observed within all three specimens for *ACN9*, while homozygosity for the alternative allele is observed in *CKM* in Batagai and heterozygosity in CGG10023. Alleles associated with racing performance are also carried by modern Yakutian horses and sample CGG101397. Additionally, two loci in *PROPI* are associated with dwarfism, and Batagai is homozygote alternate for both loci, while this condition is not observed in Late Pleistocene and modern Yakutian horses. Interestingly, Batagai also shows alternate allele homozygosity for *HMG42*, which is associated with larger body size. This condition is also shared with four modern Yakutian horses (Yak2, Yak3, Yak5 and Yak7). While CGG10022 and CGG10023 are heterozygous at four loci in *ZFAT*, Batagai is homozygous for the non-alternate allele, as the reference. These SNPs located in *ZFAT*, are associated with wither height in domesticated horses and the heterozygosity condition of one of them (at positions chr9:74,798,143) has been associated with a ~0.5 cm increase in height at the withers (40). Modern Yakutian horses and CGG101397 show both heterozygosity and homozygosity for the alternate allele, except for three horses Yak2, Yak7 and Yak8 carrying the same allelic status as Batagai.

We observed homozygosity for recessive MC1R mutations associated with chestnut coat (Yak6, Yak8, and Yak11), suggesting that these horses were chesnut in color. Specimens Yak3 and Yak7 were homozygous for the 11 bp recessive deletion associated with black coat color, suggesting these horses were black. No allele associated with Tobiano and Sabino spotting, Leopard complex spotting, silver coat color, and champagne dilution were detected across modern and ancient horses from Yakutia. Finally, none of the mutations associated with various coat color phenotypes was observed in the ancient samples Batagai, CGG101397 and some modern Yakutian horses (Yak5 and Yak9).

4.2 Screening for segmental duplications

We identified segmental duplications using mrCaNaVaR v0.31 and mrFAST v2.0.0.5 (41). BED files were manipulated using BEDTools v2.0.17 (42). The analysis was carried out using the Thoroughbred horse (Twilight) and the modern Yakutian horses (Yak1 to Yak9).

We first masked the reference sequence to account for existing duplication in the EquCab2.0 reference genome. To do this, we generated overlapping 36 bp kmers across the entire nuclear genome, using a step size of 5 bp. The genome was then indexed using mrFAST (using a window-size of 12), the 36-mers were mapped back to this genome, and the location of any 36-mer mapping to more than one region was masked in the genome. We additionally masked the regions corresponding to the UCSC repeat-tracts (“Interrupted repeats”, “Repeat Masker”, and “Simple repeats”). Consequently, a total of 1.2 Gbp of the reference genome was masked, representing ~49% of the EquCab2.0 reference genome. The masked FASTA reference genome was then indexed using mrFAST as above. We next split the reads of the genomes of interest into non-overlapping 36-mers, starting 10 bp from the 5'-end, thereby excluding the more variable (quality-wise) 5'- and 3'-regions of the read. These were mapped to the masked FASTQ using mrFAST as described above. Before investigating the copy-number variation in our samples, we expanded the masked regions in the FASTQ sequences by 36 bp, to account for lower coverage in regions proximate to the masked regions, and indexed the resulting FASTQ sequences using mrCaNaVaR, specifying no gaps.

We then called read-depth and copy-numbers for each window in each specimen with mrCaNaVaR using the alignments generated by mrFAST above. We defined segmental duplications as any region consisting of at least 5 continuous copy-windows (“CW”), covering at least a total of 10 Kb. In this region the copy-number exceeds the mean by at least three standard deviations as calculated using the control regions identified by mrCaNaVaR, while allowing one non-trailing window exceeding the mean by at least 2 standard deviations. The mean and standard deviation were calculated separately for the X chromosome in male specimens. Before we collected regions with segmental duplications, we excluded putative mis-assembled regions where the copy number exceeded 50-fold the ploidy of the given chromosome in any sample. We also excluded any region in which segmental duplications were present in the Illumina sequence data from the Thoroughbred individual underlying the horse reference genome, in order to account for some segmental duplications existing in other domesticated horses and duplications not recorded in the EquCab2.0 reference genome (which was originally assembled based on Sanger sequencing (29)). This resulted in the exclusion of 176 million bp. We then plotted the distribution of copy-numbers called for control regions for each sample (excluding the X chromosome). In order to ensure that results were comparable across samples, we excluded from downstream analyses Yak2 and Yak7, for which the distribution deviated from the remaining samples (**Figure S4.1**), possibly because these genomes were sequenced at a much higher coverage (18.38 and 21.63X versus 9.48-11.64X for the other Yakutian samples). We then called segmental duplications using the same method described above.

We next concatenated the filtered BED files with BEDTools v2.0.17 for the seven Yakutian horse genomes considered and calculated the number of individuals for which a given region was called. We employed the BEDTools command ‘genomcov’ with arguments ‘-bg’, and determined overlap with annotated sequences from Ensembl v76 (excluding pseudo-genes and introns) using the BEDTools intersect command with arguments ‘-loj’. For each Ensembl v76 transcript, we recorded the maximum number of samples for which a given segmental duplication overlapped that transcript at any

window. Overall, we identified a total number of 260 regions affected by segmental duplications within Yakutian horses.

We compared these results with previous scans for CNVs in the horse (43, 44) and observed that a large proportion of putative segmental duplications from these studies were contained in the set of regions collected for the Thoroughbred (Twilight). For (43), we found an overlap accounting for 2.8 Mbp of the 5.0 Mbp (their Table S4) of regions called in that study, and for (44), we found an overlap accounting for 12.0 Mbp of the 28.5Mbp they analysed ((44); Table S3). These regions may thus represent a combination of common segmental duplications among the domesticated horses, and false positives common to our and their studies.

When examining the functional characterization of the segmental duplications identified in Yakutian horses, we found 178 annotated genomic regions, of which 170 were genes coding for 91 proteins of known function (**Table S4.12**) and 79 uncharacterized proteins (**Table S4.13**). In the remaining regions covered by segmental duplications, we found four small nuclear RNA, one RNA, one small nucleolar RNA, one ribosomal RNA, and one microRNA.

We carried out functional enrichment (GO-terms, pathways, phenotypes, disease) for the genes encompassed by the detected segmental duplications as described in **section 7.3**. No GO-term was found to be significantly enriched; other enrichment results are presented in **Tables S4.13-S4.15**.

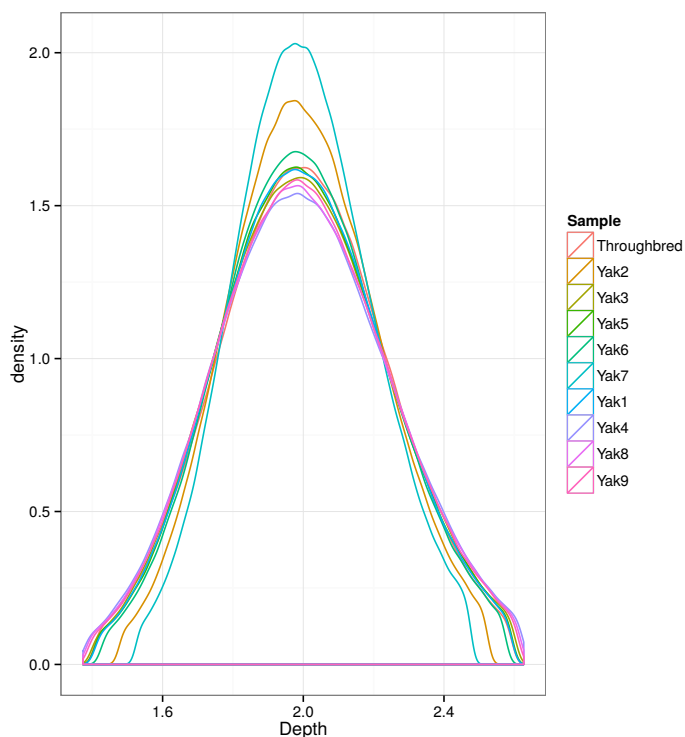


Figure S4.1. Distribution of copy-numbers called for control regions in modern Yakutian horses and the Thoroughbred Twilight individual underpinning the horse reference genome.
Chromosome X was excluded from these analyses.

4.3 Inbreeding and heterozygosity

4.3.1 Genome-wide heterozygosity estimates

The average heterozygosity of each horse described in this study was estimated as

the number of segregating sites by calculating the Watterson estimator (θ_w) (45), in 50 kb sliding windows (step-size of 10 Kb). This was done using the program ANGSD (46), which accounts for genotype uncertainties by using genotype likelihoods and priors based on site frequency spectrum (SFS). Priors for the autosomes were constructed using the SFS (47) for the chromosome 22. For high-quality genomes we excluded windows in which less than 45 out of 50 kb (90%) were covered. Additionally, θ_w was calculated either considering all substitution classes or disregarding transitions, as the latter represent the most typical nucleotide mis-incorporation at damaged sites.

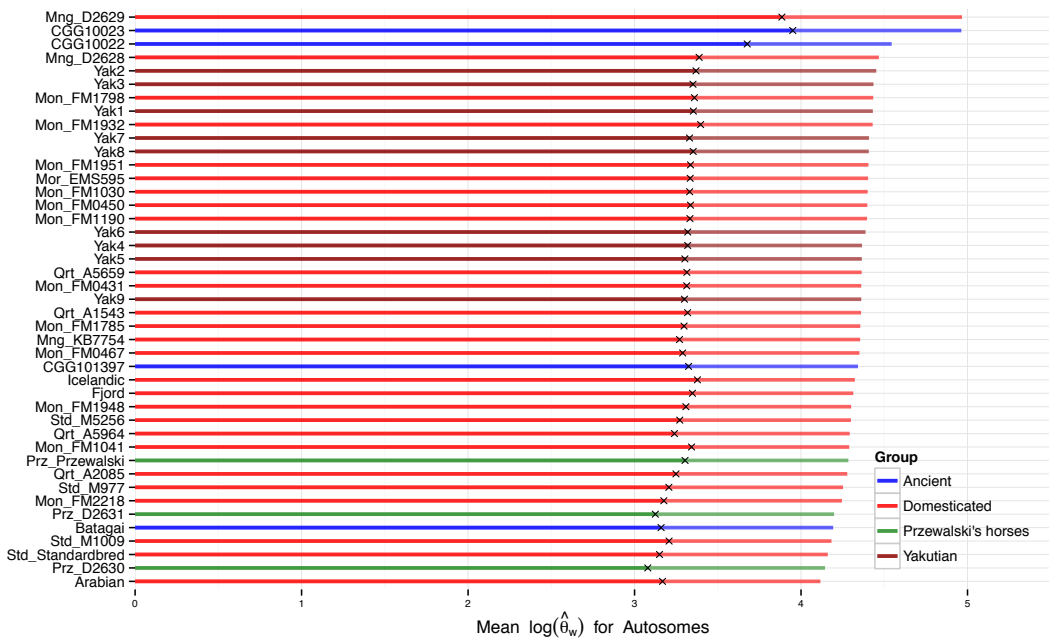


Figure S4.2. Average autosomal heterozygosity in ancient and modern horses.

Black dots indicate average $\log(\theta_w)$ values estimated considering both transitions and transversions, while black crosses indicate average $\log(\theta_w)$ values estimated disregarding transitions. Heterozygosity estimates of two Late Pleistocene horse genomes characterized by (16) (specimens CGG10022 and CGG10023), and all the genomes from our comparative panel are shown for comparison.

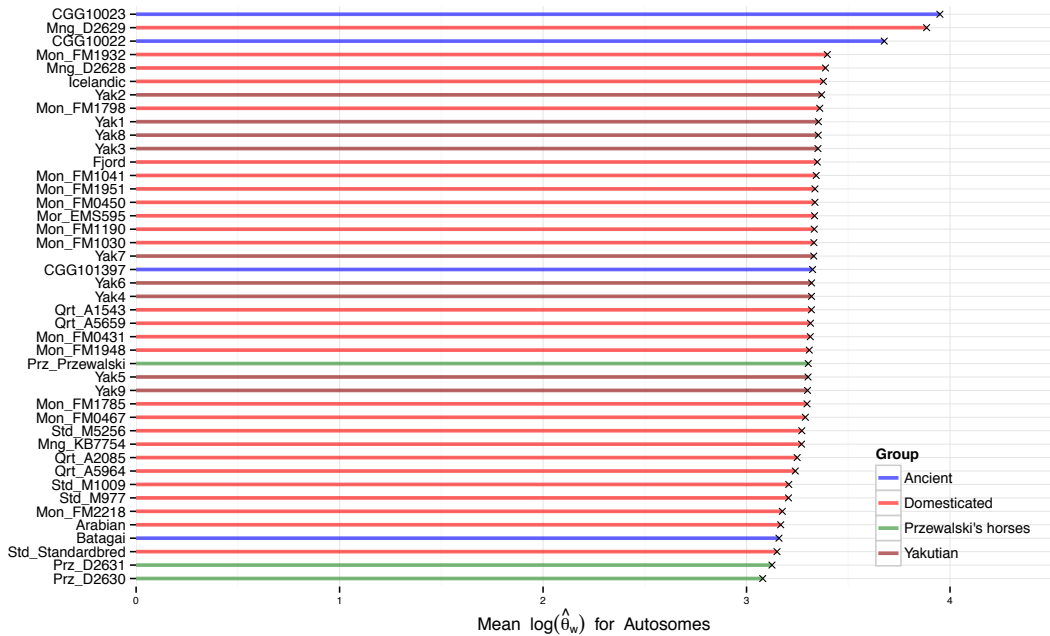


Figure S4.3. Average autosomal heterozygosity in ancient and modern horses, disregarding transitions.

See Figure S4.2 for additional captions.

4.3.2 Inbreeding estimates

We estimated inbreeding in Yakutian horses as the proportion of genomic fragments being mostly homozygous, or “homozygous-by-descent” (HBD), following terminologies and methodologies similar to those in (48), and applied to complete horse and equid genomes in (16) and (30). We used the θ_w estimator across the genome (see section S4.3.1) to detect HBD regions. In these analyses, we replaced missing data by the closest neighboring valid values on a per-chromosome basis. We determined the coordinates of the HBD genomic tracks by identifying segments with local changes in the average θ_w estimates along the genome using the R package ‘changepoints’ ((49); <http://cran.r-project.org/web/packages/changepoint/index.html>) and the binary segmentation algorithm (method=“BinSeg”) allowing up to 12 breakpoints per chromosome ($Q=12$). For each segment, we calculated the heterozygosity estimates given by the average of $\log(\theta_w)$, which were used to weigh genomic track lengths (deduced from their external coordinates) before their density was plotted with the ‘density’ R function (from 100,000 points). A bimodal distribution of the θ_w estimate values indicates inbreeding in the corresponding individual. We determined the coordinate of the lowest point (pit) between the two modes using numerically estimates of first and second derivatives of the density function (using absolute tolerance of 10^{-7}). The pit coordinate provided a threshold used to classify genomic segments as showing “high” or “low” heterozygosity (vertical red line). The total size of the “low” heterozygosity regions was divided by the total size of all regions to give the proportion of HBD tracks, or “inbreeding coverage estimate” (value shown adjacent to the vertical line). The average $\log(\theta_w)$ values and positions of the genomic tracks were determined both including (full lines) and excluding transitions (dashed lines) to account for mis-

incorporations arising from post-mortem DNA damage in ancient genomes (**Figure S4.4-4.5**).

Results suggest low levels of inbreeding (4.1-10.1% with transitions; 4.0%-10.4% without transitions) among modern Yakutian horses and low to not existing levels among the ancient horses (CGG101397: 6.7/6.6%; CGG10022: 1.1/0.2%; CGG10023: 0.0/0.0%; Batagai: 9.6/8.3%; with and without transitions respectively; **Figure S4.4**).

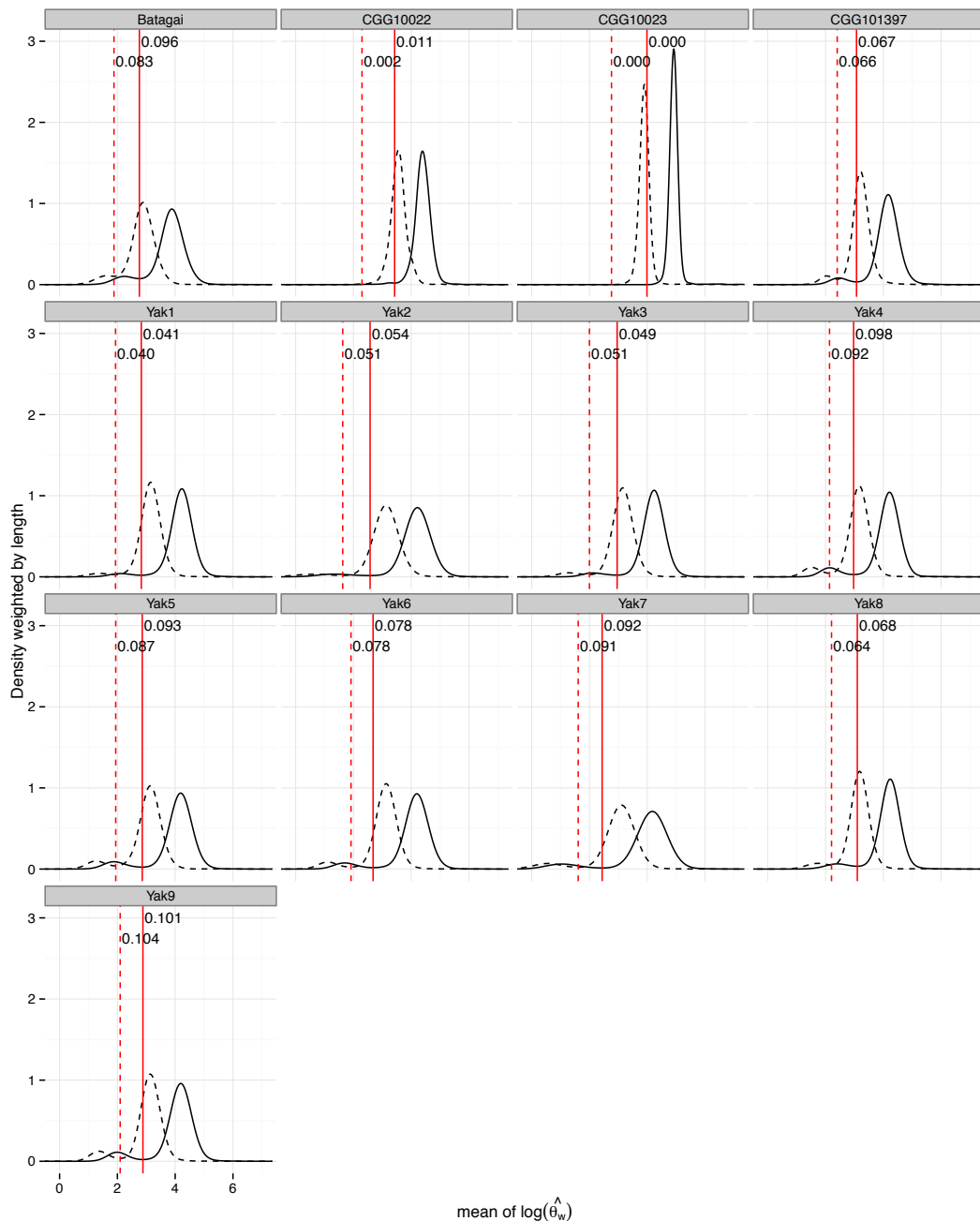


Figure S4.4. Inbreeding coverage estimates for Yakutian and Late Pleistocene horses.

Bimodal distributions are typical of inbred individuals. The red vertical line indicates the local minimum separating the two modes of the distribution, whenever present. The number adjacent to the line is the area under the left peak, and provides an estimate for inbreeding. Solid lines indicate that both transition and transversions are considered, in contrast to dashed lines for which only transversions were used.

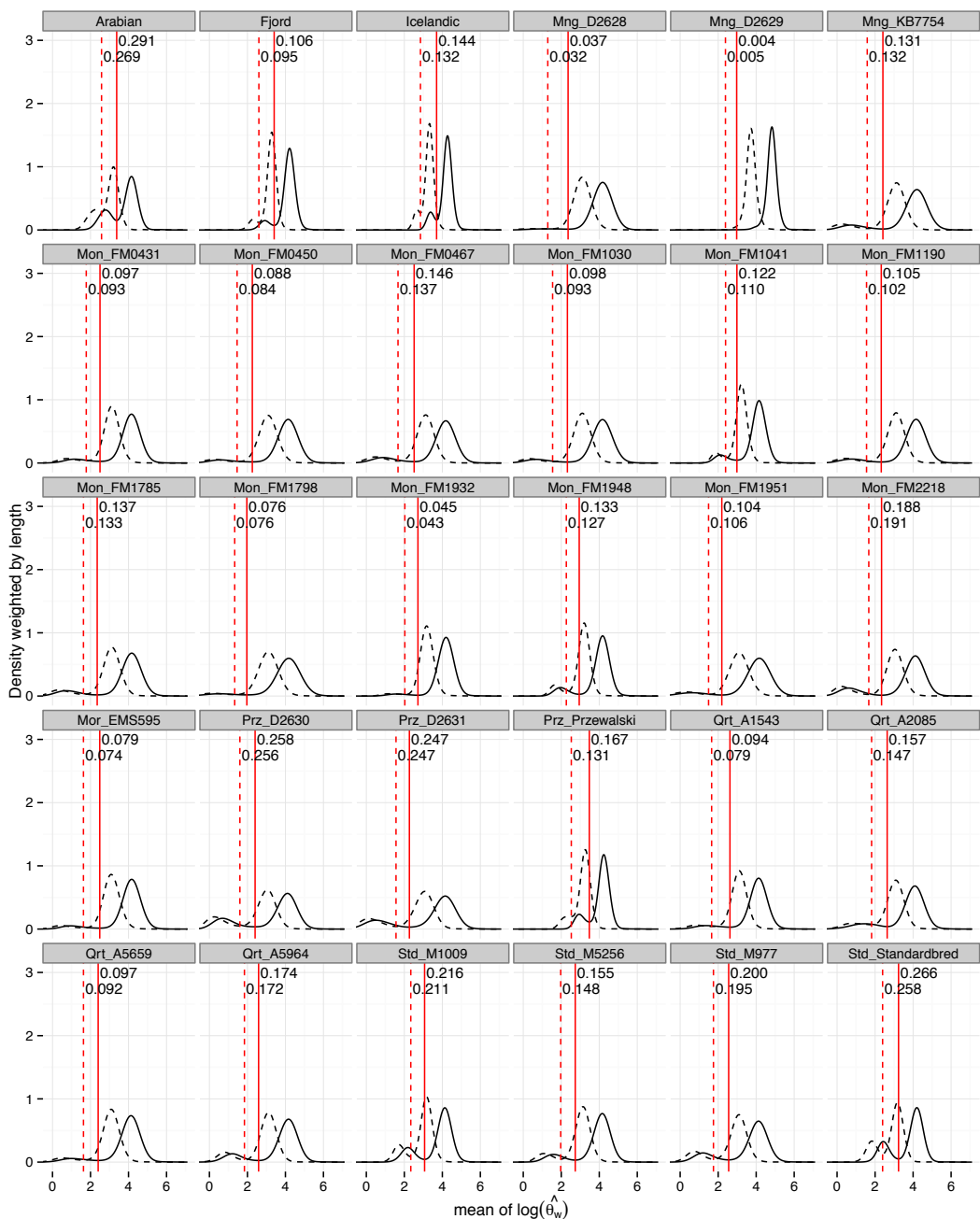


Figure S4.5. Inbreeding coverage estimates for other domesticated horses.
See Figure S4.4 for figure caption.

4.4 Supplementary Tables for Section 4

Table S4.1. Maximum per-sample depth used to filter base calls.

Sample	Maximum Depth
Batagai	54
CGG10023	35
CGG10022	72
CGG101397	84
Yak1	25
Yak2	39
Yak3	25
Yak4	23
Yak5	25
Yak6	27
Yak7	48
Yak8	23
Yak9	23

Sample	Maximum Depth
Arabian	39
Fjord	23
Icelandic	30
Mng D2629	54
Mng D2628	52
Mon FM0431	65
Mon FM0450	66
Mon FM0467	86
Mon FM1030	109
Mon FM1041	52
Mon FM1190	102
Mon FM1785	80
Mon FM1798	130
Mon FM1932	60
Mon FM1948	51
Mon FM1951	104
Mon FM2218	73
Mor EMS595	95
Prz D2631	56
Prz Przewalski	30
Prz D2630	39
Qrt A1543	80
Qrt A5659	83
Qrt A5964	114
Qrt A2085	65
Std M977	82
Std M5256	74
Std M1009	51
Std Standardbred	37
Thoroughbred	81

Table S4.2. Classification of functional variants identified across the Yakutian horse genomes.

	Batagai		CGG101397		Yak1		Yak2		Yak3		Yak4	
Variant class	Genes	Variants	Genes	Variants	Genes	Variants	Genes	Variants	Genes	Variants	Genes	Variants
All variants	26,697	6,762,877	26,648	5,814,974	26,639	6,536,920	26,653	7,084,640	26,650	6,647,543	26,637	6,369,435
Not genic		5,115,400		4,390,671		4,951,567		5,405,329		5,040,171		4,827,587
Intergenic		4,494,040		3,837,388		4,358,504		4,757,343		4,434,041		4,242,032
Upstream		337,303		306,259		319,064		350,223		325,963		315,292
Downstream		312,317		273,186		300,076		326,709		306,393		296,183
Genic	21,425	1,746,322	20,800	1,513,251	21,249	1,679,096	21,582	1,780,726	21,408	1,703,005	21,145	1,634,953
Intron	16,190	1,686,836	16,069	1,456,391	16,080	1,623,215	16,111	1,721,301	16,093	1,646,300	16,035	1,580,269
Non-coding Exon	2,755	6,844	2,368	5,634	2,740	7,132	2,967	8,518	2,836	7,503	2,692	6,962
5' UTR	1,837	3,219	1,895	3,518	1,571	2,597	1,679	2,871	1,586	2,538	1,562	2,474
3' UTR	2,487	4,010	2,212	3,541	2,406	3,794	2,439	4,004	2,429	3,909	2,275	3,621
Splice Site	4,613	6,985	4,553	7,002	4,357	6,369	4,589	6,937	4,317	6,383	4,205	6,157
Mature miRNA	28	29	33	38	36	40	44	47	32	32	38	39
Coding Exon	11,349	29,000	11,004	28,535	10,900	26,673	11,107	27,849	11,033	26,743	10,670	26,205
Frameshift	1,588	2,080	1,799	2,675	1,272	1,503	1,463	1,801	1,242	1,482	1,237	1,466
Synonymous	10,610	25,288	10,131	23,938	10,176	23,777	10,349	24,518	10,330	23,883	9,934	23,378
Non-synonymous	9,051	21,853	8,736	20,837	8,799	20,956	8,808	21,933	8,827	21,346	8,618	20,734
Stop gain	185	190	189	194	204	211	202	212	214	224	191	197
Stop loss	13	13	20	20	15	15	16	16	18	18	13	13

	Yak5		Yak6		Yak7		Yak8		Yak9	
Variant class	Genes	Variants								
All variants	26,650	6,508,075	26,634	6,625,881	26,655	7,098,114	26,662	6,482,224	26,632	6,499,579
Not genic		4,944,158		5,033,776		5,414,527		4,908,118		4,932,067
Intergenic		4,347,364		4,426,444		4,749,072		4,313,267		4,336,606
Upstream		321,281		326,825		362,115		320,938		321,250
Downstream		301,749		307,257		333,333		300,303		300,417
Genic	21,225	1,658,515	21,315	1,687,337	21,572	1,788,196	21,275	1,668,031	21,178	1,660,380
Intron	16,041	1,602,973	16,072	1,630,665	16,092	1,726,180	16,079	1,611,908	16,013	1,604,752
Non-coding Exon	2,725	7,264	2,795	7,293	2,947	8,800	2,740	6,965	2,703	7,186
5' UTR	1,583	2,579	1,684	2,784	1,837	3,328	1,612	2,656	1,586	2,578
3' UTR	2,352	3,756	2,358	3,823	2,440	3,992	2,389	3,782	2,302	3,656
Splice Site	4,289	6,271	4,403	6,456	4,696	7,280	4,297	6,375	4,280	6,319
Mature miRNA	38	38	36	38	49	52	41	41	41	42
Coding Exon	10,876	26,684	10,941	27,071	11,296	28,998	10,993	26,967	10,726	26,416
Frameshift	1,306	1,566	1,366	1,654	1,646	2,146	1,284	1,532	1,277	1,518
Synonymous	10,162	23,698	10,199	23,972	10,436	25,065	10,268	24,018	10,027	23,523
Non-synonymous	8,659	20,614	8,713	21,160	8,933	23,006	8,739	21,089	8,603	20,965
Stop gain	185	191	177	183	208	218	205	210	188	198
Stop loss	14	15	17	18	17	18	17	18	11	11

Table S4.3. Non-synonymous markers specific to Yakutian horses, ordered by specificity (1).

Gene ID	Transcript ID	Gene Name	Strand	Chr	Pos	NucRef	NucAlt	Codon	CodonPos	AARef	AAAlt	Delta
ENSECAG00000003780	ENSECAT00000003667	<i>OR6A2</i>	-	7	76242089	C	T	GCG	2	Arg	His	0.7188
ENSECAG00000010259	ENSECAT00000010674	<i>TRIM45</i>	+	5	51983000	G	A	CGG	2	Arg	Gln	0.6701
ENSECAG00000004104	ENSECAT00000004094		+	7	76318945	T	A	ATT	2	Ile	Asn	0.6597
ENSECAG00000019446	ENSECAT00000020625	<i>SH3RF3</i>	-	15	535504	C	T	TAC	3	Val	Ile	0.6287
ENSECAG00000010259	ENSECAT00000010674	<i>TRIM45</i>	+	5	51984595	G	A	GCA	1	Ala	Thr	0.6188
ENSECAG00000009561	ENSECAT0000009811	<i>FDX4CB1</i>	-	7	20458010	C	T	GCG	2	Arg	His	0.6042
ENSECAG00000016457	ENSECAT00000017372	<i>E2F8</i>	-	7	87149752	C	G	GTC	3	Asp	His	0.6029
ENSECAG00000023844	ENSECAT00000024681	<i>LAMA2</i>	+	10	75723569	G	A	CGC	2	Arg	His	0.5972
ENSECAG00000023844	ENSECAT00000028988	<i>LAMA2</i>	+	10	75723569	G	A	CGC	2	Arg	His	0.5972
ENSECAG00000011862	ENSECAT00000012267	<i>C11orf1</i>	+	7	20464163	C	A	CGT	1	Arg	Ser	0.5956
ENSECAG00000021446	ENSECAT00000029043	<i>GRID1</i>	+	1	84439712	A	G	ATT	1	Ile	Val	0.5799
ENSECAG00000013829	ENSECAT00000014395	<i>LRRK3</i>	+	5	88176264	C	G	ACA	2	Thr	Arg	0.5699
ENSECAG00000017119	ENSECAT00000017998	<i>PIGV</i>	-	2	28826835	C	G	CAA	1	Leu	Phe	0.5654
ENSECAG00000025066	ENSECAT00000027056	<i>PLA2G3</i>	+	8	5892549	G	A	CGC	2	Arg	His	0.5556
ENSECAG0000000258	ENSECAT0000000196	<i>STX11</i>	-	31	21771618	G	T	GAG	3	Leu	Ile	0.5523
ENSECAG00000011135	ENSECAT00000011552	<i>GPATCH4</i>	+	5	41675513	C	G	CCC	2	Pro	Arg	0.5486
ENSECAG00000021537	ENSECAT00000023007	<i>FNDC7</i>	-	5	59259538	T	C	GAT	3	Ile	Val	0.5389
ENSECAG00000016463	ENSECAT00000017364	<i>TMEM72</i>	-	1	69377220	G	C	TTT	1	Asn	Lys	0.5359
ENSECAG00000008441	ENSECAT00000008613	<i>ADORA2B</i>	-	11	58222333	G	C	TGG	3	Pro	Ala	0.5278
ENSECAG00000017257	ENSECAT00000018273		+	21	28288290	C	T	CGT	1	Arg	Cys	0.5229
ENSECAG00000001015	ENSECAT00000000878		+	5	38598787	C	T	CAC	1	His	Tyr	0.5211
ENSECAG00000001626	ENSECAT00000002010	<i>FAM35A</i>	-	1	83411985	G	T	AGT	2	Thr	Asn	0.5188
ENSECAG00000000955	ENSECAT00000000829		-	7	73858338	G	A	ACG	3	Arg	Cys	0.5147
ENSECAG00000000955	ENSECAT00000000829		-	7	73858980	A	G	AAA	3	Phe	Leu	0.5147
ENSECAG00000017255	ENSECAT00000018215		-	12	20100747	T	A	CTT	2	Lys	Met	0.5139
ENSECAG00000016678	ENSECAT00000017506		-	3	69502178	C	T	CAT	1	Met	Ile	0.5139
ENSECAG00000007957	ENSECAT00000008003		+	4	96520769	T	G	CTC	2	Leu	Arg	0.5062
ENSECAG00000024755	ENSECAT00000026678		-	11	41661616	C	T	GCG	2	Arg	His	0.5056
ENSECAG00000002127	ENSECAT0000001972		+	7	72759229	G	A	TGT	2	Cys	Tyr	0.5035
ENSECAG00000005646	ENSECAT00000005595		-	14	92740397	G	C	GAA	1	Phe	Leu	0.5033
ENSECAG00000024306	ENSECAT00000026216	<i>DENNDA4</i>	+	1	12674368	C	G	ACA	2	Thr	Arg	0.5029
ENSECAG00000017136	ENSECAT00000018105	<i>HEMK1</i>	-	16	36704036	A	T	CAT	2	Met	Lys	0.5000
ENSECAG00000000480	ENSECAT00000002615	<i>AB13BP</i>	+	19	54500659	A	G	ATC	1	Ile	Val	0.5000
ENSECAG00000000480	ENSECAT00000002650	<i>AB13BP</i>	+	19	54500659	A	G	ATC	1	Ile	Val	0.5000
ENSECAG00000005424	ENSECAT00000005420	<i>CABS1</i>	-	3	64622967	A	G	AAT	2	Ile	Thr	0.5000
ENSECAG00000007941	ENSECAT00000008326	<i>MYOQ10</i>	+	21	43825996	G	A	GTG	1	Val	Met	0.5000
ENSECAG00000012702	ENSECAT00000013150	<i>PPBP</i>	-	3	61847443	C	G	TCT	2	Arg	Thr	0.4965
ENSECAG00000007434	ENSECAT00000007431	<i>PRR9</i>	-	5	44362433	G	A	CGC	2	Ala	Val	0.4938
ENSECAG00000007434	ENSECAT00000007431	<i>PRR9</i>	-	5	44362443	A	C	AGA	3	Ser	Ala	0.4938
ENSECAG00000009561	ENSECAT00000009811	<i>FDX4CB1</i>	-	7	20458221	T	G	CAT	3	Met	Leu	0.4889
ENSECAG00000012474	ENSECAT00000013260	<i>TFI2</i>	-	5	52012832	A	G	CAT	2	Met	Thr	0.4882
ENSECAG00000001007	ENSECAT0000000986		-	6	25639988	C	T	GAC	3	Val	Ile	0.4869
ENSECAG00000019154	ENSECAT00000020422	<i>ADAMTSL4</i>	-	5	46533866	G	A	CCG	3	Arg	Trp	0.4861
ENSECAG00000009949	ENSECAT00000010815	<i>P2RX7</i>	+	8	21751816	G	A	GGT	1	Gly	Ser	0.4853
ENSECAG00000008940	ENSECAT00000009129	<i>TMEM40</i>	+	16	4588968	G	C	GGG	2	Gly	Ala	0.4812
ENSECAG00000026818	ENSECAT00000028860	<i>LRP11</i>	+	31	16993179	C	T	CGC	1	Arg	Cys	0.4792
ENSECAG00000010626	ENSECAT00000011724	<i>SLC47A2</i>	+	11	58820685	T	G	TTC	1	Phe	Val	0.4779
ENSECAG00000014004	ENSECAT00000014633	<i>SAMD7</i>	+	19	10364690	A	G	AAT	2	Asn	Ser	0.4779
ENSECAG0000001653	ENSECAT00000006446	<i>POLE</i>	-	8	29601827	G	A	CGG	3	Pro	Ser	0.4778
ENSECAG0000001653	ENSECAT00000006622	<i>POLE</i>	-	8	29601827	G	A	CGG	3	Pro	Ser	0.4778
ENSECAG00000003630	ENSECAT00000003501		+	25	343444	T	C	CTA	2	Leu	Pro	0.4766
ENSECAG00000012975	ENSECAT00000013485	<i>C8orf74</i>	+	2	58762175	T	C	TAC	1	Tyr	His	0.4735
ENSECAG00000014941	ENSECAT00000015992	<i>INPP5F</i>	-	1	12724544	G	A	CGA	2	Ser	Leu	0.4722
ENSECAG00000005898	ENSECAT00000005907		+	10	78715436	A	G	ATC	1	Ile	Val	0.4722
ENSECAG00000009742	ENSECAT00000009966	<i>S100A12</i>	+	5	44158614	G	A	GGT	1	Gly	Ser	0.4711
ENSECAG00000024080	ENSECAT00000025941		-	7	20387970	T	C	CAT	3	Met	Val	0.4706
ENSECAG00000010626	ENSECAT00000011724	<i>SLC47A2</i>	+	11	58820680	A	G	GAC	2	Asp	Gly	0.4688

Table S4.3. Non-synonymous markers specific to Yakutian horses, ordered by specificity (2).

Gene ID	Transcript ID	Gene Name	Strand	Chr	Pos	NucRef	NucAlt	Codon	CodonPos	AARef	AAAlt	Delta
ENSECAG00000012702	ENSECAT00000013150	<i>PPBP</i>	-	3	61847087	G	A	AGC	2	Ala	Val	0.4688
ENSECAG00000024031	ENSECAT00000025828	<i>KIAA0232</i>	+	3	114722043	A	C	ATG	1	Met	Leu	0.4688
ENSECAG00000026868	ENSECAT00000028994	<i>C6orf183</i>	+	10	58985096	C	G	GCC	2	Ala	Gly	0.4673
ENSECAG00000018781	ENSECAT00000019992	<i>MCMDC2</i>	-	9	18407831	C	T	GCG	2	Arg	His	0.4653
ENSECAG00000019768	ENSECAT00000021105	<i>GRAP2</i>	+	28	36689689	G	A	GTG	1	Val	Met	0.4653
ENSECAG00000004408	ENSECAT00000004329	<i>GPRI</i>	-	18	80490590	A	G	CAC	2	Val	Ala	0.4647
ENSECAG00000022292	ENSECAT00000023750		+	25	10628814	G	A	GGA	1	Gly	Arg	0.4632
ENSECAG00000024126	ENSECAT00000025990	<i>RFC1</i>	+	3	87992262	C	G	CTC	1	Leu	Val	0.4625
ENSECAG00000024126	ENSECAT00000025999	<i>RFC1</i>	+	3	87992262	C	G	CTC	1	Leu	Val	0.4625
ENSECAG00000000512	ENSECAT0000000397	<i>LBH</i>	-	15	66450983	T	C	GTT	2	Asn	Ser	0.4618
ENSECAG00000019204	ENSECAT00000020316		-	5	40670705	T	C	CTC	2	Glu	Gly	0.4618
ENSECAG00000005646	ENSECAT00000005595		-	14	92739894	C	T	ACT	2	Ser	Asn	0.4588
ENSECAG00000005646	ENSECAT00000005595		-	14	92740029	C	A	CCC	2	Gly	Val	0.4588
ENSECAG00000017048	ENSECAT00000017967	<i>CD101</i>	-	5	52075210	A	G	GTA	3	Tyr	His	0.4575
ENSECAG00000023120	ENSECAT00000024726	<i>ZFP69B</i>	-	2	17689694	T	C	GTT	3	Asn	Asp	0.4563
ENSECAG00000003862	ENSECAT00000004733	<i>NRD2</i>	-	24	33697644	T	G	GTT	3	Asn	His	0.4563
ENSECAG00000014425	ENSECAT00000015305	<i>PIGK</i>	+	5	85459673	T	C	GTC	2	Val	Ala	0.4549
ENSECAG00000002749	ENSECAT00000002789	<i>TKTL2</i>	+	2	71048367	C	T	CGA	1	Arg	Stop	0.4529
ENSECAG00000002041	ENSECAT00000019110	<i>OR51B5</i>	-	7	74123183	A	T	AAA	2	Phe	Tyr	0.4514
ENSECAG00000022217	ENSECAT00000024081	<i>UTP6</i>	+	11	40582906	A	C	ATC	1	Ile	Leu	0.4500
ENSECAG00000019457	ENSECAT00000020821	<i>CCDC108</i>	-	6	8596494	T	C	TGT	3	Thr	Ala	0.4500
ENSECAG00000009647	ENSECAT00000011076	<i>MGAM</i>	+	4	94831274	A	G	ACC	1	Thr	Ala	0.4500
ENSECAG00000026818	ENSECAT00000028860	<i>LRP11</i>	+	31	16993196	G	T	TGG	3	Trp	Cys	0.4479
ENSECAG00000024126	ENSECAT00000025990	<i>RFC1</i>	+	3	87992190	A	G	ACT	1	Thr	Ala	0.4477
ENSECAG00000024126	ENSECAT00000025999	<i>RFC1</i>	+	3	87992190	A	G	ACT	1	Thr	Ala	0.4477
ENSECAG00000024657	ENSECAT00000026613	<i>CHMP7</i>	+	2	51981404	T	C	GTT	2	Val	Ala	0.4449
ENSECAG00000007147	ENSECAT00000008062	<i>CAPRIN1</i>	+	12	950214	C	A	CCG	2	Pro	Gln	0.4444
ENSECAG00000008488	ENSECAT00000008751	<i>MIN4</i>	+	19	56891113	C	T	CGC	1	Arg	Cys	0.4444
ENSECAG00000026818	ENSECAT00000028860	<i>LRP11</i>	+	31	16993128	A	G	ACC	1	Thr	Ala	0.4444
ENSECAG00000007434	ENSECAT00000007431	<i>PRR9</i>	-	5	44362551	T	C	CGT	3	Thr	Ala	0.4444
ENSECAG00000011135	ENSECAT00000011552	<i>GPATCH4</i>	+	5	41672314	A	T	ACT	1	Thr	Ser	0.4444
ENSECAG00000017335	ENSECAT00000017455	<i>CDON</i>	-	7	34819663	A	G	GAA	3	Phe	Leu	0.4444
ENSECAG00000017335	ENSECAT00000028894	<i>CDON</i>	-	7	34819663	A	G	GAA	3	Phe	Leu	0.4444
ENSECAG00000017136	ENSECAT00000018105	<i>HEMK1</i>	-	16	36705050	G	T	TGC	2	Ala	Glu	0.4444
ENSECAG000000022378	ENSECAT000000023985	<i>IGSF3</i>	+	5	52444326	G	T	GCG	1	Ala	Ser	0.4444
ENSECAG000000022378	ENSECAT000000023989	<i>IGSF3</i>	+	5	52444326	G	T	GCG	1	Ala	Ser	0.4444
ENSECAG00000012533	ENSECAT00000013153	<i>RSPH4A</i>	+	10	65262821	A	G	GAA	2	Glu	Gly	0.4441
ENSECAG00000006841	ENSECAT00000006820		-	1	155745453	A	G	CAA	2	Leu	Ser	0.4437
ENSECAG00000004238	ENSECAT00000004178		-	1	155180795	G	A	GGG	2	Pro	Leu	0.4412
ENSECAG00000008618	ENSECAT00000008785	<i>LCA5L</i>	-	26	35417731	A	C	AAC	2	Val	Gly	0.4412
ENSECAG00000001007	ENSECAT0000000986		-	6	25639957	A	G	CAT	2	Met	Thr	0.4410
ENSECAG00000001007	ENSECAT0000000986		-	6	25640327	T	C	GAT	3	Ile	Val	0.4375
ENSECAG00000000355	ENSECAT0000000276		-	21	4116690	C	A	CTT	1	Lys	Asn	0.4375
ENSECAG0000001481	ENSECAT0000001358	<i>SAMD9L</i>	-	4	36789902	A	T	TAC	2	Val	Glu	0.4375
ENSECAG000000022630	ENSECAT000000025166		-	13	7486258	A	G	AGA	3	Ser	Pro	0.4353
ENSECAG00000014333	ENSECAT00000011865	<i>TET2</i>	-	2	119545075	G	C	GCG	2	Ala	Gly	0.4324
ENSECAG00000003379	ENSECAT00000003234		+	5	38662682	G	T	GCA	1	Ala	Ser	0.4324
ENSECAG000000025154	ENSECAT00000027160	<i>ADPRM</i>	+	11	53164385	A	G	ACA	1	Thr	Ala	0.4271
ENSECAG00000002094	ENSECAT00000021523	<i>DCLK3</i>	+	16	48308428	C	T	ACG	2	Thr	Met	0.4236
ENSECAG000000024761	ENSECAT00000026831	<i>INOS</i>	-	11	41896696	A	G	ACA	3	Cys	Arg	0.4228
ENSECAG000000024761	ENSECAT00000026843	<i>INOS</i>	-	11	41896696	A	G	ACA	3	Cys	Arg	0.4228
ENSECAG000000019438	ENSECAT00000020602	<i>OSMR</i>	-	21	26835081	T	C	GTA	2	Tyr	Cys	0.4211
ENSECAG00000006186	ENSECAT00000006135		+	12	18063623	T	C	CTG	2	Leu	Pro	0.4191
ENSECAG00000005195	ENSECAT00000005083		+	17	25869085	C	A	CCT	1	Pro	Thr	0.4184
ENSECAG00000003607	ENSECAT00000003475	<i>OR6K2</i>	+	5	38692038	C	T	CCC	1	Pro	Ser	0.4184
ENSECAG000000026868	ENSECAT00000028994	<i>C6orf183</i>	+	10	58985128	G	A	GTC	1	Val	Ile	0.4167

Table S4.3. Non-synonymous markers specific to Yakutian horses, ordered by specificity (3).

Gene ID	Transcript ID	Gene Name	Strand	Chr	Pos	NucRef	NucAlt	Codon	CodonPos	AARef	AAAlt	Delta
ENSECAG00000013249	ENSECAT00000013875	<i>UTP6</i>	-	12	16368660	C	T	GCG	2	Arg	His	0.4167
ENSECAG00000013249	ENSECAT00000013907		-	12	16368660	C	T	GCG	2	Arg	His	0.4167
ENSECAG00000012220	ENSECAT00000013076		+	18	59611848	A	C	ACT	1	Thr	Pro	0.4167
ENSECAG00000012220	ENSECAT00000013233		+	18	59611848	A	C	ACT	1	Thr	Pro	0.4167
ENSECAG00000017484	ENSECAT00000019252	<i>SSFA2</i>	+	22	19469586	G	C	AGT	2	Ser	Thr	0.4167
ENSECAG00000017484	ENSECAT00000019406	<i>SSFA2</i>	+	22	19469586	G	C	AGT	2	Ser	Thr	0.4167
ENSECAG00000018766	ENSECAT00000019943	<i>C20orf194</i>	-	31	16485432	G	C	GTG	1	His	Gln	0.4167
ENSECAG0000001481	ENSECAT0000001358	<i>C20orf194</i>	-	4	36788507	C	T	ACG	2	Arg	His	0.4167
ENSECAG00000021886	ENSECAT00000024105	<i>IYD</i>	+	5	38741054	G	A	CGT	2	Arg	His	0.4167
ENSECAG00000021886	ENSECAT00000024105	<i>SAMD9L</i>	+	5	38755214	C	T	CGC	1	Arg	Cys	0.4167
ENSECAG00000004825	ENSECAT0000004694	<i>SPTA1</i>	+	6	72700073	T	G	TTG	1	Leu	Val	0.4167
ENSECAG00000014894	ENSECAT00000015620	<i>SPTA1</i>	+	21	51321926	A	G	CAT	2	His	Arg	0.415
ENSECAG00000022607	ENSECAT00000024108		-	21	25316610	T	C	TTT	3	Lys	Glu	0.415
ENSECAG00000005754	ENSECAT0000005662	<i>FASTKD3</i>	+	10	12690122	G	C	GGG	2	Gly	Ala	0.4147
ENSECAG00000013392	ENSECAT00000014067		-	13	27721333	G	C	CGG	3	Pro	Ala	0.4132
ENSECAG00000014894	ENSECAT00000015620		+	21	51321925	C	T	CAT	1	His	Tyr	0.4132
ENSECAG00000000971	ENSECAT00000002158	<i>TMC5</i>	+	5	8511547	T	C	TCT	1	Ser	Pro	0.4132
ENSECAG00000010114	ENSECAT00000010916	<i>FASTKD3</i>	+	1	149766002	G	A	AGC	2	Ser	Asn	0.4125
ENSECAG000000020841	ENSECAT00000022128	<i>SUCO</i>	-	16	3868218	C	T	GAC	3	Val	Ile	0.4125
ENSECAG00000015268	ENSECAT00000016066	<i>RASGRP1</i>	-	10	50124737	C	T	AAC	3	Val	Ile	0.4118
ENSECAG00000019873	ENSECAT00000021083	<i>MRPS25</i>	-	14	82927811	T	C	TAT	3	Ile	Val	0.4118
ENSECAG00000024820	ENSECAT00000026813	<i>FBXL4</i>	+	22	26511151	C	A	ACA	2	Thr	Lys	0.4118
ENSECAG00000004038	ENSECAT0000003883		-	6	39182395	C	T	TCC	2	Gly	Glu	0.4118
ENSECAG00000004038	ENSECAT0000003883	<i>PHF20</i>	-	6	39182421	A	T	ACT	1	Ser	Arg	0.4118
ENSECAG00000015693	ENSECAT00000017333		+	6	42936427	C	T	ACA	2	Thr	Ile	0.4111
ENSECAG00000004053	ENSECAT0000003928		-	7	74793928	C	T	ACC	2	Gly	Asp	0.4097
ENSECAG00000020783	ENSECAT00000022047	<i>PTPRO</i>	+	15	61772275	T	G	TTC	2	Phe	Cys	0.4097
ENSECAG00000008213	ENSECAT0000008276		-	4	96558253	T	C	TTG	2	Gln	Arg	0.4097
ENSECAG00000006888	ENSECAT0000006857		+	1	157012356	A	G	CAG	2	Gln	Arg	0.4085
ENSECAG000000022192	ENSECAT00000023632		+	7	15694648	T	C	ATG	2	Met	Thr	0.4085
ENSECAG0000001095	ENSECAT0000000914		+	1	48293522	A	C	GAA	3	Glu	Asp	0.4081
ENSECAG0000000536	ENSECAT0000001244	<i>ZNF77</i>	-	1	12639680	C	G	AAC	3	Val	Leu	0.4062
ENSECAG0000003940	ENSECAT0000003793		-	11	38231191	C	T	AGC	3	Ala	Thr	0.4062
ENSECAG00000013249	ENSECAT00000013875	<i>SEC23IP</i>	-	12	16356917	A	G	AAA	3	Phe	Leu	0.4062
ENSECAG00000013249	ENSECAT00000013907		-	12	16356917	A	G	AAA	3	Phe	Leu	0.4062
ENSECAG0000001046	ENSECAT0000000903		-	14	92773688	T	C	GTG	2	His	Arg	0.4062
ENSECAG00000021057	ENSECAT00000023148		-	14	77154512	A	G	AAC	2	Val	Ala	0.4062
ENSECAG00000008471	ENSECAT00000008957		-	18	53252113	A	C	GGG	3	Ser	Ala	0.4062
ENSECAG00000019644	ENSECAT00000020802	<i>GPR98</i>	-	26	30158575	C	G	CCT	1	Arg	Ser	0.4062
ENSECAG00000022735	ENSECAT00000024598	<i>GPR155</i>	+	26	32662948	A	G	CAG	2	Gln	Arg	0.4062
ENSECAG00000022735	ENSECAT00000024602	<i>DNAJC28</i>	+	26	32662948	A	G	CAG	2	Gln	Arg	0.4062
ENSECAG00000000765	ENSECAT0000000617	<i>DOPEY2</i>	+	28	35568193	T	A	CTA	2	Leu	Gln	0.4062
ENSECAG00000018887	ENSECAT00000020177	<i>DOPEY2</i>	-	20	33419570	G	T	GGC	2	Ala	Asp	0.4059
ENSECAG00000014933	ENSECAT00000015588		+	4	95785514	A	C	AGT	1	Ser	Arg	0.4056
ENSECAG00000014933	ENSECAT00000015588		+	4	95785514	T	G	ATG	2	Met	Arg	0.4052
ENSECAG00000024156	ENSECAT00000026060		+	5	51156271	A	G	AAA	1	Lys	Glu	0.4052
ENSECAG00000015712	ENSECAT00000016565		+	7	74563791	C	T	TCT	2	Ser	Phe	0.4029
ENSECAG00000022171	ENSECAT00000023882	<i>SPAG17</i>	-	4	14999961	C	T	CTC	3	Glu	Lys	0.4028
ENSECAG0000003379	ENSECAT0000003234		+	5	38662935	C	T	GCT	2	Ala	Val	0.4028
ENSECAG00000004790	ENSECAT00000004685	<i>GCK</i>	+	5	37503723	G	T	TTG	3	Leu	Phe	0.4020
ENSECAG000000020525	ENSECAT00000021931		+	1	60935252	T	C	ATT	2	Ile	Thr	0.4000
ENSECAG00000007563	ENSECAT00000008109	<i>PIGM</i>	+	11	6361518	C	T	GCG	2	Ala	Val	0.4000
ENSECAG00000007563	ENSECAT00000008256	<i>NUDT13</i>	+	11	6361518	C	T	GCG	2	Ala	Val	0.4000
ENSECAG00000007563	ENSECAT00000008344	<i>RECQL5</i>	+	11	6361518	C	T	GCG	2	Ala	Val	0.4000
ENSECAG00000002813	ENSECAT00000013374	<i>RECQL5</i>	-	16	4787031	G	A	GGG	2	Pro	Leu	0.4000

*Codon on the negative strand (-) should be reverse complemented. “Chr#”: chromosome number; “NucRef”: reference nucleotide; “NucAlt”: alternative nucleotide; “CodonPos”: codon position; “AARef”: reference amino-acid; “AAAlt”: alternative amino acid; “Delta”: difference in frequency of the alternative allele between the two populations, positive when specific to the Yakutian horses.

Table S4.4. GO-term for genes enriched in Yakutian horse specific non-synonymous mutations.

GO-term	Model organism	Adjusted p-value	Gene ID	Gene Name
Disruption of cells of other organism	Human	0.0299	ENSG00000089041	P2RX7
			ENSG0000007171	NOS2
			ENSG00000163221	S100A12
C-terminal protein lipidation	Human	0.0299	ENSG00000143315	PIGM
			ENSG00000142892	PIGK
			ENSG00000060642	PIGV
Killing of cells of other organism	Human	0.0299	ENSG00000089041	P2RX7
			ENSG0000007171	NOS2
			ENSG00000163221	S100A12
Regulation of killing of cells of other organism	Human	0.0299	ENSG00000089041	P2RX7
			ENSG0000007171	NOS2
C-terminal protein amino acid modification	Human	0.0359	ENSG00000143315	PIGM
			ENSG00000142892	PIGK
			ENSG00000060642	PIGV
GPI anchor biosynthetic process	Human	0.0498	ENSG00000143315	PIGM
			ENSG00000142892	PIGK
			ENSG00000060642	PIGV
GPI anchor biosynthetic process	Mouse	0.0015	ENSMUSG00000050229	PIGM
			ENSMUSG00000032059	ALG9
			ENSMUSG00000043257	PIGV
			ENSMUSG00000039047	PIGK
GPI anchor metabolic process	Mouse	0.0015	ENSMUSG00000050229	PIGM
			ENSMUSG00000032059	ALG9
			ENSMUSG00000043257	PIGV
			ENSMUSG00000039047	PIGK
Membrane lipid biosynthetic process	Mouse	0.0015	ENSMUSG00000050229	PIGM
			ENSMUSG00000032059	ALG9
			ENSMUSG00000043257	PIGV
			ENSMUSG00000039047	PIGK
Glycolipid biosynthetic process	Mouse	0.0025	ENSMUSG00000050229	PIGM
			ENSMUSG00000032059	ALG9
			ENSMUSG00000043257	PIGV
			ENSMUSG00000039047	PIGK
Phosphatidylinositol metabolic process	Mouse	0.0042	ENSMUSG00000050229	PIGM
			ENSMUSG00000032059	ALG9
			ENSMUSG00000043257	PIGV
			ENSMUSG00000042105	INPP5F
			ENSMUSG00000039047	PIGK
Phosphatidylinositol biosynthetic process	Mouse	0.0042	ENSMUSG00000050229	PIGM
			ENSMUSG00000032059	ALG9
			ENSMUSG00000043257	PIGV
			ENSMUSG00000039047	PIGK
Protein lipidation	Mouse	0.0042	ENSMUSG00000050229	PIGM
			ENSMUSG00000032059	ALG9
			ENSMUSG00000043257	PIGV
			ENSMUSG00000039047	PIGK
Glycolipid metabolic process	Mouse	0.0048	ENSMUSG00000050229	PIGM
			ENSMUSG00000032059	ALG9
			ENSMUSG00000043257	PIGV
			ENSMUSG00000039047	PIGK
Lipoprotein biosynthetic process	Mouse	0.0048	ENSMUSG00000050229	PIGM
			ENSMUSG00000032059	ALG9
			ENSMUSG00000043257	PIGV
			ENSMUSG00000039047	PIGK
Membrane lipid metabolic process	Mouse	0.0048	ENSMUSG00000029468	P2RX7
			ENSMUSG00000050229	PIGM
			ENSMUSG00000032059	ALG9
			ENSMUSG00000043257	PIGV
			ENSMUSG00000039047	PIGK
Mannosyltransferase activity	Mouse	0.0024	ENSMUSG00000050229	PIGM
			ENSMUSG00000032059	ALG9

Table S4.5. KEGG pathways for genes enriched in Yakutian horse specific non-synonymous mutations.

KEGG Pathway	Model organism	Adjusted p-value	Gene ID	Gene Name	Model organism	Adjusted p-value	Gene ID	Gene Name
Olfactory transduction	Human	<0.0001	ENSG00000196171	<i>OR6K2</i>	Mouse	<0.0001	ENSMUSG00000070417	<i>OLFR2</i>
			ENSG00000176925	<i>OR51F2</i>			ENSMUSG00000054526	<i>OLFR1500</i>
			ENSG00000186943	<i>OR13C8</i>			ENSMUSG00000073898	<i>OLFR713</i>
			ENSG00000177489	<i>OR2G2</i>			ENSMUSG00000055033	<i>OLFR420</i>
			ENSG00000178586	<i>OR6B3</i>			ENSMUSG00000093804	<i>OLFR1303</i>
			ENSG00000166363	<i>OR1045</i>			ENSMUSG00000073965	<i>OLFR568</i>
			ENSG00000186509	<i>OR9O1</i>			ENSMUSG00000051593	<i>OLFR272</i>
			ENSG00000184933	<i>OR6A2</i>				
Glycosylphosphatidylinositol(GPI)-anchor biosynthesis	Human	0.0003	ENSG00000143315	<i>PIGM</i>	Mouse	0.0001	ENSMUSG00000050229	<i>PIGM</i>
			ENSG00000142892	<i>PIGK</i>			ENSMUSG00000043257	<i>PIGV</i>
			ENSG00000060642	<i>PIGV</i>			ENSMUSG00000039047	<i>PIGK</i>
Metabolic pathways	Human	0.0027	ENSG00000143315	<i>PIGM</i>	Mouse	0.0001	ENSMUSG00000068587	<i>MGAM</i>
			ENSG00000177084	<i>POLE</i>			ENSMUSG00000020826	<i>NOS2</i>
			ENSG00000106633	<i>GCK</i>			ENSMUSG00000007080	<i>POLE</i>
			ENSG00000142892	<i>PIGK</i>			ENSMUSG00000025519	<i>TKTL2</i>
			ENSG00000021461	<i>CYP3A43</i>			ENSMUSG00000034579	<i>PLA2G3</i>
			ENSG00000257335	<i>MGAM</i>			ENSMUSG00000032059	<i>ALG9</i>
			ENSG00000151005	<i>TKTL2</i>			ENSMUSG00000054417	<i>CYP3A44</i>
			ENSG00000007171	<i>NOS2</i>			ENSMUSG00000041798	<i>GCK</i>
			ENSG00000100078	<i>PLA2G3</i>			ENSMUSG00000039047	<i>PIGK</i>
			ENSG00000060642	<i>PIGV</i>			ENSMUSG00000050229	<i>PIGM</i>
							ENSMUSG00000043257	<i>PIGV</i>
Galactose metabolism	Human	0.0095	ENSG00000257335	<i>MGAM</i>	Mouse	0.0053	ENSMUSG00000068587	<i>MGAM</i>
			ENSG00000106633	<i>GCK</i>			ENSMUSG00000041798	<i>GCK</i>
Linoleic acid metabolism	Human	0.0096	ENSG00000021461	<i>CYP3A43</i>	Mouse	0.0060	ENSMUSG00000034579	<i>PLA2G3</i>
			ENSG00000100078	<i>PLA2G3</i>			ENSMUSG00000054417	<i>CYP3A44</i>
DNA replication	Human	0.0113	ENSG0000035928	<i>RFC1</i>	Mouse	0.0053	ENSMUSG0000007080	<i>POLE</i>
			ENSG00000177084	<i>POLE</i>			ENSMUSG00000029191	<i>RFC1</i>
Toxoplasmosis		0.0117	ENSG00000196569	<i>LAMA2</i>	Mouse	0.0053	ENSMUSG00000020826	<i>NOS2</i>
			ENSG00000007171	<i>NOS2</i>			ENSMUSG00000034579	<i>PLA2G3</i>
			ENSG00000100078	<i>PLA2G3</i>			ENSMUSG00000019899	<i>LAMA2</i>
Nucleotide excision repair	Human	0.0127	ENSG0000035928	<i>RFC1</i>	Mouse	0.0060	ENSMUSG0000007080	<i>POLE</i>
			ENSG00000177084	<i>POLE</i>			ENSMUSG00000029191	<i>RFC1</i>
Starch and sucrose metabolism	Human	0.0169	ENSG00000257335	<i>MGAM</i>	Mouse	0.0060	ENSMUSG00000068587	<i>MGAM</i>
			ENSG00000106633	<i>GCK</i>			ENSMUSG00000041798	<i>GCK</i>
Calcium signaling pathway	Human	0.0182	ENSG00000089041	<i>P2RX7</i>	Mouse	0.0068	ENSMUSG00000029468	<i>P2RX7</i>
			ENSG00000170425	<i>ADORA2B</i>			ENSMUSG00000020826	<i>NOS2</i>
			ENSG00000007171	<i>NOS2</i>			ENSMUSG00000018500	<i>ADORA2B</i>

Table S4.6. Wikipathways for genes enriched in Yakutian horse specific non-synonymous mutations.

Wikipathway	Model organism	Adjusted p-value	Gene ID	Gene Name
DNA Replication	Human	0.0094	ENSG00000035928	<i>RFC1</i>
			ENSG00000177084	<i>POLE</i>
GPCRs, Class A Rhodopsin-like	Human	0.0094	ENSG00000166363	<i>OR10A5</i>
			ENSG00000170425	<i>ADORA2B</i>
			ENSG00000183671	<i>GPR1</i>
			ENSG00000184933	<i>OR6A2</i>
GPCRs, Other	Human	0.0339	ENSG00000166363	<i>OR10A5</i>
			ENSG00000164199	<i>GPR98</i>
DNA Replication	Human	0.0107	ENSMUSG0000007080	<i>POLE</i>
			ENSMUSG00000029191	<i>RFC1</i>
Odorant GPCRs	Mouse	0.0107	ENSMUSG00000056115	<i>TAS2R134</i>
			ENSMUSG00000041762	<i>GPR155</i>
			ENSMUSG00000046856	<i>GPR1</i>
GPCRs, Class A Rhodopsin-like	Mouse	0.0108	ENSMUSG00000070417	<i>OLFR2</i>
			ENSMUSG00000073898	<i>OLFR713</i>
			ENSMUSG00000018500	<i>ADORA2B</i>
MAPK signaling pathway	Mouse	0.0394	ENSMUSG00000041798	<i>GCK</i>
			ENSMUSG00000027347	<i>RASGRPI</i>

Table S4.7. Phenotypes for genes enriched in Yakutian horse specific non-synonymous mutations.

Phenotype	Model organism	Adjusted p-value	Gene ID	Gene Name
Abnormal bone healing	Mouse	0.0312	ENSMUSG00000020826	<i>NOS2</i>
			ENSMUSG00000040297	<i>SUCO</i>
Increased T cell number	Mouse	0.0312	ENSMUSG00000042351	<i>GRAP2</i>
			ENSMUSG00000020826	<i>NOS2</i>
			ENSMUSG00000040943	<i>TET2</i>
			ENSMUSG00000026532	<i>SPNA1</i>
			ENSMUSG00000027347	<i>RASGRPI</i>
			ENSMUSG00000001123	<i>LGALS9</i>
Increased circulating prolactin level	Mouse	0.0312	ENSMUSG00000020826	<i>NOS2</i>
			ENSMUSG00000019899	<i>LAMA2</i>
Decreased hematopoietic cell number	Mouse	0.0312	ENSMUSG00000042351	<i>GRAP2</i>
			ENSMUSG00000020826	<i>NOS2</i>
			ENSMUSG00000022146	<i>OSMR</i>
			ENSMUSG00000019899	<i>LAMA2</i>
			ENSMUSG00000001123	<i>LGALS9</i>
			ENSMUSG00000040943	<i>TET2</i>
			ENSMUSG00000086564	<i>CD101</i>
			ENSMUSG00000040297	<i>SUCO</i>
			ENSMUSG00000026532	<i>SPNA1</i>
			ENSMUSG00000027347	<i>RASGRPI</i>
Increased prolactin level	Mouse	0.0333	ENSMUSG00000020826	<i>NOS2</i>
			ENSMUSG00000019899	<i>LAMA2</i>
Abnormal hematopoietic cell number	Mouse	0.0347	ENSMUSG00000029468	<i>P2RX7</i>
			ENSMUSG00000042351	<i>GRAP2</i>
			ENSMUSG00000020826	<i>NOS2</i>
			ENSMUSG00000022146	<i>OSMR</i>
			ENSMUSG00000019899	<i>LAMA2</i>
			ENSMUSG00000001123	<i>LGALS9</i>
			ENSMUSG00000040943	<i>TET2</i>
			ENSMUSG00000086564	<i>CD101</i>
			ENSMUSG00000040297	<i>SUCO</i>
			ENSMUSG00000026532	<i>SPNA1</i>
			ENSMUSG00000027347	<i>RASGRPI</i>
Abnormal leukocyte cell number	Mouse	0.0357	ENSMUSG00000029468	<i>P2RX7</i>
			ENSMUSG00000042351	<i>GRAP2</i>
			ENSMUSG00000020826	<i>NOS2</i>
			ENSMUSG00000019899	<i>LAMA2</i>
			ENSMUSG00000001123	<i>LGALS9</i>
			ENSMUSG00000040943	<i>TET2</i>
			ENSMUSG00000086564	<i>CD101</i>
			ENSMUSG00000040297	<i>SUCO</i>
			ENSMUSG00000026532	<i>SPNA1</i>
			ENSMUSG00000027347	<i>RASGRPI</i>

Table S4.8. Diseases for genes enriched in Yakutian horse specific non-synonymous mutations.

Disease	Model organism	Adjusted p-value	Gene ID	Gene Name
Immune System Diseases	Human	0.0122	ENSG00000204264	<i>PSMB8</i>
			ENSG00000132256	<i>TRIM5</i>
			ENSG00000183671	<i>GPR1</i>
			ENSG00000089041	<i>P2RX7</i>
			ENSG00000035928	<i>RFC1</i>
			ENSG00000007171	<i>NOS2</i>
			ENSG00000172575	<i>RASGRP1</i>
			ENSG00000163221	<i>S100A12</i>
Leukemia	Human	0.0122	ENSG00000145623	<i>OSMR</i>
			ENSG00000089041	<i>P2RX7</i>
			ENSG00000168769	<i>TET2</i>
			ENSG00000151490	<i>PTPRO</i>
			ENSG00000035928	<i>RFC1</i>
			ENSG00000132704	<i>FCRL2</i>
			ENSG00000132256	<i>TRIM5</i>
Lymphatic Diseases	Human	0.0122	ENSG00000089041	<i>P2RX7</i>
			ENSG00000151490	<i>PTPRO</i>
			ENSG00000035928	<i>RFC1</i>
			ENSG00000132704	<i>FCRL2</i>
			ENSG00000135604	<i>STX11</i>
			ENSG00000172575	<i>RASGRP1</i>
Inflammation	Human	0.0214	ENSG00000145623	<i>OSMR</i>
			ENSG00000089041	<i>P2RX7</i>
			ENSG00000170425	<i>ADORA2B</i>
			ENSG00000007171	<i>NOS2</i>
			ENSG00000163221	<i>S100A12</i>
			ENSG00000163736	<i>PPBP</i>
Histiocytosis, Langerhans-Cell	Human	0.0227	ENSG00000134256	<i>CD101</i>
Thrombocytosis	Human	0.0227	ENSG00000135604	<i>STX11</i>
Nelson syndrome	Human	0.0227	ENSG00000088854	<i>C20orf194</i>
			ENSG00000168769	<i>TET2</i>
			ENSG00000021461	<i>CYP3A43</i>
			ENSG00000257335	<i>MGAM</i>
			ENSG00000138434	<i>SSFA2</i>
			ENSG00000128519	<i>TAS2R16</i>
			ENSG00000163328	<i>GPR155</i>
Trisomy	Human	0.0235	ENSG00000183671	<i>GPR1</i>
			ENSG00000163736	<i>PPBP</i>
			ENSG00000213626	<i>LBH</i>
			ENSG00000142197	<i>DOPEY2</i>
Leishmaniasis	Human	0.0235	ENSG00000035928	<i>RFC1</i>
			ENSG00000171916	<i>LGALS9C</i>
			ENSG00000007171	<i>NOS2</i>
Bronchitis	Human	0.0235	ENSG00000204264	<i>PSMB8</i>
			ENSG00000111834	<i>RSPH4A</i>
			ENSG00000007171	<i>NOS2</i>
			ENSG00000163736	<i>PPBP</i>

Table S4.9. Loci underlying Mendelian traits in horses.

Chrom.	Coordinate	Gene	Phenotype	Reference
1	74,842,283	<i>ACTN2</i>	Racing performance	Hill et al. 2010 (50)
1	108,249,293	<i>TRPM1</i>	Leopard complex spotting and cation channel congenital stationary night blindness	Bellone et al. 2010 (51)
1	128,056,148	<i>PPIB</i>	Hereditary equine dermal isomerase B asthenia	Tryon et al. 2007 (52)
1	138,235,715	<i>MYO5A</i>	Lavender foal syndrome	Brooks et al. 2010 (53)
2	13,074,277	<i>TOE1</i>	Cerebellar abiotrophy	Brault et al. 2011 (54)
3	32,772,871	<i>COX4/1</i>	Racing performance	Hill et al. 2010 (50)
3	36,259,552	<i>MCIR (1)</i>	Chestnut coat color	Marklund et al. 1996 (55)
3	36,259,554	<i>MCIR (2)</i>	Chestnut coat color	Wagner et al. 2000 (56)
3	77,735,520	<i>KIT (1)</i>	Sabino spotting	Brooks et al. 2005 (57)
3	77,740,161	<i>KIT (2)</i>	Tobiano spotting	Brooks et al. 2002 (58)
3	105,547,002	<i>LCORL/NCAPG</i>	Larger body size	Makvandi-Nejad et al. 2012 (59), Signer-Hasler et al. 2012 (40)
4	38,697,145	<i>PON1</i>	Racing performance	Hill et al. 2010 (50)
4	38,969,307	<i>PDK4 (1)</i>	Racing performance	Hill et al. 2010 (50)
4	38,973,231	<i>PDK4 (2)</i>	Racing performance	Hill et al. 2010 (50)
4	40,279,726	<i>ACN9</i>	Racing performance	Hill et al. 2010 (50)
4	96,375,588	<i>CLCN1</i>	Congenital myotonia	Wijnberg et al. 2012 (60)
5	20,256,789	<i>LAMC2</i>	Junctional epidermolysis bullosa	Spirito et al. 2002 (61)
6	11,429,753	<i>PAX3</i>	Splashed white coat	Hauswirth et al. 2012, Hauswirth et al. 2013 (62, 63)
6	73,665,304	<i>PMEL17</i> (also known as <i>SIL11</i>)	Silver coat color	Brunberg et al. 2006 (64)
6	81,481,065	<i>HMG A2</i>	Larger body size	Makvandi-Nejad et al. 2012 (59)
9	35,528,429	<i>DNAPK</i>	Severe combined immunodeficiency	Shin et al. 1997 (65)
9	74,795,013	<i>ZFAT (1)</i>	Wither height	Signer-Hasler et al. 2012 (40)
9	74,795,089	<i>ZFAT (2)</i>	Wither height	Signer-Hasler et al. 2012 (40)
9	74,795,236	<i>ZFAT (3)</i>	Wither height	Signer-Hasler et al. 2012 (40)
9	74,798,143	<i>ZFAT (4)</i>	Wither height	Signer-Hasler et al. 2012 (40)
9	75,550,059	<i>ZFAT (5)</i>	Larger body size	Makvandi-Nejad et al. 2012 (59)
10	9,554,699	<i>RYR1</i>	Malignant hyperthermia	Aleman et al. 2004 (66)
10	15,884,567	<i>CKM</i>	Racing performance	Gu et al. 2010 (67)
10	18,940,324	<i>GYS1</i>	Polysaccharide storage myopathy	McCue et al. 2012 (68)
11	15,500,439	<i>SCN4A</i>	Equine hyperkalemic periodic paralysis	Cannon et al. 1995 (69)
11	19,184,674	<i>ITGA2B</i>	Glanzmann Thrombasthenia	Christopherson et al. 2007 (70)
11	23,259,732	<i>LASP1</i>	Larger body size	Makvandi-Nejad et al. 2012 (59)
14	3,761,254	<i>PROPI (1)</i>	Dwarfism	Orr et al. 2010 (71)
14	3,761,355	<i>PROPI (2)</i>	Dwarfism	Orr et al. 2010 (71)
14	5,418,619	Intergenic	Dwarfism	Orr et al. 2010 (71)
14	26,701,092	<i>SLC36A1</i>	Champagne dilution	Cook et al. 2008 (72)
14	27,991,841	<i>SLC26A2</i>	Autosomal recessively inherited chondrodysplasia	Hansen et al. 2007 (73)
16	20,103,081	<i>MITF (1)</i>	Macchiato, hearing loss	Hauswirth et al. 2012, Hauswirth et al. 2013 (62, 63)
16	20,105,348	<i>MITF (2)</i>	Splashed white coat	Hauswirth et al. 2012, Hauswirth et al. 2013 (62, 63)
16	20,117,302	<i>MITF (3)</i>	Splashed white coat	Hauswirth et al. 2012, Hauswirth et al. 2013 (62, 63)
17	50,624,658	<i>EDNRB</i>	Lethal white foal syndrome	Yang et al. 1998 (74)
18	66,493,737	<i>MSTN</i>	Optimum racing position	Tozaki et al. 2010, Hill et al. 2012 (75, 76)
21	30,666,626	<i>SLC45A2</i> (also known as <i>MATP</i>)	Cream coat color	Mariat et al. 2003 (77)
22	22,684,390	<i>COX4/2</i>	Racing performance	Gu et al. 2010 (67)
22	25,168,579	<i>ASIP</i>	Black and bay color	Rieder et al. 2001 (78)
23	22,999,655	<i>DMRT3</i>	Pattern of locomotion (altered gait)	Andersson et al. 2012 (79)
26	30,660,224	<i>SLC5A3</i>	Foal immunodeficiency syndrome	Fox-Clipsham et al. 2011 (80)
X	49,635,250	<i>AR</i>	Androgen insensitivity syndrome (AIS)	Revay et al. 2012 (81)
X	122,833,887	<i>IKBKG</i>	Incontinentia pigmenti	Towers et al. 2013 (82)

Table S4.10. Mendelian variant genotypes in Late Pleistocene horses, ancient and present-day horses from Yakutia.

Gene	Mutation	22	23	Batagai	37	Yak1	Yak2	Yak3	Yak4	Yak5	Yak6	Yak7	Yak8	Yak9
<i>ACTN2</i>	A>G	.	A4	.	A/G	.	A/G	.	G/G	G/G	G/G	A/G	A4,G1	A6
<i>TRPM1</i>	C>T
<i>PPIB</i>	G>A	G4	G5	G6
<i>MYO5A</i>	1 DEL
<i>TOE1</i>	C>T
<i>COX4/1</i>	C>T	.	C1,T4	C/T	T/T	T/T	T/T	T/T	C/T	C/T	T/T	C/T	C/T	T/T
<i>MCIR (1)</i>	C>T	T/T	C/T	T/T	.	.	T/T	C/T	T/T	.
<i>MCIR (2)</i>	G>A	A/G	.	A/G
<i>KIT (1)</i>	A>T	.	A1	.	A6	.	.	.	A4	A7
<i>KIT (2)</i>	G>C	G6	.	.
<i>LCORL / NCAPG</i>	T>C	.	T7	.	.	C4,T14	.	T7
<i>PON1</i>	C>T
<i>PDK4 (1)</i>	C>A	.	C5	.	A/C	.	.	A/C
<i>PDK4 (2)</i>	G>A	.	G3	G5
<i>ACN9</i>	C>T	C/T	C/T	C/T	C/T	T/T	.	T/T	C/T	.	C/T	C/T	C/T	C11,T11
<i>CLCN1</i>	A>C
<i>LAMC2</i>	1C INS
<i>PAX3</i>	C>T	C3	.	C2
<i>PMEL17</i>	G>A
<i>HMG2A</i>	C>T	C2	C4	T/T	T3	T7	T/T	T/T	C/T	T/T	T6	T/T	T3	C/T
<i>DNAPK</i>	5 DEL
<i>ZFAT (1)</i>	C>T	C/T	C1,T1	.	C/T	C4,T2	.	T3	C/T	C/T	C/T	C/T	.	T/T
<i>ZFAT (2)</i>	C>A	A/C	C1	.	A/C	A/C	.	A4	A/C	A/C	A/C	A/C	.	A/A
<i>ZFAT (3)</i>	G>A	A/G	A1,G4	.	A4,G23	A1,C2,G2	.	A4,C1	A/G	A2,G11	A/G	.	.	A6
<i>ZFAT (4)</i>	G>A	A/G	A/G	.	A/G	A2,G1	.	A4	A2,G7	A/G	A/G	.	.	A/A
<i>ZFAT (5)</i>	C>T	C/T	C/T	C/T	.	.	.	C/T	.	.
<i>RYR1</i>	C>G
<i>CKM</i>	G>A	.	A/G	A/A	A/G	G7	.	A3,G1	A/G	A/G	A/A	A/G	G6	G4
<i>GYS1</i>	C>T
<i>SCN4A</i>	C>T
<i>ITGA2B</i>	10 DEL
<i>LASP1</i>	G>A	.	G4	.	A/G	A3	G3	A1,G2	G1	G1	.	A4,G3	G3	G1
<i>PROPI (1)</i>	G>C	C/G	C4,G2	C/C	C/G	C5	C/G	.	C/G	C/G	C/C	C/G	.	.
<i>PROPI (2)</i>	T>C	C/C	C4,T2	C/C	C/T	C/C	C/T	.	C/T	C/T	C/T	C/T	.	.
Intergenic	G>A	A4,G2	A/G	G8,T1	G3
<i>SLC36A1</i>	G>C
<i>SLC26A2</i>	G>A
<i>MITF (1)</i>	T>C	T5
<i>MITF (2)</i>	5 DEL
<i>MITF (3)</i>	11 DEL
<i>EDNRB</i>	GA>CT
<i>MSTN</i>	T>C	T7	T2	.	T2	.	C/T	.	T4	T7
<i>SLC45A2</i>	G>A	G7	.	.
<i>COX4/2</i>	C>T	.	.	C/T	C/T	.	.	C4	.	T/T	C/T	.	C/T	T/T
<i>ASIP</i>	11 DEL	+/?	+-	+-	+-	.	.	+-	+-	.
<i>DMRT3</i>	C>A	C4
<i>SLC5A3</i>	C>T
<i>AR</i>	A>G	A3	A4
<i>IKBKG</i>	C>T	C4	.	.

“INS”: insertion; “DEL”: bp deletion; “22”: CGG10022; “23”: CGG10023”; “97”: CGG101397. A dot (.) stands for same alleles as the common allele, otherwise alternate allele associated with the Mendelian trait. A positive sign (+) refers to the presence of indels, while a minus sign (-) stands for the absence of indels.

Table S4.11. Mendelian variant genotypes in Late Pleistocene and domesticated horses.

Gene	Mutation	FM0431	FM0450	FM0467	FM1030	FM1041	FM1190	FM1785	FM1798	FM1932	FM1948	FM1951	FM2218	EMS595	A1543	A5659	A5964	A2085	M977	M5256	M1009		
<i>ACTN2</i>	A>G						A4										A/G						
<i>TRPM1</i>	C>T	C/T	C5			C1	C/T		C/T		C4				C3								
<i>PPIB</i>	G>A	G6	G4			G4	G3	G3				G3			G1	G4		NA		G4	G4		
<i>MYO5A</i>	1 DEL																						
<i>TOE1</i>	C>T	C4				C2								C4			C4		C4		C3		
<i>COX4/1</i>	C>T	C3,T2	T/T	T/T	C/T	C1,T3	C/T	T/T	C/T	C/T	C1,T2			C1	C/T	C4	C1,T2	C2,T3	C/T	T4	C2		
<i>MCIR (I)</i>	C>T	C1	C2	T/T	C1,T4	C5,T2	C/T	C5	T/T		C2,T2		C/T	T2	T2	T3	T/T	C1,T1			C1		
<i>MCIR (2)</i>	G>A	NA	G1			G3				G5			G4		G3	G3	G4			G2			
<i>KIT (I)</i>	A>T																A3				A5		
<i>KIT (2)</i>	G>C						G6								G3						G3		
<i>LCORL / NCAPG</i>	T>C					C/T	C/T		C/T									C/T	C/T				
<i>PON1</i>	C>T	C4				C3								C4		T2		C1	C/T	C6	C2	T2	
<i>PDK4 (I)</i>	G>A	A/G			A/C	A/C	A2	A/A		A/C		G2	A/A		A/C	A/C	A/G			A2,C4			
<i>PDK4 (2)</i>	G>A				A2,G10	A/G	A1,G4	A/A		A/A				A/C	A/C	A/G	A/G			A/G			
<i>ACN9</i>	C>T		C/T	T/T		C3,T2	T/T		C/T	T6				A4				T/T	T/T	C/T	C/T	C/T	
<i>CLCN1</i>	A>C	A6																	A4		A3		
<i>LAMC2</i>	1C INS																						
<i>PAX3</i>	C>T	C2	C1			C3		C2			C2			C3	C2			C3	C4	C1	C3		
<i>PMEL17</i>	G>A					G5				G2								G3			G3		
<i>HMG2</i>	C>T	T/T	T/T	T/T	C/T	T/T	T/T	T/T	T/T	T/T	C/T	C/T	T/T	T/T	T/T	T/T	C/T	C/T	T/T	T/T	T5		
<i>DNAPK</i>	5 DEL																						
<i>ZFAT (I)</i>	C>T	C/T	C/T			T2	C/T		T/T	C2,T1	C1			C/T	C/T			C/T	C/T			C2	
<i>ZFAT (2)</i>	C>A	A/C	A/C			A/A	A/C		A/A	A1,C3	A1,C5			A/C	A/C			A/C	A/C			C6	
<i>ZFAT (3)</i>	G>A	A3,G1	A/G			A3	A/G		A/A	A4,G2	A/G			A/G	A1,G3			A/G	A5				
<i>ZFAT (4)</i>	G>A	A1,G7	A2,G2			A4	A/G		A/A	A/G	A/G			A2,G1	A3,G2	G1		A/G	A1,G2				
<i>ZFAT (5)</i>	C>T						C/T	C/T	C/T	C/T								C2,T1		C/T	T3		
<i>RYR1</i>	C>G		C2							C4					C2	C2			NA		C3	C1	
<i>CKM</i>	G>A	A/G	A/G		G3	G3	A/G	A/G		G4	A/G	A/G		A/A	A6	A6	A/A	A/G	A1,G2	A1,G2	A4	A1,G2	
<i>GYSI</i>	C>T					C2,T1				C6	C4	C5			C3						C3		
<i>SCN4A</i>	C>T	C3	C5																			C4	
<i>ITGA2B</i>	10 DEL																						
<i>LASP1</i>	G>A	A2	NA	A2	A1	A2	A/A	G1	A1	G1	NA	A1	NA	A/A	A3	G4	A1,G5	G1	G3	G2	A1		
<i>PROPI (1)</i>	G>C	C/G	G4	C/G		G5			C/G	C/C			C/G	G4				C3,G2	G5			G2	
<i>PROPI (2)</i>	T>C			C/T		T2				C/C			C/T		T3				T4	T1	T3		
Intergenic	G>A	A1,G4		A1,G1	A/G	A/G	A/G		A/G	A1	G2	A/G				A1,G1	A/G	NA	G4		G1		
<i>SLC36A1</i>	G>C					G4																	
<i>SLC26A2</i>	G>A																						
<i>MITF (I)</i>	T>C																						T4
<i>MITF (2)</i>																							
<i>MITF (3)</i>																							
<i>EDNRB</i>	GA>CT																						
<i>MSTN</i>	T>C		C/T	C/T	C/T					C/T					C2,T9	C/T	C/C	C1	C7				
<i>SLC45A2</i>	G>A										G3					A/A			G3			G4	
<i>COX4/2</i>	C>T	T5	C/T	C/T		C2,T2	C/T			C4	C3	C3		C1	T/T	C2	T/T	C3,T2	C/T	C/T	C3		
<i>ASIP</i>						+/-		+/-	+/-					+/-		+/-	+/-	+/-	+/-				
<i>DMRT3</i>	C>A	C3	C5			C4					C3			C3	C3			NA	A4	A3	A1		
<i>SLC5A3</i>	C>T	C4																			C5		
<i>AR</i>	A>G	NA	A3	A3		A2	A3	A5		A2	A2		A3					A2		A1	A1		
<i>IKBKG</i>	C>T	C4	C3	C1		C1	C4		C5	C2		C2	C2		C3	C3		C1	C3	C4	C4		

"INS": insertion; "DEL": bp deletion; "FM0431": "Mon_FM0431"; "FM0450": "Mon_FM0450"; "FM0467": "Mon_FM0467"; "FM1030": "Mon_FM1030"; "FM1041": "Mon_FM1041"; "FM1190": "Mon_FM1190"; "FM1190": "Mon_FM1190"; "FM1785": "Mon_FM1785"; "FM1798": "Mon_FM1798"; "FM1932": "Mon_FM1932"; "FM1948": "Mon_FM1948"; "FM1951": "Mon_FM1951"; "FM2218": "Mon_FM2218"; "EMS595": "Mor_EM595"; "A1543": "Qrt_A1543"; "A5659": "Qrt_A5659"; "A5964": "Qrt_A5964"; "A2085": "Qrt_A2085"; "M977": "Std_M977"; "M5256": "Std_M5256"; "M1009": "Std_M1009". A dot (.) stands for same alleles as the common allele, otherwise alternate allele associated with the Mendelian trait. A positive sign (+) refers to the presence of indels, while a minus sign (-) stands for the absence of indels.

Table S4.12. Genes contained in segmental duplications in Yakutian horses and encoding proteins of known functions (1).

Chr#	Gene ID	#Carriers	#Females	#Males	Gene Name	Gene Description
1	ENSECAG00000012176	7	4	3	<i>SNX6</i>	sorting nexin 6
19	ENSECAG00000008906	7	4	3	<i>PARP15</i>	poly (ADP-ribose) polymerase family, member 15
29	ENSECAG00000024146	7	4	3	<i>UCMA</i>	upper zone of growth plate and cartilage matrix associated
9	ENSECAG0000007583	5	4	1	<i>LY6K</i>	lymphocyte antigen 6 complex, locus K
18	ENSECAG0000009694	5	3	2	<i>IWS1</i>	IWS1 homolog (S. cerevisiae)
3	ENSECAG0000000727	4	4	0	<i>HTRA3</i>	HtrA serine peptidase 3
3	ENSECAG00000020879	4	4	0	<i>SH3TC1</i>	SH3 domain and tetratricopeptide repeats 1
12	ENSECAG00000020462	4	3	1	<i>GSTPI</i>	glutathione S-transferase pi 1
14	ENSECAG00000013199	4	3	1	<i>PCDH1</i>	protocadherin alpha 1
19	ENSECAG00000024988	4	3	1	<i>PARP14</i>	poly (ADP-ribose) polymerase family, member 14
25	ENSECAG00000017095	4	2	2	<i>CAMSAP1</i>	calmodulin regulated spectrin-associated protein 1
25	ENSECAG00000021229	4	4	0	<i>SURF6</i>	surfeit 6
28	ENSECAG00000022371	4	2	2	<i>APOBEC3Z1B</i>	Equus caballus apolipoprotein B mRNA-editing enzyme-catalytic polypeptide-like 3Z1b (APOBEC3Z1B), mRNA.
Un	ENSECAG00000004570	4	3	1	<i>OR4C3</i>	olfactory receptor, family 4, subfamily C, member 3
X	ENSECAG00000000012	4	4	0	<i>PRKX</i>	protein kinase, X-linked
X	ENSECAG00000000026	4	4	0	<i>XG</i>	Xg blood group
X	ENSECAG00000003414	4	4	0	<i>ZBED1</i>	zinc finger, BED-type containing 1
X	ENSECAG00000005751	4	4	0	<i>GYG2</i>	glycogenin 2
X	ENSECAG00000009174	4	4	0	<i>ARSD</i>	arylsulfatase D
X	ENSECAG00000010384	4	4	0	<i>ARSE</i>	arylsulfatase E (chondrodysplasia punctata 1)
X	ENSECAG00000012190	4	4	0	<i>ARSH</i>	arylsulfatase family, member H
X	ENSECAG00000014736	4	4	0	<i>OFDI</i>	oral-facial-digital syndrome 1
X	ENSECAG00000015651	4	4	0	<i>ARSF</i>	arylsulfatase F
X	ENSECAG00000017487	4	4	0	<i>MXRA5</i>	matrix-remodelling associated 5
X	ENSECAG00000022025	4	4	0	<i>SCML2</i>	sex comb on midleg-like 2 (Drosophila)
X	ENSECAG00000022295	4	4	0	<i>AKAP17A</i>	A kinase (PRKA) anchor protein 17A
X	ENSECAG00000022808	4	4	0	<i>ASMT</i>	acetylserotonin O-methyltransferase
2	ENSECAG00000021856	3	3	0	<i>PADI2</i>	Equus caballus peptidyl arginine deiminase, type II (PADI2), mRNA.
2	ENSECAG00000024136	3	2	1	<i>RHOBTB2</i>	Rho-related BTB domain containing 2
7	ENSECAG00000005132	3	1	2	<i>OR2D3</i>	olfactory receptor, family 2, subfamily D, member 3
7	ENSECAG00000011501	3	1	2	<i>ZNF215</i>	zinc finger protein 215
8	ENSECAG00000014402	3	2	1	<i>MPHOSPH9</i>	M-phase phosphoprotein 9
8	ENSECAG00000020493	3	2	1	<i>TOP3B</i>	topoisomerase (DNA) III beta
10	ENSECAG00000001193	3	2	1	<i>EQUCABV1R918</i>	Equus caballus vomeronasal 1 receptor equCabV1R918 (EQUCABV1R918), mRNA.
10	ENSECAG00000009053	3	1	2	<i>ZNF304</i>	zinc finger protein 304
13	ENSECAG00000015801	3	2	1	<i>POLR3E</i>	polymerase (RNA) III (DNA directed) polypeptide E (80kD)
16	ENSECAG00000009171	3	2	1	<i>NUP210</i>	nucleoporin 210kDa
20	ENSECAG00000013685	3	1	2	<i>TNXB</i>	tenascin XB
X	ENSECAG00000007323	3	3	0	<i>MTMR1</i>	myotubularin related protein 1
2	ENSECAG00000012961	2	0	2	<i>HSPG2</i>	heparan sulfate proteoglycan 2
3	ENSECAG00000014798	2	1	1	<i>ZNF19</i>	zinc finger protein 19
5	ENSECAG00000024827	2	1	1	<i>ATP1A2</i>	ATPase, Na+/K+ transporting, alpha 2 polypeptide
6	ENSECAG00000004076	2	2	0	<i>OR10A7</i>	olfactory receptor, family 10, subfamily A, member 7
8	ENSECAG00000011312	2	0	2	<i>RTDRI</i>	rhabdoid tumor deletion region gene 1
8	ENSECAG00000018855	2	2	0	<i>EP400NL</i>	EP400 N-terminal like

Table S4.12. Genes contained in segmental duplications in Yakutian horses and encoding proteins of known functions (2).

Chrom.#	Gene ID	#Carriers	#Females	#Males	Gene Name	Gene Description
10	ENSECAG00000011643	2	2	0	<i>KLK1E2</i>	Equus caballus glandular kallikrein precursor (KLK1E2), mRNA.
10	ENSECAG00000018268	2	2	0	<i>KLK4</i>	kallikrein-related peptidase 4
10	ENSECAG00000021708	2	1	1	<i>FAM26F</i>	family with sequence similarity 26, member F
12	ENSECAG0000002053	2	1	1	<i>OR5M8</i>	olfactory receptor, family 5, subfamily M, member 8
12	ENSECAG00000013637	2	2	0	<i>SLC22A24</i>	solute carrier family 22, member 24
23	ENSECAG00000007210	2	0	2	<i>CTSL</i>	cathepsin L
30	ENSECAG00000000283	2	1	1	<i>F13B</i>	coagulation factor XIII, B polypeptide
X	ENSECAG00000000478	2	2	0	<i>CA5B</i>	carbonic anhydrase VB, mitochondrial
X	ENSECAG00000002779	2	2	0	-	Histone H2A
X	ENSECAG00000012150	2	2	0	<i>SHROOM2</i>	shroom family member 2
1	ENSECAG0000007462	1	1	0	<i>RHOU</i>	ras homolog family member U
1	ENSECAG0000008327	1	0	1	<i>PI4K2A</i>	phosphatidylinositol 4-kinase type 2 alpha
1	ENSECAG00000016495	1	0	1	<i>NUSAPI</i>	nucleolar and spindle associated protein 1
2	ENSECAG00000008307	1	1	0	<i>UBE4B</i>	ubiquitination factor E4B
3	ENSECAG00000018979	1	1	0	<i>GRK4</i>	G protein-coupled receptor kinase 4
5	ENSECAG00000021098	1	0	1	<i>SLAMF6</i>	SLAM family member 6
6	ENSECAG00000012364	1	1	0	<i>MYEOV2</i>	myeloma overexpressed 2
7	ENSECAG00000012108	1	1	0	<i>PPP2R1B</i>	protein phosphatase 2, regulatory subunit A, beta
7	ENSECAG00000022192	1	1	0	<i>ZNF77</i>	zinc finger protein 77
8	ENSECAG00000002578	1	0	1	<i>PES1</i>	pescadillo ribosomal biogenesis factor 1
8	ENSECAG00000016242	1	0	1	-	Tuftelin-interacting protein 11
9	ENSECAG0000000565	1	1	0	<i>NSMAF</i>	neutral sphingomyelinase (N-SMase) activation associated factor
9	ENSECAG00000015053	1	1	0	<i>SDCBP</i>	Equus caballus syndecan binding protein (syntenin) (SDCBP), mRNA.
10	ENSECAG00000005998	1	0	1	<i>TAAR6</i>	trace amine associated receptor 6
10	ENSECAG00000016657	1	0	1	<i>ZNF211</i>	zinc finger protein 211
11	ENSECAG00000008934	1	1	0	<i>KRT35</i>	keratin 35
11	ENSECAG00000011417	1	1	0	<i>KRT32</i>	keratin 32
11	ENSECAG00000022015	1	0	1	<i>ALOX12</i>	arachidonate 12-lipoxygenase
12	ENSECAG00000020705	1	1	0	<i>DUSP8</i>	dual specificity phosphatase 8
15	ENSECAG00000023970	1	1	0	<i>MERTK</i>	c-mer proto-oncogene tyrosine kinase
16	ENSECAG00000011706	1	1	0	<i>DENNDA4</i>	DENN/MADD domain containing 6A
16	ENSECAG00000015620	1	0	1	<i>ZNF850</i>	zinc finger protein 850
19	ENSECAG00000011230	1	0	1	<i>SENP2</i>	SUMO1/sentrin/SMT3 specific peptidase 2
21	ENSECAG0000003563	1	1	0	<i>BST2</i>	bone marrow stromal cell antigen 2
22	ENSECAG0000006225	1	1	0	<i>EDN3</i>	endothelin 3
23	ENSECAG0000002305	1	1	0	-	Equus caballus interferon-alpha-4 (LOC100052921), mRNA.
23	ENSECAG00000007878	1	0	1	<i>FRMD3</i>	FERM domain containing 3
24	ENSECAG00000015948	1	1	0	<i>ACOT4</i>	acyl-CoA thioesterase 4
24	ENSECAG00000016290	1	1	0	<i>ACOT6</i>	acyl-CoA thioesterase 6
25	ENSECAG00000017439	1	1	0	<i>SPATA31E1</i>	SPATA31 subfamily E, member 1
Un	ENSECAG0000000039	1	0	1	<i>PFKFB1</i>	6-phosphofructo-2-kinase/fructose-2,6-biphosphatase 1
Un	ENSECAG00000007364	1	1	0	<i>COMT</i>	Equus caballus catechol-O-methyltransferase (COMT), transcript variant MB-COMT, mRNA.
Un	ENSECAG00000013435	1	1	0	<i>OAS1</i>	Equus caballus 2',5'-oligoadenylate synthetase 1, 40/46kDa (OAS1), mRNA.
Un	ENSECAG00000026951	1	1	0	<i>ARVCF</i>	armadillo repeat gene deleted in velocardiofacial syndrome
X	ENSECAG00000009398	1	1	0	<i>STS</i>	Equus caballus steroid sulfatase (microsomal), isozyme S (STS), mRNA.
X	ENSECAG00000017572	1	1	0	<i>ZNF280C</i>	zinc finger protein 280C

Table S4.13. KEGG and Wikipathway pathways for genes enriched in Yakutian horse segmental duplications.

Database	Pathways	Model organism	Adjusted p-value	Gene ID	Gene Name
KEGG	Olfactory transduction	Human	0.00002	ENSG00000175619	<i>OR4B1</i>
				ENSG00000258817	<i>OR4C13</i>
				ENSG00000166368	<i>OR2D2</i>
				ENSG00000178358	<i>OR2D3</i>
				ENSG00000179919	<i>OR10A7</i>
				ENSG00000177693	<i>OR4F4</i>
				ENSG00000181371	<i>OR5M8</i>
		Mouse	0.00280	ENSMUSG0000043267	<i>OLFR1031</i>
				ENSMUSG0000094970	<i>OLFR943</i>
				ENSMUSG0000073896	<i>OLFR716</i>
				ENSMUSG0000075063	<i>OLFR142</i>
				ENSMUSG0000061798	<i>OLFR1204</i>
				ENSMUSG0000061195	<i>OLFR1289</i>
KEGG	Steroid hormone biosynthesis	Human	0.01110	ENSG00000109193	<i>SULT1E1</i>
		Human	0.01110	ENSG00000179142	<i>CYP11B2</i>
		Mouse	0.00280	ENSMUSG0000029272	<i>SULT1E1</i>
				ENSMUSG0000022589	<i>CYP11B2</i>
KEGG	Wnt signaling pathway	Human	0.02940	ENSG00000137713	<i>PPP2R1B</i>
		Human	0.02940	ENSG00000163904	<i>SENP2</i>
		Mouse	0.01210	ENSMUSG0000022855	<i>SENP2</i>
				ENSMUSG0000032058	<i>PPP2R1B</i>
KEGG	Ubiquitin mediated proteolysis	Human	0.02940	ENSG0000008853	<i>RHOBTB2</i>
		Human	0.02940	ENSG00000130939	<i>UBE4B</i>
		Mouse	0.01170	ENSMUSG0000028960	<i>UBE4B</i>
				ENSMUSG0000022075	<i>RHOBTB2</i>
KEGG	RNA transport	Human	0.02940	ENSG00000132182	<i>NUP210</i>
		Human	0.02940	ENSG00000163904	<i>SENP2</i>
		Mouse	0.01250	ENSMUSG0000030091	<i>NUP210</i>
				ENSMUSG0000022855	<i>SENP2</i>
KEGG	Fatty acid metabolism	Mouse	0.00280	ENSMUSG0000029455	<i>ALDH2</i>
KEGG	Valine, leucine and isoleucine degradation	Mouse	0.00280	ENSMUSG0000030861	<i>ACADS</i>
KEGG	Valine, leucine and isoleucine degradation	Mouse	0.00280	ENSMUSG0000029455	<i>ALDH2</i>
KEGG	Valine, leucine and isoleucine degradation	Mouse	0.00280	ENSMUSG0000030861	<i>ACADS</i>
KEGG	Metabolic pathways	Mouse	0.01070	ENSMUSG0000029455	<i>ALDH2</i>
				ENSMUSG0000030861	<i>ACADS</i>
				ENSMUSG000000320	<i>ALOX12</i>
				ENSMUSG0000025178	<i>PI4K2A</i>
				ENSMUSG0000022589	<i>CYP11B2</i>
Wikipathways	Metapathway biotransformation	Human	0.01160	ENSG00000084207	<i>GSTP1</i>
				ENSG00000109193	<i>SULT1E1</i>
				ENSG00000179142	<i>CYP11B2</i>
Wikipathways	Lymphocyte TarBase	Human	0.02120	ENSG00000104689	<i>TNFRSF10A</i>
				ENSG00000137575	<i>SDCBP</i>
				ENSG00000160886	<i>LY6K</i>
				ENSG00000129515	<i>SNX6</i>
				ENSG00000137575	<i>SDCBP</i>
Wikipathways	Epithelium TarBase	Human	0.02310	ENSG00000160886	<i>LY6K</i>
				ENSG00000129515	<i>SNX6</i>

Table S4.14. Phenotypes for genes enriched in Yakutian horse segmental duplications.

Database	Phenotype	Model organism	Adjusted p-value	Gene ID	Gene Name
PheWAS	Circumscribed scleroderma	Human	0.00480	ENSG00000104689	<i>TNFRSF10A</i>
				ENSG00000153208	<i>MERTK</i>
PheWAS	Other hemoglobinopathies	Human	0.00480	ENSG00000116574	<i>RHOU</i>
				ENSG00000104689	<i>TNFRSF10A</i>
PheWAS	Disturbances in tooth eruption	Human	0.00480	ENSG00000116574	<i>RHOU</i>
				ENSG00000153208	<i>MERTK</i>
PheWAS	Disorders of tooth development	Human	0.00520	ENSG00000116574	<i>RHOU</i>
				ENSG00000153208	<i>MERTK</i>
PheWAS	Hereditary hemolytic anemias	Human	0.00970	ENSG00000116574	<i>RHOU</i>
				ENSG00000104689	<i>TNFRSF10A</i>
PheWAS	Chronic airway obstruction	Human	0.03380	ENSG00000116574	<i>RHOU</i>
				ENSG00000104689	<i>TNFRSF10A</i>
PheWAS	Pneumonia	Human	0.03380	ENSG00000104689	<i>TNFRSF10A</i>
				ENSG00000153208	<i>MERTK</i>
PheWAS	Type 1 diabetes	Human	0.03590	ENSG00000116574	<i>RHOU</i>
				ENSG00000153208	<i>MERTK</i>
PheWAS	Disorders of menstruation	Human	0.04080	ENSG00000116574	<i>RHOU</i>
				ENSG00000153208	<i>MERTK</i>
Phenotype	Abnormality of temperature regulation	Human	0.02120	ENSG00000196177	<i>ACADSB</i>
				ENSG00000142798	<i>HSPG2</i>
				ENSG0000018625	<i>ATPIA2</i>
				ENSG00000179142	<i>CYP1B2</i>
Phenotype	Increased circulating interleukin-12b level	Mouse	0.01900	ENSMUSG0000022074	<i>TNFRSF10B</i>
				ENSMUSG0000015314	<i>SLAMF6</i>
Phenotype	Abnormal circulating interleukin-12b level	Mouse	0.04620	ENSMUSG0000022074	<i>TNFRSF10B</i>
				ENSMUSG0000015314	<i>SLAMF6</i>

Table S4.15. Phenotypes for genes enriched in Yakutian horse segmental duplications (Humans as model organisms).

Disease	Adjusted p-value	Gene ID	Gene Name
Urogenital Neoplasms	0.02500	ENSG00000167749	<i>KLK4</i>
		ENSG00000170801	<i>HTRA3</i>
		ENSG00000108839	<i>ALOX12</i>
		ENSG00000084207	<i>GSTP1</i>
		ENSG00000109193	<i>SULT1E1</i>
Essential hypertension	0.02500	ENSG00000125388	<i>GRK4</i>
		ENSG00000167748	<i>KLK1</i>
		ENSG00000179142	<i>CYP11B2</i>
Hypertension, Renal	0.02500	ENSG00000125388	<i>GRK4</i>
		ENSG00000167748	<i>KLK1</i>
		ENSG00000179142	<i>CYP11B2</i>
Demyelinating Diseases	0.03110	ENSG00000153208	<i>MERTK</i>
		ENSG00000051825	<i>MPHOSPH9</i>
		ENSG00000117115	<i>PADI2</i>
Beckwith-Wiedemann Syndrome	0.03110	ENSG00000157429	<i>ZNF19</i>
		ENSG00000149054	<i>ZNF215</i>
Multiple Sclerosis	0.03110	ENSG00000153208	<i>MERTK</i>
		ENSG00000051825	<i>MPHOSPH9</i>
		ENSG00000117115	<i>PADI2</i>
Hypertension	0.03110	ENSG00000125388	<i>GRK4</i>
		ENSG00000167748	<i>KLK1</i>
		ENSG00000179142	<i>CYP11B2</i>
Ototoxicity	0.03110	ENSG00000084207	<i>GSTP1</i>
		ENSG00000109193	<i>SULT1E1</i>
Cholestasis	0.03110	ENSG00000132182	<i>NUP210</i>
		ENSG00000067066	<i>SP100</i>
Brenner tumour of ovary	0.03110	ENSG00000167749	<i>KLK4</i>
		ENSG00000167748	<i>KLK1</i>
		ENSG00000108839	<i>ALOX12</i>

5 Section 5: Phylogenomic inference

We reconstructed the phylogenetic relationships amongst the Yakutian horses sequenced here, by comprehensively comparing their genetic variability against a set of previously sequenced genomes from both, present-day and Late Pleistocene specimens (13, 16). More specifically, we compared their mitochondrial, Y-chromosome and nuclear genomes.

5.1 *Phylogenetic inference from mitochondrial sequences*

5.1.1 Dataset and substitution models

Following the procedure described in **section S2.5**, we mapped the sequencing reads of 12 modern (**Table S2.5**) and 9 ancient (**Table S2.6**) Yakutian horses against the reference mitochondrial genome (Accession Nb. NC_001640; (83)). Samples for which the average depth-of-coverage was inferior to 4X were disregarded, resulting in a total of 16 mitochondrial genomes analyzed. BAM alignments were converted into pileup format, and subsequently used in bcftools (84) to call genotypes (depth ≥ 3 , and baseQ ≥ 30). The final mtDNA consensus sequences were generated using a strict majority rule at each position (disregarding 16,129-16,360 bp corresponding to tandem repeats), which resulted in an average depth-of-coverage of 30.6-3,277.4X. The final consensus sequences were submitted to GenBank, under Accession numbers KT368723-KT368738.

We aligned our 16 mitochondrial genome sequences to the collection of 105-horse mitochondrial genomes that was previously presented in (16). This collection is comprised by ancient and modern specimens, and encompasses most of the mitochondrial diversity present in horses (**Table S5.1**).

We applied ModelGenerator v0.851 (85) to determine which nucleotide substitution model best fitted the mitochondrial data. The mitochondrial sites were first split into six categories, including the control region, rRNAs, tRNAs, and the three codon positions (detailed in **Table S5.2**). We also generated a global alignment corresponding to the concatenation of the six categories. For each site category, as well as the global alignment, the best-fit nucleotide substitution model was selected by means of the Bayesian Information Criterion (BIC) (86), and used for the corresponding Maximum Likelihood (from the global alignment) and Bayesian (from the six partitions) phylogenetic inferences.

5.1.2 Maximum likelihood phylogeny

We inferred the maximum likelihood (ML) phylogenetic tree from the global mitochondrial alignment by using PhyML3.0 (87) with the corresponding best-fit substitution model (TrN+I+ Γ 8). Node robustness was assessed using three statistics based on approximate Likelihood Ratio Tests (88): (i) Approximate-Unbiased test (aLRT); (ii) aLRT parametric Chi2-based (Chi2-aLRT); and (iii) aLRT non-parametric branch support based on a Shimodaira-Hasegawa-like procedure (SH-aLRT) (89). The unrooted phylogenetic tree, drawn using Dendroscope 3 (90), is shown in **Figure S5.1**.

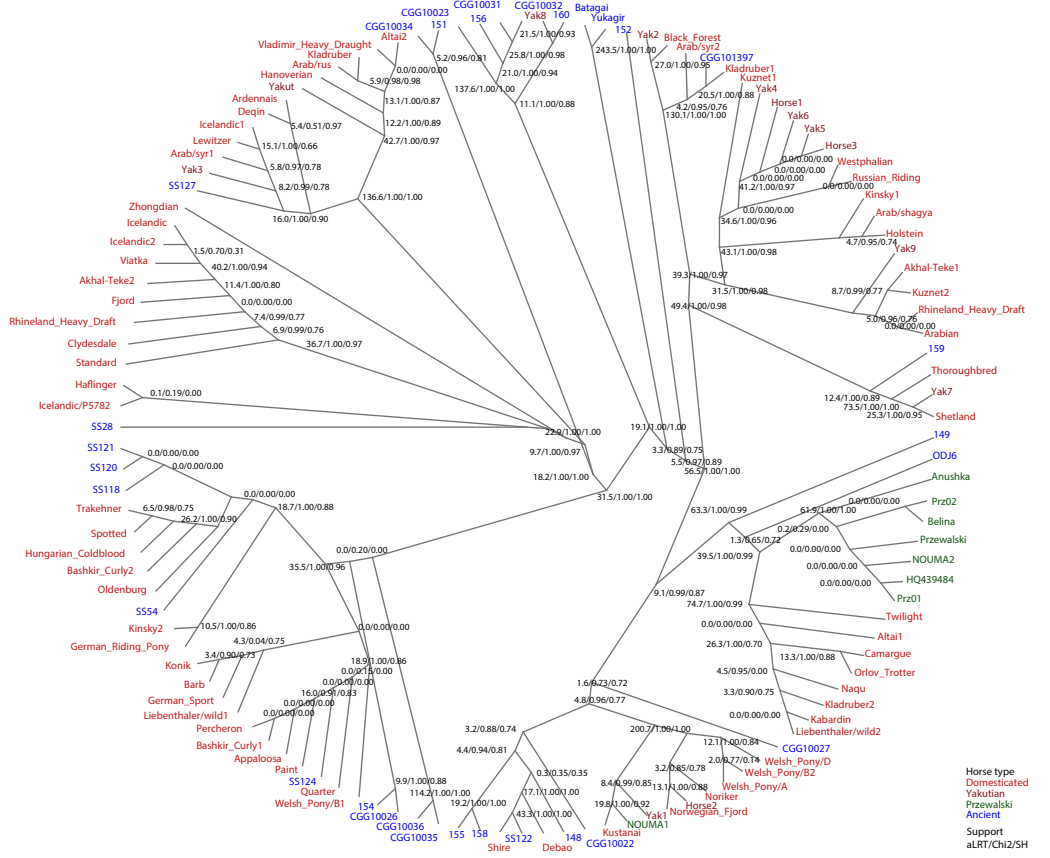


Figure S5.1. Mitochondrial ML phylogeny of ancient and modern horses.

The mitochondrial horse genomes considered are described in (Table S5.1) and the phylogeny was estimated using PhyML 3.0 (87). Node support values (aLRT/Chi2-aLRT/SH-aLRT) are indicated at each node. Samples are color-coded as ancient (in blue), domestic (red), Przewalski's (green), and modern Yakutian horses (brown).

5.1.3 Bayesian phylogeny

We also performed Bayesian phylogenetic inference using BEAST 1.8.0 (91). The six site categories were treated as unlinked partitions. Divergence dates were estimated using a log-uncorrelated molecular clock model, with radiocarbon dates (or stratigraphic context information) of the ancient specimens employed for tip calibration (**Table S5.1**). The Bayesian phylogenetic inference was run for 150 millions generations, sampling the chain every 1,000 (thin-in interval), and discarding the first 10% chains (burn-in). We analysed the MCMC samples with TRACER 1.5 (92), which indicated convergence and adequate mixing of the Markov chains. We thus used the TREEANNOTATOR 1.7.5 program to summarize the MCMC samples as the maximum clade credibility topology (91). The tree, drawn with Figtree v1.4.2 (<http://tree.bio.ed.ac.uk/software/figtree/>), is shown in (**Figure S5.2**) with the corresponding node support values (posterior probabilities).

We also evaluated the fit of three demographic models to the mitochondrial data, including a constant population size, a Bayesian Skyline (93) and a Bayesian Skyride (94). We then compared their marginal likelihoods through the Bayes factors, which were calculated in TRACER v1.5 (92) via importance sampling (1,000 bootstraps), and using the harmonic mean of the sampled likelihoods. The comparison supported the Bayesian Skyline as the best-fit demographic model to the mtDNA data (**Table S5.3**). We therefore reconstructed the Bayesian Skyline demographic profile (N_e x generation time) with TRACER 1.5 (92), and plotted its log10-transformed value using the ggplot2 (95) package of the R programming language (**Figure S5.3**).

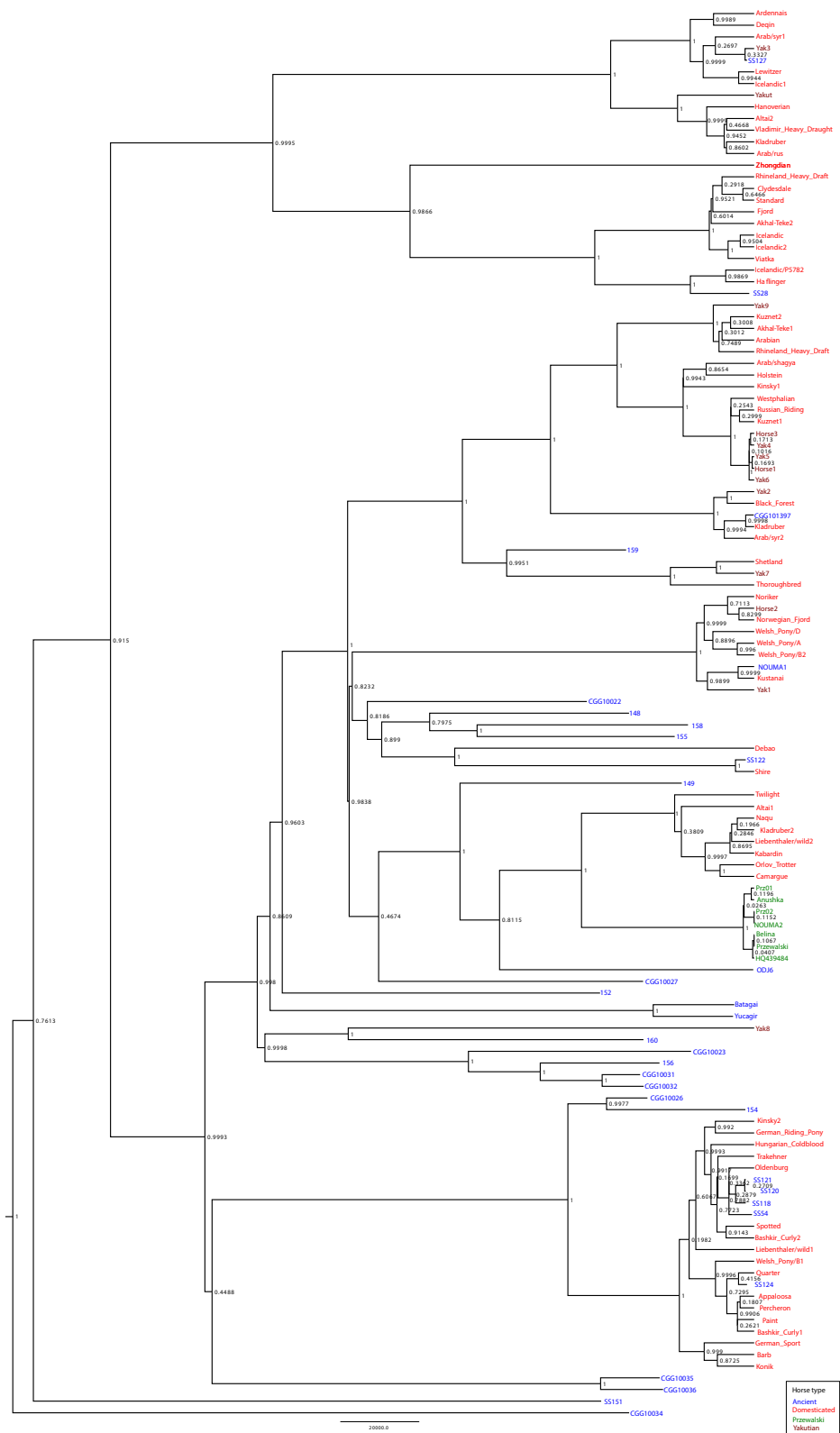


Figure S5.2. Mitochondrial Bayesian phylogeny of ancient and modern horses.

The mitochondrial horse genomes considered are described in **(Table S5.1)** and the phylogeny was estimated using BEAST and six unlinked site partitions (**Table S5.2**). The node labels depict the clade support (posterior probabilities). Samples are color-coded as ancient (in blue), domestic (red), Przewalski's (green), and modern Yakutian horses (brown).

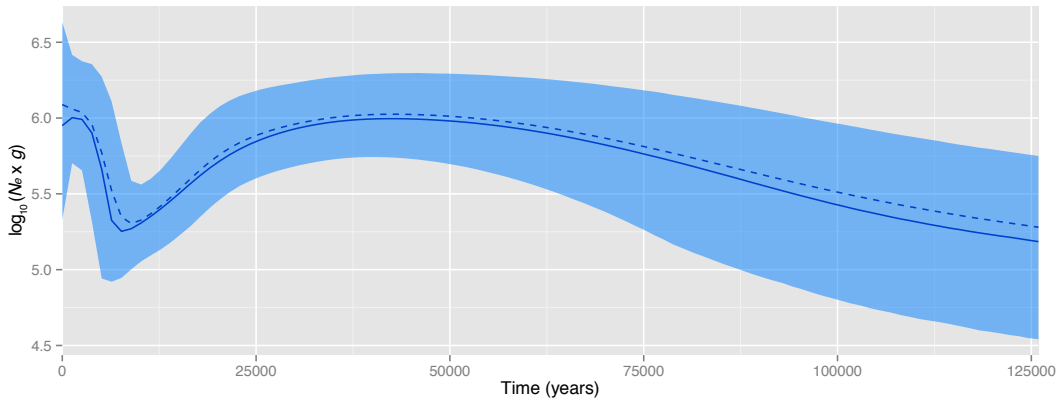


Figure S5.3: Bayesian Skyline plot reconstructed from mitochondrial genome data.

The y-axis provides a \log_{10} -transformed measure of the product of the effective population size (N_e) and the generation time (g). The full and dashed blue lines represent the median and the mean of demographic traces, respectively. The blue shaded area delimits the 95% confidence intervals of the mean.

5.2 Y-chromosome phylogenetic inference

We first prepared FASTA files corresponding to the Y-chromosome contigs characterised by Wallner et al. (96) and Lippold et al. (97). We excluded sequence G72337.1 as it overlaps between both studies, resulting in a total of 193,857bp.

We mapped the sequencing reads of six Yakutian horse samples, including four modern stallions (Yak1, Yak4, Yak8 and Yak9) and the two ancient specimens, Batagai and CGG101397, against these Y-chromosome contigs. To assure we retained Y-specific sequencing reads, we followed a two-step mapping approach. The first step involved mapping against the Y-chromosome contigs (without filtering for quality and PCR duplicates). This provided an initial list of Y-chromosome read candidates that were further mapped against both the EquCab2.0 nuclear and the Y-chromosome sequences. Only candidate reads mapping again uniquely to the Y-chromosome were considered to be Y-specific, provided they showed a minimal mapping quality of 25 and were not PCR duplicates.

We called genotypes as described in section S4.1.1, except that a minimum depth of 4 (as the Y-chromosome is haploid) and a maximum depth of 50 were required. Based on the genomic coordinates of the reference sequence, we then merged the Y-linked genotypes with the sequence information previously characterized for two modern domesticated horses (Standarbred and Icelandic; from (13) and (16) and one Late Pleistocene stallion (CGG10023, from (16)).

The phylogenetic relationships among these samples was inferred by Maximum Likelihood (ML) with PhyML3.0 (87), under the GTR substitution model with eight rate categories, as estimated by ModelGenerator v0.851 (85). Node support was assessed using three statistics based on two approximate Likelihood Ratio Tests (88): the aLRT parametric Chi₂-based (Chi₂-aLRT), and the aLRT non-parametric branch support based on a Shimodaira-Hasegawa-like procedure (SH-aLRT) (89). The unrooted phylogenetic tree, drawn using Dendroscope 3 (90), is shown in **Figure S5.4**.

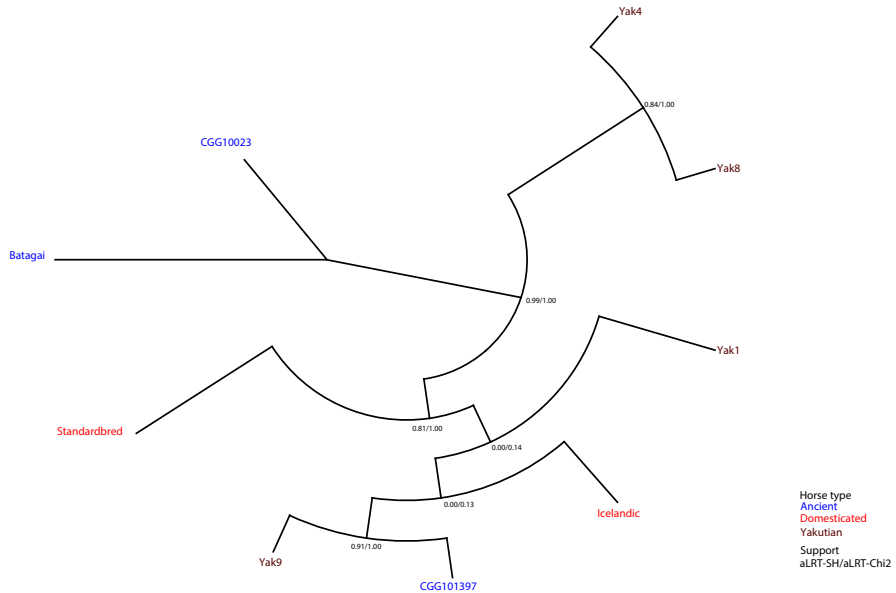


Figure S5.4. Y-chromosome Maximum Likelihood phylogeny.

Phylogenetic inference was performed using PhyML 3.0 (87). Node support values (Chi2-aLRT/SH-aLRT) are indicated at each node. Samples are color-coded as ancient (in blue), domestic (red), Przewalski's (green), and modern Yakutian horses (brown).

5.3 Phylogenetic inference using a super-matrix of nuclear coding sequences

We inferred the phylogenetic relationship amongst the 9 modern and 2 ancient Yakutian samples (Batagai and CGG101397), by comparing their nuclear genetic variability with that present in Przewalski's and domesticated horses (**Table S5.4**) (13, 16, 30). The low-coverage genomes of other Yakutian horses were not compatible with this analysis (**Table S2.5** and **S2.6**).

More specifically, we used the VCF genotyping calls produced in **section S4.1** to build a partitioned super-matrix based on the 50% longest protein-coding genes annotated in EquCab v2.76 (98). Support was calculated based on 100 bootstrap trees. Maximum Likelihood phylogenetic inference was performed using ExaML v2.04 (<http://sco.h-its.org/exelixis/software.html>) and RAxML v8.1.3 (99), with default parameters. The resulting tree was rooted using the divergence from the outgroup *Equus africanus somaliensis* (Somali wild ass) (**Figure S5.5**).

We found that the specimens Batagai (dating ~5,200 BP ago) and CGG101397 (dating to the 19th century) did not cluster together. Instead, sample CGG101397 grouped within the diversity of modern Yakutian horses (which is also forming a monophyletic clade, included within that of modern domesticated horses), while Batagai clustered with two previously characterised Late Pleistocene horses (CGG10022 and CGG10023). Przewalski's horses were found to represent a third phylogenetic cluster.

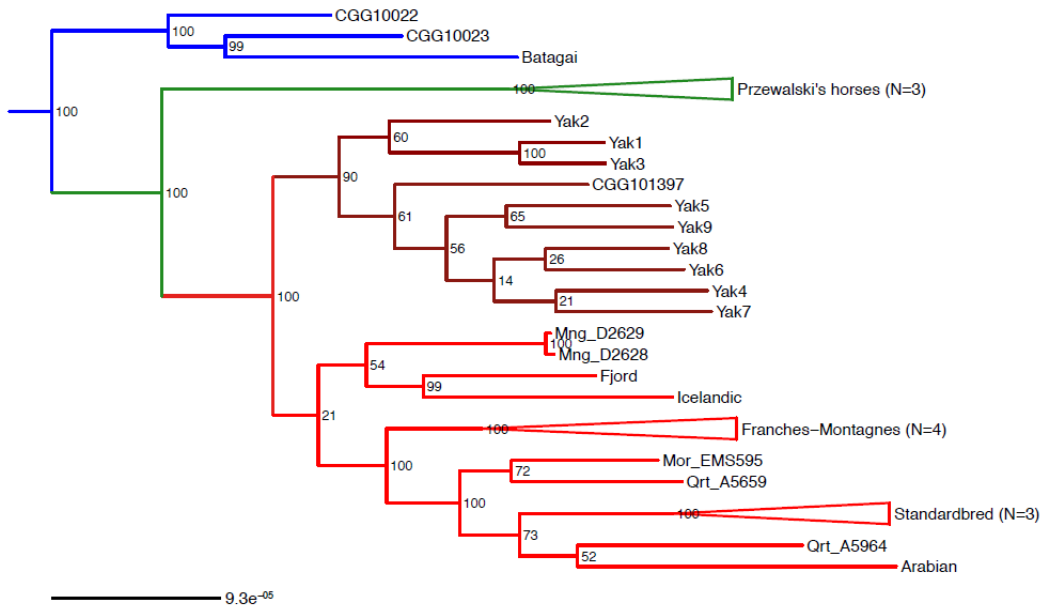


Figure S5.5. Exome-based phylogenetic inference.

Individual samples are color-coded as: ancient horses (blue), modern domesticated horses (red), Przewalski's horses (green) and modern Yakutian horses (brown). Node labels show the corresponding support values using 100 bootstrap pseudo-replicates. For improving readability, we collapsed all individuals from the same breeds that clustered together. The number of horses (N) in collapsed tips is listed after the breed name. The topology presented is rooted using the divergence from the outgroup *Equus africanus somaliensis* (Somali wild ass, not shown), previously characterized by (30).

5.4 Supplementary Tables for Section 5

Table S5.1. Complete mitochondrial genome sequences used for phylogenetic inference.

Horse type/Sample name	Accession number	Reference	Tip Age for Calibration in BEAST (yBP)
Ancient/Batagai	KT368725	This study	5,088
Ancient/CGG101397	KT368726	This study	100
Ancient/Yukagir	KT368723	This study	5,384
Ancient/ODJ6	KT368724	This study	225
Yakutian/Yak1	KT368730	This study	0
Yakutian/Yak2	KT368731	This study	0
Yakutian/Yak3	KT368732	This study	0
Yakutian/Yak4	KT368733	This study	0
Yakutian/Yak5	KT368734	This study	0
Yakutian/Yak6	KT368735	This study	0
Yakutian/Yak7	KT368736	This study	0
Yakutian/Yak8	KT368737	This study	0
Yakutian/Yak9	KT368738	This study	0
Yakutian/Horse2	KT368727	This study	0
Yakutian/Horse1	KT368728	This study	0
Yakutian/Horse3	KT368729	This study	0
Przewalski/Belina	AP012267	Goto et al. 2011 (100)	0
Przewalski/Anushka	AP012268	Goto et al. 2011 (100)	0
Przewalski/NOUMA2	AP013095	n/a	0
Przewalski/NOUMA1	NC_024030	n/a	0
Przewalski/Prz01	JN398402	Achilli et al. 2012 (101)	0
Przewalski/Prz02	JN398403	Achilli et al. 2012 (101)	0
Zhongdian	EF597512	Xu et al. 2007 (102)	0
Naqu	EF597513	Xu et al. 2007 (102)	0
Deqin	EF597514	Xu et al. 2007 (102)	0
Debao	EU939445	Jiang et al. 2010 (103)	0
Akhal-Teke1	HQ439441	Lippold et al. 2011 (97)	0
Akhal-Teke2	HQ439442	Lippold et al. 2011 (97)	0
Altai1	HQ439443	Lippold et al. 2011 (97)	0
Altai2	HQ439444	Lippold et al. 2011 (97)	0
Kladruber	HQ439445	Lippold et al. 2011 (97)	0
Appaloosa	HQ439446	Lippold et al. 2011 (97)	0
Arabian/rus	HQ439447	Lippold et al. 2011 (97)	0
Arabian/syr1	HQ439448	Lippold et al. 2011 (97)	0
Arabian/syr2	HQ439449	Lippold et al. 2011 (97)	0
Ardennais	HQ439450	Lippold et al. 2011 (97)	0
Bashkir Curly1	HQ439451	Lippold et al. 2011 (97)	0
Bashkir Curly2	HQ439452	Lippold et al. 2011 (97)	0
Barb	HQ439453	Lippold et al. 2011 (97)	0
Camargue	HQ439454	Lippold et al. 2011 (97)	0
Clydesdale	HQ439455	Lippold et al. 2011 (97)	0

German Sport	HQ439456	Lippold et al. 2011 (97)	0
Hanoverian	HQ439457	Lippold et al. 2011 (97)	0
Holstein	HQ439458	Lippold et al. 2011 (97)	0
Oldenburg	HQ439459	Lippold et al. 2011 (97)	0
Westphalian	HQ439460	Lippold et al. 2011 (97)	0
German Riding Pony	HQ439461	Lippold et al. 2011 (97)	0
Thoroughbred	HQ439462	Lippold et al. 2011 (97)	0
Norwegian Fjord	HQ439463	Lippold et al. 2011 (97)	0
Haffinger	HQ439464	Lippold et al. 2011 (97)	0
Icelandic1	HQ439465	Lippold et al. 2011 (97)	0
Icelandic2	HQ439466	Lippold et al. 2011 (97)	0
Yakut	HQ439467	Lippold et al. 2011 (97)	0
Kabardin	HQ439468	Lippold et al. 2011 (97)	0
Kinsky1	HQ439469	Lippold et al. 2011 (97)	0
Kinsky2	HQ439470	Lippold et al. 2011 (97)	0
Kladruber1	HQ439471	Lippold et al. 2011 (97)	0
Kladruber2	HQ439472	Lippold et al. 2011 (97)	0
Konik	HQ439473	Lippold et al. 2011 (97)	0
Kuznet1	HQ439474	Lippold et al. 2011 (97)	0
Kuznet2	HQ439475	Lippold et al. 2011 (97)	0
Kustamai	HQ439476	Lippold et al. 2011 (97)	0
Lewitzer	HQ439477	Lippold et al. 2011 (97)	0
Liebenthaler/wild1	HQ439478	Lippold et al. 2011 (97)	0
Liebenthaler/wild2	HQ439479	Lippold et al. 2011 (97)	0
Noriker	HQ439480	Lippold et al. 2011 (97)	0
Orlov Trotter	HQ439481	Lippold et al. 2011 (97)	0
Paint	HQ439482	Lippold et al. 2011 (97)	0
Percheron	HQ439483	Lippold et al. 2011 (97)	0
Przewalski	HQ439484	Lippold et al. 2011 (97)	0
Rhineland Heavy Draft	HQ439485	Lippold et al. 2011 (97)	0
Russian Riding Horse	HQ439486	Lippold et al. 2011 (97)	0
Black Forest	HQ439487	Lippold et al. 2011 (97)	0
Arab/shagya	HQ439488	Lippold et al. 2011 (97)	0
Shetland	HQ439489	Lippold et al. 2011 (97)	0
Shire	HQ439490	Lippold et al. 2011 (97)	0
Rhineland Heavy Draft	HQ439491	Lippold et al. 2011 (97)	0
Spotted	HQ439492	Lippold et al. 2011 (97)	0
Trakehner	HQ439493	Lippold et al. 2011 (97)	0
Hungarian Cold Blood	HQ439494	Lippold et al. 2011 (97)	0
Viatka	HQ439495	Lippold et al. 2011 (97)	0
WelshPony/D	HQ439496	Lippold et al. 2011 (97)	0
WelshPony/A	HQ439497	Lippold et al. 2011 (97)	0
WelshPony/B1	HQ439498	Lippold et al. 2011 (97)	0
WelshPony/B2	HQ439499	Lippold et al. 2011 (97)	0
Vladimir Heavy Draught	HQ439500	Lippold et al. 2011 (97)	0
Przewalski	n/a	Orlando et al. 2013 (13)	0
Arabian	n/a	Orlando et al. 2013 (13)	0
Fjord	n/a	Orlando et al. 2013 (13)	0
Twilight	n/a	Orlando et al. 2013 (13)	0
Standard	n/a	Orlando et al. 2013 (13)	0
Icelandic/P5782	n/a	Orlando et al. 2013 (13)	0

Icelandic	n/a	Orlando et al. 2013 (13)	0
Quarter	n/a	Orlando et al. 2013 (13)	0
Ancient/CGG10022	n/a	Schubert et al. 2014 (16)	42,692
Ancient/CGG10023	n/a	Schubert et al. 2014 (16)	16,099
Ancient/CGG10026	n/a	Orlando et al. 2013 (13)	27,230
Ancient/CGG10027	n/a	Orlando et al. 2013 (13)	28,336
Ancient/CGG10031	n/a	Orlando et al. 2013 (13)	29,081
Ancient/CGG10032	n/a	Orlando et al. 2013 (13)	28,198
Ancient/CGG10034	n/a	Orlando et al. 2013 (13)	31,890
Ancient/CGG10035	n/a	Orlando et al. 2013 (13)	24,104
Ancient/CGG10036	n/a	Orlando et al. 2013 (13)	23,244
Ancient/148	n/a	Orlando et al. 2013 (13)	31,917
Ancient/149	n/a	Orlando et al. 2013 (13)	18,471
Ancient/151	n/a	Orlando et al. 2013 (13)	39,022
Ancient/152	n/a	Orlando et al. 2013 (13)	39,311
Ancient/154	n/a	Orlando et al. 2013 (13)	2,235
Ancient/155	n/a	Orlando et al. 2013 (13)	20,273
Ancient/156	n/a	Orlando et al. 2013 (13)	24,154
Ancient/158	n/a	Orlando et al. 2013 (13)	16,880
Ancient/159	n/a	Orlando et al. 2013 (13)	32,667
Ancient/160	n/a	Orlando et al. 2013 (13)	28,242
Ancient/SS127	n/a	Sawyer et al. 2012 (104)	1,815
Ancient/SS28	n/a	Sawyer et al. 2012 (104)	1,250
Ancient/SS54	n/a	Sawyer et al. 2012 (104)	550
Ancient/SS118	n/a	Sawyer et al. 2012 (104)	2,150
Ancient/SS120	n/a	Sawyer et al. 2012 (104)	2,150
Ancient/SS121	n/a	Sawyer et al. 2012 (104)	2,150
Ancient/SS122	n/a	Sawyer et al. 2012 (104)	2,150
Ancient/SS124	n/a	Sawyer et al. 2012 (104)	1,815

yBP, years Before Present; cal. yBP, calibrated years Before Present.

Table S5.2. Best-fit nucleotide substitution model, according to the Bayesian Information Criterion (BIC) in ModelGenerator v0.851.

Partition	#Sites*	Model BIC
1 st codon position	3,626	HKY+I
2 nd codon position	3,623	HKY+I
3 rd codon position	3,623	TrN+Γ8
Control Region	965	TrN+I+Γ8
rRNA	2,561	HKY+I+Γ8
tRNA	1,521	TrN+I+Γ8
Global alignment	15,919	TrN+I+Γ8

Number of sites considered in each partition/dataset, based on the horse reference mtDNA genome (Accession number NC_001640.1). The global dataset corresponds to the concatenate of the other six categories; HKY, Hasegawa-Kishino-Yano substitution model (89). TrN, Tamura-Nei substitution model (105). I, Invariant sites; Γ8, 8 Gamma categories to model of substitution rate variation among sites.

Table S5.3. Bayes Factor for three demographic models fitted in the BEAST phylogenetic analyses.

Tree model	Bayes factor (ln P (model data))
Constant population size	-30,841.2
Skyline	-30,857.7
Skyride	-30,851.2

Table S5.4. Samples used for phylogenetic inference based on nuclear coding sequences.

Sample	Horse type	Reference
Arabian	Arabian	Orlando et al. 2013 (13)
Batagai	Ancient Yakutia	this study
CGG10022	Ancient Taymyr peninsula	Schubert et al. 2014 (16)
CGG10023	Ancient Taymyr peninsula	Schubert et al. 2014 (16)
CGG101397	Ancient Yakutia	this study
Fjord	Fjord	Orlando et al. 2013 (13)
Icelandic	Icelandic	Orlando et al. 2013 (13)
Mng_D2628	Mongolian	Do et al. 2014 (19)
Mng_D2629	Mongolian	Do et al. 2014 (19)
Mon_FM1030	Franches-Montagnes	this study
Mon_FM1785	Franches-Montagnes	this study
Mon_FM1932	Franches-Montagnes	this study
Mon_FM1951	Franches-Montagnes	this study
Mor_EM595	Morgan	this study
Prz_D2630	Przewalski	Do et al. 2014 (19)
Prz_D2631	Przewalski	Do et al. 2014 (19)
Prz_Przewalski	Przewalski	Orlando et al. 2013 (13)
Qrt_A5659	Quarter	this study
Qrt_A5964	Quarter	this study
Std_M5256	Standardbred	this study
Std_M977	Standardbred	this study
Std_Standardbred	Standardbred	Orlando et al. 2013 (13)
Yak1	Yakutian	this study
Yak2	Yakutian	this study
Yak3	Yakutian	this study
Yak4	Yakutian	this study
Yak5	Yakutian	this study
Yak6	Yakutian	this study
Yak7	Yakutian	this study
Yak8	Yakutian	this study
Yak9	Yakutian	this study

6 Section 6: Demographic history of the Yakutian horses

In this section, we addressed a long-standing debate about the demographic history of the Yakutian horses, namely whether they arrived with the Yakut people a few centuries ago, or rather descend or were admixed with wild Late Pleistocene horses. We tested these hypotheses by applying a range of methods (i) characterizing the effective population size (N_e) changes of Yakutian horses over time, (ii) estimating their genetic distances with other populations/breeds, as well as (iii) detecting the presence of admixture events.

6.1 Reconstructing their long and short-term effective population sizes

6.1.1 Pairwise Sequentially Markov Coalescent

We used PSMC (106) to trace N_e changes over the last two million years. The method operates on a single diploid genome, exploiting the local density of heterozygous positions along unlinked loci to date the distribution of coalescent events (and thus N_e in a temporal scale).

Because deep sequencing is required to accurately call heterozygous positions, a minimum coverage of 20X is required for appropriate PSMC inferences (13). Two Yakutian genomes in our data set meet this requirement, namely the historical sample CGG101397 (20.24x) and the modern Yakutian horse Yak7 (21.63x) (**Tables S2.5 and S2.6**). The genomes of Batagai and Yak2 were sequenced at an average coverage of 18.29X and 18.38X, respectively, which is sub-optimal for PSMC inference. In order to include these genomes in the analyses, we therefore applied the correction method based on uniform false negative rates (uFNR) of heterozygous calls, devised in (13) and suggested in (106). Briefly, Yak7 (which has the highest genome coverage) was first randomly down-sampled to an average depth-of-coverage of 18.3X (corresponding to the average genome coverage observed for both ancient Yakutian genomes). We then tested a different set of uFNR of heterozygous calls (from 1% to 30%), searching for the one that minimizes the differences with the PSMC profile recovered from the original Yak7 sequence. We found that PSMC inference on 18.3X depth-of-coverage datasets could be satisfactorily corrected with ~2% as uFNR of heterozygous calls.

PSMC analyses were performed as described in the Supplementary section S9.2 of (13), except that we defined a per-sample maximum coverage threshold to avoid overestimating heterozygosity in the presence of unidentified repetitive regions (see **section S4.2**). Briefly, consensus FASTA sequences were generated for autosomal chromosomes from BAM files. SNPs were then called with samtools v0.1.18 (84) and filtered with the ‘vcf2fq’ command from vcftools.pl, using the following settings:

- Minimum depth-of-coverage: 8X.
- Maximum depth-of-coverage: 0.995 quantile of the coverage distribution.
- InDels filtered in a windows size of 5 bp.
- Minimum RMS mapping quality: 10.
- Sites with genotyping quality scores inferior to 35 were also excluded, but during the conversion to the PSMC input file format.

PSMC inference was run using the parameters recommended in (13) and (16), including *Number of iterations* = 25; *maximum $2N_0$ coalescent time* = 15; *initial θ_0/ρ* = 5. We evaluated the variance of the PSMC reconstructions, by splitting chromosomal sequences into shorter segments of 500 Kb and generating 100 genome bootstrap pseudo-replicates (with replacement). Unscaled PSMC profiles are shown in **Figure S6.1**. For scaling PSMC profiles, we used a calibration point of $T = 4.5$ million years (Myr), a mutation rate of $\mu = 7.242 \times 10^{-9}$ per site per generation, and a generation time of $g = 8$ years. These parameters are in agreement with the recent findings from Orlando and colleagues (13) and (16). Scaled PSMC profiles are shown in **Figure 3A**.

PSMC profiles reported virtually identical demographic trajectories for modern Yakutian horses and the historical Yakutian horse CGG101397. In contrast, the 5.2 kyr-old Yakutian sample Batagai showed a similar pattern to that observed for the Late Pleistocene horse CGG10022, which was originally analysed in (16) and is included here for comparative purposes (**Figure 3A**).

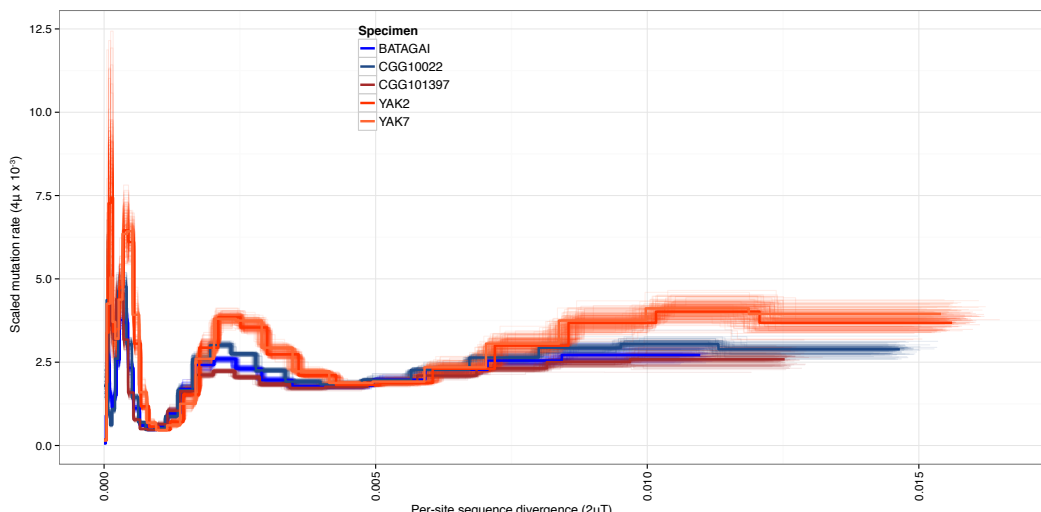


Figure S6.1. Unscaled PSMC profiles.

Bootstrap pseudo-replicates are indicated with thin lines around the corresponding PSMC profile.

6.1.2 Diffusion approximation for demographic inference

We reconstructed the recent demographic history of Yakutian horses using the software *dadi* (version 1.6.3), where the estimation of demographic parameters is based on the diffusion approximation to the site frequency spectrum (SFS) (107).

We first considered the SFS calculated from 4d-fold degenerate sites (see definition in **section S7.2.1**), as a proxy for neutrally evolving and approximately independent sites. We used the reference (Thoroughbred; **Table S2.4**), Mongolian (Mng_D2628; **Table S2.4**), and Donkey (*Equus africanus somaliensis*) outgroup species to infer derived alleles. After masking monomorphic sites, the unfolded SFS resulted in 9,381 to 9,573 entries, depending on the ancestral sequence used. As additional analyses, we also considered the SFS computed across the whole genome, comprised of a total of 2,843,575 to 2,933,002 SNPs.

We fixed the ancient demographic history of Yakutian horses from the model inferred by PSMC analyses (see **section S6.1.1**). The ancestral effective

population size was therefore set to 136,337, and it changed instantaneously over time until approximately 18,000 yBP, as detailed in **Table S6.1**, which was calibrated considering a generation time of 8 years. We then tested three demographic models of recent evolution for Yakutian horses (from 18,000 yBP to the present):

- **Model PSMC:** at 18,545 yBP (see **Table S6.1**) the effective population size drops instantaneously to 5,107, exactly as estimated by PSMC analyses;
- **Model one epoch:** is the same as Model PSMC, but assuming that at 5,500 yBP (domestication time; (108), the effective population size exponentially decays to N_2 , which represents the current size (N_1 and N_2 are free parameters to be estimated);
- **Model three epochs:** the same as the one epoch model, but assuming that at a putative founder time (700 yBP; (1, 2)) the effective population size instantaneously drops to N_3 and exponential recovers to N_4 , which represents the current size. N_1 , N_2 , N_3 , N_4 are free parameters to be estimated.

During each model optimization, we also estimated an additional parameter, i.e. the probability of misidentification (P_{misid}) of the derived state based on the ancestral sequence used. For each model, we ran the program 20 times from different initial values to ensure convergence, and retained the parameters set with the highest likelihood (**Table S6.2**). To compare fitting between models, we performed a likelihood ratio test (LRT) with two degrees of freedom, equal to the difference of free parameters.

Our analyses show that the model assuming constant size starting ~18,000 yBP, as estimated by PSMC analyses, provides a poor fit to the data, suggesting that PSMC performs poorly for recent times (**Table S6.2**). Conversely, imposing a population size change at the domestication time greatly improves the model fitting and the current effective population size is estimated at approximately 3,000, irrespective of the ancestral sequence used (**Table S6.2**). Furthermore, when assuming a bottleneck event at a hypothetical founder time (700 yBP), we observe a significant increase in the likelihood ($P = 0.041, 0.045, 0.020$ using the reference, Mongolian, or Donkey sequence as ancestral state, respectively). Current effective population size was estimated to be between 5,600 and 7,900 (**Table S6.2**).

We finally tested whether a different assumption on the founder event provided a better fit to the data. We therefore used as initial values the parameters for the best-fit model and let vary the founder (bottleneck) event at different arbitrary times: 5,000, 4,000, 3,000, 2,000, 1,000, 500 and 200 yBP. To improve the optimization, we fixed N_1 and N_2 parameters (old population size changes) as estimated in the best-fit models. We recorded the best model likelihood at these different times (**Tables S6.3**).

We observed that more recent times appear to provide greater model likelihood (**Table S6.3, Fig. S1**). These results are not an artefact of sequencing heterogeneity, as this trend is observed even when the whole-genome data set is used (**Table S6.3**). We could not pinpoint a precise timing for the founder event, as FS-based methods (like the one adopted here) may have low power for characterising bottlenecks (109). However, these results show that it is more likely that this event occurred within the last 1,000 years, in agreement with historical records (1, 2).

6.2 Genome projections of Yakutian and other domesticated horses

We next applied the method of projecting test genomes onto reference populations (110). The projection value w summarizes the past relationship between a single test genome and a reference population, by exploiting differences in their

derived allele frequencies. Projections of $w = 1$ across all mutation frequency classes indicate that the test genome is randomly sampled from the reference population. Otherwise, it highlights a more complex demographic history of the tested individual and/or the reference population, being especially sensitive to recent N_e changes and small amounts of admixture. For this analysis, we compared the genomes detailed in **Table S6.4**, and grouped them according to their corresponding breeds/population.

6.2.1 Test horse genomes and reference panels

We first considered the refDOM panel, which includes all of the 27 horse genomes from non-Yakutian domesticated breeds. By including a high number of individuals, this panel may provide greater resolution of the projection for rare alleles. However, it is composed of genomes from several horse breeds/types, which violates the random mating assumption made for the reference population. Therefore, to avoid the confounding effects originating from the refDOM structure, we focused our subsequent projections onto refFM and refYAK populations.

In panel refFM, we only considered a subset of refDOM, exclusively comprised of 12 Franches-Montagnes horses. Whereas panel refYAK grouped all of the nine modern Yakutian horse genomes characterized in this study.

6.2.2 Projection results

Projections of modern Yakutian horse genomes onto the reference panels, refYAK and refFM

Projections of modern Yakutian horses onto refYAK mostly lie around $w = 1$ (**Figure S6.2**), which corresponds to the expectation of a random mating population, including a slight departure for rare alleles (110). For three genomes, namely Yak1, Yak3 and notably Yak2, the projections rose above the $w = 1$ line for alleles found at a low frequency, suggesting they experienced reduced levels of admixture, which is in agreement with our admixture test (see **section S6.5**).

All nine Yakutian horse genomes have similar projections relative to refFM, with minimum projection values (MPV) below one (mean MPV = 0.7724), and a standard deviation (sd) of 0.0092 (**Table S6.5**), suggesting that modern Yakutian and FM horses do not belong to the same breed, as expected.

Projections of Przewalski's and Yakutian horse genomes onto refFM

When projected onto refFM, the mean MPV is interestingly lower for Przewalski's horses (mean MPV = 0.6762; sd = 0.0109) than for modern Yakutian horses (mean MPV = 0.7724; sd = 0.0092; **Table S6.5**), indicating that Franches-Montagnes horses are more closely related to modern Yakutian horses than to the Przewalski's horses (**Figure S6.3** and **S6.4**). This is consistent with the phylogenetic position of modern Yakutian horses within the domesticated horse clade, and outside the monophyletic group of Przewalski's horses (see **section S5.3**).

Projections of non-Yakutian modern horse genomes onto refYAK

Further evidence that the modern Yakutian horses belong to the clade of domesticated horses is provided by the reciprocal projections onto refYAK (**Figure S6.5**), which report relatively high MPVs when testing either the Franches-Montagnes horse genomes (mean MPV = 0.8038; sd = 0.0062) or non-Franches-Montagnes domesticated horses (MPV = 0.8073; sd = 0.0246) (**Table S6.5**). These MPVs are

higher than the MPVs observed when projecting the Przewalski's horse genomes onto refYAK (mean MPV = 0.6926; sd = 0.0009; **Table S6.5**), in line with their early phylogenetic divergence (see **section S5.3**). Although the two mean MPVs obtained when testing Franches-Montagnes and non-Franches-Montagnes are comparable, the standard deviation is about four fold larger for non-Franches-Montagnes, nicely reflecting their heterogeneous genetic background, consisting of a mixture from eight different domesticated breeds.

Projections of ancient horse genomes onto the reference panels, refYAK and refFM

Projections of test ancient genomes onto refYAK show that CGG101397 on the one hand, and the other three surveyed ancient horses on the other hand (namely, CGG10022, CGG10023 and Batagai), have very different demographic histories (**Figure S6.6**). The genome of specimen CGG101397 shows mean MPVs of 0.8719 and 0.7637, when projected onto refYAK and refFM panels, respectively (**Table S6.5**). This suggests a closer relationship to modern Yakutian horses than to the Franches-Montagnes horses. These findings are in agreement with the results from phylogenetic analyses (see **section S5.3**), where CGG101397 clustered within the modern Yakutian diversity, supporting genetic discontinuity in the horse population of Yakutia, with the ancient population represented by sample Batagai (~5.2 kyr sample) being replaced by the population of present-day domesticated horses.

The projections of the CGG10022, CGG10023 and Batagai ancient horse genomes onto refYAK (mean MPV = 0.5977; sd = 0.0085) and refFM (mean MPV = 0.5955; sd = 0.0050) are very similar. The extremely reduced variance observed in the projections of these three genomes further suggests that they share a similar demographic history, despite spanning a ~40 kyr-long temporal range. The mean MPV obtained for the projections of the CGG10022, CGG10023 and Batagai genomes onto refYAK (mean MPV = 0.5977) is much lower than those obtained for the modern domesticated horses (mean MPV = 0.8038-0.8073), and even than those observed when projecting Przewalski's horses (mean MPV = 0.6926) (**Table S6.5**). This, again, supports that Late Pleistocene horses and the Batagai sample diverged prior to the most recent common ancestor of Przewalski's, Yakutian (including CGG101397), and other domesticated horses.

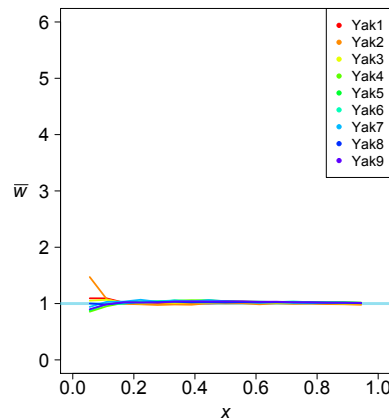


Figure S6.2. Projections of modern Yakutian horses onto the refYAK panel.

The x-axis represents the categories of derived allele frequencies, while w their corresponding projection (a w value above 1 indicates that the test genome has more alleles at that frequency than reference panel, and vice versa).

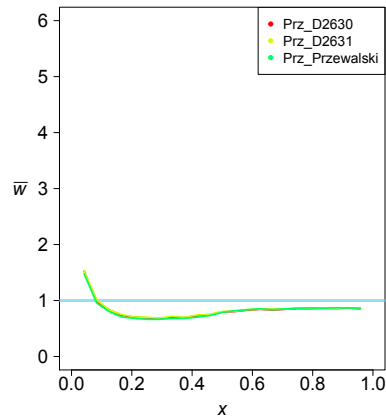


Figure S6.3. Projections of Przewalski's horses onto the refFM panel.
See Figure S6.2 for captions.

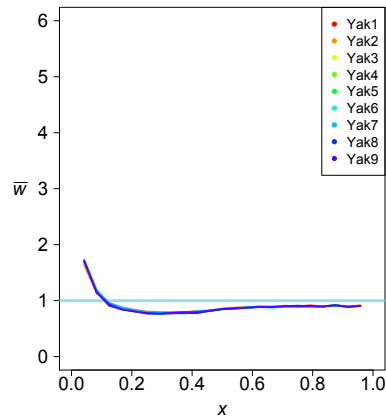


Figure S6.4. Projections of modern Yakutian horses onto the refFM panel.
See Figure S6.2 for captions.

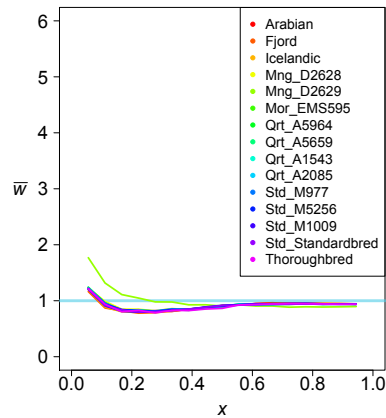


Figure S6.5. Projections of non-Yakutian and non-Franches-Montagnes modern horses onto the refYAK panel.

See **Figure S6.2** for captions.

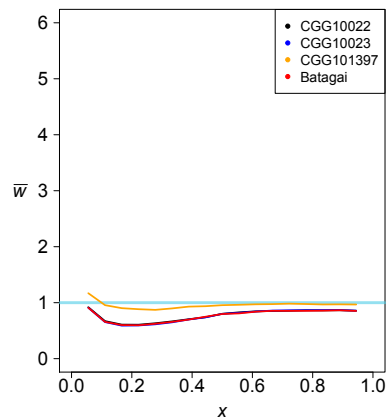


Figure S6.6. Projections of ancient horse genomes onto the refYAK panel.
See **Figure S6.2** for captions.

6.3 Principal component analysis

Principal Component Analysis (PCA) was used to investigate the genetic distances amongst ancient (including the two Late Pleistocene horses CGG10022 and CGG10023, and the two ancient Yakutian horses Batagai and CGG101397) and modern horses (including Przewalski's horses and modern domesticated horses, either Yakutian or not).

6.3.1 PCA based on genotype calls

VCF files encoding individual-based genotypes were collected (see **section 4.1.1**), and merged with bcftools (111). We restricted the analysis to biallelic sites called for every individual (-g ^miss), with a minimum frequency for the alternate allele of -q 0.00001. This merged VCF file, containing a total of 356,720 variants, was converted into plink format with vcftools v0.1.12 (111). This plink file was used as input for the EIGENSTRAT program vEIG5.0.1 (112), which was run with no outlier iterations (numoutlieriter: 0). Finally, the first three principal components, which explain 27.71% of the total variance, were plotted with ggplot2 (95) in R 3.02.

We found three main clusters (**Figure S6.7**). The first included all Przewalski's horses, while the second included the two Late Pleistocene horses and the ancient Yakutian sample Batagai. The third cluster consisted in all other horses, including the historical Yakutian horse from the 19th century (CGG101397), which grouped together within the diversity of modern domesticated horses, especially within the Yakutian breed. This is in line with our phylogenomic inference based on the exome (see **section S5.3**) and the topology recovered from TreeMix analyses (see **section S6.5.2**).

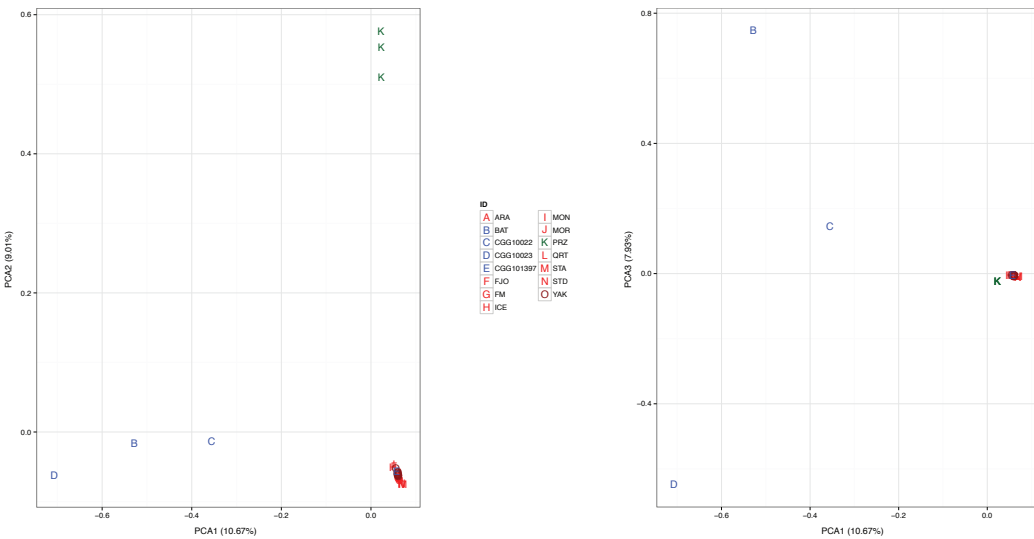


Figure S6.7. PCA plot depicting the genetic affinities of ancient and modern horses, based on genotype calls.

Left: first two principal components. Right: first and third principal components. The proportion of the variance explained by each principal component is indicated on each axis, between parentheses. For clarity, labels only refer to breeds or populations, except for Yakutian and Late Pleistocene horses.

6.3.2 PCA in a genotype likelihood framework

We also performed PCA with the ngsCovar program of the ngsTools package (113), which accounts for genotype uncertainties. Briefly, priors for the allele frequencies of each position (saf files) were estimated with ANGSD v0.615 (46). For that, we assumed Hardy-Weinberg equilibrium, and considered reads showing a mapping quality greater than or equal to 25 (-minMapQ), as well as sites showing a minimum base quality of 20 (-minBQ) and for which data was available in at least five individuals (-minInd). The saf files were then used as input for ngsCovar.

PCA plots were generated for the first three components, which explained 13.33% of the total variance (**Figure S6.8**). Although we consistently recovered the same three main clusters as in the SNP-based analysis (**Figure S6.7**), the PCA relying on genotype likelihoods revealed finer sub-clustering patterns, especially the separation of domesticated horses into their corresponding breeds/populations. For example, modern Yakutian horses form a clearly separated subgroup together with the historical horse CGG101397, with Yak2 being genetically closer to the Mongolian horses.

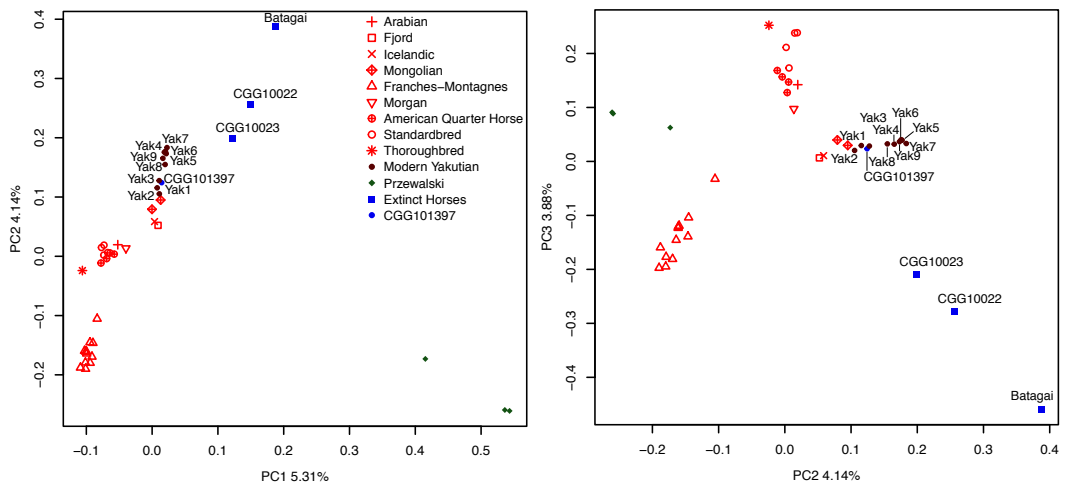


Figure S6.8. PCA plot depicting the genetic affinities of ancient and modern horses, based on genotype likelihoods.

The analysis was based on genotype likelihoods and 43 genomes representative of present-day Yakutian horses, nine domestic breeds, the Przewalski's horse population, CGG101397 and extinct horses. The fraction of the total variance explained by each of the three principal components is indicated on the corresponding axes. Left: first two principal components. Right: second and third principal components.

As the over-representation of one group of related individuals can impact the overall structure reflected in PCA, we also ran PCA on a subset of genomes, considering a maximum three individuals per population/breed of the comparative panel (**Figure 2**). These were selected to represent the genomes characterised with the highest average depth-of-coverage: Yak1, Yak2, Yak3, Yak4, Yak5, Yak6, Yak7, Yak8, Yak9, Arabian, Fjord, Icelandic, Mng_D2628, Mng_D2629, Mon_FM1951, Mon_FM1798, Mor_EMS595, Qrt_A5659, Qrt_A5964, Std_M977, Std_Standardbred, Thoroughbred, Prz_D2630, Prz_D2631, Prz_Przewalski, Batagai, CGG10022, CGG10023, and CGG101397. The resulting structure was in agreement with that from the analyses presented above, showing 1) three clusters represented by domesticated horses, Przewalski's horses, and extinct horses, respectively, 2) close affinities between the historical (CGG101397) and the modern Yakutian horses, and 3) close genetic proximity between Mongolian horses and historical/modern Yakutian horses.

6.4 Admixture tests

We explored whether modern and ancient Yakutian horses showed evidence of genetic admixture using a range of admixture tests based on D-statistics (114) f3-statistics (115), Tree-Graph reconstructions in TreeMix (116), and NGSadmix (117).

6.4.1 D-statistics

The D-statistics, also known as ABBA-BABA test (114), assesses whether the genetic data of three taxa deviate from their tree-like relationship. Briefly, given three taxa (H_1 , H_2 and H_3), an outgroup (O) and a tree topology $((H_1, H_2), H_3, O)$, the D-statistics quantifies the occurrence of two incomplete sorting patterns, so called ABBA and BABA events, where A and B refer to ancestral (namely, identical to O)

and derived allelic states. ABBA events occur when H₂ and H₃ share the derived allele (B) while the ancestral allele (A) is carried by H₁. Conversely, in BABA events the ancestral allele (A) is carried by H₂ while H₁ and H₃ share the derived one. Under the null hypothesis that the tree is correct and there is no gene flow connecting H₃ to either H₁ or H₂, the ABBA and BABA events result from incomplete lineage sorting, and, thus, occur with equal frequency. Enrichment of ABBA sites (or BABA), therefore, indicates the possible presence of gene flow between the H₂ and H₃) lineages (H₁ and H₃, respectively).

Such deviations from equal proportion of ABBA-BABA events can however result from ancestral substructure prior to the divergence of H₁, H₂ and H₃, as well as to heterogeneities in genome-wide sequencing error rates (118). The latter was ruled out by only using samples with large differences in sequencing error rates as H₃. Moreover, to reduce the effect of base calling errors in ancient genomes (and to a lower extent those of some modern Yakutian horse genomes also showing an excess of GC→AT substitutions, see **section S2.6**), we restricted the calculation of D-statistics to transversions.

To comprehensively assess the amount of gene flow between horse lineages, we calculated multiple D-statistics, corresponding to different taxa combinations as H₁, H₂ or H₃ compatible with the inferred tree topology (**Figure S5.5**). As outgroup species, we used *Equus africanus somaliensis* from (30), because it was re-sequenced at higher depth-of-coverage than the domestic donkey (*Equus asinus asinus*) originally reported and used by Orlando and colleagues (13). The full list of surveyed scenarios is illustrated in (**Figure S6.9**).

Our significance assessment of D-statistics follows (13), where we applied a 10Mb block jackknife procedure to accommodate for the large levels of linkage disequilibrium in horses. The D-statistics significance was expressed as Z-scores, which are generally considered significant when their absolute values are higher than 3. However, in order to control the family-wise error rate arising from the large number of tests performed, we corrected the Z-scores for multiple testing using the function ‘p.adjust’ with the Holm correction (Holm 1979) in R. A test was considered significant when showing an adjusted p-value smaller than 0.05.

When one ancient horse was considered as H₃ and two Yakutian or two non-Yakutian domesticated horses as H₁ and H₂, the vast majority of the D-statistics were not significantly different from zero (**Figure S6.9A-B**). Conversely, the topology tested was rejected when including Przewalski’s horses as H₁ or H₂ (**Figure S6.9C-D**). Interestingly, all D-statistics calculated for the tree topology with non-Yakutian domesticated horses (**Figure S6.9D**) were significantly positive ($2.95 < \text{Z-scores} < 22.91$), in agreement with the findings from Schubert and colleagues based on a more limited genome dataset (16). This confirms that the extinct population of ancient horses (represented by Batagai, CGG10022 and CGG10023) contributed genetically to the population of domesticated horses, prior to or in the early stages of horse domestication.

The tree topology was rejected when non-Yakutian and Yakutian modern domesticated horses were placed as H₁ and H₂ and CGG101397 as H₃ (**Figure S6.9E**). This was not the case when any other ancient horse (Batagai, CGG10022, and CGG10023) was used as H₃ (**Figure S6.9E**). This not only agrees with a high genetic affinity between CGG101397 and modern Yakutian horses, but also rejects genetic continuity from more ancient Yakutian horses (here represented with the 5.2-kyr old Batagai sample) to modern Yakutian horses (see **sections S5.3, S6.3 and S6.4**). Finally, the tree topology could not be rejected when Przewalski’s horses were placed

as H₃ and modern Yakutian horses were placed as H₁/H₂, suggesting that no Yakutian individual is particular closer to Przewalski's horses (**Figure S6.9F**).

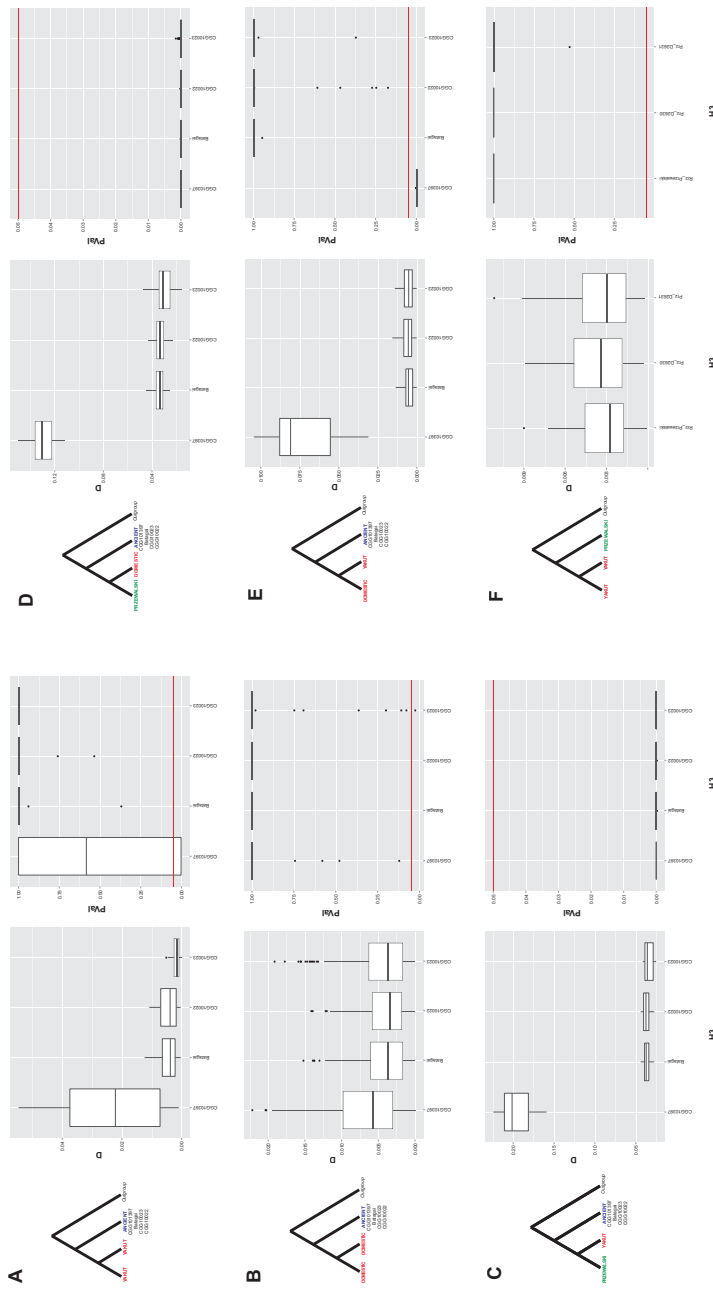


Figure S6.9. Admixture tests based on D-statistics and transversions.

The combinations tested are shown in the first and fourth columns. The D-statistics and p-values are indicated in the second/fifth columns and in the third/sixth columns, respectively. The red line indicates the p-value significance threshold of 0.05, following correction for multiple testing. In panels A-E, we tested ancient specimens (as H_3) against modern horses (considered as H_1 and H_2), while in panel F, Przewalski's horses were tested (as H_3) against our panel of domesticated breeds (considered as H_1 and H_2), including Yakutian horses. Ancient: Batagai, CGG10022, CGG10023, CGG101397. Domestic: Arabian, Fjord, Icelandic, Mng_D2629, Mng_D2628, Mon_FM0431, Mon_FM0450, Mon_FM0467, Mon_FM1030, Mon_FM1041, Mon_FM1190, Mon_FM1785, Mon_FM1798, Mon_FM1932, Mon_FM1948, Mon_FM1951, Mon_FM2218, Mor_EMS595, Qrt_A1543, Qrt_A5659, Qrt_A5964, Qrt_A2085, Std_Standardbred, Std_M977, Std_M5256, Std_M1009, Thoroughbred. Przewalski: Prz_Przewalski, Prz_D2631, Prz_D2630. Yakut: Yak1, Yak2, Yak3, Yak4, Yak5, Yak6, Yak7, Yak8, Yak9. Outgroup: *Equus africanus somaliensis*.

6.4.2 f_3 -statistics and TreeMix analyses

The plink file already generated for the PCA based on genotype calls (see **section S6.3.1**) was converted into a TreeMix input file (116). For that, we used the Python plink2treemix.py script provided by the TreeMix package (<https://code.google.com/p/treemix/>), grouping samples as indicated in **Table S6.6**. We ran TreeMix using a block resampling procedure of groups of 1,500 variants (-k 1,500).

f_3 -statistics

We calculated the $f_3(C;A,B)$ -statistic (115), which assesses whether a population C is the result of an admixture of ancestral populations A and B (**Figure S6.10**). In this section, we use the notation from (115) for the expected value of f_3 :

$$E [f_3(C;A,B)] = c + \alpha^2 d + \beta^2 e - \alpha\beta(g+f)$$

where f , g , d , e and c represent the branch lengths illustrated in **Figure S6.10**, while α and β the corresponding admixture proportions. If the f_3 -statistic is negative, it supports a complex population history whereby population C descends from both A and B populations. However, we found no significant results when ancient specimens were placed as the test population C (**Table S6.7**), suggesting an absence of admixture for each combination tested.

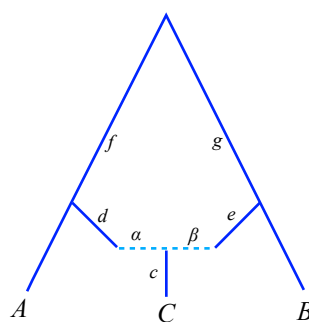


Figure S6.10. Schematic illustration depicting the notation used to estimate f_3 -statistics values.

For three hypothetical populations (A, B and C) branch lengths (f , g , d , e and c) and admixture proportions (α and β). Migration edges are depicted with a light blue dashed line.

TreeMix: estimation of the population trees with admixture

We used TreeMix (116) to infer horse population splits, and subsequent admixture events. TreeMix analyses were run considering up to four migration events (-m 0-4). We performed a round of global rearrangements after all populations were added (-global), and placed the root of the inferred trees at the root of the clade represented by the ancient specimens CGG10022, CGG10023, Batagai (option -root CGG10022, CGG10023, Batagai). The resulting trees were plotted using the supplied TreeMix R functions. The total fraction of the variance explained by each migration model was estimated with the 'get_f()' R function.

TreeMix recovers the same tree topologies as the one inferred from our phylogenomic analysis (see **section S5.3; Figures 1B and S6.11**), regardless of the number of migration events considered. The Late Pleistocene horses (CGG10022 and CGG10023) cluster with the ancient Yakutian sample Batagai, forming a sister

lineage clearly separated from the modern horses and CGG101397. The majority of the allele frequency variation (variance = 98.6669%) is solely explained by the tree topology, with migration events only providing a marginal increment (from up to 0.26%). The first migration edge is between the Prz_Przewalski and the population ancestral to the domesticated breeds (0.17% increase in variance). The variance explained by the additional migration edges is much smaller than the first migration edge (<0.09%), and simply involves admixture within modern Yakutian horses, probably reflecting their shared ancestry.

6.4.3 Genetic Clustering based on genotype likelihoods

The genetic structure of our panel of modern and ancient horses was investigated using the function “NGSAdmix” implemented in ANGSD, which handles genotype uncertainties in a Maximum Likelihood framework (46, 117). The analyses were run considering two to 20 ancestral populations (-K), a minimum minor allele frequency of 5% (-minMaf) and a maximum number of Expectation Maximization iterations of 5,000 (-maxiter) (**Figure S6.12**). We retained K = 6 as the plausible number of ancestral populations, as it retrieves the known genetic structure among present-day domesticated horse breeds, including: (K1) Arabian horses, Morgan horses, Thoroughbred horses, Standardbred horses, American Quarter horses, in accordance with the latter three descending from Arabian horses; (K2) Franches-Montagnes; (K3) Przewalski’s horses; (K4) Mongolian horses, Icelandic horses and Norwegian Fjord horses, in agreement with the genetic affinities reported in (13, 16, 119), and in our phylogenetic results (see **section S5**). Importantly, the last two clusters consist of (K5) Batagai and the Late Pleistocene horses CGG10022 and CGG10023, and (K6) all modern Yakutian horses, including sample CGG101397. No ancestry component is shared between clusters (K5) and (K6), confirming that samples Batagai and CGG101397 reflect two different population ancestries, in line with the results from our other analyses. Of note, some horses such as Yak2 seem to share some of their ancestry with modern Mongolian horses, as also suggested by our genome projections (see **section S6.2**).

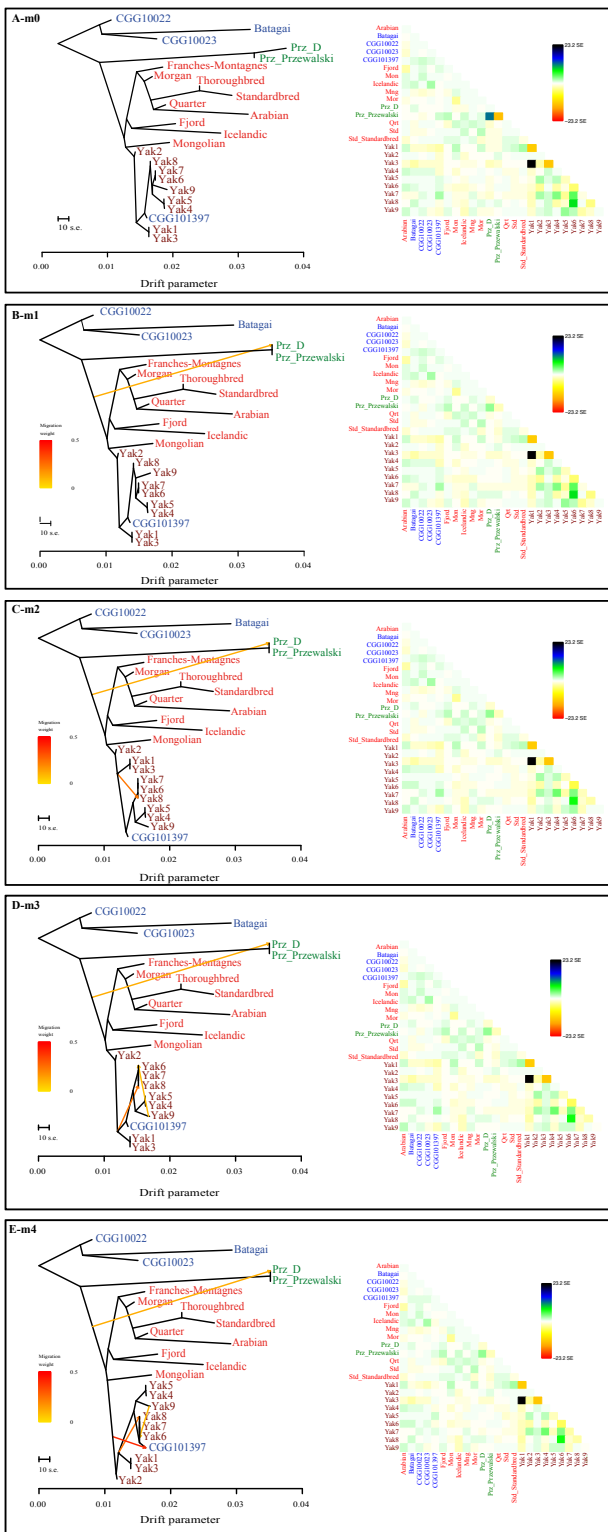


Figure S6.11. TreeMix population splits between modern and ancient horses.

Left: population relationships as inferred from Treemix analyses, considering 0-4 possible migration edges (m0-m4). Right: Residuals of the covariance matrix. Individuals belonging to the same domesticated breed were grouped together, and branch labels are provided in **Table S6.4**. Proportion of the variance explained by the tree: A. 98.6669%; B. 98.8381%; C. 98.9042%; D. 98.9049%; E. 98.9270%.

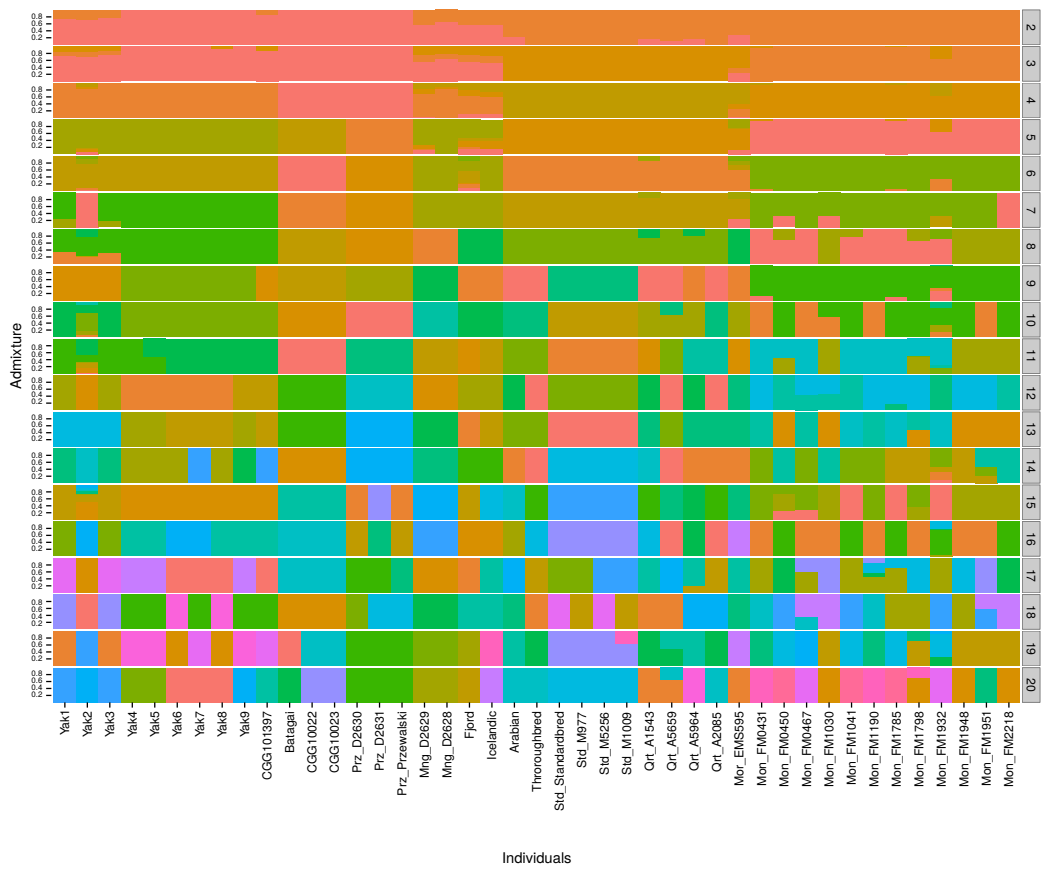


Figure S6.12. Admixture plot representing from $K=2$ to 20 ancestry components.

6.5 Supplementary Tables for Section 6

Table S6.1. Ancestral population size changes estimated from PSMC analyses, used as non-free (fixed) parameters in the estimation of recent history

Time (yBP)	Effective population size*
8509835	136338
6009540	142062
5047854	129485
4238467	105545
3557261	80974
2983935	66227
2501405	64800
2095293	76820
1753495	101314
1465827	129322
1223716	131287
1019947	89860
848449	43198
704110	20871
582631	16067
480389	23631
394339	55064
321917	135346
260963	221906
209664	219181
166488	151155
130149	110403
99566	128007
73826	174071
52162	147017
33930	146775
18584	n.a. [#]

* parameter to be estimated

Table S6.2. Demographic parameters estimated using *dadi* and the reference, Mongolian, and donkey genome sequence as ancestral state.

Outgroup	Parameters	Model PSMC	Model one epoch	Model three epochs
Thoroughbred (EquCab2.0 Reference sequence)	Log-likelihood	-867.86	-124.25	-121.05
	N ₁	5,107*	16,352	48,152
	N ₂	-	3,072	17,878
	N ₃	-	-	<15
	N ₄	-	-	6,582
	P _{misid}	<0.001	0.012	0.012
Mng_D2628 (Mongolian)	Log-likelihood	-872.43	-126.49	-123.39
	N ₁	5,107*	16,339	47,958
	N ₂	-	3,059	17,763
	N ₃	-	-	<15
	N ₄	-	-	7,968
	P _{misid}	<0.001	0.0093	0.0097
Equus africanus somaliensis (donkey)	Log-likelihood	-872.43	-126.49	-123.39
	N ₁	5,107*	16,339	47,958
	N ₂	-	3,059	17,763
	N ₃	-	-	<15
	N ₄	-	-	7,968
	P _{misid}	<0.001	0.0093	0.0097

* parameter set as fixed value

Table S6.3. Likelihood surface assuming different values for the founder effect.

Data set	Founder time (yBP)	Reference	Mongolian	Donkey
4d-fold sites	5,000	-127.17	-129.48	-119.55
	4,000	-124.94	-127.25	-116.67
	3,000	-123.20	-125.52	-114.44
	2,000	-121.95	-124.28	-112.84
	1,000	-121.18	-123.52	-111.84
	500	-120.98	-123.32	-111.57
	200	-120.90	-123.24	-111.47
Genome-wide SFS	5,000	-16,183.96	-14,444.93	-13,312.14
	4,000	-15,531.13	-13,757.58	-12,390.05
	3,000	-15,034.58	-13,225.16	-11,663.36
	2,000	-14,691.63	-12,845.11	-11,125.64
	1,000	-14,499.94	-12,615.29	-10,771.32
	500	-14,460.18	-12,556.14	-10,661.38
	200	-14,454.12	-12,538.36	-10,616.59

Table S6.4. Horse genomes used for projection analyses.

Horse ID	Horse type	Reference	Reference panel(s)
Yak1	Yakutian	this study	refYAK
Yak2	Yakutian	this study	refYAK
Yak3	Yakutian	this study	refYAK
Yak4	Yakutian	this study	refYAK
Yak5	Yakutian	this study	refYAK
Yak6	Yakutian	this study	refYAK
Yak7	Yakutian	this study	refYAK
Yak8	Yakutian	this study	refYAK
Yak9	Yakutian	this study	refYAK
CGG10022	Ancient Taymyr peninsula	Orlando et al. 2013 (13)	n/a
CGG10023	Ancient Taymyr peninsula	Schubert et al. 2014 (16)	n/a
CGG101397	Ancient Yakutia	this study	n/a
Batagai	Ancient Yakutia	this study	n/a
Prz_D2630	Przewalski	Do et al. 2014 (19)	n/a
Prz_D2631	Przewalski	Do et al. 2014 (19)	n/a
Prz_Przewalski	Przewalski	Orlando et al. 2013 (13)	n/a
Arabian	Arabian	Orlando et al. 2013 (13)	refDOM
Fjord	Norwegian Fjord	Orlando et al. 2013 (13)	refDOM
Icelandic	Icelandic	Orlando et al. 2013 (13)	refDOM
Mng_D2628	Mongolian	Do et al. 2014 (19)	refDOM
Mng_D2629	Mongolian	Do et al. 2014 (19)	refDOM
Mor_EMS595	Morgan	this study	refDOM
Qrt_A5964	Quarter	this study	refDOM
Qrt_A5659	Quarter	this study	refDOM
Qrt_A1543	Quarter	this study	refDOM
Qrt_A2085	Quarter	this study	refDOM
Std_M977	Standardbred	this study	refDOM
Std_M5256	Standardbred	this study	refDOM
Std_M1009	Standardbred	this study	refDOM
Std_Standardbred	Standardbred	Orlando et al. 2013 (13)	refDOM
Thoroughbred	Thoroughbred	Wade et al. 2009 (29)	refDOM
Mon_FM1798	Franches-Montagnes	this study	refDOM, refFM
Mon_FM1932	Franches-Montagnes	this study	refDOM, refFM
Mon_FM1948	Franches-Montagnes	this study	refDOM, refFM
Mon_FM2218	Franches-Montagnes	this study	refDOM, refFM
Mon_FM1190	Franches-Montagnes	this study	refDOM, refFM
Mon_FM1041	Franches-Montagnes	this study	refDOM, refFM
Mon_FM1951	Franches-Montagnes	this study	refDOM, refFM
Mon_FM0467	Franches-Montagnes	this study	refDOM, refFM
Mon_FM_431	Franches-Montagnes	this study	refDOM, refFM
Mon_FM1785	Franches-Montagnes	this study	refDOM, refFM
Mon_FM1030	Franches-Montagnes	this study	refDOM, refFM
Mon_FM0450	Franches-Montagnes	this study	refDOM, refFM

Table S6.5. Minimum projection values.

Test genome(s)	refYAK		refFM	
	MPV	sd	MPV	sd
Yakutian horses	*	*	0.7724	0.0092
Przewalski's horses	0.6926	0.0009	0.6762	0.0109
Non-Franches-Montagnes	0.8073	0.0246	0.8088	0.0283
Franches-Montagnes	0.8038	0.0062	*	*
CGG101397	0.8719	n/a	0.7637	n/a
Batagai	0.5967	n/a	0.5943	n/a
CGG10022	0.6067	n/a	0.6010	n/a
CGG10023	0.5898	n/a	0.5913	n/a
Ancient horses (excl. CGG101397)	0.5977	0.0085	0.5955	0.0050

“MPV”: Minimum Projection Value; “sd”: standard deviation.

Table S6.6. Samples used for the f_3 -statistics and TreeMix analyses.

Group	Samples	Horse type
Batagai	Batagai	Ancient
CGG10022	CGG10022	
CGG10023	CGG10023	
CGG101397	CGG101397	
Icelandic	Icelandic	Domesticated
Mng	Mng D2629	
	Mng D2628	
Mon	Mon_FM1932	
	Mon_FM1951	
	Mon_FM1785	
	Mon_FM1030	
Mor	Mor_EMS595	
Qrt	Qrt_A5964	
	Qrt_A5659	
Std	Std_M977	Przewalski
	Std_M5256	
Std Standardbred	Std Standardbred	
Arabian	Arabian	
Fjord	Fjord	Yakutian
Prz_D	Prz_D2630	
	Prz_D2631	
Prz Przewalski	Prz Przewalski	
Yak	Yak1	
	Yak2	
	Yak3	
	Yak4	
	Yak5	
	Yak6	
	Yak7	
	Yak8	
	Yak9	

Table S6.7. f_3 -statistics for topologies where ancient specimens are considered as population C. None f_3 statistics are significantly negative.

7 Section 7: Genetic determinants of the Yakutian horse adaptations

Our demographic analyses (see **section S6**) show that contemporary Yakutian horses derive from a recent founder event, likely associated with the arrival of Yakut people in the area a few centuries ago (1, 2). It follows that Yakutian horses have evolved striking physiological and morphological adaptations to extreme climate conditions in a small number of generations. Here, we analyzed the genetic basis and evolutionary mechanisms underlying these adaptations.

7.1 Selection scans

7.1.1 Genetically differentiated regions: F_{ST} -outlier approach

We estimated the F_{ST} index by comparing the genomes of modern Yakutian horses against two different domestic populations, including one comprising 12 Franches-Montagnes horses (hereafter referred to as YAK-FM), and another one encompassing all 27 individuals from nine different domestic breeds (YAK-DOM). The genome of the 19th century specimen CGG101397 was included within the set of modern Yakutian horse genomes, as it is genetically undifferentiated from modern individuals (see **sections S5.3** and **S6**). A schematic description of the compared populations is summarized in **Table S7.1**.

The F_{ST} values were estimated in 50 Kb sliding windows (step 10 Kb), using the ngsFst program of the ngsPopGen package (113). Briefly, for each compared population pair (i.e. YAK-DOM and YAK-FM), priors for the allele frequencies of each position (saf files) were estimated with ANGSD v0.615, which implements a statistical framework to integrate over genotype uncertainties (46). To generate saf files, we assumed Hardy-Weinberg equilibrium, and only considered autosomal sites with a minimum mapping quality of 25 (-minMapQ), a minimum base quality of 20 (-minBQ), and for which data were available in at least half of the individuals (-minInd). The saf files were then used as input information for the realSFS 2dsfs command in ANGSD, which generated the 2D Site Frequency Spectrum between each pair of populations considered. The saf files and the 2D SFS were then used as input for the ngsFST command from the ngsPopGen package (113).

Outlier F_{ST} regions were detected following two different approaches. In the first approach (hereafter referred to as “Gene-max”), we simply extracted those genes located in regions ranking in the top-1% (or 5%) F_{ST} values. This provided a total number of 251 (top-1%) or 1,255 (top-5%) gene candidates underpinning significant population differentiation for the two data sets considered (YAK-DOM and YAK-FM). In the second approach (“Region-peaks”), we applied the smoothing procedure described in the Supplementary section S7.2 of (30). This provided 312 (or 1,489) and 318 (1,350) outlier genes for the YAK-DOM and YAK-FM data sets, respectively. Significant outcomes “Region-peaks” smooting method are shown for five different chromosomes in **Figures S7.1** and **S7.2**, which are representative of the profiles observed across all chromosomes. **Table S7.2** summarizes the number of significant genes for each approach. **Table S7.3** shows the complete list of genes within the top-1% F_{ST} -outlier windows, and **Tables S7.4-S7.7** the corresponding enrichment tests.

Outlier F_{ST} windows were found to be depleted of protein-coding genes (**Figure S7.3**), pointing to a long-term effect of negative selection in reducing their

genetic differentiation, but also to ongoing adaptive pressures in non-coding loci, and thus in potentially regulatory regions.

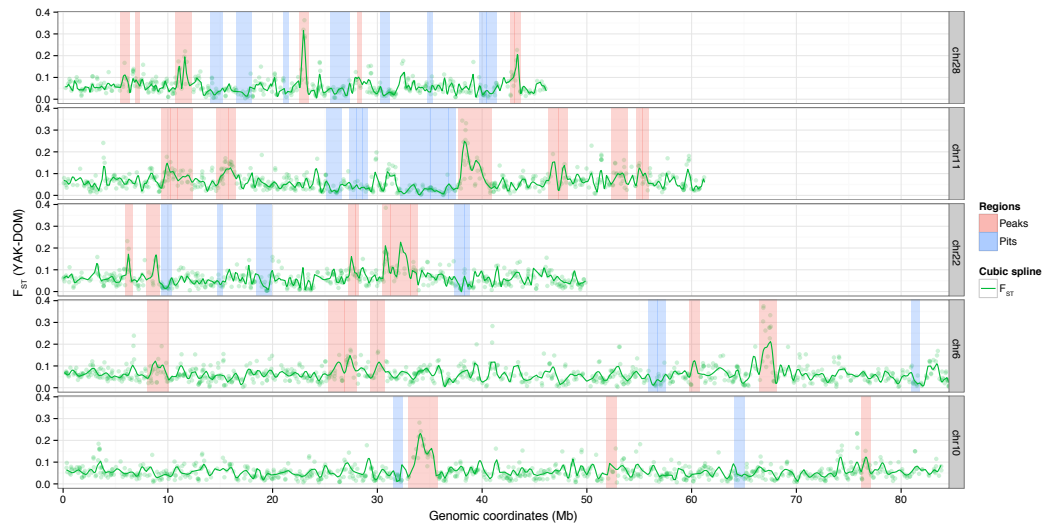


Figure S7.1. Illustrative examples of F_{ST} outlier regions identified by the “Region peaks” smoothing method (YAK-DOM).

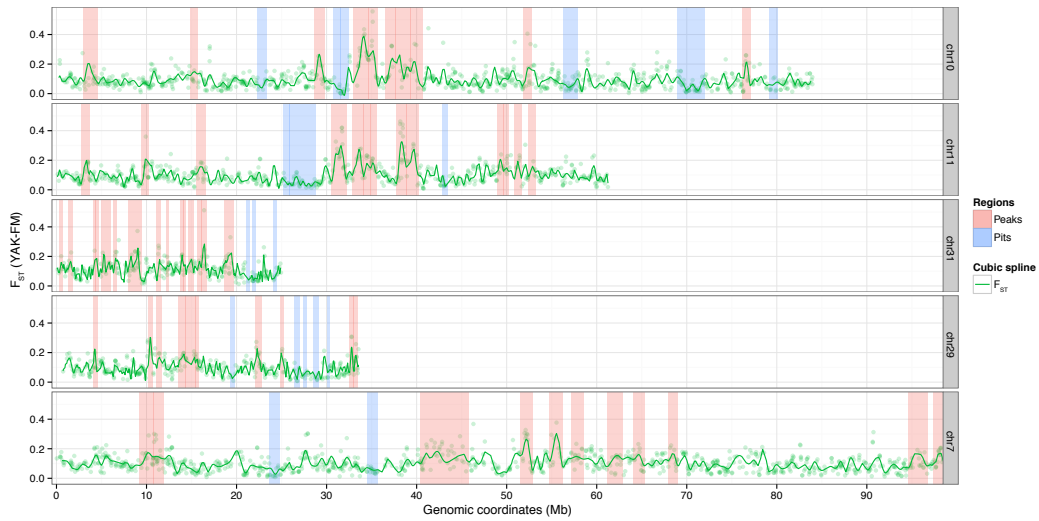


Figure S7.2. Illustrative examples of F_{ST} outlier regions identified by the “Region-peaks” smoothing method (YAK-FM).

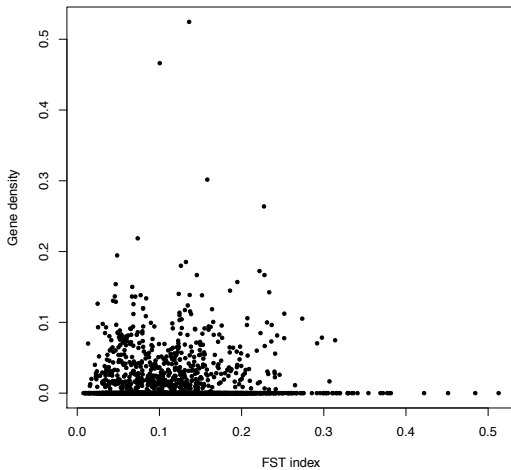


Figure S7.3. Relationship between protein-coding gene density and F_{ST} in 50Kb sliding windows.

7.2 Coding vs. non-coding contribution to adaptation

It is well known that mutations affecting the function of *cis*-regulatory elements (CREs) are a major force driving the evolution of transcriptional regulation, significantly contributing to the phenotypic variation within and between species (120). Nevertheless, the relative contribution of the CRE and non-synonymous mutations to adaptation remains one of the most controversial issues in evolutionary genetics (121–125).

At one end of the spectrum, adaptive changes are believed to mainly involve CRE mutations, because they can alter gene expression in very specific spatio-temporal frames, thereby fine-tuning transcriptional expression to optimize individual fitness (122). Unlike CRE mutations, protein-coding variants have a larger potential for high pleiotropic effects, as they can introduce phenotypic changes in all the developmental stages and/or cell types where the underlying gene is expressed. This may reduce the “evolvability” of the protein-coding regions, often yielding low evolutionary rates, especially if they have high levels of expression breadth, such as those housekeeping genes.

The critics of such extreme view argue that there are other mechanisms decreasing the functional constraints imposed by pleiotropy, such as increasing redundancy through gene duplication. Indeed, it is generally accepted that gene duplications are a major evolutionary mechanism for generating functional innovation, either through neofunctionalization or subfunctionalization, which may also play an important role in adaptation (124, 126).

7.2.1 Genetic distances across functional site categories

We used current gene model annotations (Ensembl version 2.78) to classify the horse genome positions into functional categories. In particular, we split protein-coding regions into zero-fold (0d-fold), two-fold (2d-fold) and four-fold (4d-fold) positions, depending on their degeneracy. Mutations at zero-fold degenerate positions always result in amino acid replacement, implying non-synonymous changes. In contrast, mutations at four-fold positions, which are synonymous, provide proxies for sites putatively evolving under neutrality. Changes at two-fold positions involve both

synonymous and non-synonymous changes. Additionally, we partitioned the 10Kb located upstream of Translation Start Sites (TSS) into non-overlapping 1Kb bins.

We then calculated the genetic distance (average net number of pairwise nucleotide differences, or d_A) (127) between the Yakutian horse population (including the sequence information from contemporary horses and the historical horse CGG1101397) and two panels of domesticated horses (**Table S7.1**). The first encompasses all the 27 domesticated horses considered in this study (YAK-DOM, see **section S7.1.1**), while the second is restricted to the 12 horses within the Franches-Montagnes breed (YAK-FM, see **section S7.1.1**). The inclusion of different breeds in the YAK-DOM panel alleviates possible breed-specific selective processes, while YAK-FM reduces the bias caused by the inherent breed structure. We used mstatspop (http://bioinformatics.cragenomica.es/numgenomics/people/sebas/software/files/page_3_4.zip) to calculate d_A on those positions with up to 10% of missing alleles.

The neutral expectation of nucleotide divergence was approximated by the d_A values at four-fold degenerate positions, using the top-0.001% quantile as the minimal threshold for detecting sites putatively evolving under positive selection (**Figure 4A** for the YAK-FM panel, and **Figure S7.4** for YAK-DOM). Comparing the proportion of adaptive mutations across sites is not straightforward, because the sample size is unbalanced across site categories, i.e. the more sites analyzed in a particular category, the higher the probability of observing positively selected mutations. We therefore applied a bootstrapping approach to circumvent this issue, re-sampling with replacement the same number of sites within each category (e.g. zero-fold, first 1Kb located upstream of TSS) as those analyzed for the neutral reference. For each of the 10,000 bootstrap replicates, we estimated the proportion of adaptive mutations within each site category, obtaining full data distributions that are shown in **Figure 4B** (YAK-FM panel) and **Figure S7.5** (YAK-DOM panel). The complete list of genes harbouring significant instances of adaptive alleles at their upstream regions is available upon request.

We also verified that the identification of dA-outliers was not biased by underlying segmental duplications, as the presence of unidentified paralogs could lead to spurious read alignments and, hence the calculation of erroneous dA values. To achieve this, we recovered any site under selection (as identified by the dA-based selection scans using DOM and FM as reference panels) that was also found in regions identified as segmental duplications (see **section S4.2**) extended by 1 Kb upstream and downstream of the duplicated region. The overlap was found to be negligible when considering both the FM (2/184 = 1.1%) and the DOM (14/1,486 = 0.9%) panels, suggesting a limited impact of segmental duplications on the detection of sites under selection. Similarly, only ~1% of the genes with dA outlier sites at their upstream regions were embedded within CNVs. Consequently, the functional enrichment analyses reported almost identical results (methods for functional enrichment analyses described in **section S7.3**), corroborating the biological significance of our findings.

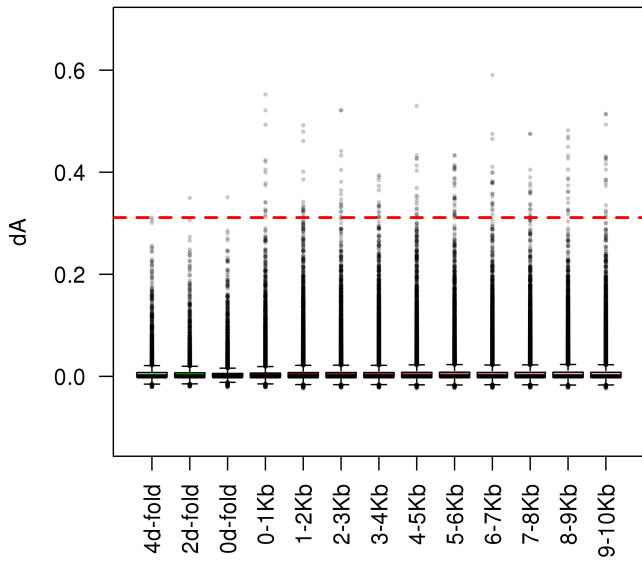


Figure S7.4. Boxplot of the d_A estimates across different site categories, for the YAK-DOM population pair.

The red line delimits the threshold of neutrality (i.e. the top 0.001% of the 4d-fold degenerate sites). Points above this red line represent nucleotide positions genetically more differentiated than this threshold, and therefore sites positively selected since the ancestral population split.

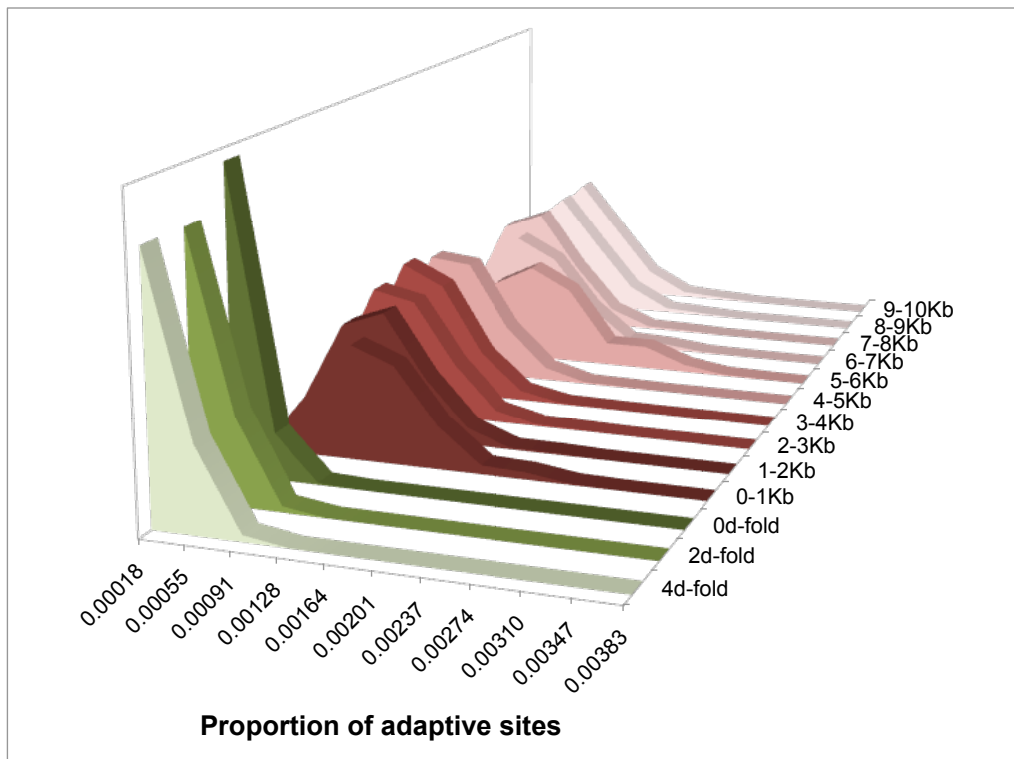


Figure S7.5. Proportion of adaptive sites for each site category in the YAK-DOM population pair.

7.3 Functional enrichment analyses

We tested for functional enrichment among the genes targeted by positive selection, either at their protein-coding (F_{ST}) or upstream regions (d_A -based analysis). Functional enrichment was carried out on the online platform WebGestalt (WEB-based Gene SeT AnaLysis Toolkit; (128)), separately using the functional annotations of either the humans or mice ortholog genes as query (orthologs were downloaded from Ensembl, using the BioMart query tool), and the following databases:

- Pathways: KEGG (03/21/2011), WikiPathways (11/11/2012),
- Phenotypes: Mammalian Phenotype Ontology (for mouse gene ID, 04/10/2013) and Human Phenotype Ontology (for human gene ID 04/10/2013),
- Phenome-Wide Association Study: PheWAS catalog (05/20/2014; for human gene ID only),
- Disease associated genes: GLAD4U (1/26/2013, for human gene ID only).

We used default parameters and Benjamini-Hochberg correction for multiple tests (129), and retained the top-10 significant enrichment clusters. Enrichment results are in **Tables S4.4-S4.8** (for the ancestral informative markers), **Tables S4.13-S4.15** (for the Copy Number Variants), **Tables S7.4-S7.7** (for the F_{ST} -outlier windows), and **S7.8-S7.13** (for d_A -outlier positions).

7.4 Supplementary Tables for Section 7

Table S7.1. Specimens used in FST selection scan.

Horse ID	Horse type	Reference	Reference panel(s)
Yak1	Yakutian	this study	refYAK
Yak2	Yakutian	this study	refYAK
Yak3	Yakutian	this study	refYAK
Yak4	Yakutian	this study	refYAK
Yak5	Yakutian	this study	refYAK
Yak6	Yakutian	this study	refYAK
Yak7	Yakutian	this study	refYAK
Yak8	Yakutian	this study	refYAK
Yak9	Yakutian	this study	refYAK
CGG101397	Yakutian 19 th century	this study	refYAK
Arabian	Arabian	Orlando et al., 2013 (13)	refDOM
Fjord	Norwegian Fjord	Orlando et al., 2013 (13)	refDOM
Icelandic	Icelandic	Orlando et al., 2013 (13)	refDOM
Mng_D2628	Mongolian	Do et al., 2014 (19)	refDOM
Mng_D2629	Mongolian	Do et al., 2014 (19)	refDOM
Mor_EMS595	Morgan	this study	refDOM
Qrt_A5964	Quarter	this study	refDOM
Qrt_A5659	Quarter	this study	refDOM
Qrt_A1543	Quarter	this study	refDOM
Qrt_A2085	Quarter	this study	refDOM
Std_M977	Standardbred	this study	refDOM
Std_M5256	Standardbred	this study	refDOM
Std_M1009	Standardbred	this study	refDOM
Std_Standardbred	Standardbred	Orlando et al., 2013 (13)	refDOM
Thoroughbred	Thoroughbred	Wade et al., 2009 (29)	refDOM
Mon_FM1798	Franches-Montagnes	this study	refDOM, refFM
Mon_FM1932	Franches-Montagnes	this study	refDOM, refFM
Mon_FM1948	Franches-Montagnes	this study	refDOM, refFM
Mon_FM2218	Franches-Montagnes	this study	refDOM, refFM
Mon_FM1190	Franches-Montagnes	this study	refDOM, refFM
Mon_FM1041	Franches-Montagnes	this study	refDOM, refFM
Mon_FM1951	Franches-Montagnes	this study	refDOM, refFM
Mon_FM0467	Franches-Montagnes	this study	refDOM, refFM
Mon_FM_431	Franches-Montagnes	this study	refDOM, refFM
Mon_FM1785	Franches-Montagnes	this study	refDOM, refFM
Mon_FM1030	Franches-Montagnes	this study	refDOM, refFM
Mon_FM0450	Franches-Montagnes	this study	refDOM, refFM

We compared Yakutian horses (including the CGG101397 specimen) against the YAK-DOM and YAK-FM panels.

Table S7.2. Number of outlier genes identified through F_{ST} selection scans.

Population 1	Population 2	Method	Significance threshold	Outlier genes
YAK	DOM	Region-peaks	0.01	312
			0.05	1,489
		Gene-max	0.01	251
			0.05	1,255
YAK	FM	Region-peaks	0.01	318
			0.05	1,350
		Gene-max	0.01	251
			0.05	1,255

We used two different detection methods (“Gene-max” and “Region-peaks”) and two significance thresholds ($\alpha = 0.01$ and 0.05).

Table S7.3. Genes within the top 1% FST-outlier windows.

GeneID	TranscriptID	QValue(Min)	QValue(Max)	Overlap	Biotype	Name	Description
ENSECAG00000000384	ENSECAT00000000362	6.58E-05	6.58E-05	1,108	protein coding	<i>ERP29</i>	endoplasmic reticulum protein 29
ENSECAG00000000395	ENSECAT00000000572	1.09E-02	3.67E-02	516	protein coding	<i>RAPGEF5</i>	Rap guanine nucleotide exchange factor (GEF) 5
ENSECAG00000000420	ENSECAT00000000470	6.58E-05	1.62E-04	1,526	protein coding	<i>BANP</i>	BTG3 associated nuclear protein
ENSECAG00000000658	ENSECAT00000001905	1.97E-02	4.04E-02	1,190	protein coding	<i>GPNMB</i>	glycoprotein (transmembrane) nmb
ENSECAG00000001022	ENSECAT00000000843	4.07E-03	4.07E-03	339	protein coding	<i>UCN2</i>	urocortin 2
ENSECAG00000001103	ENSECAT00000000912	6.58E-05	6.58E-05	825	protein coding		Uncharacterized protein
ENSECAG00000001493	ENSECAT00000001322	2.60E-04	2.60E-04	891	protein coding		Uncharacterized protein
ENSECAG00000001843	ENSECAT00000001659	1.04E-04	1.04E-04	681	protein coding		Uncharacterized protein
ENSECAG00000001866	ENSECAT00000001683	1.46E-04	1.46E-04	597	protein coding		Uncharacterized protein
ENSECAG00000001999	ENSECAT00000001963	2.61E-02	2.86E-02	258	protein coding	<i>GMDS</i>	GDP-mannose 4,6-dehydratase
ENSECAG00000002212	ENSECAT00000002055	6.58E-05	6.58E-05	1,437	protein coding	<i>FOXO1</i>	forkhead box O1
ENSECAG00000002894	ENSECAT00000002734	1.62E-04	1.62E-04	294	protein coding	<i>SPATA45</i>	spermatogenesis associated 45
ENSECAG00000002985	ENSECAT00000002828	6.58E-05	6.58E-05	540	protein coding		Uncharacterized protein
ENSECAG00000003561	ENSECAT00000003425	1.32E-03	1.32E-03	519	protein coding	<i>TMEM11</i>	transmembrane protein 11
ENSECAG00000003600	ENSECAT00000003692	6.58E-05	6.58E-05	1,097	protein coding	<i>MRPS31</i>	mitochondrial ribosomal protein S31
ENSECAG00000003664	ENSECAT00000003504	1.62E-04	1.62E-04	1,290	protein coding		Uncharacterized protein
ENSECAG00000003992	ENSECAT00000003872	1.62E-04	1.62E-04	954	protein coding		Uncharacterized protein
ENSECAG00000004727	ENSECAT00000004599	3.38E-02	4.29E-02	1,059	protein coding	<i>S1PR2</i>	sphingosine-1-phosphate receptor 2
ENSECAG00000004819	ENSECAT00000008274	3.77E-03	3.12E-02	3,164	protein coding	<i>DNAH11</i>	dynein, axonemal, heavy chain 11
ENSECAG00000005550	ENSECAT00000005515	1.62E-04	1.62E-04	747	protein coding	<i>SFN</i>	stratin
ENSECAG00000006237	ENSECAT00000006194	1.27E-03	1.48E-03	1,526	protein coding		Uncharacterized protein
ENSECAG00000006490	ENSECAT00000006548	2.49E-03	2.49E-03	906	protein coding	<i>OR4K14</i>	olfactory receptor, family 4, subfamily K, member 14
ENSECAG00000006608	ENSECAT00000006575	8.96E-04	1.41E-03	872	protein coding	<i>OR4K13</i>	olfactory receptor, family 4, subfamily K, member 13
ENSECAG00000006635	ENSECAT00000006635	5.60E-04	5.60E-04	927	protein coding	<i>OR4N5</i>	olfactory receptor, family 4, subfamily N, member 5
ENSECAG00000006720	ENSECAT00000006683	1.62E-04	1.62E-04	939	protein coding		Uncharacterized protein
ENSECAG00000007163	ENSECAT00000007206	1.62E-04	1.62E-04	1,162	protein coding	<i>NR0B2</i>	nuclear receptor subfamily 0, group B, member 2
ENSECAG00000007531	ENSECAT00000007542	1.62E-04	1.62E-04	900	protein coding	<i>OR4C16</i>	olfactory receptor, family 4, subfamily C, member 16 (gene/pseudogene)
ENSECAG00000007653	ENSECAT00000007936	1.62E-04	1.62E-04	1,591	protein coding	<i>GPATCH3</i>	G patch domain containing 3
ENSECAG00000007790	ENSECAT00000007819	1.73E-03	1.73E-03	903	protein coding	<i>OR4P4</i>	olfactory receptor, family 4, subfamily P, member 4
ENSECAG00000008082	ENSECAT00000008235	7.83E-03	2.83E-02	2,225	protein coding	<i>PJA2</i>	praia ring finger 2, E3 ubiquitin protein ligase
ENSECAG00000008109	ENSECAT000000029102	3.20E-02	3.61E-02	694	protein coding	<i>BANK1</i>	B-cell scaffold protein with ankyrin repeats 1
ENSECAG00000008110	ENSECAT00000008250	6.58E-05	6.58E-05	1,368	protein coding	<i>TMEM116</i>	transmembrane protein 116
ENSECAG00000008220	ENSECAT00000008357	2.07E-02	2.07E-02	565	protein coding	<i>FDXIL</i>	ferredoxin 1-like
ENSECAG00000008513	ENSECAT00000008623	1.62E-04	1.62E-04	828	protein coding	<i>TATDN3</i>	TatD DNase domain containing 3
ENSECAG00000008638	ENSECAT00000009209	6.95E-03	8.77E-03	522	protein coding	<i>RERE</i>	arginine-glutamic acid dipeptide (RE) repeats
ENSECAG00000008659	ENSECAT00000008879	2.36E-04	3.31E-04	792	protein coding	<i>SHISA5</i>	shisa family member 5
ENSECAG00000008754	ENSECAT00000009442	6.58E-05	6.58E-05	2,913	protein coding	<i>NAA25</i>	N(alpha)-acetyltransferase 25, NatB auxiliary subunit
ENSECAG00000008821	ENSECAT00000009135	6.58E-05	6.58E-05	1,086	protein coding	<i>FCAR</i>	Equus caballus Fc fragment of IgA, receptor for (FCAR), mRNA.
ENSECAG00000009092	ENSECAT00000009245	1.50E-03	1.50E-03	930	protein coding		Uncharacterized protein
ENSECAG00000009299	ENSECAT00000009838	1.94E-02	1.94E-02	2,755	protein coding	<i>ICAM5</i>	intercellular adhesion molecule 5, telencephalin
ENSECAG00000009341	ENSECAT00000009505	1.62E-04	1.62E-04	831	protein coding		Uncharacterized protein
ENSECAG00000009355	ENSECAT00000009653	1.62E-04	1.62E-04	944	protein coding	<i>NSL1</i>	NSL1, MIS12 kinetochore complex component
ENSECAG00000009384	ENSECAT00000009603	1.62E-04	9.51E-03	1,122	protein coding	<i>NECAB1</i>	N-terminal EF-hand calcium binding protein 1

ENSECAG00000009599	ENSECAT00000009793	6.58E-05	6.58E-05	3,736	protein coding		Uncharacterized protein
ENSECAG00000009723	ENSECAT00000010381	3.03E-02	3.03E-02	739	protein coding	<i>IGF2BP1</i>	insulin-like growth factor 2 mRNA binding protein 1
ENSECAG00000009737	ENSECAT00000009944	6.58E-05	6.58E-05	622	protein coding	<i>IL17C</i>	interleukin 17C
ENSECAG00000009769	ENSECAT00000010081	1.11E-03	3.29E-02	1,303	protein coding	<i>CNTN4</i>	contactin 4
ENSECAG00000009796	ENSECAT00000010439	5.43E-04	9.58E-03	862	protein coding	<i>FER</i>	fer (fps/fes related) tyrosine kinase
ENSECAG00000010327	ENSECAT00000011267	4.81E-03	1.33E-02	590	protein coding	<i>INPP4B</i>	inositol polyphosphate-4-phosphatase, type II, 105kDa
ENSECAG00000010723	ENSECAT00000011174	1.62E-04	1.62E-04	1,656	protein coding	<i>ANGEL2</i>	angel homolog 2 (Drosophila)
ENSECAG00000010761	ENSECAT00000011071	2.36E-04	2.36E-04	1,021	protein coding	<i>TREX1</i>	three prime repair exonuclease 1
ENSECAG00000010784	ENSECAT00000011297	2.36E-04	3.11E-04	2,200	protein coding	<i>ATRIP</i>	ATR interacting protein
ENSECAG00000010790	ENSECAT00000011790	4.81E-03	3.81E-02	1,864	protein coding	<i>COG6</i>	component of oligomeric golgi complex 6
ENSECAG00000010806	ENSECAT00000011160	6.58E-05	6.58E-05	1,095	protein coding		Uncharacterized protein
ENSECAG00000010965	ENSECAT00000011277	6.58E-05	6.58E-05	645	protein coding	<i>CYBA</i>	cytochrome b-245, alpha polypeptide
ENSECAG00000011042	ENSECAT00000011367	2.36E-04	3.31E-04	297	protein coding	<i>BATF3</i>	basic leucine zipper transcription factor, ATF-like 3
ENSECAG00000011206	ENSECAT00000011581	6.58E-05	1.46E-02	1,308	protein coding	<i>MVD</i>	mevalonate (diphospho) decarboxylase
ENSECAG00000011234	ENSECAT00000012935	4.07E-03	1.43E-02	6,098	protein coding	<i>COL7A1</i>	collagen, type VII, alpha 1
ENSECAG00000011296	ENSECAT00000011993	1.62E-04	7.05E-04	2,991	protein coding	<i>SLC9A1</i>	solute carrier family 9, subfamily A (NHE1, cation proton antiporter 1), member 1
ENSECAG00000011483	ENSECAT00000011960	2.28E-02	2.60E-02	381	protein coding	<i>MORN1</i>	MORN repeat containing 1
ENSECAG00000011486	ENSECAT00000011931	3.15E-03	4.07E-03	1,198	protein coding	<i>ATF3</i>	activating transcription factor 3
ENSECAG00000011508	ENSECAT00000012117	6.58E-05	6.58E-05	1,276	protein coding	<i>TRA2A</i>	transformer 2 alpha homolog (Drosophila)
ENSECAG00000011599	ENSECAT00000012512	6.58E-05	6.58E-05	2,846	protein coding	<i>ZC3H18</i>	zinc finger CCCH-type containing 18
ENSECAG00000012131	ENSECAT00000012555	3.84E-02	3.84E-02	846	protein coding	<i>SNAI3</i>	snail family zinc finger 3
ENSECAG00000012403	ENSECAT00000012989	1.62E-04	1.62E-04	1,458	protein coding	<i>GPN2</i>	GPN-loop GTPase 2
ENSECAG00000012543	ENSECAT00000013268	2.56E-02	2.56E-02	826	protein coding	<i>C-SKI</i>	Equus caballus SKI (C-SKI), mRNA.
ENSECAG00000012669	ENSECAT00000013543	1.71E-02	4.31E-02	726	protein coding	<i>TANC2</i>	tetratricopeptide repeat, ankyrin repeat and coiled-coil containing 2
ENSECAG00000012768	ENSECAT00000013265	6.58E-05	6.58E-05	1,258	protein coding		Uncharacterized protein
ENSECAG00000012805	ENSECAT00000013279	1.94E-02	2.01E-02	818	protein coding	<i>ICAM4</i>	intercellular adhesion molecule 4 (Landsteiner-Wiener blood group)
ENSECAG00000013354	ENSECAT00000014009	4.00E-03	5.20E-03	752	protein coding	<i>B4GALNT2</i>	beta-1,4-N-acetyl-galactosaminyl transferase 2
ENSECAG00000013436	ENSECAT00000014189	3.17E-02	3.95E-02	848	protein coding	<i>TCEA1</i>	transcription elongation factor A (SII), 1
ENSECAG00000013539	ENSECAT00000014564	1.25E-03	1.87E-02	1,321	protein coding	<i>ITFG1</i>	integrin alpha FG-GAP repeat containing 1
ENSECAG00000013677	ENSECAT00000016045	1.62E-04	5.79E-04	8,088	protein coding	<i>FRY</i>	furry homolog (Drosophila)
ENSECAG00000013762	ENSECAT00000014568	3.21E-02	3.21E-02	924	protein coding	<i>NCRI</i>	Natural cytotoxicity triggering receptor 1; Uncharacterized protein
ENSECAG00000013883	ENSECAT00000014969	2.01E-02	2.01E-02	1,584	protein coding	<i>ICAMI</i>	intercellular adhesion molecule 1
ENSECAG00000014089	ENSECAT00000014815	5.06E-03	4.60E-02	3,639	protein coding	<i>NFATC3</i>	nuclear factor of activated T-cells, cytoplasmic, calcineurin-dependent 3
ENSECAG00000014169	ENSECAT00000014974	1.91E-03	3.34E-02	1,908	protein coding	<i>CCSER2</i>	coiled-coil serine-rich protein 2
ENSECAG00000014285	ENSECAT00000014882	1.27E-02	1.33E-02	958	protein coding	<i>INHBB</i>	inhibin, beta B
ENSECAG00000014543	ENSECAT00000015156	3.31E-04	5.43E-04	1,476	protein coding	<i>CCDC51</i>	coiled-coil domain containing 51
ENSECAG00000014555	ENSECAT00000015455	6.60E-03	6.60E-03	158	protein coding	<i>PLA2G15</i>	phospholipase A2, group XV
ENSECAG00000014577	ENSECAT00000015968	1.62E-04	1.62E-04	2,054	protein coding	<i>ADAM28</i>	ADAM metallopeptidase domain 28
ENSECAG00000014767	ENSECAT00000015985	5.43E-04	5.43E-04	287	protein coding	<i>PLXNB1</i>	plexin B1
ENSECAG00000014888	ENSECAT00000015647	5.60E-04	2.81E-03	2,087	protein coding	<i>NEK5</i>	NIMA-related kinase 5
ENSECAG00000015180	ENSECAT00000016039	2.70E-02	3.37E-02	1,299	protein coding	<i>NEXN</i>	nexilin (F actin binding protein)
ENSECAG00000015839	ENSECAT00000016675	1.62E-04	1.62E-04	831	protein coding	<i>ZDHHC18</i>	zinc finger, DHHC-type containing 18
ENSECAG00000015846	ENSECAT00000016670	1.62E-04	1.62E-04	1,063	protein coding	<i>VASH2</i>	vasohibin 2
ENSECAG00000015967	ENSECAT00000016728	5.65E-03	2.43E-02	644	protein coding	<i>ASF1B</i>	anti-silencing function 1B histone chaperone
ENSECAG00000016105	ENSECAT00000016879	6.53E-03	8.53E-03	540	protein coding	<i>MALSU1</i>	mitochondrial assembly of ribosomal large subunit 1
ENSECAG00000016156	ENSECAT00000016906	6.58E-05	6.58E-05	1,080	protein coding		Uncharacterized protein
ENSECAG00000016313	ENSECAT00000017650	6.58E-05	6.58E-05	2,966	protein coding	<i>PTPN4</i>	protein tyrosine phosphatase, non-receptor type 4 (megakaryocyte)

ENSECAG00000016336	ENSECAT00000017427	1.22E-02	1.90E-02	1,745	protein coding	<i>CDC25A</i>	cell division cycle 25A
ENSECAG00000016418	ENSECAT00000018285	6.58E-05	6.58E-05	1,487	protein coding	<i>KIR3DL</i>	Equus caballus killer cell immunoglobulin-like receptor with three domains and long cytoplasmic tail (KIR3DL), mRNA.
ENSECAG00000016637	ENSECAT00000018108	6.58E-05	1.04E-04	2,421	protein coding	<i>EPB41L5</i>	erythrocyte membrane protein band 4.1 like 5
ENSECAG00000016792	ENSECAT00000017817	3.07E-02	3.09E-02	2,520	protein coding		Uncharacterized protein
ENSECAG00000016797	ENSECAT00000018011	6.58E-05	6.53E-03	2,129	protein coding	<i>IGF2BP3</i>	insulin-like growth factor 2 mRNA binding protein 3
ENSECAG00000017013	ENSECAT00000018069	2.30E-02	2.69E-02	771	protein coding	<i>MRPL4</i>	mitochondrial ribosomal protein L4
ENSECAG00000017119	ENSECAT00000017998	1.62E-04	1.62E-04	1,671	protein coding	<i>PIGV</i>	phosphatidylinositol glycan anchor biosynthesis, class V
ENSECAG00000017338	ENSECAT00000019133	5.24E-04	1.59E-03	1,449	protein coding	<i>PFKFB4</i>	6-phosphofructo-2-kinase/fructose-2,6-biphosphatase 4
ENSECAG00000017375	ENSECAT00000018683	5.36E-03	5.36E-03	2,126	protein coding	<i>ESRP2</i>	epithelial splicing regulatory protein 2
ENSECAG00000017458	ENSECAT00000018629	4.35E-03	4.35E-03	297	protein coding	<i>BNIP3</i>	BCL2/adenovirus E1B 19kDa interacting protein 3
ENSECAG00000017514	ENSECAT00000018710	1.62E-04	1.62E-04	812	protein coding		60S ribosomal protein L6
ENSECAG00000017527	ENSECAT00000018479	1.86E-02	2.14E-02	131	protein coding	<i>NDUFAF2</i>	NADH dehydrogenase (ubiquinone) complex I, assembly factor 2
ENSECAG00000017787	ENSECAT00000019051	1.62E-04	1.62E-04	1,765	protein coding	<i>FLVCR1</i>	feline leukemia virus subgroup C cellular receptor 1
ENSECAG00000017894	ENSECAT00000018991	1.62E-04	1.62E-04	2,203	protein coding	<i>CKAP2</i>	cytoskeleton associated protein 2
ENSECAG00000017967	ENSECAT00000018959	1.85E-02	1.85E-02	226	protein coding	<i>METAP1</i>	methionyl aminopeptidase 1
ENSECAG00000017991	ENSECAT00000019703	1.62E-04	3.31E-04	5,032	protein coding	<i>ARID1A</i>	AT rich interactive domain 1A (SWI-like)
ENSECAG00000018146	ENSECAT00000019570	1.04E-04	1.62E-04	434	protein coding	<i>VPS36</i>	vacuolar protein sorting 36 homolog (S. cerevisiae)
ENSECAG00000018216	ENSECAT00000019228	1.04E-04	1.04E-04	216	protein coding		
ENSECAG00000018240	ENSECAT00000019411	1.47E-03	4.08E-03	617	protein coding	<i>PHKB</i>	phosphorylase b kinase regulatory subunit beta
ENSECAG00000018281	ENSECAT00000019301	1.04E-04	1.04E-04	1,425	protein coding	<i>LENG9</i>	leukocyte receptor cluster (LRC) member 9
ENSECAG00000018321	ENSECAT00000019431	6.31E-03	1.43E-02	1,563	protein coding	<i>ALG11</i>	ALG11, alpha-1,2-mannosyltransferase
ENSECAG00000018343	ENSECAT00000019558	1.04E-04	1.04E-04	2,867	protein coding	<i>LENG8</i>	leukocyte receptor cluster (LRC) member 8
ENSECAG00000018372	ENSECAT00000019403	1.04E-04	1.04E-04	1,401	protein coding		Uncharacterized protein
ENSECAG00000018510	ENSECAT00000019719	3.34E-02	3.67E-02	806	protein coding	<i>RGS20</i>	regulator of G-protein signaling 20
ENSECAG00000018676	ENSECAT00000019971	1.62E-04	1.62E-04	1,281	protein coding	<i>RAD52</i>	RAD52 homolog (S. cerevisiae)
ENSECAG00000018785	ENSECAT00000019859	1.69E-03	1.69E-03	393	protein coding		Uncharacterized protein
ENSECAG00000018835	ENSECAT00000020002	1.62E-04	1.62E-04	1,601	protein coding	<i>FAM46B</i>	family with sequence similarity 46, member B
ENSECAG00000019161	ENSECAT00000021056	4.37E-02	4.37E-02	788	protein coding	<i>DIAPH3</i>	diaphanous-related formin 3
ENSECAG00000019742	ENSECAT00000020901	6.58E-05	6.58E-05	576	protein coding	<i>CCDC126</i>	coiled-coil domain containing 126
ENSECAG00000019817	ENSECAT00000021018	6.46E-03	6.46E-03	347	protein coding	<i>SNRPF</i>	small nuclear ribonucleoprotein polypeptide F
ENSECAG00000019922	ENSECAT00000021251	1.62E-04	1.62E-04	1,383	protein coding	<i>ADAMDEC1</i>	ADAM-like, decysin 1
ENSECAG00000019943	ENSECAT00000021835	1.43E-02	1.43E-02	140	protein coding	<i>ATP7B</i>	ATPase, Cu++ transporting, beta polypeptide
ENSECAG00000020102	ENSECAT00000021747	6.58E-05	1.62E-04	3,368	protein coding	<i>ZEB1</i>	zinc finger E-box binding homeobox 1
ENSECAG00000020537	ENSECAT00000022031	1.62E-04	1.18E-03	1,370	protein coding	<i>ADAM7</i>	ADAM metallopeptidase domain 7
ENSECAG00000020561	ENSECAT00000021824	1.62E-04	1.62E-04	1,444	protein coding	<i>KDF1</i>	keratinocyte differentiation factor 1
ENSECAG00000020725	ENSECAT00000021995	2.75E-02	2.75E-02	1,342	protein coding		Uncharacterized protein
ENSECAG00000021107	ENSECAT00000022541	6.58E-05	6.58E-05	2,079	protein coding	<i>TRAFD1</i>	TRAF-type zinc finger domain containing 1
ENSECAG00000021311	ENSECAT00000022834	1.62E-04	1.62E-04	1,139	protein coding	<i>NUDC</i>	nudC nuclear distribution protein
ENSECAG00000021316	ENSECAT00000022692	6.58E-05	6.58E-05	881	protein coding	<i>FAM221A</i>	family with sequence similarity 221, member A
ENSECAG00000021555	ENSECAT00000023706	8.59E-04	1.54E-03	3,350	protein coding	<i>LPHN1</i>	latrophilin 1
ENSECAG00000021688	ENSECAT00000023337	2.36E-04	5.60E-04	1,579	protein coding	<i>NEK3</i>	NIMA-related kinase 3
ENSECAG00000021706	ENSECAT00000023249	1.62E-04	3.72E-02	1,727	protein coding	<i>RPS6KC1</i>	ribosomal protein S6 kinase, 52kDa, polypeptide 1
ENSECAG00000021735	ENSECAT00000023334	1.85E-03	2.46E-03	492	protein coding	<i>EPHA6</i>	EPH receptor A6
ENSECAG00000021801	ENSECAT00000023283	9.33E-03	9.33E-03	414	protein coding	<i>CCDC38</i>	coiled-coil domain containing 38
ENSECAG00000021842	ENSECAT00000023428	6.58E-05	6.58E-05	3,165	protein coding	<i>STK31</i>	Equus caballus serine/threonine kinase 31 (STK31), mRNA.
ENSECAG00000021879	ENSECAT00000023271	2.02E-02	2.02E-02	399	protein coding		Uncharacterized protein

ENSECAG00000022031	ENSECAT00000023479	4.93E-02	4.93E-02	196	protein coding	<i>GRID2</i>	glutamate receptor, ionotropic, delta 2
ENSECAG00000022100	ENSECAT00000023675	5.60E-04	2.82E-03	1,001	protein coding	<i>DHRS7B</i>	dehydrogenase/reductase (SDR family) member 7B
ENSECAG00000022220	ENSECAT00000023894	1.86E-02	1.99E-02	276	protein coding		Uncharacterized protein
ENSECAG00000022238	ENSECAT00000023679	4.52E-04	5.60E-04	234	protein coding	<i>NATD1</i>	N-acetyltransferase domain containing 1
ENSECAG00000022242	ENSECAT00000024114	1.62E-04	1.62E-04	1,031	protein coding	<i>MAP2K3</i>	mitogen-activated protein kinase kinase 3
ENSECAG00000022846	ENSECAT00000024378	1.56E-02	1.56E-02	945	protein coding		Uncharacterized protein
ENSECAG00000022854	ENSECAT00000024382	1.56E-02	1.56E-02	945	protein coding		Uncharacterized protein
ENSECAG00000022858	ENSECAT00000024390	4.92E-03	4.92E-03	945	protein coding		Uncharacterized protein
ENSECAG00000022863	ENSECAT00000024401	3.67E-03	3.67E-03	669	protein coding		Uncharacterized protein
ENSECAG00000022876	ENSECAT00000024415	1.50E-03	1.50E-03	960	protein coding		Uncharacterized protein
ENSECAG00000022882	ENSECAT00000024420	1.50E-03	1.50E-03	945	protein coding		Uncharacterized protein
ENSECAG00000023324	ENSECAT00000025006	7.82E-04	1.04E-03	1,719	protein coding	<i>SP4</i>	Sp4 transcription factor
ENSECAG00000023403	ENSECAT00000025178	1.25E-03	4.35E-03	3,277	protein coding	<i>OTUD4</i>	OTU deubiquitinase 4
ENSECAG00000023501	ENSECAT00000025447	1.62E-04	4.52E-04	5,396	protein coding	<i>WNK1</i>	WNK lysine deficient protein kinase 1
ENSECAG00000023602	ENSECAT00000025656	6.58E-05	1.04E-04	11,976	protein coding	<i>HECTD4</i>	HECT domain containing E3 ubiquitin protein ligase 4
ENSECAG00000023648	ENSECAT00000025599	6.15E-04	1.04E-03	1,909	protein coding	<i>ABCE1</i>	ATP-binding cassette, sub-family E (OABP), member 1
ENSECAG00000023701	ENSECAT00000025441	2.09E-03	1.23E-02	474	protein coding	<i>CA5A</i>	carbonic anhydrase VA, mitochondrial
ENSECAG00000024340	ENSECAT00000026285	1.04E-04	1.04E-04	1,230	protein coding	<i>TTYH1</i>	tweety family member 1
ENSECAG00000024416	ENSECAT00000026243	6.15E-04	1.48E-03	682	protein coding	<i>ANAPC10</i>	anaphase promoting complex subunit 10
ENSECAG00000024476	ENSECAT00000026328	6.15E-04	6.36E-04	3,822	protein coding		Uncharacterized protein
ENSECAG00000024560	ENSECAT00000026567	1.09E-03	3.45E-03	753	protein coding	<i>PTPN11</i>	protein tyrosine phosphatase, non-receptor type 11
ENSECAG00000024908	ENSECAT00000026919	1.04E-04	1.62E-04	2,836	protein coding	<i>ERC1</i>	ELKS/RAB6-interacting/CAST family member 1
ENSECAG00000024966	ENSECAT00000026953	2.56E-02	2.56E-02	1,856	protein coding	<i>RAVER1</i>	ribonucleoprotein, PTB-binding 1
ENSECAG00000026276	ENSECAT00000028288	1.43E-02	1.43E-02	61	miRNA	eca-mir-711	eca-mir-711
ENSECAG00000027193	ENSECAT00000029359	3.12E-02	3.12E-02	103	miRNA		
ENSECAG00000027275	ENSECAT00000029441	1.46E-04	1.46E-04	75	miRNA		
ENSECAG00000026627	ENSECAT00000028639	1.62E-04	1.62E-04	128	rRNA	5S rRNA	5S ribosomal RNA
ENSECAG00000026538	ENSECAT00000028550	8.95E-03	8.95E-03	146	snoRNA	<i>SNORA12</i>	Small nucleolar RNA SNORA12
ENSECAG00000027212	ENSECAT00000029378	1.62E-04	1.62E-04	72	snoRNA	<i>SNORD112</i>	Small nucleolar RNA SNORD112
ENSECAG00000026565	ENSECAT00000028577	6.58E-05	6.58E-05	108	snRNA	U6	U6 spliceosomal RNA

Table S7.4: GO-term enrichment for genes showing 1% top FST values.

Panel	Model Organism	GO terms	Adjusted p-value	Number of Genes
DOM	human	fluid transport GO:0042044	1.60E-03	6
		water transport GO:0006833	1.60E-03	6
		positive regulation of response to nutrient levels GO:0032109	5.62E-02	3
		positive regulation of response to extracellular stimulus GO:0032106	5.62E-02	3
		cellular component organization GO:0016043	8.99E-02	55
		cellular component organization or biogenesis GO:0071840	9.37E-02	56
		neuron apoptotic process GO:0051402	9.63E-02	7
		neuron death GO:0070997	9.84E-02	7
		natural killer cell chemotaxis GO:0035747	1.17E-01	2
		eosinophil chemotaxis GO:0048245	1.17E-01	2
		water transmembrane transporter activity GO:0005372	3.00E-04	4
		water channel activity GO:0015250	3.00E-04	4
		anion binding GO:0043168	9.00E-04	41
		purine ribonucleotide binding GO:0032555	1.20E-03	33
		purine ribonucleoside triphosphate binding GO:0035639	1.20E-03	33
		purine ribonucleoside binding GO:0032550	1.20E-03	33
		Rab GTPase binding GO:0017137	1.20E-03	5
		ribonucleoside binding GO:0032549	1.20E-03	33
		ribonucleotide binding GO:0032553	1.20E-03	33
		purine nucleoside binding GO:0001883	1.20E-03	33
		neuronal cell body GO:0043025	2.14E-01	8
		mitotic spindle GO:0072686	2.14E-01	2
		cell body GO:0044297	2.14E-01	8
		cytoplasmic part GO:0044444	2.14E-01	73
		dendritic spine GO:0043197	2.14E-01	5
		dendrite GO:0030425	2.14E-01	8
		endoplasmic reticulum GO:0005783	2.14E-01	20
		neuron spine GO:0044309	2.14E-01	5
		extracellular region part GO:0044421	2.14E-01	18
		neuron projection GO:0043005	2.14E-01	13
	mouse	water transport GO:0006833	4.60E-03	4
		fluid transport GO:0042044	5.70E-03	4
		protein splicing GO:0030908	5.90E-03	2
		phosphorus metabolic process GO:0006793	5.90E-03	35
		phosphate-containing compound metabolic process GO:0006796	5.90E-03	34
		regulation of apoptotic process GO:0042981	5.90E-03	20
		cellular process GO:0009987	5.90E-03	114
		organophosphate catabolic process GO:0046434	5.90E-03	13
		regulation of programmed cell death GO:0043067	5.90E-03	20
		apoptotic process GO:0006915	5.90E-03	23
		protein binding GO:0005515	5.15E-06	76
		anion binding GO:0043168	7.38E-06	39
		binding GO:0005488	1.76E-05	108
		water channel activity GO:0015250	2.31E-05	4
		water transmembrane transporter activity GO:0005372	2.31E-05	4
		ribonucleoside binding GO:0032549	2.31E-05	31
		purine ribonucleoside triphosphate binding GO:0035639	2.31E-05	31
		purine nucleoside binding GO:0001883	2.31E-05	31
		purine ribonucleoside binding GO:0032550	2.31E-05	31

		nucleoside binding GO:0001882	2.34E-05	31
		cell part GO:0044464	1.00E-04	120
		cell GO:0005623	1.00E-04	120
		intracellular part GO:0044424	6.00E-04	104
		intracellular GO:0005622	1.30E-03	104
		cytoplasmic part GO:0044444	1.50E-03	61
		cytoplasm GO:0005737	1.70E-03	82
		organelle GO:0043226	1.70E-03	91
		intracellular organelle GO:0043229	1.70E-03	91
		dendritic spine GO:0043197	2.80E-03	7
		neuron spine GO:0044309	2.80E-03	7
FM	human	positive regulation of response to food GO:0032097	6.99E-02	2
		response to food GO:0032094	6.99E-02	4
		positive regulation of appetite GO:0032100	6.99E-02	2
		cellular trivalent inorganic anion homeostasis GO:0072502	1.80E-01	2
		heme transport GO:0015886	1.80E-01	2
		neurological system process GO:0050877	1.80E-01	23
		cellular phosphate ion homeostasis GO:0030643	1.80E-01	2
		positive regulation of multicellular organism growth GO:0040018	1.85E-01	3
		phosphate ion homeostasis GO:0055062	1.85E-01	2
		cellular anion homeostasis GO:0030002	1.85E-01	2
		adenosine receptor binding GO:0031685	4.50E-02	2
		microfilament motor activity GO:0000146	4.50E-02	3
		carbon-carbon lyase activity GO:0016830	4.50E-02	4
		malate dehydrogenase activity GO:0016615	5.31E-02	2
		caldmodulin binding GO:0005516	6.37E-02	6
		carboxy-lyase activity GO:0016831	6.37E-02	3
		alkali metal ion binding GO:0031420	6.37E-02	2
		actin-dependent ATPase activity GO:0030898	6.37E-02	2
		ATPase activity, coupled GO:0042623	6.37E-02	8
		heme transporter activity GO:0015232	6.37E-02	2
		cell body GO:0044297	3.14E-02	10
		neuronal cell body GO:0043025	3.14E-02	10
		perikaryon GO:0043204	3.66E-02	4
		neuron projection GO:0043005	4.71E-02	14
		cell projection part GO:0044463	4.71E-02	14
		presynaptic membrane GO:0042734	4.71E-02	4
		axolemma GO:0030673	7.40E-02	2
		anchored to membrane GO:0031225	1.08E-01	5
		terminal button GO:0043195	1.08E-01	3
		extracellular region part GO:0044421	1.08E-01	18
	mouse	cellular process GO:0009987	3.10E-03	116
		cellular trivalent inorganic anion homeostasis GO:0072502	6.82E-02	2
		positive regulation of response to food GO:0032097	6.82E-02	2
		positive regulation of appetite GO:0032100	6.82E-02	2
		cellular ketone body metabolic process GO:0046950	6.82E-02	2
		cellular metabolic process GO:0044237	6.82E-02	70
		response to food GO:0032094	6.82E-02	3
		cellular phosphate ion homeostasis GO:0030643	6.82E-02	2
		fat cell differentiation GO:0045444	7.88E-02	5
		regulation of systemic arterial blood pressure by baroreceptor feedback GO:0003025	7.88E-02	2

	anion binding GO:0043168	1.20E-03	32
	small molecule binding GO:0036094	3.70E-03	32
	nucleotide binding GO:0000166	9.20E-03	29
	ATP binding GO:0005524	9.20E-03	21
	nucleoside phosphate binding GO:1901265	9.20E-03	29
	adenyl nucleotide binding GO:0030554	1.00E-02	21
	adenyl ribonucleotide binding GO:0032559	1.00E-02	21
	neuron spine GO:0044309	6.10E-03	7
	cell part GO:0044464	6.10E-03	114
	clathrin-coated endocytic vesicle GO:0045334	6.10E-03	3
	cell GO:0005623	6.10E-03	114
	dendritic spine GO:0043197	6.10E-03	7
	AP-2 adaptor complex GO:0030122	1.09E-02	2
	neuronal cell body GO:0043025	1.09E-02	10
	clathrin-coated endocytic vesicle membrane GO:0030669	1.30E-02	2
	clathrin coat of endocytic vesicle GO:0030128	1.30E-02	2
	cell projection part GO:0044463	1.30E-02	12

Table S7.5: Pathway enrichment for genes showing 1% top FST values.

Database	Panel	Model Organism	Pathway	Gene Name	Adjusted p-value
KEGG	DOM	human	Chemokine signaling pathway	<i>CCL13, CCL7, GRK4, PIK3CD, RAPIA, ADCY5, CCLI</i>	6.00E-04
			Vasopressin-regulated water reabsorption	<i>AQP2, NSF, DYNCIL2, AQP4</i>	6.00E-04
			Valine, leucine and isoleucine degradation	<i>OXCT1, BCKDHB, HADHA, ALDH9A1</i>	6.00E-04
			Riboflavin metabolism	<i>ENPP1, ACP6</i>	1.32E-02
			Amyotrophic lateral sclerosis (ALS)	<i>APAF1, GPX1, PRPH</i>	1.43E-02
			Glutathione metabolism	<i>RRM2B, GPX1, MGST3</i>	1.43E-02
			Adipocytokine signaling pathway	<i>PRKAG1, MAPK10, NPY</i>	2.45E-02
			Phagosome	<i>TUBA1C, COLEC12, TUBA1A, DYNCIL2</i>	2.57E-02
			beta-Alanine metabolism	<i>HADHA, ALDH9A1</i>	2.57E-02
			Purine metabolism	<i>ENPP1, RRM2B, ADCY5, PDE4B</i>	2.71E-02
	mouse	mouse	Chemokine signaling pathway	<i>Pik3cd, Adcy5, Rap1a, Grk4, Ccl11, Ccl1</i>	9.02E-05
			Valine, leucine and isoleucine degradation	<i>Oxct1, Aldh9a1, Hadha, Bckdhb</i>	3.00E-04
			Vasopressin-regulated water reabsorption	<i>Acp2, Dyncil2, Acp4, Nsf</i>	3.00E-04
			Amyotrophic lateral sclerosis (ALS)	<i>Prph, Apaf1, Gpx1</i>	6.40E-03
	FM	human	Glutathione metabolism	<i>Gpx1, Mgst3, Rrm2b</i>	6.40E-03
			Riboflavin metabolism	<i>Acp6, Enpp1</i>	6.40E-03
			Metabolic pathways	<i>Dgat1, Pigg, Inpp4b, B4galnt7, Aldh9a1, Hadha, Bckdhb, Uck2, Enpp1, Smpd1, Rrm2b</i>	7.30E-03
			Adipocytokine signaling pathway	<i>Mapk10, Prkag1, Npy</i>	8.80E-03
			Phagosome	<i>Dyncil2, Tubala1, Colec12, Tubal1c</i>	1.13E-02
			Gap junction	<i>Adcy5, Tubala1, Tubal1c</i>	1.13E-02
			Neuroactive ligand-receptor interaction	<i>CTSG, HTR1E, OPRK1, CGA, GRIK2, ADRA1D, GHSR, GPR35</i>	5.00E-04
			Glutathione metabolism	<i>RRM2B, ODC1, GPX1</i>	1.80E-02
			Metabolic pathways	<i>GAD2, ENPP1, RRM2B, BCKDHB, MDH2, SMPD1, UCK2, PIGB, ME1, RPN2, NDUFA7, ODC1</i>	2.28E-02
			Gastric acid secretion	<i>SST, ADCY5, MYLK2</i>	2.88E-02
	mouse	mouse	Butanoate metabolism	<i>GAD2, OXCT1</i>	4.37E-02
			GnRH signaling pathway	<i>MAPK10, CGA, ADCY5</i>	4.37E-02
			Primary immunodeficiency	<i>ICOS, CIITA</i>	4.37E-02
			Vascular smooth muscle contraction	<i>ADRA1D, ADCY5, MYLK2</i>	4.48E-02
			Pyruvate metabolism	<i>ME1, MDH2</i>	4.48E-02
			Valine, leucine and isoleucine degradation	<i>OXCT1, BCKDHB</i>	4.79E-02
			Neuroactive ligand-receptor interaction	<i>Ctsg, Grik2, Cga, Oprk1, Adrald, Gpr35, Ghsr</i>	6.00E-04
			Metabolic pathways	<i>Rpn2, Mdh2, Odc1, Gad2, Ndufa7, Pigg, Bckdhb, Uck2, Enpp1, Smpd1, Rrm2b, Me1</i>	3.60E-03
			Glutathione metabolism	<i>Odc1, Gpx1, Rrm2b</i>	6.00E-03
			Gastric acid secretion	<i>Adcy5, Mylk2, Sst</i>	1.08E-02
			Butanoate metabolism	<i>Oxct1, Gad2</i>	2.04E-02
			GnRH signaling pathway	<i>Adcy5, Mapk10, Cga</i>	2.04E-02
			Primary immunodeficiency	<i>Citta, Icos</i>	2.21E-02
			Vascular smooth muscle contraction	<i>Adcy5, Mylk2, Adra1d</i>	2.40E-02
			Toxoplasmosis	<i>Lama3, Citta, Mapk10</i>	2.40E-02
			Pyruvate metabolism	<i>Mdh2, Me1</i>	2.45E-02
WikiPathway	DOM	human	Oxidative Stress	<i>MAPK10, GPX1, SOD2</i>	8.60E-03
			Integrated Pancreatic Cancer Pathway	<i>APAF1, RAPIA, ESR2, TOP1, PDE4B</i>	1.72E-02
			Insulin Signaling	<i>ENPP1, PIK3CD, MAPK10, STXBP1</i>	3.75E-02
			Wnt Signaling Pathway and Pluripotency	<i>RACGAP1, MAPK10, PPM1J</i>	3.75E-02
			Apoptosis Modulation by HSP70	<i>APAF1, MAPK10</i>	3.75E-02
			G13 Signaling Pathway	<i>PIK3CD, MAPK10</i>	3.75E-02
			Matrix Metalloproteinases	<i>TIMP2, MMP17</i>	3.75E-02
			Ovarian Infertility Genes	<i>ESR2, SMPD1</i>	3.75E-02
			Hedgehog Signaling Pathway	<i>DHH, IHH</i>	3.75E-02

		Integrin-mediated cell adhesion	<i>Rap1a, Mapk10, Itga4</i>	3.75E-02
mouse		Chemokine signaling pathway	<i>Pik3cd, Adcy5, Rap1a, Grk4, Ccl7, Ccl11, Ccl1</i>	4.96E-05
		Oxidative Stress	<i>Sod2, Mapk10, Gpx1</i>	1.30E-03
		Insulin Signaling	<i>Pik3cd, Mapk10, Sxbp1, Enpp1</i>	1.11E-02
		Oxidative Damage	<i>Mapk10, Apaf1</i>	1.11E-02
		Apoptosis Modulation by HSP70	<i>Mapk10, Apaf1</i>	1.40E-02
		Matrix Metalloproteinases	<i>Timp2, Mmp17</i>	1.40E-02
		Integrin-mediated cell adhesion	<i>Rap1a, Mapk10, Itga4</i>	1.40E-02
		Wnt Signaling Pathway and Pluripotency	<i>Racgap1, Mapk10, Ppmlj</i>	1.40E-02
		Ovarian Infertility Genes	<i>Esr2, Smpd1</i>	1.70E-02
		G13 Signaling Pathway	<i>Pik3cd, Mapk10</i>	1.90E-02
FM	human	GPCRs, Class A Rhodopsin-like	<i>HTR1E, OPRK1, OR10J1, OR2B6, ADRA1D, GHSR, GPR35</i>	1.80E-03
		Lymphocyte TarBase	<i>MS12, HDAC4, MYO10, BCKDHB, TTK, FNDC3B, NCEH1, DHX40, RHOB</i>	3.20E-03
		miRNA regulation of DNA Damage Response	<i>RFC1, RRM2B, SESN1</i>	1.12E-02
		Endochondral Ossification	<i>ENPP1, HDAC4, IHH</i>	1.12E-02
		DNA damage response	<i>RFC1, RRM2B, SESN1</i>	1.12E-02
		Epithelium TarBase	<i>FNDC3B, HDAC4, MYO10, BCKDHB, DHX40, RHOB</i>	1.12E-02
		Monoamine GPCRs	<i>HTR1E, ADRA1D</i>	1.77E-02
		Muscle cell TarBase	<i>FNDC3B, HDAC4, NCEH1, MYO10, DHX40, TTK</i>	1.77E-02
		Oxidative Stress	<i>MAPK10, GPX1</i>	1.77E-02
		mRNA processing	<i>DDX20, RNGTT, SRPK1</i>	3.11E-02
	mouse	miRNA regulation of DNA Damage Response	<i>Rfc1, Rrm2b, Sesn1</i>	1.15E-02
		Endochondral Ossification	<i>Hdac4, Ihh, Enpp1</i>	1.15E-02
		mRNA processing	<i>Ddx20, Rngtt, Ms12, Rps28, Srpk1, Zfml</i>	1.52E-02
		Oxidative Stress	<i>Mapk10, Gpx1</i>	1.52E-02
		GPCRs, Class A Rhodopsin-like	<i>Olf716, Oprk1, Adra1d, Gpr35</i>	1.76E-02
		GPCRs, Other	<i>Oprk1, Olf711, Ghsr</i>	2.99E-02
		Selenium metabolism-Selenoproteins	<i>Sepsecs, Gpx1</i>	2.99E-02
		One carbon metabolism and related pathways	<i>Gad2, Gpx1</i>	2.99E-02
		Peptide GPCRs	<i>Oprk1, Ghsr</i>	3.65E-02
		Focal Adhesion	<i>Lama3, Mylk2, Rhob</i>	3.65E-02

Table S7.6: Phenotype-term enrichment for genes showing 1% top FST values.

Database	Panel	Model Organism	Phenotype	Gene Name	Adjusted p-value
Phenotype	DOM	human	Aplasia/Hypoplasia of the fallopian tube	<i>DHH, DCAF17,</i>	4.33E-02
			Hypoplasia of the fallopian tube	<i>DHH, DCAF17,</i>	4.33E-02
			Abnormality of the fallopian tube	<i>DHH, DCAF17,</i>	4.33E-02
			Spastic tetraplegia	<i>SEPSECS, TUBA1A, ELOVL4, STXBPI,</i>	4.33E-02
			Thin corpus callosum	<i>SEPSECS, TUBA1A, STXBPI, MAPK10,</i>	5.77E-02
			Abnormal thickness of corpus callosum	<i>SEPSECS, TUBA1A, STXBPI, MAPK10,</i>	5.77E-02
			Protracted diarrhea	<i>MYO5B, CIITA,</i>	1.18E-01
			Generalized myoclonic seizures	<i>ELOVL4, STXBPI, MAPK10,</i>	1.89E-01
			Autoimmune thrombocytopenia	<i>MLL2, NDRG1,</i>	2.17E-01
			Hypoplasia of the uterus	<i>DHH, DCAF17,</i>	2.24E-01
	mouse	nervous system phenotype		<i>Ctnm5, Stxbp1, Tuba1a, Tmbim6, Ubr5, Gpx1, Smpd1, Slc24a4, Mapk10, Slc6a15, Apaf1, Dhh, Faim2, Accn1, Sod2, Lrpap1, Ihh, Tim2, Esr2, Prph, Grid2, Ndrg1, Pask, Atoh1, Rrm2b, Oxct1, Mterf2, Trim3, Tg, Elov4, Enpp1, Sh2d3c, Hsfl, Aqp4, Npy,</i>	4.90E-02
			abnormal trigeminal motor nucleus morphology	<i>Grid2, Sod2,</i>	4.90E-02
			abnormal nervous system physiology	<i>Accn1, Sod2, Ctnm5, Stxbp1, Tuba1a, Tim2, Esr2, Grid2, Tmbim6, Ndrg1, Pask, Gpx1, Atoh1, Smpd1, Oxct1, Slc24a4, Mapk10, Trim3, Apaf1, Tg, Faim2, Elov4, Sh2d3c, Aqp4, Npy,</i>	4.90E-02
			failure of zygotic cell division	<i>Racgap1, Dax20, Hsfl,</i>	4.90E-02
FM	human	human	abnormal brainstem morphology	<i>Accn1, Grid2, Sod2, Atoh1, Apaf1, Smpd1, Esr2,</i>	4.90E-02
			abnormal erythrocyte morphology	<i>App2, Sod2, Ikkf1, Tg, Esr2, Ctsg, Prkag1, Elov4, Rrm2b, Tmpo, Ulkl,</i>	5.10E-02
			abnormal hematocrit	<i>App2, Sod2, Ikkf1, Prkag1, Tg, Rrm2b, Tmpo,</i>	5.10E-02
			decreased susceptibility to pharmacologically induced seizures	<i>Mapk10, Trim3, Npy,</i>	5.10E-02
			increased circulating pituitary hormone level	<i>Grid2, Lhx9, Tg, Dhh, Esr2,</i>	5.44E-02
			abnormal erythropoiesis	<i>App2, Sod2, Ikkf1, Tg, Esr2, Ctsg, Prkag1, Elov4, Rrm2b, Tmpo, Ulkl,</i>	6.44E-02
			Subvalvular aortic stenosis	<i>HDAC4, MYLK2,</i>	4.99E-01
			Protracted diarrhea	<i>MYO5B, CIITA,</i>	4.99E-01
			Recurrent lower respiratory tract infections	<i>ICOS, WDR19, CIITA,</i>	4.99E-01
			Anxiety	<i>TMC01, RRM2B, ADCY5,</i>	4.99E-01
PheWAS	DOM	human	Abnormality of the left ventricular outflow tract	<i>HDAC4, MYLK2,</i>	4.99E-01
			Reduced tendon reflexes	<i>DYSE, TMC01, HDAC4, RRM2B, FLVCR1, BCKDHB, SMPD1,</i>	4.99E-01
			Abnormality of the urinary system	<i>TMC01, LAMA3, HDAC4, OXCT1, RRM2B, BCKDHB, WDR19, TNFRSF11B, COL14A1, FLVCR1, AP2SI, CIITA,</i>	5.83E-01
			Gingival overgrowth	<i>TMC01, MAPK10,</i>	5.83E-01
			Abnormality of immune system physiology	<i>LAMA3, ELOVL4, WDR19, SMPD1, FLVCR1, ICOS, MAPK10, CIITA,</i>	5.83E-01
			Abnormal respiratory system morphology	<i>TMC01, LAMA3, HDAC4, ELOVL4, BCKDHB, WDR19, SMPD1, MAPK10, ICOS, CIITA, SLC34A2,</i>	5.83E-01
			decreased susceptibility to pharmacologically induced seizures	<i>Mapk10, Grik2, Trim3, Npy,</i>	5.50E-03
			abnormal seizure response to inducing agent	<i>Hdac4, Mapk10, Grik2, Ctnmap2, Ctnm5, Trim3, Npy,</i>	2.86E-02
			behavior/neurological phenotype	<i>Foxi1, Trib2, Ctnmap2, Adra1d, Gad2, Lmo7, Ctnn5, Ctnn6, Apbb1, Ghsr, Adcy5, Lhfp15, Oprk1, Clps, Smpd1, Me1, Mapk10, Trim3, Dysf, Prox1, Sst, Hdac4, Add2, Grik2, Elov4, Anxa4, Enpp1, Npy,</i>	5.93E-02
			abnormal behavior	<i>Foxi1, Trib2, Ctnmap2, Adra1d, Gad2, Lmo7, Ctnn5, Ctnn6, Apbb1, Ghsr, Adcy5, Lhfp15, Oprk1, Clps, Smpd1, Me1, Mapk10, Trim3, Dysf, Prox1, Sst, Hdac4, Add2, Grik2, Elov4, Anxa4, Enpp1, Npy,</i>	5.93E-02
			decreased body size	<i>Trib2, Ctnmap2, Gad2, Lmo7, Jhh, Mfsd7b, Ghsr, Clps, Ghrh, Gpx1, Rrm2b, Smpd1, Me1, Lama3, Cga, Robh, Hdac4, Msi2, Grik2, Elov4, Tfnsf11b, Enpp1, Npy,</i>	5.93E-02
			pancreas inflammation	<i>Ctla4, Ciita, Gad2, Icos,</i>	6.59E-02
			seizures	<i>Hdac4, Mapk10, Grik2, Ctnmap2, Gad2, Ctnm5, Trim3, Npy,</i>	6.59E-02
			abnormal body size	<i>Foxi1, Trib2, Ctnmap2, Gad2, Lmo7, Jhh, Mfsd7b, Ghsr, Clps, Ghrh, Gpx1, Rrm2b, Smpd1, Me1, Lama3, Cga, Robh, Prox1, Sst, Hdac4, Msi2, Grik2, Elov4, Tfnsf11b, Enpp1, Npy,</i>	6.59E-02
			environmentally induced seizures	<i>Hdac4, Ctnmap2, Ctnm5,</i>	6.59E-02
			decreased body weight	<i>Trib2, Gad2, Lmo7, Ghsr, Clps, Gpx1, Ghrh, Rrm2b, Smpd1, Me1, Lama3, Cga, Hdac4, Msi2, Grik2, Elov4, Enpp1, Npy</i>	8.21E-02

		Other nonspecific findings on examination of urine PheWAS:598.9	<i>TIMP2, NSF, PALM2-AKAP2, PLXDC2,</i>	2.78E-01
		Other benign neoplasm of connective and other soft tissue PheWAS:215	<i>IKZF1, ADCY5,</i>	2.78E-01
		Urinary tract infection PheWAS:591	<i>DTNB, CIITA,</i>	2.78E-01
		Chronic glomerulonephritis PheWAS:580.14	<i>NSF, PALM2-AKAP2</i>	2.78E-01
		Generalized anxiety disorder PheWAS:300.11	<i>MYO1D, SEL1L3, PRPH,</i>	2.78E-01
		Dermatophytosis of the body PheWAS:110.13	<i>TMCO1, CNTN5, SLC24A4,</i>	2.78E-01
		Other disorders of thyroid PheWAS:246	<i>PROXI, GPC5, CLEC16A,</i>	3.00E-01
		Cholangitis PheWAS:575.1	<i>SNTB1, ICOS,</i>	3.00E-01
		Other infectious diseases PheWAS:136	<i>CNTN4, GRIK2,</i>	3.00E-01
		Functional disorders of bladder PheWAS:596.5	<i>CTLA4, ADCY5,</i>	3.00E-01
		Nervous system congenital anomalies PheWAS:752	<i>CNTN4, GHRSR,</i>	3.00E-01
		Psoriatic arthropathy PheWAS:696.42	<i>SEL1L3, CIITA,</i>	3.00E-01
		Other abnormal blood chemistry PheWAS:790.6	<i>PROXI, CNTN4,</i>	3.00E-01
		Oliguria and anuria PheWAS:599.6	<i>DYSF, SH3BP5,</i>	3.00E-01
		Pulmonary embolism and infarction PheWAS:415.1	<i>PROXI, FAM13A,</i>	3.00E-01
		Stricture and stenosis of esophagus PheWAS:530.3	<i>CLEC16A, MICAL3,</i>	3.00E-01

Table S7.7: Disease-term enrichment for genes showing 1% top Fst values (human model).

Panel	Disease	Gene Name	Adjusted p-value
DOM	Disease Susceptibility DB ID:PA443919	<i>ENPP1, BANK1, CNTN5, FAIM2, TIMP2, NOD1, ADCY5, CLEC16A, NPY, SOD2, TG, ESR2, GPX1, CIITA, CCL1</i>	4.00E-04
	Genetic Predisposition to Disease DB ID:PA446882	<i>ENPP1, BANK1, FAIM2, TIMP2, NOD1, ADCY5, CLEC16A, NPY, PDE4B, SOD2, ESR2, GPX1, CIITA, CCL1</i>	6.00E-04
	Metabolic Diseases DB ID:PA444938	<i>ENPP1, OXCT1, BCKDHB, ADCY5, CLEC16A, HADHA, SMPDI, NPY, DGAT1, DCAF17, PRPH, SETX</i>	6.00E-04
	Immune System Diseases DB ID:PA444602	<i>CCL7, BANK1, NOD1, ITGA4, CLEC16A, AQP4, WIF1, TG, SEPSECS, PIK3CD, IKZF1, CIITA, CCL1</i>	6.00E-04
	diabetes mellitus type 2 and obesity DB ID:PA447306	<i>ENPP1, FAIM2, RASAL2, ADCY5, NPY, BCDFIN3D</i>	1.20E-03
	Stress DB ID:PA445752	<i>RRM2B, NDRG1, NPY, SOD2, HSF1, PRKAG1, TMBIM6, MAPK10, GPX1, STK4</i>	1.20E-03
	Meniere Disease DB ID:PA444911	<i>AQP6, AQP2, AQP4</i>	1.30E-03
	Immunologic Deficiency Syndromes DB ID:PA444601	<i>CCL7, WIF1, TUBA1C, PIK3CD, PDCD6IP, TUBA1A, MAPK10, ITGA4, CIITA</i>	1.50E-03
	HIV DB ID:PA447230	<i>CCL7, PDCD6IP, TUBA1A, ADCY5, ITGA4, PRKAG1, TUBA1C, PIK3CD, MOV10, MAPK10, CCL1, TOP1</i>	2.10E-03
	Diabetes Mellitus DB ID:PA443886	<i>ENPP1, ADCY5, CLEC16A, NPY, SOD2, DCAF17, GPX1, BCDFIN3D</i>	2.20E-03
FM	Disease Susceptibility DB ID:PA443919	<i>CTLA4, CNTN5, CNTNAP2, FAM13A, ICOS, CIITA, ENPP1, GAD2, CNTN4, CLEC16A, ADCY5, NPY, RFC1, GPC5, AFF3, GPX1, CCL1</i>	1.14E-05
	Genetic Predisposition to Disease DB ID:PA446882	<i>GAD2, ENPP1, CTLA4, ADCY5, CLEC16A, NPY, RFC1, CNTNAP2, GPC5, FAM13A, AFF3, ICOS, GPX1, CIITA, CCL1</i>	1.00E-04
	Diabetes Mellitus DB ID:PA443886	<i>GAD2, ENPP1, CTLA4, ADCY5, CLEC16A, NPY, PROX1, TNFRSF11B, DCAF17, GPX1</i>	1.00E-04
	Anxiety Disorders DB ID:PA447196	<i>CNTN6, GAD2, CNTN5, CNTNAP2, OPRK1, GRIK2, NPY</i>	2.00E-04
	Mental Disorders DB ID:PA447208	<i>GAD2, CNTN5, OPRK1, ASIC2, CNTN4, GRIK2, APBB1, NPY, SST, CNTNAP2, DCAF17</i>	1.00E-03
	Immune System Diseases DB ID:PA444602	<i>GAD2, CTLA4, CLEC16A, TNFSF10, TNFRSF11B, SEPSECS, RFC1, GPC5, AFF3, ICOS, CIITA, CCL1</i>	1.00E-03
	Endocrine disorder NOS DB ID:PA165109147	<i>GAD2, ENPP1, CTLA4, ADCY5, CLEC16A, TNFRSF11B, DCAF17, GHRH, SLC34A2</i>	1.60E-03
	Autoimmune Diseases DB ID:PA443464	<i>GAD2, CTLA4, CLEC16A, TNFRSF11B, SEPSECS, GPC5, AFF3, ICOS, CIITA</i>	1.60E-03
	Endocrine System Diseases DB ID:PA444037	<i>GAD2, ENPP1, CTLA4, ADCY5, CLEC16A, TNFRSF11B, DCAF17, GHRH, SLC34A2</i>	1.60E-03
	Endocrine disturbance NOS DB ID:PA165108435	<i>GAD2, ENPP1, CTLA4, ADCY5, CLEC16A, TNFRSF11B, DCAF17, GHRH, SLC34A2</i>	1.60E-03

Table S7.8: Genes harboring top-1% d_4 sites.

Panel	Site category	Genes
DOM	0d-fold	ENSECAG00000021537 (FNDC7)
	2d-fold	ENSECAG00000017796 (NCAPD2)
	0-1Kb	ENSECAG0000000628, ENSECAG00000002575, ENSECAG00000002739, ENSECAG00000003284, ENSECAG00000003576, ENSECAG00000003780 (OR6A2), ENSECAG00000008324 (LECT2), ENSECAG00000008749 (VTCN1), ENSECAG00000011862 (C1orf1), ENSECAG00000015087 (PFKM), ENSECAG00000015444 (SLC37A1), ENSECAG00000017048 (CD101), ENSECAG00000024694 (KIF14)
	1-2Kb	ENSECAG00000008247, ENSECAG00000008324 (LECT2), ENSECAG00000010259 (TRIM45), ENSECAG00000011995 (FTS13), ENSECAG00000013724 (FAS), ENSECAG00000014017 (PRKG1), ENSECAG00000015087 (PFKM), ENSECAG00000016463 (TMEM72), ENSECAG00000020193 (TGFBI), ENSECAG00000022355 (EIF4E1B), ENSECAG00000023727 (IL1A), ENSECAG00000023803 (TM9SF2), ENSECAG00000024187 (SMARCA2), ENSECAG00000024824 (LPHN2)
	2-3Kb	ENSECAG00000002070, ENSECAG00000002739, ENSECAG00000003576, ENSECAG00000004219 (ZNF831), ENSECAG00000004271 (OR10A4), ENSECAG00000005669, ENSECAG00000009983, ENSECAG00000010259 (TRIM45), ENSECAG00000012980 (TRNA1AP), ENSECAG00000018025 (SIGLEC15), ENSECAG00000019408 (CAT), ENSECAG00000020193 (TGFBI), ENSECAG00000022313 (COL2A1)
	3-4Kb	ENSECAG00000005530 (ACAD9), ENSECAG00000005652, ENSECAG00000005669, ENSECAG00000008046 (EIF4GI), ENSECAG00000008324 (LECT2), ENSECAG00000008754 (NAA25), ENSECAG00000011330, ENSECAG00000013741 (MORC1), ENSECAG00000016069 (CLYBL), ENSECAG00000016256 (HPCA), ENSECAG00000018825 (SIK2), ENSECAG00000019542 (SLC35D1), ENSECAG00000019681 (MANIA2), ENSECAG00000022357 (EIF4E1B)
	4-5Kb	ENSECAG0000000598 (C19orf18), ENSECAG0000000765, ENSECAG0000001160, ENSECAG0000002084, ENSECAG0000004271 (OR10A4), ENSECAG0000005669, ENSECAG0000010259 (TRIM45), ENSECAG0000012474 (TTF2), ENSECAG0000013724 (FAS), ENSECAG0000016463 (TMEM72), ENSECAG0000017078 (CYLC1), ENSECAG0000020193 (TGFBI), ENSECAG0000021563 (CLEC2D), ENSECAG0000022497 (AFM), ENSECAG0000023832 (GAK)
	5-6Kb	ENSECAG00000002070, ENSECAG00000005585, ENSECAG00000005669, ENSECAG00000008494, ENSECAG0000011154 (CHRD), ENSECAG0000011444 (THOC5), ENSECAG0000013938 (ZDHHC13), ENSECAG0000016463 (TMEM72), ENSECAG0000017707 (HCK), ENSECAG0000018025 (SIGLEC15), ENSECAG0000020193 (TGFBI), ENSECAG0000021490, ENSECAG0000022438 (CTSS), ENSECAG0000024981 (HFE), ENSECAG0000026829
	6-7Kb	ENSECAG00000002070, ENSECAG00000003148, ENSECAG00000003256 (KRTAP8-1), ENSECAG00000004271 (OR10A4), ENSECAG00000005669, ENSECAG00000007401, ENSECAG00000008247, ENSECAG00000012584 (GNG2), ENSECAG00000012715, ENSECAG00000015637 (NREP), ENSECAG00000016463 (TMEM72), ENSECAG00000019471 (RASSF6), ENSECAG0000021706 (RPS6KC1), ENSECAG0000022588, ENSECAG0000023832 (GAK)
	7-8Kb	ENSECAG00000002084, ENSECAG00000003256 (KRTAP8-1), ENSECAG00000008247, ENSECAG00000009430 (C16orf72), ENSECAG00000009983, ENSECAG00000015200, ENSECAG00000015637 (NREP), ENSECAG00000016463 (TMEM72), ENSECAG00000017260 (DPEP2), ENSECAG00000017796 (NCAPD2), ENSECAG00000018725 (OGFOD3), ENSECAG00000019542 (SLC35D1)
	8-9Kb	ENSECAG0000000765, ENSECAG00000002084, ENSECAG00000005669, ENSECAG00000008980 (FBXL21), ENSECAG00000009066 (GABBR2), ENSECAG00000009983, ENSECAG00000010461 (LSM1), ENSECAG00000013392 (TMC5), ENSECAG00000015255 (ARMC4), ENSECAG00000016463 (TMEM72), ENSECAG00000018662 (CCDC66), ENSECAG00000018825 (SIK2), ENSECAG00000019471 (RASSF6), ENSECAG00000019634 (DMC1)
	9-10Kb	ENSECAG00000003383, ENSECAG00000005132 (OR2D3), ENSECAG00000008940 (TMEM40), ENSECAG00000009430 (C16orf72), ENSECAG00000011222 (NGE1), ENSECAG00000012507 (CRYAB), ENSECAG00000014389 (MTRF1), ENSECAG00000015637 (NREP), ENSECAG00000015821 (ZERI), ENSECAG00000016463 (TMEM72), ENSECAG00000018401 (CNDP2), ENSECAG00000019137 (MAML3), ENSECAG00000019408 (CAT), ENSECAG00000022355, ENSECAG00000023616 (DDX4)
FM	0d-fold	ENSECAG0000000557 (RPUSD4), ENSECAG0000000955, ENSECAG00000002300 (OR51S1), ENSECAG00000003064, ENSECAG00000003576, ENSECAG00000003780 (OR6A2), ENSECAG00000004548, ENSECAG00000005898, ENSECAG00000006970 (DS4), ENSECAG00000008040 (ADGRB3), ENSECAG00000008864 (CD1A1), ENSECAG00000009003 (APC), ENSECAG00000009483 (PRLR), ENSECAG00000009561 (FDXACB1), ENSECAG00000010259 (TRIM45), ENSECAG00000011688 (TRIOBP), ENSECAG00000011862 (C1orf1), ENSECAG00000012312 (ARHGAP15), ENSECAG0000001265 (DYRK4), ENSECAG00000012702 (PPBP), ENSECAG00000013471 (ZNF599), ENSECAG00000013505, ENSECAG00000014894 (FASTKD3), ENSECAG00000015622 (CDH4), ENSECAG00000016457 (E2F8), ENSECAG00000017249 (TRPS1), ENSECAG00000017257, ENSECAG00000017335 (CDON), ENSECAG00000017400 (SMURF1), ENSECAG00000019282 (HDC), ENSECAG00000019670 (UBA7), ENSECAG00000022699 (PKHD1), ENSECAG00000023231, ENSECAG00000024047 (IL6R)
	2d-fold	ENSECAG0000000701 (FNI), ENSECAG00000003240 (CCR9), ENSECAG00000005293, ENSECAG00000005669, ENSECAG00000008864 (CD1A1), ENSECAG00000008931 (C1orf112), ENSECAG00000009483 (PRLR), ENSECAG00000010684 (PHIP), ENSECAG00000011081, ENSECAG00000011478 (NLN), ENSECAG00000012060 (MYO3A), ENSECAG00000012881 (NME6), ENSECAG00000013742 (MAEA), ENSECAG00000014187 (RSPH3), ENSECAG00000014289 (ARHGAP12), ENSECAG00000014404 (WDR62), ENSECAG00000014894 (FASTKD3), ENSECAG00000017249 (TRPS1), ENSECAG00000017707 (HCK), ENSECAG00000017796 (NCAPD2), ENSECAG00000019159 (NUP85), ENSECAG00000021706 (RPS6KC1), ENSECAG00000021797 (LRRC39), ENSECAG00000022011 (AKAP7), ENSECAG00000022294 (EEF2K), ENSECAG0000002344 (USP28), ENSECAG00000025133 (SYDE2)
	0-1Kb	ENSECAG0000000159 (C16orf78), ENSECAG0000000628, ENSECAG0000000937, ENSECAG00000002155 (NUP93), ENSECAG00000002739, ENSECAG00000003284, ENSECAG00000003576, ENSECAG00000003780 (OR6A2), ENSECAG00000004562, ENSECAG00000005289 (SP7SB), ENSECAG00000005585, ENSECAG00000005914 (PRR29), ENSECAG00000006876 (UTP20), ENSECAG00000007954, ENSECAG00000008049 (EPOR), ENSECAG00000008289 (C1orf27), ENSECAG00000008324 (LECT2), ENSECAG00000008404, ENSECAG00000008749 (VTCN1), ENSECAG00000008980 (FBXL21), ENSECAG00000009482 (PPRC1), ENSECAG00000010221, ENSECAG00000010421 (SLC25A19), ENSECAG000000010723 (ANGEL2), ENSECAG00000001143 (FBXO2), ENSECAG00000011212 (TTC23L), ENSECAG00000011330, ENSECAG00000011689 (SLBP), ENSECAG00000011801 (FHIT), ENSECAG00000011862 (C1orf1), ENSECAG00000012189 (PDE8B), ENSECAG000000013335, ENSECAG00000013471 (ZNF599), ENSECAG00000013489 (GPATCH11), ENSECAG00000013623 (PIK3AP1), ENSECAG00000013682 (VSNL1), ENSECAG00000013712 (ECATH-3), ENSECAG00000014004 (SAMD7), ENSECAG000000014103 (RXFP2), ENSECAG000000014397 (C1orf146), ENSECAG000000014518, ENSECAG000000014680 (MLLT4), ENSECAG000000014825 (LRPAP1), ENSECAG000000015182 (OBSP11A), ENSECAG000000015444 (SLC37A1), ENSECAG000000016216 (ITCH), ENSECAG000000016256 (HPCA), ENSECAG000000016950 (KCNJ8), ENSECAG000000017048 (CD101), ENSECAG000000017484 (C20orf194), ENSECAG000000017907 (RNFT2), ENSECAG000000017924 (KCNG1), ENSECAG000000018022, ENSECAG000000018025 (SIGLEC15), ENSECAG000000018133 (C1orf54), ENSECAG000000018356, ENSECAG000000018847, ENSECAG000000018864 (CPNE2), ENSECAG000000019757, ENSECAG000000019825 (TRDC), ENSECAG000000019842 (NAA15), ENSECAG000000020278 (RAP1GAP2), ENSECAG000000020594 (ELAVL3), ENSECAG000000020638 (NEB), ENSECAG000000020724 (TPR), ENSECAG000000021095, ENSECAG000000021647, ENSECAG000000022355, ENSECAG000000022430 (TOX), ENSECAG000000022924 (EEF2K), ENSECAG000000022986 (CNDP1), ENSECAG000000023176, ENSECAG000000023475, ENSECAG000000023607 (DOCK5), ENSECAG000000024187 (SMARCA2)
	1-2Kb	ENSECAG0000000243, ENSECAG0000000377 (BRIXI), ENSECAG0000000867, ENSECAG0000000937, ENSECAG0000000995, ENSECAG0000000987 (PSMB3), ENSECAG00000001022 (UCN2), ENSECAG00000002070, ENSECAG00000002127, ENSECAG00000002739, ENSECAG00000002922, ENSECAG00000003765, ENSECAG00000004023 (SSBP1), ENSECAG00000005006, ENSECAG00000005111 (RFX4), ENSECAG00000005530 (ACAD9), ENSECAG00000005585, ENSECAG00000005781 (SCPEPI), ENSECAG00000006451 (DX28), ENSECAG00000006779 (USP12), ENSECAG00000006876 (UTP20), ENSECAG00000007032 (KLHL29), ENSECAG00000007192 (PTPRC), ENSECAG00000007458 (SPRR4), ENSECAG00000007806 (PTPN3), ENSECAG00000007841 (CUX2), ENSECAG00000008247, ENSECAG00000008289 (C1orf27), ENSECAG00000008324 (LECT2), ENSECAG00000008846 (LGALS2), ENSECAG00000009315 (DHTKD1), ENSECAG000000010075 (COG2), ENSECAG000000010259 (TRIM45), ENSECAG000000010422 (DNAJC16), ENSECAG00000001143 (FBXO2), ENSECAG000000011330, ENSECAG000000011794 (C6orf141), ENSECAG000000011995 (FTS13), ENSECAG00000001207, ENSECAG000000012312 (ARHGAP15), ENSECAG000000012326 (CD1D), ENSECAG000000012560, ENSECAG000000012628 (EPB41L4A), ENSECAG000000012881 (NME6), ENSECAG000000013122 (ZNF544), ENSECAG000000013623 (PIK3AP1), ENSECAG000000013682 (VSNL1), ENSECAG000000013724 (FAS), ENSECAG000000013881 (DHX35), ENSECAG000000014004 (SAMD7), ENSECAG000000014425 (PIGK), ENSECAG000000014560 (KPNB1), ENSECAG000000014737 (HEATR5B), ENSECAG000000014865 (ADGRA3), ENSECAG000000014918 (ZNF154), ENSECAG000000014926 (MRPL16), ENSECAG000000015043 (CLNS1A), ENSECAG000000015465 (NCOA5), ENSECAG000000015782, ENSECAG000000016069 (CLYBL), ENSECAG000000016546 (GALNT12), ENSECAG000000017074 (FSD2), ENSECAG000000017087 (ACSBG2), ENSECAG000000017400 (SMURF1), ENSECAG000000017513 (DTHD1), ENSECAG000000017789 (SIX2), ENSECAG000000017924 (KCNG1), ENSECAG000000018025 (SIGLEC15),

		ENSECAG00000018068 (MROH2B), ENSECAG00000018160 (TBX21), ENSECAG00000019245 (ACSF2), ENSECAG00000019757, ENSECAG00000019825 (TRDC), ENSECAG00000019927, ENSECAG00000020341, ENSECAG00000020724 (TPR), ENSECAG00000020955, ENSECAG00000021003 (ARMCT), ENSECAG00000021355 (STAM2), ENSECAG00000021447 (ASPH), ENSECAG00000021621 (MOB3B), ENSECAG00000022192 (ZNF77), ENSECAG00000022296 (SGSM3), ENSECAG00000022510 (CD1E2), ENSECAG00000022924 (EEF2K), ENSECAG00000022986 (CNDP1), ENSECAG00000023424 (GABRA4), ENSECAG00000023475, ENSECAG00000024187 (SMARCA2), ENSECAG00000024647 (MLBLAC2), ENSECAG00000024700 (NOLC1), ENSECAG00000024824 (LPHN2), ENSECAG00000024875, ENSECAG00000025178 (PMP22)
2-3Kb		ENSECAG0000000324 (RASEF), ENSECAG0000000869 (RPL26L1), ENSECAG0000000937, ENSECAG0000001326 (FZD1), ENSECAG0000001775 (RAB38), ENSECAG0000001934, ENSECAG0000002070, ENSECAG0000002084, ENSECAG0000002491 (WTIP), ENSECAG0000002581, ENSECAG0000002739, ENSECAG0000003367 (RAD51C), ENSECAG0000003576, ENSECAG0000003791 (NR2C2), ENSECAG0000003916, ENSECAG0000004023 (SSBP1), ENSECAG0000004024 (GGA3), ENSECAG0000004087, ENSECAG0000004219 (ZNF831), ENSECAG0000004242 (AQP4), ENSECAG0000004271 (OR10A4), ENSECAG0000004709 (C2), ENSECAG0000005530 (ACAD9), ENSECAG0000005585, ENSECAG0000005667, ENSECAG0000005998 (TAAR8), ENSECAG0000006170, ENSECAG0000006228, ENSECAG0000006451 (DDX28), ENSECAG0000007241 (PDYN), ENSECAG0000007790 (QR4P4), ENSECAG0000007841 (CUX2), ENSECAG0000008178 (CPNE5), ENSECAG0000008324 (LECT2), ENSECAG0000008846 (LGALS2), ENSECAG0000008980 (FBXL21), ENSECAG0000009159 (PLXND1), ENSECAG0000009665 (DAG1), ENSECAG0000009720 (RIMBP2), ENSECAG0000009759 (TNRC6B), ENSECAG0000009920 (POLR3F), ENSECAG0000009983, ENSECAG0000010259 (TRIM45), ENSECAG0000010684 (PHIP), ENSECAG0000010989 (SH3YL1), ENSECAG0000010990, ENSECAG0000011081, ENSECAG0000011435 (MSI2), ENSECAG0000011794 (C6orf141), ENSECAG0000012326 (CD1D), ENSECAG0000012957 (RHAG), ENSECAG0000013671 (EIF3B), ENSECAG0000014004 (SAMD7), ENSECAG0000014173 (ZRANB2), ENSECAG0000014242, ENSECAG0000014425 (PIKG), ENSECAG0000014706 (RAD51AP2), ENSECAG0000014825 (LRPAPI), ENSECAG0000014927 (AZGP1), ENSECAG0000015152 (SERPINA6), ENSECAG0000015444 (SLC37A1), ENSECAG0000016143 (ANKS6), ENSECAG0000016404 (SLC22A1), ENSECAG0000016989 (OTOL1), ENSECAG0000017081 (DZANK1), ENSECAG0000017087 (ACSBG2), ENSECAG0000017484 (C20orf194), ENSECAG0000018025 (SIGLEC15), ENSECAG0000018068 (MROH2B), ENSECAG0000019067 (OSBPL7), ENSECAG0000019408 (CAT), ENSECAG0000019617 (ATP8B4), ENSECAG0000019853 (AMIGO2), ENSECAG0000019882 (CALHM3), ENSECAG0000021431 (MOB3B), ENSECAG0000021706 (RPS6KC1), ENSECAG0000021851 (DGKE), ENSECAG0000021875 (USP42), ENSECAG0000022290 (GCA), ENSECAG0000022313 (COL2A1), ENSECAG0000022510 (CD1E2), ENSECAG0000022815 (RNFI23), ENSECAG0000022894 (CNDP1), ENSECAG0000023239 (SSR3), ENSECAG0000023441 (E2F3), ENSECAG0000023475, ENSECAG0000023641 (SNX8), ENSECAG0000023805 (ZSWIM6), ENSECAG0000023818 (UVRAG), ENSECAG0000023949 (CCL2), ENSECAG0000024176 (SIGLECL1), ENSECAG0000024301 (DLG4), ENSECAG0000024345 (SUCNR1), ENSECAG0000024875
3-4Kb		ENSECAG0000000159 (C16orf78), ENSECAG0000000324 (RASEF), ENSECAG0000000377 (BRIX1), ENSECAG0000000879 (CAB39L), ENSECAG0000000937, ENSECAG0000001808, ENSECAG0000002021, ENSECAG0000002070, ENSECAG0000002408 (ZNF329), ENSECAG0000002494, ENSECAG0000002548 (RNF182), ENSECAG0000003099, ENSECAG0000004085 (FAM78B), ENSECAG0000004735, ENSECAG0000004808, ENSECAG0000005111 (RFX4), ENSECAG0000005153, ENSECAG0000005193, ENSECAG0000005530 (ACAD9), ENSECAG0000005585, ENSECAG0000005669, ENSECAG0000006451 (DDX28), ENSECAG0000006802 (KCNAB1), ENSECAG0000007740 (HESX1), ENSECAG0000008135 (TRPM3), ENSECAG0000008324 (LECT2), ENSECAG0000008404, ENSECAG0000008426 (PAPSP2), ENSECAG0000008494, ENSECAG0000008754 (NAA25), ENSECAG0000008843 (PODXL2), ENSECAG0000008846 (LGALS2), ENSECAG0000008864 (CD1A1), ENSECAG0000008890 (FBXL21), ENSECAG0000009103 (MLANA), ENSECAG0000009759 (TNRC6B), ENSECAG0000010102, ENSECAG0000010259 (TRIM45), ENSECAG0000010990, ENSECAG0000011212 (TTC23L), ENSECAG0000011330, ENSECAG0000011783 (PDS5A), ENSECAG0000012859 (SP2), ENSECAG0000012864 (ZNF530), ENSECAG0000012957 (RHAG), ENSECAG0000013057 (MREG), ENSECAG0000013270 (CNP134), ENSECAG0000013638 (DCDC2C), ENSECAG0000013671 (PARD6B), ENSECAG0000013893 (SCAR1), ENSECAG0000014242 (MAD1L1), ENSECAG0000016069 (CYLB1), ENSECAG0000016256 (HPCA), ENSECAG0000016682 (RIT2), ENSECAG0000016934 (IL31RA), ENSECAG0000016973 (FILIP1), ENSECAG0000016984 (RANBP3L), ENSECAG0000016989 (OTOL1), ENSECAG0000017249 (ACSBG2), ENSECAG0000017338 (PFKFB4), ENSECAG0000017413 (TELO2), ENSECAG0000017484 (C20orf194), ENSECAG0000018025 (SIGLEC15), ENSECAG0000018068 (MROH2B), ENSECAG0000018069 (ARAP2), ENSECAG0000018094 (TBC1D16), ENSECAG0000018120, ENSECAG0000018966 (FBXO48), ENSECAG0000019067 (OSBPL7), ENSECAG0000019401 (TRIM77), ENSECAG0000019408 (CAT), ENSECAG0000019659, ENSECAG0000019681 (MAN1A2), ENSECAG0000019757, ENSECAG0000019803 (GALK1), ENSECAG0000019927, ENSECAG0000020113 (SEMA3C), ENSECAG0000020495 (CALHM2), ENSECAG0000020684 (C1orf49), ENSECAG0000020722, ENSECAG0000020904 (ZNF438), ENSECAG0000020955, ENSECAG0000021262 (MMPT), ENSECAG0000022357 (E1F4E1B), ENSECAG0000023063 (PTX4), ENSECAG0000023441 (E2F3), ENSECAG0000023641 (SNX8), ENSECAG0000024133 (FGF14), ENSECAG0000024176 (SIGLECL1), ENSECAG0000024181, ENSECAG0000024722 (SCARB2), ENSECAG0000024996
4-5Kb		ENSECAG0000000765, ENSECAG0000000937, ENSECAG0000001160, ENSECAG0000001479, ENSECAG0000001775 (RAB38), ENSECAG0000001796, ENSECAG0000001934, ENSECAG0000002070, ENSECAG0000002084, ENSECAG0000002127, ENSECAG0000002408 (ZNF329), ENSECAG00000030765, ENSECAG0000004023 (SSBP1), ENSECAG0000004271 (OR10A4), ENSECAG0000004674, ENSECAG0000005111 (RFX4), ENSECAG0000005153, ENSECAG0000005585, ENSECAG0000005669, ENSECAG0000005981, ENSECAG0000007007 (STT3B), ENSECAG0000007214 (CACNG4), ENSECAG0000007543 (LLRC46), ENSECAG0000007740 (HESX1), ENSECAG0000008107 (FERMT3), ENSECAG0000008289 (C1orf27), ENSECAG0000008334 (SMARCA4), ENSECAG0000008494, ENSECAG0000008545 (ECM1), ENSECAG0000008980 (FBXL21), ENSECAG0000009476, ENSECAG0000009558 (SLC16A12), ENSECAG0000009642 (ADAMTS5), ENSECAG0000009759 (TNRC6B), ENSECAG0000010259 (TRIM45), ENSECAG0000010794 (SPACA1), ENSECAG0000010609 (IL7R), ENSECAG0000010990, ENSECAG0000011061 (ZNF789), ENSECAG0000011435 (MSI2), ENSECAG0000011602, ENSECAG0000011801 (FHIT), ENSECAG0000012474 (ITF2), ENSECAG0000012607 (ABTB1), ENSECAG0000012653 (DYRK4), ENSECAG0000012853 (SP6), ENSECAG0000012864 (ZNF530), ENSECAG0000012881 (NME6), ENSECAG0000012980 (TRNAU1AP), ENSECAG0000013070 (DAGLB), ENSECAG0000013238 (FAM83D), ENSECAG0000013328 (TMOD2), ENSECAG0000013370, ENSECAG0000013616 (DSG2), ENSECAG0000013671 (EIF3B), ENSECAG0000013724 (FAM106), ENSECAG0000013938 (ZDHHC13), ENSECAG0000014153 (CLK4), ENSECAG0000014304 (ATP11A), ENSECAG0000014425 (PIKG), ENSECAG0000015053 (SDCBP), ENSECAG0000015443 (OSBP2), ENSECAG0000016024, ENSECAG0000016463 (TMEM72), ENSECAG0000016682 (RIT2), ENSECAG0000016984 (RANBP3L), ENSECAG0000017078 (CYLC2), ENSECAG0000017081 (DZANK1), ENSECAG0000017087 (ACSBG2), ENSECAG0000017484 (C20orf194), ENSECAG0000017658 (CRNN), ENSECAG0000018025 (SIGLEC15), ENSECAG0000018068 (MROH2B), ENSECAG0000019067 (OSBPL7), ENSECAG0000019401 (TRIM77), ENSECAG0000019621, ENSECAG0000019626 (FAM46C), ENSECAG0000019757, ENSECAG0000019825 (TRDC), ENSECAG0000020170 (ARP12P), ENSECAG0000020479 (GEMIN5), ENSECAG0000020955, ENSECAG0000021355 (STAM2), ENSECAG0000021609 (SLC40A1), ENSECAG0000022128, ENSECAG0000022141 (TSLP), ENSECAG0000022359 (FOXRED1), ENSECAG0000022584 (DOCK6), ENSECAG0000023244 (TAF1B), ENSECAG0000023475, ENSECAG0000023616 (DDX4), ENSECAG0000023724 (ZNF235), ENSECAG0000023731 (ABCD3), ENSECAG0000023832 (GAK), ENSECAG0000024176 (SIGLECL1), ENSECAG0000024187 (SMARCA2), ENSECAG0000024198 (SEL1)
5-6Kb		ENSECAG000000188 (NMD3), ENSECAG0000000765, ENSECAG0000001096, ENSECAG0000001302, ENSECAG0000002070, ENSECAG0000002183, ENSECAG0000002548 (RNF182), ENSECAG0000002803, ENSECAG0000003137 (P4HTM), ENSECAG0000003256 (KRTAP8-1), ENSECAG0000003791 (NR2C2), ENSECAG0000003992, ENSECAG0000004271 (OR10A4), ENSECAG0000004589 (SPTSSB), ENSECAG0000005585, ENSECAG0000005669, ENSECAG0000005676, ENSECAG0000005765 (ADII), ENSECAG0000005889 (TIMMD1), ENSECAG0000006371, ENSECAG0000006851, ENSECAG0000007176 (ELOVL7), ENSECAG0000007214 (CACNG4), ENSECAG0000007525 (CPSF4), ENSECAG0000008046 (EIF4GI), ENSECAG0000008486 (PAPSS2), ENSECAG0000008494, ENSECAG0000008660 (YAP1), ENSECAG0000008846 (LGALS2), ENSECAG0000008980 (FBXL21), ENSECAG0000009197 (LANCL1), ENSECAG0000009430 (C16orf72), ENSECAG0000009521 (WNT8B), ENSECAG0000010117, ENSECAG0000010331 (PCGF3), ENSECAG0000010407 (BAG4), ENSECAG0000010684 (PHIP), ENSECAG0000011015, ENSECAG000001154 (CHRD), ENSECAG0000011444 (THOC5), ENSECAG0000011801 (FHIT), ENSECAG0000011824, ENSECAG0000012653 (DYRK4), ENSECAG0000012859 (SP2), ENSECAG0000012864 (ZNF530), ENSECAG0000012870 (NEURL1), ENSECAG0000012927 (KIAA0319L), ENSECAG0000012957 (RHAG), ENSECAG0000012980 (TRNAU1AP), ENSECAG0000013418 (ICT1), ENSECAG0000013471 (ZNF8), ENSECAG0000013553 (ZNF8), ENSECAG0000013582 (DHRS3), ENSECAG0000013671 (EIF3B), ENSECAG0000013938 (ZDHHC13), ENSECAG0000014153 (CLK4), ENSECAG0000014304 (ATP11A), ENSECAG0000014737 (HEATR5B), ENSECAG0000015063 (ADGRG6), ENSECAG0000015545 (ARHGEF15), ENSECAG0000015612 (FAM212A), ENSECAG0000016256 (HPCA), ENSECAG0000016463 (TMEM72), ENSECAG0000016790, ENSECAG0000016894 (PPM1A), ENSECAG0000016984 (RANBP3L), ENSECAG0000016989 (OTOL1), ENSECAG0000017087 (ACSBG2), ENSECAG0000017155, ENSECAG0000017249 (TRPS1), ENSECAG0000017337 (PDE6B), ENSECAG0000018022, ENSECAG0000018025 (SIGLEC15), ENSECAG0000018068 (MROH2B), ENSECAG0000018160 (TBX21), ENSECAG0000018688 (CDK5RAP3), ENSECAG0000019401 (TRIM77), ENSECAG0000019659, ENSECAG0000019757, ENSECAG0000019825 (TRDC), ENSECAG0000019853 (AMIGO2), ENSECAG0000019882 (CALHM3), ENSECAG0000020684 (C12orf49), ENSECAG0000021001 (SEN P6), ENSECAG0000021077 (FGF23), ENSECAG0000021355 (STAM2), ENSECAG0000021361 (ANXA13), ENSECAG0000021490, ENSECAG0000022082 (C12orf4), ENSECAG0000022290 (GCA), ENSECAG0000023756 (SMYD4), ENSECAG0000024761 (INOS), ENSECAG0000024875, ENSECAG0000024981 (HFE), ENSECAG0000026829
6-7Kb		ENSECAG000000011 (ADGRA2), ENSECAG0000000869 (RPL26L1), ENSECAG0000000971 (SUCO), ENSECAG0000000999, ENSECAG0000001219 (OR1B4), ENSECAG0000001479, ENSECAG0000002070, ENSECAG0000002084,

		ENSECAG0000002155 (NUP93), ENSECAG0000002373, ENSECAG0000002408 (ZNF329), ENSECAG0000003148, ENSECAG0000003256 (KRTAP8-1), ENSECAG0000004271 (OR10A4), ENSECAG0000005111 (RFX4), ENSECAG0000005132 (OR2D3), ENSECAG0000005669, ENSECAG0000005765 (ADII), ENSECAG0000007434 (PRR9), ENSECAG0000007740 (HESX1), ENSECAG0000008090 (TAS2R41), ENSECAG0000008247, ENSECAG0000008324 (LECT2), ENSECAG0000008426 (PAPSS2), ENSECAG0000008494, ENSECAG0000008959 (SAMHD1), ENSECAG0000009759 (TNRC6B), ENSECAG0000010011 (MAP1LC3A), ENSECAG0000010117, ENSECAG0000010367 (RAD51AP1), ENSECAG0000010461 (LSM1), ENSECAG0000011353 (MFS7D), ENSECAG0000011435 (MSI2), ENSECAG0000011602, ENSECAG0000011754 (RPIA), ENSECAG0000011794 (C6orf141), ENSECAG0000011824, ENSECAG0000012312 (ARHGAP15), ENSECAG0000012584 (GNG2), ENSECAG0000012607 (ABTB1), ENSECAG0000012715, ENSECAG0000012853 (SP6), ENSECAG0000012870 (NEURL1), ENSECAG0000012957 (RHAG), ENSECAG0000013070 (DAGLB), ENSECAG0000013553 (ZNF8), ENSECAG0000013671 (EIF3B), ENSECAG0000013706 (SMAD6), ENSECAG0000013859, ENSECAG0000014425 (PIKG), ENSECAG0000014491 (NLRC5), ENSECAG0000014501 (TMEM54), ENSECAG0000014891 (NRCAM), ENSECAG0000015012 (MARCH1), ENSECAG0000015200, ENSECAG0000015444 (SLC37A1), ENSECAG0000015637 (NREP), ENSECAG0000016336 (CDC25A), ENSECAG0000016463 (TMEM72), ENSECAG0000016984 (RANBP3L), ENSECAG0000017151 (LYPD5), ENSECAG0000017337 (PDE6B), ENSECAG0000017400 (SMURF1), ENSECAG0000017484 (C20orf194), ENSECAG0000018022, ENSECAG0000018068 (MROH2B), ENSECAG0000018617 (RPRD2), ENSECAG0000018688 (CDK5RAP3), ENSECAG0000018721, ENSECAG0000018901 (FAM120B), ENSECAG0000019182 (GPRC6A), ENSECAG0000019210 (FNDC5), ENSECAG0000019282 (HDC), ENSECAG0000019393 (ALS2CR11), ENSECAG0000019401 (TRIM77), ENSECAG0000019471 (RASSF6), ENSECAG0000019661 (RPF1), ENSECAG0000019757, ENSECAG0000019825 (TRDC), ENSECAG0000020113 (SEMA3C), ENSECAG0000020278 (RAP1GAP2), ENSECAG0000020341, ENSECAG0000020638 (NEB), ENSECAG0000021077 (FGF23), ENSECAG0000021239 (CCDC92), ENSECAG0000021355 (STAM2), ENSECAG0000021492 (ADSL), ENSECAG0000021706 (RPS6KC1), ENSECAG0000021776, ENSECAG0000021797 (LRRC39), ENSECAG0000021923 (GTF2F2), ENSECAG0000021984 (WBSRCL16), ENSECAG000002202 (ADGRD1), ENSECAG0000022402 (GFOD1), ENSECAG0000022588, ENSECAG0000023141 (LAMC17), ENSECAG0000023326 (TMEM175), ENSECAG0000023832 (GAK), ENSECAG0000024181, ENSECAG0000024345 (SUCNR1), ENSECAG0000024700 (NOLC1), ENSECAG0000026877 (C1orf98)
FM	7-8Kb	ENSECAG000000327 (RNFL18), ENSECAG0000004040 (CCDC174), ENSECAG0000004937, ENSECAG0000001022 (UCN2), ENSECAG0000001808, ENSECAG0000002084, ENSECAG0000002155 (NUP93), ENSECAG0000002599, ENSECAG0000003265 (KRTAP8-1), ENSECAG0000003791 (NR2C2), ENSECAG0000003846 (ANKR), ENSECAG0000004045 (P2R), ENSECAG0000004085 (FAM78B), ENSECAG0000004526, ENSECAG0000004649, ENSECAG0000004742, ENSECAG0000005291, ENSECAG0000005585, ENSECAG0000005676, ENSECAG0000006818, ENSECAG0000007032 (KLHL29), ENSECAG0000007147 (CAPRIN1), ENSECAG0000007950, ENSECAG0000007979 (PLG), ENSECAG0000008311 (CHMP4B), ENSECAG0000008494, ENSECAG0000008576 (CD300E), ENSECAG0000008738 (ID2), ENSECAG0000008987 (TRIM42), ENSECAG0000008980 (FBXL21), ENSECAG0000009066 (GABBR2), ENSECAG0000009430 (C16orf72), ENSECAG0000009846 (RAD1), ENSECAG0000009897 (CIPC), ENSECAG0000009990, ENSECAG0000009983, ENSECAG0000010117, ENSECAG0000010461 (LSM1), ENSECAG0000010476 (L3MBTL2), ENSECAG0000010669 (CRB1), ENSECAG0000010973 (IL7R), ENSECAG0000010990, ENSECAG0000011699 (PDSSA), ENSECAG0000011783 (PPDS5A), ENSECAG0000012073 (FBXL21), ENSECAG0000012918 (ZNF704), ENSECAG0000012952 (UV420H1), ENSECAG0000013489 (GPATCH11), ENSECAG0000013553 (ZNF8), ENSECAG0000013671 (EIF3B), ENSECAG0000015182 (OBSP1A), ENSECAG0000015200, ENSECAG0000015567 (FREM1), ENSECAG0000015637 (NREP), ENSECAG0000016312 (CD274), ENSECAG0000016322 (CYP24A1), ENSECAG0000016463 (TMEM72), ENSECAG0000016506 (PIWIL1), ENSECAG0000016577 (ZNF211), ENSECAG0000017074 (FSD2), ENSECAG0000017482 (TCAF1), ENSECAG0000017484 (C20orf194), ENSECAG0000017796 (NCAPD2), ENSECAG0000017907 (RNFT2), ENSECAG0000017924 (KNG1), ENSECAG0000018068 (MROH2B), ENSECAG0000018094 (TBC1D16), ENSECAG0000018146 (PRAME), ENSECAG0000018151 (SORBS1), ENSECAG0000018172, ENSECAG0000019847 (NADK2), ENSECAG0000019853 (AMIGO2), ENSECAG0000019882 (CALHM3), ENSECAG0000020025 (HMGN3), ENSECAG0000020278 (RAP1GAP2), ENSECAG0000020356 (MEF2D), ENSECAG0000020722, ENSECAG0000021001 (SEN6P), ENSECAG0000021233 (MSANTD3), ENSECAG0000021556, ENSECAG0000021615 (PMSB1), ENSECAG0000022068 (F1G6), ENSECAG0000022068 (ROR2), ENSECAG0000022352 (SPL140), ENSECAG0000022474 (CALU), ENSECAG0000024055 (JUN), ENSECAG0000024187 (SMARCA2), ENSECAG0000024990 (SLC17A6), ENSECAG0000024996, ENSECAG0000026817 (ALDH1B1)
FM	8-9Kb	ENSECAG000000159 (C16orf78), ENSECAG000000537, ENSECAG0000005040 (CCDC174), ENSECAG000000616 (BARX2), ENSECAG000000647, ENSECAG000000721 (MYCBPAP), ENSECAG000000765, ENSECAG0000001096, ENSECAG000001273, ENSECAG000001326 (FZD1), ENSECAG000002084, ENSECAG000002155 (NUP93), ENSECAG000002739, ENSECAG000003056 (TM6SF1), ENSECAG000003256 (KRTAP8-1), ENSECAG000003791 (NR2C2), ENSECAG000004045 (F2R), ENSECAG000004085 (FAM78B), ENSECAG000004085 (BMP2D), ENSECAG000004085 (SPTSSB), ENSECAG0000045291, ENSECAG000005669, ENSECAG000006442 (ADAM9), ENSECAG000006875 (IPK62), ENSECAG000007463, ENSECAG000007670 (BMP10), ENSECAG000007974 (GALNT3), ENSECAG000008404, ENSECAG000008763 (LYPD3), ENSECAG000008846 (LGALS2), ENSECAG000008939 (RBM17), ENSECAG000008980 (FBXL21), ENSECAG000009066 (GABBR2), ENSECAG000009430 (C16orf72), ENSECAG000009506, ENSECAG000009809 (ENDOG), ENSECAG000009841 (AKAP1), ENSECAG000009983, ENSECAG0000010123 (UP3P4), ENSECAG0000010190 (FEZ2), ENSECAG0000010242 (MCTP1), ENSECAG0000010259 (TRIM45), ENSECAG0000010461 (LSM1), ENSECAG0000010642, ENSECAG0000010807 (PYXLP1), ENSECAG0000011222 (NGEF), ENSECAG0000011688 (TRIOBP), ENSECAG0000011754 (RPIA), ENSECAG0000011801 (FHIT), ENSECAG0000011824, ENSECAG0000012333 (MRPS23), ENSECAG0000012607 (ABTB1), ENSECAG0000012834 (RRNAD1), ENSECAG0000012859 (SP2), ENSECAG0000013070 (DAGLB), ENSECAG0000013238 (FAM83D), ENSECAG000001392 (TM5C), ENSECAG0000013682 (VSNL1), ENSECAG0000013706 (SMAD6), ENSECAG0000014336 (ENKRD32), ENSECAG0000014397 (C1orf146), ENSECAG0000014604 (PNPLA3), ENSECAG0000015255 (NC0A5), ENSECAG0000015567 (FREM1), ENSECAG0000015637 (NREP), ENSECAG0000015790 (ANKR32), ENSECAG0000015852 (GOT1L), ENSECAG0000015989 (ABRA), ENSECAG0000016024, ENSECAG0000016069 (CYBLY), ENSECAG0000016322 (CYP24A1), ENSECAG0000016454 (NTSR2), ENSECAG0000016463 (TMEM72), ENSECAG0000016710 (UPK3B), ENSECAG0000017337 (PDE6B), ENSECAG0000017484 (C20orf194), ENSECAG0000017658 (CRNN), ENSECAG0000018068 (MROH2B), ENSECAG0000018094 (ARAP2), ENSECAG0000018166 (RBM17), ENSECAG0000018662 (CCDC66), ENSECAG0000018825 (SIK2), ENSECAG0000019401 (TRIM77), ENSECAG0000019471 (RASSF6), ENSECAG0000019570 (GRAMD4), ENSECAG0000019634 (DMC1), ENSECAG0000019708 (PIK3CG), ENSECAG0000019739 (PXDN), ENSECAG0000019757, ENSECAG0000019853 (AMIGO2), ENSECAG0000020638 (NEB), ENSECAG0000020684 (C1orf49), ENSECAG0000020955, ENSECAG0000021355 (STAM2), ENSECAG0000021875 (USP42), ENSECAG0000021993 (GCLM), ENSECAG0000022077 (ELF2), ENSECAG0000022162 (TBC1D1), ENSECAG0000023607 (DOCK5), ENSECAG0000023860 (TGM3), ENSECAG0000025029 (C1orf52)
FM	9-10Kb	ENSECAG000000159 (C16orf78), ENSECAG000000170, ENSECAG000000647, ENSECAG000000721 (MYCBPAP), ENSECAG000000765, ENSECAG0000001326 (FZD1), ENSECAG0000001479, ENSECAG0000002155 (NUP93), ENSECAG0000003256 (KRTAP8-1), ENSECAG0000003367 (RAD51C), ENSECAG0000003838 (ENP22), ENSECAG0000003976 (ENP22), ENSECAG0000004049, ENSECAG0000004469, ENSECAG0000005111 (RFX4), ENSECAG0000005132 (OR2D3), ENSECAG0000005676, ENSECAG0000006548 (SPATA3), ENSECAG0000006855, ENSECAG0000007280, ENSECAG0000007543 (LRRC46), ENSECAG0000007881 (IFIH1), ENSECAG0000008528, ENSECAG0000008738 (ID2), ENSECAG0000008893 (PARVB), ENSECAG0000008939 (RBM17), ENSECAG0000008980 (FBXL21), ENSECAG0000009384 (NECAB1), ENSECAG0000009430 (C16orf72), ENSECAG0000009476, ENSECAG0000010723 (ANGEL2), ENSECAG0000010776 (TERF2IP1), ENSECAG0000010807 (PYXLP1), ENSECAG0000011222 (NGEF), ENSECAG0000011338 (ABCBS5), ENSECAG0000011600 (WNT9B), ENSECAG0000011754 (RPIA), ENSECAG0000011797 (MN-SOD), ENSECAG0000011933, ENSECAG0000012531 (ACY2P), ENSECAG0000012607 (ABTB1), ENSECAG0000012667 (RBF0X1), ENSECAG0000012715, ENSECAG0000012859 (SP2), ENSECAG0000012881 (NME6), ENSECAG0000012942, ENSECAG0000012991, ENSECAG0000013682 (VSNL1), ENSECAG0000014153 (CLK4), ENSECAG0000014610 (PRTT3), ENSECAG0000015003 (PLGRKT), ENSECAG0000015053 (SDCBP), ENSECAG0000015070 (PRPSAP2), ENSECAG0000015133 (FOXX1), ENSECAG0000015567 (FREM1), ENSECAG0000015637 (NREP), ENSECAG0000015821 (ZER1), ENSECAG0000016183 (STAR4D), ENSECAG0000016256 (HPCA), ENSECAG0000016463 (TMEM72), ENSECAG0000016894 (OTOL1), ENSECAG0000017115, ENSECAG0000017211 (ASCI1), ENSECAG0000017473 (APPL1), ENSECAG0000017478 (B4GALT1), ENSECAG0000017484 (C20orf194), ENSECAG0000018068 (MROH2B), ENSECAG0000018094 (TBC1D16), ENSECAG0000018341 (CA11), ENSECAG0000018367 (ZWILCH), ENSECAG0000018401 (CNDP2), ENSECAG0000018465 (MS4A5), ENSECAG0000018751, ENSECAG0000018901 (FAM120B), ENSECAG0000019126 (SLC12A5), ENSECAG0000019137 (MAML3), ENSECAG0000019210 (FNDC5), ENSECAG0000019401 (TRIM77), ENSECAG0000019471 (RASSF6), ENSECAG0000019708 (PIK3CG), ENSECAG0000019757, ENSECAG0000019842 (NAA15), ENSECAG0000019847 (NADK2), ENSECAG0000019853 (AMIGO2), ENSECAG0000019882 (CALHM3), ENSECAG0000019955 (ADCK3), ENSECAG0000020025 (HMGN3), ENSECAG0000020392 (AZI2), ENSECAG0000020433 (TENM3), ENSECAG0000020638 (NEB), ENSECAG0000020684 (C1orf49), ENSECAG0000020710 (DRC1), ENSECAG0000020724 (TPR), ENSECAG0000020791 (FRMPD1), ENSECAG0000020843, ENSECAG0000021207 (THRAP3), ENSECAG0000021355 (STAM2), ENSECAG0000021662 (STMN1), ENSECAG0000021867 (MRPS7), ENSECAG0000021889 (ABR), ENSECAG0000022290 (GCA), ENSECAG0000023416, ENSECAG0000023475, ENSECAG0000023616 (DDX4), ENSECAG0000024176 (SIGLECL1), ENSECAG0000024277 (CYTH4), ENSECAG0000024850, ENSECAG0000025029 (C1orf52)

Table S7.9. GO term enrichment for genes harbouring adaptive alleles at their 0-1Kb and 0-10Kb site categories.

Site category	Panel	Model organism	GO Term
0-10Kb	DOM	mouse	ATP binding (0.0206)
			dipeptidase activity (0.0206)
			adenyl nucleotide binding (0.0206)
			small molecule binding (0.0206)
			adenyl ribonucleotide binding (0.0206)
			nucleotide binding (0.0248)
			translation factor activity, nucleic acid binding (0.0248)
			anion binding (0.0248)
			nucleoside phosphate binding (0.0248)
			ribonucleoside binding (0.0314)
	FM	mouse	metabolic process (0.0016)
			single-organism metabolic process (0.0027)
			cellular metabolic process (0.0027)
			organic substance metabolic process (0.0039)
			primary metabolic process (0.0039)
			anatomical structure morphogenesis (0.0168)
			biological regulation (0.0180)
			localization (0.0180)
			cartilage condensation (0.0323)
			RNA binding (0.0091)
			R-SMAD binding (0.0411)
			cell periphery (0.0073)
			plasma membrane (0.0073)
			membrane (0.0080)
			intracellular organelle (0.0080)
			organelle (0.0080)
			cytoplasm (0.0080)

Table S7.10. KEGG pathway enrichment for genes harbouring adaptive alleles at their 0-1Kb and 0-10Kb site categories.

Site category	Panel	Model organism	KEGG Pathway
0-1Kb	DOM	mouse	Olfactory transduction (0.0100)
		human	Purine metabolism (0.0159)
			RNA transport (0.0159)
			Ubiquitin mediated proteolysis (0.0159)
	FM	mouse	RNA transport (0.0145)
			Ubiquitin mediated proteolysis (0.0145)
			Purine metabolism (0.0145)
			Graft-versus-host disease (0.0077)
0-10Kb	DOM	human	RNA transport (0.0077)
			Type I diabetes mellitus (0.0077)
			Olfactory transduction (0.0097)
			Apoptosis (0.0182)
		mouse	RNA transport (0.0083)
			Graft-versus-host disease (0.0083)
			Type I diabetes mellitus (0.0083)
			Apoptosis (0.0130)
			Olfactory transduction (0.0170)
			Protein processing in endoplasmic reticulum (0.0317)
	FM	human	Chemokine signaling pathway (0.0320)
			Cytokine-cytokine receptor interaction (0.0470)
			MAPK signaling pathway (0.0491)
			RNA transport (0.0002)
			Pathways in cancer (0.0002)
		mouse	Metabolic pathways (0.0109)
			Melanoma (0.0143)
			Endocytosis (0.0148)
			Small cell lung cancer (0.0219)
			Histidine metabolism (0.0340)

Table S7.11. Wiki pathways enrichment for genes harbouring adaptive alleles at their 0-1Kb and 0-10Kb site categories.

Site category	Panel	Model organism	WikiPathway
0-1Kb	DOM	mouse	GPCRs, Class A Rhodopsin-like (0.0005)
			GPCRs, Other (0.0005)
	FM	human	Muscle cell TarBase (0.0278)
			GPCRs, Other (0.0378)
	DOM	mouse	GPCRs, Class A Rhodopsin-like (0.0378)
			FAS pathway and Stress induction of HSP regulation (0.0180)
0-10Kb	DOM	human	TSH signaling pathway (0.0180)
			TCR Signaling Pathway (0.0266)
			Focal Adhesion (0.0450)
			MAPK signaling pathway (0.0450)
			GPCRs, Class A Rhodopsin-like (0.0010)
		mouse	Iron Homeostasis (0.0010)
			FAS pathway and Stress induction of HSP regulation (0.0063)
			MAPK signaling pathway (0.0324)
			Focal Adhesion (0.0324)
			GPCRs, Other (0.0324)
	FM	human	Chemokine signaling pathway (0.0324)
			Muscle cell TarBase (0.0195)
		mouse	B Cell Receptor Signaling Pathway (0.0325)
			ESC Pluripotency Pathways (0.0058)
			Non-odorant GPCRs (0.0058)
			mRNA processing (0.0058)
			serotonin and anxiety (0.0101)
			Complement and Coagulation Cascades (0.0128)

Table S7.12. Phenotype term enrichment for genes harbouring adaptive alleles at their 0-1Kb and 0-10Kb site categories.

Site category	Panel	Model organism	Phenotype
0-1Kb	DOM	mouse	abnormal hematopoietic cell number (0.0064)
			abnormal hematopoiesis (0.0072)
			abnormal blood cell morphology/development (0.0072)
			abnormal immune system morphology (0.0072)
			abnormal hematopoietic system morphology/development (0.0078)
			increased hematopoietic cell number (0.0078)
			hematopoietic system phenotype (0.0078)
			increased circulating glucose level (0.0096)
			abnormal leukocyte cell number (0.0146)
			increased T cell number (0.0160)
0-10Kb	DOM	human	Prominent interphalangeal joints (0.0116)
			Dumbbell-shaped long bone (0.0155)
			Anterior rib cupping (0.0155)
			Cupped ribs (0.0232)
			Edema (0.0232)
			Flat acetabular roof (0.0232)
			Abnormal tarsal ossification (0.0232)
			Abnormal foot bone ossification (0.0261)
			Arthropathy (0.0284)
		mouse	Abnormality of fluid regulation (0.0371)
			platyspondylia (0.0140)
	FM	mouse	mortality/aging (0.0031)
			abnormal survival (0.0336)
			abnormal nervous system physiology (0.0459)

Table S7.13. PheWas term enrichment for genes harbouring adaptive alleles at their 0-1Kb and 0-10Kb site categories.

Site category	Panel	PheWas
0-1Kb	FM	Biliary cirrhosis (0.0184)
		Adverse effects of opiates and related narcotics in therapeutic use (0.0184)
		Viral infection (0.0184)
		First degree AV block (0.0184)
		Cellulitis and abscess of trunk (0.0184)
		Peripheral arterial disease (0.0219)
		Superficial cellulitis and abscess (0.0391)
		Atrial fibrillation & flutter (0.0460)
		Disorders of fluid, electrolyte, and acid-base balance (0.0460)
		Chronic sinusitis (0.0460)
0-10Kb	DOM	Lump or mass in breast (0.0420)
		Other rheumatic heart disease (0.0420)
		Chronic rheumatic disease of the heart valves (0.0420)
		Torticollis (0.0420)
		Retinal detachments and defects (0.0420)
		Other peripheral nerve disorders (0.0420)
		Posterior pituitary disorders (0.0420)
		Malignant neoplasm of ovary (0.0420)
		Cancer of other female genital organs (0.0420)
		Enthesopathy (0.0420)

Table S7.14. Disease enrichment for genes harbouring adaptive alleles at their 0-1Kb and 0-10Kb sites categories.

Site category	Panel	Disease
0-1Kb	FM	Kidney Neoplasms (0.0057)
		Gallbladder Neoplasms (0.0057)
		Drug-induced chronic hepatitis (0.0057)
		Encephalomyelitis (0.0057)
		Gallbladder Diseases (0.0057)
		Endocrine disorder NOS (0.0057)
		Endocrine System Diseases (0.0057)
		Endocrine disturbance NOS (0.0057)
		Anemia, Refractory (0.0057)
		Hypothyroidism (0.0090)
0-10Kb	DOM	Arthritis, Rheumatoid (0.0033)
		Occupational Diseases (0.0033)
		Autoimmune Diseases (0.0033)
		Arthritis (0.0033)
		Lens Diseases (0.0095)
		Wounds and Injuries (0.0095)
		Sunburn (0.0095)
		Liver Failure, Acute (0.0111)
		Liver Cirrhosis, Alcoholic (0.0111)
		Degeneration of lumbar intervertebral disc (0.0111)
	FM	Demyelinating Diseases (0.0010)
		Tooth, Supernumerary (0.0018)
		Encephalomyelitis (0.0018)
		Hypophosphatemia, Familial (0.0018)
		Osteomalacia (0.0018)

REFERENCES

1. Pakendorf B, et al. (2006) Investigating the effects of prehistoric migrations in Siberia: genetic variation and the origins of Yakuts. *Hum Genet* 120(3):334–353.
2. Crubézy E, et al. (2010) Human evolution in Siberia: from frozen bodies to ancient DNA. *BMC Evol Biol* 10(1):25.
3. Fedorova SA, et al. (2013) Autosomal and uniparental portraits of the native populations of Sakha (Yakutia): implications for the peopling of Northeast Eurasia. *BMC Evol Biol* 13(1):127.
4. Keyser C, et al. (2015) The ancient Yakuts: a population genetic enigma. *Philos Trans R Soc Lond B Biol Sci* 370(1660):20130385.
5. West BA (2009) *Encyclopedia of the Peoples of Asia and Oceania* (Facts On File, Incorporated).
6. Ferret C (2009) *Une civilisation du cheval* (BELIN). BELIN edition.
7. Bonnie LH (1995) International Encyclopedia of Horse Breeds.
8. Solomonov NG, Anufriev AI, Yadrikhinskii VF, Isaev AP (2009) Body temperature changes in purebred and hybrid Yakut horses under the conditions of Yakutia. *Dokl Biol Sci* 427(1):358–361.
9. Grigoreva NN, Koryakina LP (2008) Dynamics of products of a metabolism glycoproteide and activity of enzymes AcAT, AAT at different type the Yakut breed of a horse. *Dokl Ross Akad Selskokhozyaistvennykh Nauk* (3):44–46.
10. Sarkissian C Der, et al. (2014) Shotgun microbial profiling of fossil remains. *Mol Ecol* 23(7):1780–1798.
11. Gilbert MTP, et al. (2004) Ancient mitochondrial DNA from hair. *Curr Biol CB* 14(12):R463–464.
12. Vilstrup JT, et al. (2013) Mitochondrial Phylogenomics of Modern and Ancient Equids. *PLoS ONE* 8(2):e55950.
13. Orlando L, et al. (2013) Recalibrating *Equus* evolution using the genome sequence of an early Middle Pleistocene horse. *Nature* 499(7456):74–78.
14. Meyer M, Kircher M (2010) Illumina sequencing library preparation for highly multiplexed target capture and sequencing. *Cold Spring Harb Protoc* 2010(6):db.prot5448.
15. Pedersen JS, et al. (2014) Genome-wide nucleosome map and cytosine methylation levels of an ancient human genome. *Genome Res* 24(3):454–466.
16. Schubert M, et al. (2014) Prehistoric genomes reveal the genetic foundation and cost of horse domestication. *Proc Natl Acad Sci U A* 111(52):E5661–9.
17. Seguin-Orlando A, et al. (2013) Ligation Bias in Illumina Next-Generation DNA Libraries: Implications for Sequencing Ancient Genomes. *PLoS ONE* 8(10):e78575.

18. Der Sarkissian C, et al. (2015) Evolutionary Genomics and Conservation of the Endangered Przewalski's Horse. *Curr Biol.* doi:10.1016/j.cub.2015.08.032.
19. Do K-T, et al. (2014) Genomic characterization of the Przewalski's horse inhabiting Mongolian steppe by whole genome re-sequencing. *Livest Sci* 167(0):86–91.
20. Schubert M, et al. (2014) Characterization of ancient and modern genomes by SNP detection and phylogenomic and metagenomic analysis using PALEOMIX. *Nat Protoc* 9(5):1056–1082.
21. Botchkareva NV, Ahluwalia G, Shander D (2006) Apoptosis in the Hair Follicle. *J Invest Dermatol* 126(2):258–264.
22. Rasmussen M, et al. (2010) Ancient human genome sequence of an extinct Palaeo-Eskimo. *Nature* 463(7282):757–762.
23. Olalde I, et al. (2014) Derived immune and ancestral pigmentation alleles in a 7,000-year-old Mesolithic European. *Nature*. doi:10.1038/nature12960.
24. Enk JM, et al. (2014) Ancient whole genome enrichment using baits built from modern DNA. *Mol Biol Evol* 31(5):1292–1294.
25. Briggs AW, et al. (2007) Patterns of damage in genomic DNA sequences from a Neandertal. *Proc Natl Acad Sci* 104(37):14616–14621.
26. Jónsson H, Ginolhac A, Schubert M, Johnson PLF, Orlando L (2013) mapDamage2.0: fast approximate Bayesian estimates of ancient DNA damage parameters. *Bioinformatics* 29(13):1682–1684.
27. Star B, et al. (2014) Palindromic Sequence Artifacts Generated during Next Generation Sequencing Library Preparation from Historic and Ancient DNA. *PLoS One* 9(3):e89676.
28. Reich D, et al. (2010) Genetic history of an archaic hominin group from Denisova Cave in Siberia. *Nature* 468(7327):1053–1060.
29. Wade CM, et al. (2009) Genome sequence, comparative analysis, and population genetics of the domestic horse. *Science* 326(5954):865–867.
30. Jónsson H, et al. (2014) Speciation with gene flow in equids despite extensive chromosomal plasticity. *Proc Natl Acad Sci U A* 111(52):18655–18660.
31. Langmead B, Salzberg SL (2012) Fast gapped-read alignment with Bowtie 2. *Nat Methods* 9(4):357–359.
32. Segata N, et al. (2012) Metagenomic microbial community profiling using unique clade-specific marker genes. *Nat Methods* 9(8):811–814.
33. Suzuki R, Shimodaira H (2006) Pvclust: an R package for assessing the uncertainty in hierarchical clustering. *Bioinformatics* 22(12):1540–1542.
34. The Human Microbiome Project Consortium (2012) Structure, function and diversity of the healthy human microbiome. *Nature* 486(7402):207–214.
35. Fierer N, et al. (2012) Cross-biome metagenomic analyses of soil microbial communities and their functional attributes. *Proc Natl Acad Sci U A* 109(52):21390–21395.

36. McLaren W, et al. (2010) Deriving the consequences of genomic variants with the Ensembl API and SNP Effect Predictor. *Bioinformatics* 26(16):2069–2070.
37. Baye TM, Tiwari HK, Allison DB, Go RC (2009) Database mining for selection of SNP markers useful in admixture mapping. *BioData Min* 2(1):1.
38. Nicholas FW (2003) Online Mendelian Inheritance in Animals (OMIA): a comparative knowledgebase of genetic disorders and other familial traits in non-laboratory animals. *Nucleic Acids Res* 31(1):275–277.
39. Doan R, et al. (2012) Whole-genome sequencing and genetic variant analysis of a Quarter Horse mare. *BMC Genomics* 13:78.
40. Signer-Hasler H, et al. (2012) A genome-wide association study reveals loci influencing height and other conformation traits in horses. *PLoS One* 7(5):e37282.
41. Alkan C, et al. (2009) Personalized copy number and segmental duplication maps using next-generation sequencing. *Nat Genet* 41(10):1061–1067.
42. Quinlan AR (2014) BEDTools: The Swiss-Army Tool for Genome Feature Analysis. *Curr Protoc Bioinforma* 47:11.12.1–11.12.34.
43. Wang W, et al. (2014) Genome-wide detection of copy number variations among diverse horse breeds by array CGH. *PLoS One* 9(1):e86860.
44. Ghosh S, et al. (2014) Copy number variation in the horse genome. *PLoS Genet* 10(10):e1004712.
45. Watterson GA (1979) Estimating and Testing Selection: The Two-Alleles, Genic Selection Diffusion Model. *Adv Appl Probab* 11(1):14–30.
46. Korneliussen TS, Albrechtsen A, Nielsen R (2014) ANGSD: Analysis of Next Generation Sequencing Data. *BMC Bioinformatics* 15(1):356.
47. Korneliussen TS, Moltke I, Albrechtsen A, Nielsen R (2013) Calculation of Tajima's D and other neutrality test statistics from low depth next-generation sequencing data. *BMC Bioinformatics* 14:289.
48. Prüfer K, et al. (2014) The complete genome sequence of a Neanderthal from the Altai Mountains. *Nature* 505(7481):43–49.
49. Killick R, Eckley I (2014) changepoint:an R package for changepoint analysis. *J Stat Softw* 58(3):1–19.
50. Hill EW, Gu J, McGivney BA, MacHugh DE (2010) Targets of selection in the Thoroughbred genome contain exercise-relevant gene SNPs associated with elite racecourse performance. *Anim Genet* 41 Suppl 2:56–63.
51. Bellone RR, et al. (2010) Fine-mapping and mutation analysis of TRPM1: a candidate gene for leopard complex (LP) spotting and congenital stationary night blindness in horses. *Brief Funct Genomics* 9(3):193–207.
52. Tryon RC, White SD, Bannasch DL (2007) Homozygosity mapping approach identifies a missense mutation in equine cyclophilin B (PPIB) associated with HERDA in the American Quarter Horse. *Genomics* 90(1):93–102.

53. Brooks SA, et al. (2010) Whole-Genome SNP Association in the Horse: Identification of a Deletion in Myosin Va Responsible for Lavender Foal Syndrome. *PLoS Genet* 6(4):e1000909.
54. Brault LS, Cooper CA, Famula TR, Murray JD, Penedo MCT (2011) Mapping of equine cerebellar abiotrophy to ECA2 and identification of a potential causative mutation affecting expression of MUTYH. *Genomics* 97(2):121–129.
55. Marklund L, Moller MJ, Sandberg K, Andersson L (1996) A missense mutation in the gene for melanocyte-stimulating hormone receptor (MCIR) is associated with the chestnut coat color in horses. *Mamm Genome* 7(12):895–899.
56. Wagner H-J, Reissmann M (2000) New polymorphism detected in the horse MC1R gene. *Anim Genet* 31(4):289–290.
57. Brooks SA, Bailey E (2005) Exon skipping in the KIT gene causes a Sabino spotting pattern in horses. *Mamm Genome* 16(11):893–902.
58. Brooks SA, Terry RB, Bailey E (2002) A PCR-RFLP for KIT associated with tobiano spotting pattern in horses. *Anim Genet* 33(4):301–303.
59. Makvandi-Nejad S, et al. (2012) Four Loci Explain 83% of Size Variation in the Horse. *PLoS ONE* 7(7):e39929.
60. Wijnberg ID, et al. (2012) A missense mutation in the skeletal muscle chloride channel 1 (CLCN1) as candidate causal mutation for congenital myotonia in a New Forest pony. *Neuromuscul Disord* 22(4):361–367.
61. Spirito F, et al. (2002) Animal Models for Skin Blistering Conditions: Absence of Laminin 5 Causes Hereditary Junctional Mechanobullous Disease in the Belgian Horse. *J Invest Dermatol* 119(3):684–691.
62. Hauswirth R, et al. (2012) Mutations in MITF and PAX3 Cause “Splashed White” and Other White Spotting Phenotypes in Horses. *PLoS Genet* 8(4):e1002653.
63. Hauswirth R, et al. (2013) Novel variants in the KIT and PAX3 genes in horses with white-spotted coat colour phenotypes. *Anim Genet* 44(6):763–765.
64. Brunberg E, et al. (2006) A missense mutation in PMEL17 is associated with the Silver coat color in the horse. *BMC Genet* 7:46.
65. Shin EK, Perryman LE, Meek K (1997) A kinase-negative mutation of DNA-PK(CS) in equine SCID results in defective coding and signal joint formation. *J Immunol* 158(8):3565–3569.
66. Aleman M, et al. (2004) Association of a mutation in the ryanodine receptor 1 gene with equine malignant hyperthermia. *Muscle Nerve* 30(3):356–365.
67. Gu J, et al. (2010) Association of sequence variants in CKM (creatine kinase, muscle) and COX4I2 (cytochrome c oxidase, subunit 4, isoform 2) genes with racing performance in Thoroughbred horses: SNP association with elite racing performance. *Equine Vet J* 42:569–575.

68. McCue ME, et al. (2012) A High Density SNP Array for the Domestic Horse and Extant Perissodactyla: Utility for Association Mapping, Genetic Diversity, and Phylogeny Studies. *PLoS Genet* 8(1):e1002451.
69. Cannon SC, Hayward LJ, Beech J, Brown RH (1995) Sodium channel inactivation is impaired in equine hyperkalemic periodic paralysis. *J Neurophysiol* 73(5):1892–1899.
70. Christopherson PW, Santen VL, Livesey L, Boudreaux MK (2007) A 10-Base-Pair Deletion in the Gene Encoding Platelet Glycoprotein IIb Associated with Glanzmann Thrombasthenia in a Horse. *J Vet Intern Med* 21(1):196–198.
71. Orr N, et al. (2010) Genome-wide SNP association-based localization of a dwarfism gene in Friesian dwarf horses: SNP association of a dwarfism gene. *Anim Genet* 41:2–7.
72. Cook D, Brooks S, Bellone R, Bailey E (2008) Missense Mutation in Exon 2 of SLC36A1 Responsible for Champagne Dilution in Horses. *PLoS Genet* 4(9):e1000195.
73. Hansen M, Knorr C, Hall AJ, Broad TE, Brenig B (2007) Sequence analysis of the equine SLC26A2 gene locus on chromosome 14q15→q21. *Cytogenet Genome Res* 118(1):55–62.
74. Yang G (1998) A dinucleotide mutation in the endothelin-B receptor gene is associated with lethal white foal syndrome (LWFS); a horse variant of Hirschsprung disease. *Hum Mol Genet* 7(6):1047–1052.
75. Tozaki T, et al. (2010) A genome-wide association study for racing performances in Thoroughbreds clarifies a candidate region near the MSTN gene: A genome-wide scan for racing performances. *Anim Genet* 41:28–35.
76. W. Hill E, P. Ryan D, E. MacHugh D (2012) Horses for Courses: a DNA-based Test for Race Distance Aptitude in Thoroughbred Racehorses. *Recent Pat DNA Gene Seq* 6(3):203–208.
77. Mariat D, Taourit S, Guérin G (2003) A mutation in the MATP gene causes the cream coat colour in the horse. *Genet Sel Evol* 35(1):119.
78. Rieder S, Taourit S, Mariat D, Langlois B, Guérin G (2001) Mutations in the agouti (ASIP), the extension (MC1R), and the brown (TYRP1) loci and their association to coat color phenotypes in horses (*Equus caballus*). *Mamm Genome* 12(6):450–455.
79. Andersson LS, et al. (2012) Mutations in DMRT3 affect locomotion in horses and spinal circuit function in mice. *Nature* 488(7413):642–646.
80. Fox-Clipsham LY, et al. (2011) Identification of a Mutation Associated with Fatal Foal Immunodeficiency Syndrome in the Fell and Dales Pony. *PLoS Genet* 7(7):e1002133.
81. Révay T, Villagómez DAF, Brewer D, Chenier T, King WA (2012) GTG Mutation in the Start Codon of the Androgen Receptor Gene in a Family of Horses with 64,XY Disorder of Sex Development. *Sex Dev* 6(1-3):108–116.
82. Towers RE, et al. (2013) A Nonsense Mutation in the IKBKG Gene in Mares with Incontinentia Pigmenti. *PLoS ONE* 8(12):e81625.

83. Xu X, Arnason U (1994) The complete mitochondrial DNA sequence of the horse, *Equus caballus*: extensive heteroplasmy of the control region. *Gene* 148(2):357–362.
84. Li H, et al. (2009) The Sequence Alignment/Map format and SAMtools. *Bioinformatics* 25(16):2078–2079.
85. Keane T, Creevey C, Pentony M, Naughton T, McInerney J (2006) Assessment of methods for amino acid matrix selection and their use on empirical data shows that ad hoc assumptions for choice of matrix are not justified. *BMC Evol Biol* 6(1):29.
86. Schwarz G (1978) Estimating the Dimension of a Model. *Ann Stat* 6(2):461–464.
87. Guindon S, et al. (2010) New algorithms and methods to estimate maximum-likelihood phylogenies: assessing the performance of PhyML 3.0. *Syst Biol* 59(3):307–321.
88. Anisimova M, Gascuel O (2006) Approximate likelihood-ratio test for branches: A fast, accurate, and powerful alternative. *Syst Biol* 55(4):539–552.
89. Hasegawa M, Kishino H, Yano T (1985) Dating of the human-ape splitting by a molecular clock of mitochondrial DNA. *J Mol Evol* 22(2):160–174.
90. Huson DH, Scornavacca C (2012) Dendroscope 3: an interactive tool for rooted phylogenetic trees and networks. *Syst Biol* 61(6):1061–1067.
91. Drummond AJ, Suchard MA, Xie D, Rambaut A (2012) Bayesian phylogenetics with BEAUti and the BEAST 1.7. *Mol Biol Evol* 29(8):1969–1973.
92. Rambaut A, Suchard MA, Xie D, Drummond AJ (2014) *Tracer v1.6*.
93. Drummond AJ, Rambaut A, Shapiro B, Pybus OG (2005) Bayesian Coalescent Inference of Past Population Dynamics from Molecular Sequences. *Mol Biol Evol* 22(5):1185–1192.
94. Minin VN, Bloomquist EW, Suchard MA (2008) Smooth skyride through a rough skyline: Bayesian coalescent-based inference of population dynamics. *Mol Biol Evol* 25(7):1459–1471.
95. Wickham H (2009) *ggplot2: Elegant Graphics for Data Analysis* (Springer New York).
96. Wallner B, et al. (2013) Identification of Genetic Variation on the Horse Y Chromosome and the Tracing of Male Founder Lineages in Modern Breeds. *PLoS One* 8(4):e60015.
97. Lippold S, Matzke NJ, Reissmann M, Hofreiter M (2011) Whole mitochondrial genome sequencing of domestic horses reveals incorporation of extensive wild horse diversity during domestication. *BMC Evol Biol* 11:328.
98. Flicek P, et al. (2013) Ensembl 2013. *Nucleic Acids Res* 41(D1):D48–D55.
99. Stamatakis A (2006) RAxML-VI-HPC: maximum likelihood-based phylogenetic analyses with thousands of taxa and mixed models. *Bioinformatics* 22(21):2688–2690.
100. Goto H, et al. (2011) A massively parallel sequencing approach uncovers ancient origins and high genetic variability of endangered Przewalski's horses. *Genome Biol Evol* 3:1096–1106.

101. Achilli A, et al. (2012) Mitochondrial genomes from modern horses reveal the major haplogroups that underwent domestication. *Proc Natl Acad Sci U S A* 109(7):2449–2454.
102. Xu S, et al. (2007) High altitude adaptation and phylogenetic analysis of Tibetan horse based on the mitochondrial genome. *J Genet Genomics* 34(8):720–729.
103. Jiang Q, et al. (2011) The complete mitochondrial genome and phylogenetic analysis of the Deba pony (*Equus caballus*). *Mol Biol Rep* 38(1):593–599.
104. Sawyer S, Krause J, Guschanski K, Savolainen V, Pääbo S (2012) Temporal Patterns of Nucleotide Misincorporations and DNA Fragmentation in Ancient DNA. *PLoS ONE* 7(3):e34131.
105. Tamura K, Nei M (1993) Estimation of the number of nucleotide substitutions in the control region of mitochondrial DNA in humans and chimpanzees. *Mol Biol Evol* 10(3):512–526.
106. Li H, Durbin R (2011) Inference of human population history from individual whole-genome sequences. *Nature* 475(7357):493–496.
107. Gutenkunst RN, Hernandez RD, Williamson SH, Bustamante CD (2009) Inferring the joint demographic history of multiple populations from multidimensional SNP frequency data. *PLoS Genet* 5(10):e1000695.
108. Outram AK, et al. (2009) The Earliest Horse Harnessing and Milking. *Science* 323(5919):1332–1335.
109. Terhorst J, Song YS (2015) Fundamental limits on the accuracy of demographic inference based on the sample frequency spectrum. *Proc Natl Acad Sci* 112(25):7677–7682.
110. Yang MA, Harris K, Slatkin M (2014) The projection of a test genome onto a reference population and applications to humans and archaic hominins. *Genetics* 198(4):1655–1670.
111. Danecek P, et al. (2011) The Variant Call Format and VCFtools. *Bioinformatics*. doi:10.1093/bioinformatics/btr330.
112. Price AL, et al. (2006) Principal components analysis corrects for stratification in genome-wide association studies. *Nat Genet* 38(8):904–909.
113. Fumagalli M, Vieira FG, Linderöth T, Nielsen R (2014) ngsTools: methods for population genetics analyses from next-generation sequencing data. *Bioinformatics* 30(10):1486–1487.
114. Green RE, et al. (2010) A Draft Sequence of the Neandertal Genome. *Science* 328(5979):710–722.
115. Patterson N, et al. (2012) Ancient Admixture in Human History. *Genetics* 192(3):1065–1093.
116. Pickrell JK, Pritchard JK (2012) Inference of Population Splits and Mixtures from Genome-Wide Allele Frequency Data. *PLoS Genet* 8(11):e1002967.

117. Skotte L, Korneliussen TS, Albrechtsen A (2013) Estimating individual admixture proportions from next generation sequencing data. *Genetics* 195(3):693–702.
118. Durand EY, Patterson N, Reich D, Slatkin M (2011) Testing for ancient admixture between closely related populations. *Mol Biol Evol* 28(8):2239–2252.
119. Petersen JL, et al. (2013) Genome-wide analysis reveals selection for important traits in domestic horse breeds. *PLoS Genet* 9(1):e1003211.
120. Wittkopp PJ, Kalay G (2011) Cis-regulatory elements: molecular mechanisms and evolutionary processes underlying divergence. *Nat Rev Genet* 13(1):59–69.
121. King MC, Wilson AC (1975) Evolution at two levels in humans and chimpanzees. *Science* 188(4184):107–116.
122. Carroll SB (2005) Evolution at two levels: on genes and form. *PLoS Biol* 3(7):e245.
123. Carroll SB (2008) Evo-devo and an expanding evolutionary synthesis: a genetic theory of morphological evolution. *Cell* 134(1):25–36.
124. Hoekstra HE, Coyne JA (2007) The locus of evolution: evo devo and the genetics of adaptation. *Evolution* 61(5):995–1016.
125. Fraser HB (2013) Gene expression drives local adaptation in humans. *Genome Res* 23(7):1089–1096.
126. Ohno S (1970) *Evolution by Gene Duplication*: (Springer Berlin Heidelberg).
127. Nei M (1987) *Molecular Evolutionary Genetics* (Columbia University Press).
128. Zhang B, Kirov S, Snoddy J (2005) WebGestalt: an integrated system for exploring gene sets in various biological contexts. *Nucleic Acids Res* 33(Web Server issue):W741–8.
129. Benjamini Y, Hochberg Y (1995) Controlling the False Discovery Rate: A Practical and Powerful Approach to Multiple Testing. *J R Stat Soc Ser B Stat Methodol* 57(1):289–300.